Establishing an *Ex Vivo* Model of Acanthamoeba Keratitis and Investigating the Phenotypic Similarities between the Protozoan *Acanthamoeba* and Human Macrophages

Noor Tawfiq Mohamad Al-Antary (M.B.B.S,
Higher Specialization Degree in Pathology)

A thesis submitted in partial fulfilment of the requirements of the University of Wolverhampton for the degree of Doctor of Philosophy

April 2021

Declaration

This work or any part thereof has not previously been presented in any form to the University or to any other body whether for the purposes of assessment, publication or for any other purpose (unless otherwise indicated in page 3). Save for any express acknowledgements, references and/or bibliographies cited in the work, I confirm that the intellectual content of the work is the result of my own efforts and of no other person.

The right of Noor Tawfiq Mohamad Al-Antary to be identified as author of this work is asserted in accordance with ss.77 and 78 of the Copyright, Designs and Patents Act 1988. At this date copyright is owned by the author.

Signature:

Date: 19 / 4 / 2021

Publications and Posters Related to The Work Presented in This Thesis

Al-Antary, N. Heaselgrave, W. and Hau, S., 2021. Correlation of *Ex vivo* and *In vivo* Confocal Microscopy Imaging of *Acanthamoeba*. American Journal of Ophthalmology (manuscript submitted).

Al-Antary, N. Heaselgrave, W. ,2021. Establishing *Ex-vivo* Acanthamoeba Keratitis Model (manuscript ready for submission).

Al-Antary, N. Heaselgrave, W., 2021. Phenotypic Similarities Between *Acanthamoeba* and Macrophages (manuscript ready for submission).

Al-Antary, N. Heaselgrave, W., 2018. Developing an *ex vivo* model of Acanthamoeba keratitis. Proceedings of the Internal Annual Research Symposium, Poster no. 17, University of Wolverhampton, UK. (3rd place winner in poster competition).

Abstract

Acanthamoeba is a small free-living amoeba found in tap water and soil with two life stages: the trophozoite and cyst. *Acanthamoeba* species are opportunistic pathogens of humans that cause two main diseases including a potentially blinding infection of the cornea called Acanthamoeba keratitis (AK) in immunocompetent individuals, and a fatal granulomatous encephalitis in the immunocompromised.

In this study, an *ex vivo* model of AK was developed to better understand the pathophysiological processes that occur in this disease. The model has several applications such as studying the interaction of *Acanthamoeba* with cells of innate immunity, investigating the efficacy of different pharmaceutical products in stopping the progression of the disease beside using the model to correlate between *in vivo* and *ex vivo* confocal microscopy findings of various morphologies of *Acanthamoeba* cysts and trophozoites. Furthermore, the study evaluated the phenotypic similarities between *Acanthamoeba* and cells of the innate immune system mainly macrophages using flow cytometry analysis to enhance the understanding of how immune cells interact with *Acanthamoeba*.

Porcine corneas were used to establish a reproducible *ex vivo* model which was maintained for four weeks and optimised by the supplement of CO_2 and the use of air – liquid interface rocking system that mimics natural eye blinking. Once the model was established, *Acanthamoeba* trophozoites and cysts were added to the corneal model to evaluate the pathogenesis of Acanthamoeba keratitis, and the study successfully demonstrated the development of the infection in the model. This study was also able to demonstrate that the addition of macrophages and neutrophils to the AK model did not limit the process of the infection as these cells were phagocytosed by *Acanthamoeba*.

The model was also used to investigate the efficacy of doxycycline and polyhexamethylene biguanide (PHMB) in stopping the disease progression and the results demonstrated the ability of PHMB to inactivate *Acanthamoeba* trophozoites with minimal toxicity to the corneal epithelium. Doxycycline was not found to have any major antimicrobial effect on the viability of *Acanthamoeba.*

The model was also utilized to study the *ex vivo* confocal microscopy (EVCM) features of various forms of *Acanthamoeba* and correlate these findings to *in vi*vo confocal microscopy (IVCM) images from culture positive AK cases. The study demonstrated similarity in the

morphological features of *Acanthamoeba* in both *ex vivo* and *in vivo* confocal microscopy images, which makes EVCM images a reliable reference to validate IVCM findings.

Finally, this study evaluated the phenotypic similarities between *Acanthamoeba* and macrophages using flow cytometry analysis which identified various degrees of positive reactivity of amoebic cell surface to a limited number of anti-human monoclonal antibodies. This suggests some structural and functional similarities in protein surfaces between amoeba and macrophages which can potentially offer a future tool for screening.

Acknowledgement

First and foremost, I thank and praise God the almighty who blessed me with health, knowledge and persistence to complete this work.

I would like to show my greatest appreciation to my supervisor and mentor Dr Wayne Heaselgrave for his support, guidance and continuous encouragement without which this work would not have been possible.

I am very thankful for my second supervisor Dr Kesley Attridge for his assistance and advice especially in the immunology part of this work.

I would also like to thank Dr Hau Scott for his invaluable input about confocal microscopy.

I would also express my gratitude to my lab colleagues for their help and support: Dr Enas Al-Ani, Dr Anas Hamad, Ogechi Onuoha. I send special thanks to the technician team who provided great support to my lab work: David Luckhurst, Clare Murcott, Andy Brook, and Angela Williams.

Finally, my deepest gratitude goes to my dear parents, brother and sisters for their support throughout the years, my lovely kids Jad, Leen and Ward and my beloved husband Rakan for joining me on this journey.

Dedication

I dedicate this thesis to my beloved and best companion Rakan for being a great husband and friend. Thank you for all the support, care and love you have been giving me.

Abbreviations

°C	Degree Celsius
AK	Acanthamoeba keratitis
CD	Cluster of Differentiation
CNS	Central nervous system
CO_2	Carbon dioxide
DMEM	Dulbecco's minimum essential medium
DMSO	Dimethyl sulphoxide
DNA	Deoxyribonucleic acid
DPBS	Dulbecco's phosphate buffered saline
E. coli	*Escherichia coli*
EBP	Encystment stimulating protein
EDTA	Ethylenediaminetetraacetic acid
EGF	Epidermal growth factor
EVCM	Ex vivo confocal microscopy
HEp-2	Human epithelial cells type 2
HEPES	N-(2-Hydroxyethyl)piperazine-N′-(2-ethanesulfonic acid)
HRT II/RCM	Heidelberg Retina Tomograph II with the Rostock Corneal Module
IFN	Interferon
IgA	Immunoglobulin A
IL	Interleukin
IPA	Isopropyl alcohol (Propan-2-ol)

I-PVP	Povidone-iodine
IVCM	In vivo confocal microscopy
KH_2PO_4	Potassium dihydrogen orthophosphate
LPG	Lipophosphoglycans
M	Molar
mAb	Monoclonal antibodies
MAPD	Myristamidopropyl dimethylamine
MAPK/ERK	Mitogen Activated Protein Kinases/ Extracellular Signal-Regulated Kinases
MCC	Minimum cysticidal concentration
MCT	Minimum cytotoxic concentration
MEM	Minimum essential medium
MHC-II	Major histocompatibility complex
MIC	Minimum inhibitory concentration
MIP-2	Macrophage inflammatory protein 2
MKP-1	MAP kinase phosphatase -1
mL	Milliliter
mM	Millimolar
MTAC	Minimum trophozoite amoebicidal concentration
MTIC	Minimum trophozoite inhibitory concentration
NaOH	Sodium hydroxide
NEM	Neff's encystment medium
NF-kB	Nuclear factor kappa B
NNA	Non-nutrient agar
PCR	Polymerase chain reaction

PES	Phenazine ethosulfate
PHMB	Polyhexamethylene biguanide
PMA	Phorbol 12-myristate 13-acetate
PRRs	Pattern recognition receptors
PTPRC	Protein tyrosine phosphatase, receptor type, C
PYG	Peptone yeast glucose
RNA	Ribonucleic acid
rpm	Revolutions per minute
SEM	Scanning electron microscope
TGF-β	Transforming growth factor β
TLR	Toll-like receptor
TNF-α	Tumour necrosis factor alpha
TSA	Tryptic soy agar
TSB	Tryptic soy broth
TUNEL	Terminal deoxynucleotidyl transferase dUTP nick end labelling
v/v	Volume/volume
w/v	Weight/volume
x g	Gravity
α-SMA	Alpha smooth muscle actin
µg	Microgram
µm	Micrometre
µL	Microliter
µM	Micromolar

Table of Contents

Abstract…… 4

Acknowledgments…… 7

Abbreviations…… 9

Table of contents…….. 12

List of Tables…….. 19

List of Figures…… 20

Chapter 1: General Introduction…… 24

1.1 Brief History…….. 25

1.2 Amoebic Discovery History……... 26

1.3 *Acanthamoeba*: Trophozoite Stage……. 28

1.4 *Acanthamoeba*: Cyst Stage…….. 30

1.5 *Acanthamoeba* Feeding……. 32

1.6 *Acanthamoeba* Distribution……... 33

1.7 *Acanthamoeba* Classification…… 34

1.7.1 Genetic Grouping ……. 36

1.8 *Acanthamoeba* as a Reservoir for Other Microorganisms…….. 38

1.9 Pathogenicity of *Acanthamoeba*……. 39

1.9.1 Granulomatous Amoebic Encephalitis (GAE)…….. 40

1.9.2 *Acanthamoeba* Keratitis (AK) ……. 42

1.9.2.1 Pathogenesis of Acanthamoeba Keratitis…… 43

1.9.2.2 Risk Factors…….. 44

1.9.2.3 Incidence……... 44

1.9.2.4 Contact Lens Disinfection…….. 45

1.9.2.5 Diagnosis of *Acanthamoeba* Keratitis…….. 46

1.9.2.6 Treatment of Acanthamoeba Keratitis…….. 47

1.9.2.7 Surgical Treatment…….. 49

1.10 Brief Description of the Immune System……. 50

1.11 The Human Eye…… 52

1.11.1 Defense Mechanisms…… 53

1.11.1.1 Tear Film……. 54
1.11.1.2 Immunological Factors……. 55
1.12 Aims and Objectives…… 56
1.12.1 Objectives for Aim 1: Developing *ex vivo* model..... 56
1.12.2 Objectives for Aim 2: Using the model to study Acanthamoeba keratitis (AK)…… 57
1.12.3 Objectives for Aim 3: Correlation between *ex vivo* (EVCM) and *in vivo* confocal microscopy (IVCM) Findings……. 57
1.12.4 Objectives for Aim 4: Investigating similarities between *Acanthamoeba* and human macrophages…….. 57
Chapter 2: Materials and Methods…… 58
2.1 Chemicals…… 59
2.2 Test Organisms…… 59
2.3 *Acanthamoeba C*ell Culture…… 60
2.4 Cryopreservation of *Acanthamoeba*…… 60
2.5 Preparation of *Acanthamoeba* Food *E. coli* Stock……. 61
2.6 Preparation of *Acanthamoeba* Mature Cysts in Neff's Medium…….. 62
2.7 The Preparation of *Acanthamoeba* Mature Cysts in NNA Medium… 62
2.8 Human Epithelial Cell Line Culture (HEp-2)…….…. 63
2.9 HEp-2 Cells Sub-culture…….…….…… 64
2.10 Cryopreservation of HEp-2 Cells…..……..…….. 64
2.11 THP-1 and HL-60 Cell Culture……..…… 65
2.12 Cryopreservation of THP-1 and HL-60 Cell……. 65
2.13 THP-1 Differentiation to Macrophages…….…… 66
2.14 Excision of Cornea from Porcine Ocular Globe……..……. 66
2.15 Culture of Corneal Tissue……..……. 68
2.16 Histological Techniques…….…… 68
2.17 Capturing Microscopic Slides……..…… 78
Chapter 3: Establishing *Ex Vivo* Corneal Model……... 79
3.1 Introduction…… 80
3.1.1 Cornea…… 80
3.1.1.1 The Epithelium……..…….. 82
3.1.1.2 Bowman's Layer…..…… 83

3.1.1.3 The Stroma..…… 83
3.1.1.4 Descemet's Membrane and Endothelium…… 84
3.1.2 Previous Models…… 84
3.1.2.1 *In vivo* Animal Models…… 84
3.1.2.2 *In vitro* Models…….. 85
3.1.2.3 *Ex vivo* Animal Model…….. 88
3.1.2.4 *Ex vivo* Human Model……..…….. 89
3.1.3 Rationale…… 90
3.1.4 Aims and objectives…….. 90
3.2 Methods…….. 91
3.2.1 Excision of Cornea from Porcine Ocular Globe……..…….. 91
3.2.2 Culture of Corneal Tissue…….. 91
3.2.2.1 Immersion System……..…… 92
3.2.2.2 Air/Liquid Interface System……..…….. 92
3.2.3 Assessment Methodology…… 97
3.3 Results…… 99
3.3.1 Immersion System……..……. 99
3.3.2 Air/Liquid Interface System……..…… 101
3.3.2.1 Cornea Culture in Petri Dish, Static with CO_2 ……..…… 101
3.3.2.2 Cornea Culture in Petri Dish, Rocking without CO_2 ……. 105
3.3.2.3 Cornea Culture in Petri Dish, Rocking with CO_2 ……..…… 108
3.4 Discussion…….. 111
3.4.1 Previous Studies…… 113
3.4.2 Eye Banks- Corneal Storage Techniques……. 123
3.5 Conclusion and Future Work……..…….. 125
Chapter 4: Establishing *Ex-vivo* Acanthamoeba Keratitis Model…… 126
4.1 Introduction…… 127
4.1.1 *Acanthamoeba* ……. 127
4.1.2 Acanthamoeba Keratitis……..…… 127
4.1.3 Pathogenesis……. 128
4.1.4 Pharmacological Treatment……. 130
4.1.5 Previous Models…… 130
4.1.6 Rationale……. 131

4.1.7 Aim and Objectives…….. 132
4.2 Methods…….. 133
4.2.1 *Acanthamoeba* Culture……. 133
4.2.2 Developing *Acanthamoeba* Passage Cells……... 133
4.2.3 Culture of Mammalian Cells……..……. 134
4.2.3.1 THP-1 Cell Culture…….. 134
4.2.3.2 HL-60 Cell Culture. ……. 134
4.2.3.3 Human Epithelial Cell Line Culture (HEp-2) Cell Culture…..…. 134
4.2.4 Cornea Culture…….. 135
4.2.5 Inducing Infection…….. 135
4.2.6 Adding Macrophages and HL-60…… 136
4.2.7 Assessment Methodology…… 136
4.3 Results…… 138
4.3.1 Macroscopic Level……..……. 138
4.3.2 Microscopic Level……..……... 140
4.3.2.1 Day 0 (control)…….. 140
4.3.2.2 Day 3……. 141
4.3.2.3 Day 8……. 143
4.3.2.4 Day 13…….. 144
4.3.2.5 Day 18……... 145
4.3.2.6 Day 23……... 147
4.3.2.7 Day 28……... 148
4.3.3 Outcome of Adding *Acanthamoeba* Cysts to Cornea……..… 149
4.3.4 Outcome of Adding or Injecting Macrophages and HL-60 Cells to the Infected Cornea……. 149
4.4 Discussion …… 151
4.4.1 Summary of Results……. 151
4.4.2 Inducing the Infection…… 152
4.4.3 Pathogenesis and Previous Studies…….. 154
4.4.4 Previous Studies on Macrophages……... 157
4.5 Conclusion and Future Work…… 158

Chapter 5: Application of the Porcine *Ex Vivo* Model: Drugs…… 159
5.1 Introduction…… 160
5.1.1 Acanthamoeba Keratitis……... 160
5.1.2 Treatment- PHMB……. 160
5.1.3 Treatment- Doxycycline……. 162
5.1.4 Rationale ……. 163
5.1.5 Aim…….. 163
5.2 Methods…….. 164
5.2.1 Test Organism Strains and Culture……. 164
5.2.2 Drug Sensitivity Testing…….……. 164
5.2.2.1 Amoebicidal Assay……. 164
5.2.2.2 Cysticidal Assay……... 166
5.2.3 Toxicology Assay ……..…….. 166
5.2.4 Applying the Drugs on the *Ex Vivo* Model…….. 167
5.3 Results……. 169
5.3.1 Drug Assays……... 169
5.3.2 Histological Sections – PHMB……. 170
5.3.2.1 Day 3, Control……..……... 170
5.3.2.2 Day 7 – Control and Test Corneas……..……. 172
5.3.2.3 Day 10 – Control and Test Corneas……..……... 174
5.3.2.4 Day 14- Control and Test Corneas……..……. 176
5.3.3 Histological Sections – Doxycycline……..…… 178
5.3.3.1 Day 3, Controls……..……. 178
5.3.3.2 Day 7, Control and Test Corneas……..…… 179
5.3.3.3 Day 10, Control and Test Corneas……..……. 181
5.3.3.4 Day 14, Control and Test Corneas……..…. 183
5.3.3.5 Day 18, Control and Test Corneas……... 185
5.3.3.6 Day 22, Control and Test Corneas……... 187
5.4 Discussion ……. 189
5.4.1 PHMB- Assay Results…….. 189
5.4.2 PHMB- Light Microscope Results…….. 189
5.4.3 PHMB- Previous Studies……. 191
5.4.4 Doxycycline- Assay and Histology Results……... 194

5.4.5 Doxycycline- Previous Studies…… 194
5.5 Conclusion and Future Work…… 196
Chapter 6: Correlation of *Ex Vivo* and *In Vivo* Confocal Microscopy Imaging of *Acanthamoeba*…….. 197
6.1 Introduction…… 198
6.2 Aim and Objectives…….. 200
6.3 Methods…….. 201
6.3.1 *Acanthamoeba* Strains and Culture……... 201
6.3.2 Preparation of Dead *Acanthamoeba Cysts*……... 201
6.3.3 Preparation of *Acanthamoeba* Empty Cysts…… 202
6.3.4 Preparation of Eye Globes…….. 202
6.3.5 Inoculation of *Acanthamoeba*…….. 203
6.3.6 *Ex vivo* Confocal Microscopy (EVCM)..... 203
6.3.7 EVCM and IVCM Image Comparison…… 205
6.3.8 Phase Contrast Images…… 206
6.4 Results…… 207
6.4.1 Control Cornea…….. 207
6.4.2 Live *Acanthamoeba* Cysts……... 209
6.4.3 Dead *Acanthamoeba* Cysts…… 211
6.4.4 Empty *Acanthamoeba* Cysts……... 213
6.4.5 Live *Acanthamoeba* Trophozoites……..... 215
6.5 Discussion …… 217
6.6 Conclusion and Future Work…….. 220
Chapter 7: Phenotypic Similarities between *Acanthamoeba* and Macrophages Using Flow Cytometry…… 221
7.1 Introduction…… 222
7.1.1 Macrophages…… 222
7.1.2 Function…….. 222
7.1.3 History…… 223
7.1.4 Activation of Macrophages…….. 224
7.1.5 *Acanthamoeba* and Macrophages…… 227
7.1.6 Rationale…… 230
7.1.7 Aim and Objectives…….. 230

7.2 Methods…….. 231
7.2.1 Organisms…….. 231
7.2.2 Culture……. 232
7.2.2.1 THP-1 Cells …….. 232
7.2.2.2 Microorganisms…… 232
7.2.3 Flow Cytometry…….. 232
7.3 Results…… 235
7.3.1 Macrophages……. 236
7.3.2 *Acanthamoeba castellanii*…… 237
7.3.3 *Naegleriae gruberi* …… 238
7.3.4 *Acanthamoeba* (clinical isolate)…….. 239
7.3.5 *Acanthamoeba polyphaga* ……... 240
7.3.6 *Acanthamoeba culbertsoni*……... 241
7.4 Discussion…… 242
7.4.1 Previous Studies…… 244
7.5 Conclusion and future work…….. 246
Chapter 8: General Conclusions……... 247
List of References…… 253

List of Tables

Table 1.1:	Classification of Acanthamoeba based on morphology……	36
Table 1.2:	Morphology groups and genotypes of Acanthamoeba based on 18s ribosomal RNA sequence……	37
Table 2.1:	Organisms and cell lines……..	59
Table 2.2:	Histology processing - dehydration steps……...	69
Table 2.3:	Histology processing - clearing steps……..	70
Table 2.4:	Histology processing - infiltration steps……..	71
Table 2.5:	Histology processing - clearing and rehydration process……	75
Table 2.6:	Histology processing - staining process…….	76
Table 3.1:	Outcome of current study and 'Deshpande *et al.'* study ….....	116
Table 3.2:	Outcome of current study and 'Marlo *et al.'* study…….	121
Table 5.1:	Activities of tested drugs against the trophozoites and cysts of *A. castellanii* (ATCC 50370) and *A. polyphaga* (ATCC 30461) and shows their toxicity for HEp-2 cells…….	169
Table 6.1:	*Acanthamoeba* morphological structures on IVCM……..	205
Table 7.1:	Organisms and cells used for flow cytometry analysis…….	231
Table 7.2:	Anti-human leukocyte monoclonal antibodies used in flow cytometry analysis of amoebic cell surfaces……..	234

List of Figures

Figure 1.1:	Trophozoite stage of *Acanthamoeba castellanii* (ATCC 50370) demonstrating contractile vacuoles and acanthopodia at 200X…….	28
Figure 1.2:	Mature cysts of *Acanthamoeba castellanii* demonstrating endocyst and ectosyst at 400X……..	32
Figure 1.3:	Scanning electron microscope of Acanthamoeba trophozoites showing the food cup……	33
Figure 1.4:	Transmission electron microscopy image of *Acanthamoeba* cyst containing *Legionella*……..	38
Figure 1.5:	Life cycle of *Acanthamoeba* in environment and human body……	41
Figure 1.6:	Normal eye compared to *Acanthamoeba*-infected eye ……	42
Figure 1.7:	The pathogenesis of Acanthamoeba keratitis……	43
Figure 1.8:	Penetrating keratoplasty: full thickness donor graft placed using interrupted sutures in radial distribution……	49
Figure 1.9:	Schematic diagram of the human eye……..	52
Figure 1.10:	Schematic diagram of corneal layers……	53
Figure 2.1:	Corneal harvesting……...	67
Figure 2.2:	Histology processing - fixation process……	69
Figure 2.3:	Dehydration processor……	70
Figure 2.4:	Histology processing - embedding process…….	72
Figure 2.5:	Histology processing - sectioning process……...	73
Figure 2.6:	Histology processing - mounting process……	74
Figure 2.7:	Histology processing - rehydration and staining process…..	77
Figure 2.8:	Mounting the sections under a coverslip…….	77
Figure 2.9:	Storage of slides and examination…….	78
Figure 3.1:	Schematic diagram of the human eye……..	80
Figure 3.2:	Schematic presentation of different layers of the cornea …	81
Figure 3.3:	Histology section from cornea of pig eye……	82
Figure 3.4:	Haematoxylin-eosin-stained histological cross-section of the EpiOcular™ tissue model……	87

Figure 3.5:	Immersion method. Corneas cultured in storage medium in 50 mL tissue culture flat tubes.....	92
Figure 3.6:	Culture in Petri dish, static with CO_2. Corneas cultured in storage medium in 90 mm Petri dish.....	93
Figure 3.7:	Cornea culture in Petri dish, rocking system.....	94
Figure 3.8:	Schematic diagram of the box – containing the egg incubator- placed on a platform rocker.....	95
Figure 3.9:	Cornea culture in Petri dish, rocking system with 5% CO_2 ...	96
Figure 3.10:	Corneal transparency, immersion system.....	100
Figure 3.11:	Histology sections, immersion system.....	101
Figure 3.12:	Corneal transparency, static with CO_2	102
Figure 3.13:	Histology sections, static with CO_2	104
Figure 3.14:	Corneal transparency, rocking without CO_2.....	105
Figure 3.15:	Histology sections, rocking without CO_2.....	107
Figure 3.16:	Corneal transparency, rocking with CO_2.....	108
Figure 3.17:	Histology sections, rocking with CO_2.....	110
Figure 4.1:	The pathogenic cascade of Acanthamoeba keratitis.....	129
Figure 4.2:	Corneal transparency.....	139
Figure 4.3:	Normal cornea at day 0.....	140
Figure 4.4:	Control and infected corneas at day 3.....	142
Figure 4.5:	Control and infected corneas at day 8.....	143
Figure 4.6:	Control and infected corneas at day 13.....	144
Figure 4.7:	Control and infected corneas at day 18.....	146
Figure 4.8:	Control and infected corneas at day 23.....	147
Figure 4.9:	Control and infected corneas at day 28.....	149
Figure 4.10:	The addition of macrophages and HL-60 to the infected cornea.....	150
Figure 5.1:	Molecular structure of PHMB.....	161
Figure 5.2:	The layout of the microtiter plate for the sensitivity testing..	165
Figure 5.3:	Adding the drug to the corneal surface.....	168
Figure 5.4:	Histology sections, control versus infected cornea, day 3....	171
Figure 5.5:	Histology sections, healthy versus infected cornea, day 7, added PHMB.....	173

Figure 5.6: Histology sections, healthy versus infected cornea, day 10, added PHMB…… 175
Figure 5.7: Histology sections, healthy versus infected cornea, day 14, added PHMB……. 177
Figure 5.8: Histology sections, control versus infected cornea, day 3…. 178
Figure 5.9: Histology sections, healthy versus infected cornea, day 7, added doxycycline…… 180
Figure 5.10: Histology sections, healthy versus infected cornea, day 10, added doxycycline…… 182
Figure 5.11: Histology sections, healthy versus infected cornea, day 14, added doxycycline…… 184
Figure 5.12: Histology sections, healthy versus infected cornea, day 18, added doxycycline…… 186
Figure 5.13: Histology sections, healthy versus infected cornea, day 22, added doxycycline…… 188
Figure 6.1: Eye globe held in place using a three-pronged clamp attached to a retort stand with the cornea in contact with the TomoCap during the ex vivo scanning process…… 204
Figure 6.2: EVCM images of control cornea…… 208
Figure 6.3: EVCM, IVCM and phase contrast images of live cysts……. 210
Figure 6.4: EVCM, IVCM and phase contrast images of dead *Acanthamoeba* cysts…….. 212
Figure 6.5: EVCM, IVCM and phase contrast images of empty *Acanthamoeba* cysts……... 214
Figure 6.6: EVCM, IVCM and phase contrast images of live *Acanthamoeba* trophozoites…….. 216
Figure7.1: Schematic diagram showing different stimuli and signalling pathways in activation and polarization of macrophages….. 226
Figure 7.2: Transmission electron microscope images showing similar appearance of *Acanthamoeba castellanii* and alveolar macrophage…….. 229
Figure 7.3: Flow cytometry results for macrophages stained with anti-human mAbs…… 236

Figure 7.4: Flow cytometry result for *Acanthamoeba castellanii* stained with anti-human mAbs……. 237
Figure 7.5: Flow cytometry result for *Naegleriae gruberi* stained with anti-human mAbs……. 238
Figure 7.6: Flow cytometry result for *Acanthamoeba* (clinical isolate) stained with anti-human mAbs…… 239
Figure 7.7: Flow cytometry result for *Acanthamoeba polyphaga* stained with anti-human mAbs……. 240
Figure 7.8: Flow cytometry result for *Acanthamoeba culbertsoni* stained with anti-human mAbs……. 241

Chapter One

General Introduction

Chapter 1: General Introduction

1.1 Brief History

Cells are divided into two main categories: prokaryotic and eukaryotic (Whittaker, 1969). The unicellular organisms of bacteria and archaea domains are classified as prokaryotes (Murat *et al.,*2010). Animal cells, plant cells, fungi, and protists are eukaryotes (Youngson ,2006). Eukaryotic cells have four components in common: a plasma membrane which separates the internal structures of the cell from the outside environment, cytoplasm within which other cellular organelles are located, deoxyribonucleic acid (DNA) which is the genetic material of the cell, and ribosomes which are the particles that synthesize proteins (Whittaker, 1969). Prokaryotes are structurally different from eukaryotic cells as they are single-cell organisms with no nucleus or other membrane-bound organelles (Charles *et al.,*2012).

The invention of the microscope in the 1600s was a revolutionary step in enabling scientists to study objects that cannot be observed by the naked eye. In 1676, the Dutch scientist Antonie Van Leeuwenhoek was the first to identify microorganisms when he was studying a drop of water under the microscope and noticed some microorganisms, and he was the first to identify free-living protozoa (Lane, 2015)

Protozoa are unicellular eukaryotes that have complicated internal structure and perform complex metabolic functions like feeding in which they ingest food by a process called pinocytosis to engulf liquids or small particles, and another process called phagocytosis for larger food particles (Flannagan *et al.,* 2009).

Living organisms are subtyped into two super kingdoms: prokaryotes and eukaryotes; The eukaryotes are divided into five kingdoms: animalia, plantae, fungi, chromista and protista (Ruggiero *et al.,* 2015). Amoebozoa is classified as a phylum

in the Protozoa subkingdom within the Protista kingdom, it has a characteristic ability to change its shape by forming projections called pseudopodia, and all amoebae share a common amoeboid motion (Singleton and Sainsbury 2006).

1.2 Amoebic Discovery History

In 1875, Lösch described the relationship between *Entamoeba* and chronic dysentery in a young farmer (Lesh,1875). In 1899, Schadinger correlated the clinical symptoms of a patient with dysentery with a flagellate amoeba he isolated from the patient's stool and named it *Amoeba gruberi* (Martinez and Visvesvara 1997). In 1903, Schaudinn stated that the underlying cause of chronic dysentery is the parasite *Entamoeba histolytica* (Martinez and Visvesvara 1997).

In 1909, Kurt Naegler reported that *Amoeba gruberi* is a harmless amoeba and renamed it *Naegleria gruberi* (Martinez and Visvesvara 1997). In 1930, *Acanthamoeba* was discovered as a contamination of a yeast culture of *Cryptococcus pararoseus* by the British/Italian scientist Sir Aldo Castellani who classified the organism in genus *Hartmannella* and named it *Hartmannella castellanii* (Castellani 1930; Douglas 1930; Volkonsky 1931), however the new classification has classified *Hartmannella* and *Acanthamoeba* as separate genera (Martinez and Visvesvara 1997).

During the development of the polio vaccine Clyde Culbertson reported the pathogenic effect of *Acanthamoeba* on monkey kidney cells at the Eli Lily Laboratory in Indianapolis, USA. This contamination was the first time that the free-living

amoeba *Acanthamoeba* was reported to exhibit a pathogenic effect (Culbertson *et al.,*1958) and Singh named it *Acanthamoeba culbertsoni* (Singh and Das 1970).

In 1972, the first case of Granulomatous Amoebic encephalitis (GAE) in humans was discovered by Jager and Stamm. In 1974, Naginton reported the first published case of *Acanthamoeba* keratitis in a healthy schoolteacher who had been complaining of blurred vision with no prior eye trauma, his symptoms worsened over a period of six weeks and a ring infiltrate formed around the cornea which ended up with ulceration resistant to conventional treatment. The second case was a farmer with a history of eye trauma who started to complain from pain in his eye then developed a painful ring abscess surrounding the cornea which was refractory to treatment. The histology sections for the cornea of both patients showed heavy infiltration of *Acanthamoeba* cysts (Naginton *et al.,* 1974).

The pathogenic types of free-living amoeba are the most significant to study because of their relevance and implications on human health. *Acanthamoeba* species cause keratitis and GAE, *Naegleria fowleri* causes primary amoebic meningoencephalitis (PAM) in children and adults, *Sappinia diploidea* is known to cause brain infection (Visvesvara *et al.,*1990, Visvesvara *et al*.,2007), *Balamuthia mandrillaris* causes skin and lung infections and lethal encephalitis in young patients and it was first isolated from a mandrill baboon that died at the San Diego Zoo Park in California in 1986 with the first human infection reported in 1990, and the name Balamuthia was given by Visvesvara after his mentor, parasitologist William Balamuth in recognition of his contribution to the field of studying amoeba (Kaneshiro *et al.,*2014).

1.3 *Acanthamoeba*: Trophozoite Stage

Acanthamoeba is a virtually ubiquitous free-living amoeba with a life cycle characterized by a phenotypic switch between the trophozoite (active) stage and the cyst (dormant) stage. The trophozoite stage is the active, feeding and replicating stage where the organism moves by contraction of protoplasmic tooth-like projections called acanthopodia which are 1-2 μm in diameter that extend several microns from the amoeba and are formed of hyaline cytoplasm (Bowers and Korn, 1968) giving the trophozoite its characteristic 'thorny' appearance (acanthus is Latin for thorny-like) (Figure 1.1).

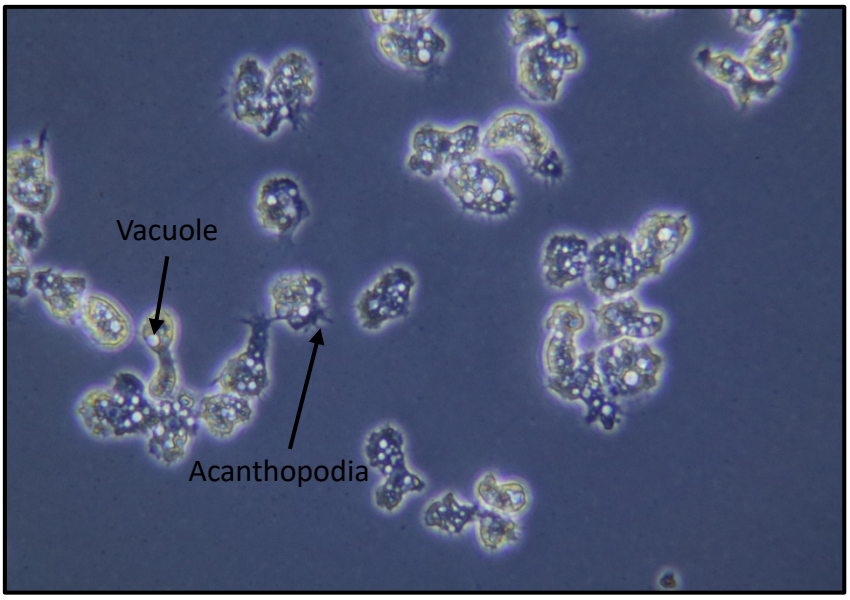

Figure 1.1:Trophozoite stage of *Acanthamoeba castellanii* (ATCC 50370) demonstrating contractile vacuoles and acanthopodia at 200X.

The average size of trophozoites ranges from 25 μm to 40 μm (Marciano-Cabral and Cabral 2003). It is composed of a plasma membrane formed of two layers of phospholipids and embedded proteins, and the cytoplasm and the organelles within

that include mitochondria, a network of rough endoplasmic reticulum, contractile vacuoles which control the concentration of water inside the cell by their contractile ability that expels extra water out of cell, food vacuoles scattered throughout the cytoplasm which form after ingestion of food material , and a central nucleus that contains a large nucleolus (Marciano-Cabral and Cabral 2003).

The plasma membrane consists of proteins, phospholipids, sterols and lipophysphoglycan (Dearborn and Kornl 1974). The lipophosphoglycan component forms 31% of the cell membrane of *Acanthamoeba* and 14% of the lipophosphonoglycan of the *Acanthamoeba* plasma membrane is formed of classes of long chain fatty acids as saturated, unsaturated and branched (Korn *et al.,*1974).

Acanthamoeba grows and replicates by mitosis (Neelam and Niederkorn 2017), and feeds on organic matter such as algae, yeast and bacteria (Marciano-Cabral and Cabral 2003). When feeding on bacteria in monoxenic culture, *Acanthamoeba* trophozoites feed on both gram-negative bacilli (including *Escherichia coli, Enterobacter aerogenes*) and gram-positive bacteria like *Staphylococcus epidermis* (Marciano-Cabral and Cabral 2003). It can also be grown axenically in Peptone Yeast Glucose extract (PYG) medium consisting of 2% proteose peptone, 0.2% yeast extract and 0.1% M glucose (Marciano-Cabral and Cabral, 2003) which was first described by Neff (Neff, 1957). *Acanthamoeba castellanii* can grow and replicate in media containing amino acids, vitamins and any carbon sources or salts (Byers *et al.,*1980).

1.4 *Acanthamoeba*: Cyst Stage

The cyst is smaller than the trophozoite and is approximately 12-20 μm in diameter depending on the species. In this stage, *Acanthamoeba* is mitotically inactive securing itself within a tough cyst wall to survive difficult environmental conditions (Figure 1.2). The alterations to ribonucleic acid (RNA), proteins, lipids and glycogen during the encystment process lead to a decline in cellular volume and weight (Weisman 1976) as the encystment process completes. *Acanthamoeba castellanii* has a specific amount of cAMP that increases two- to threefold before starting to decline when cyst formation starts, cAMP helps in glycogen breakdown by activating glycogen phosphorylase and changing glycogen synthase to the less-active glucose 6-phosphate-dependent form, a mechanism that may account for glycogen degradation in the encystment stage (Weisman 1976).

Cellulose is mainly detected in the cyst stage; it is fibrous in nature and its rigidity and high tensile strength explains its presence in many rigid cell walls like the cyst stage (Weisman,1976). The dormant cyst stage is responsible of the ubiquity of *Acanthamoeba* due to its ability to respond to adverse environmental conditions such as extremes of temperature, change in pH, starvation and change in osmolarity (Page 1988). *Acanthamoeba castellanii* trophozoite has a surface receptor called 'Encystment Stimulating Protein' (ESP) that initiates the encystment process after binding to its natural ligand in the environment which could be an antibody on the target cell and the trophozoite remains encysted as long as this binding is present (Yang and Villemez,1994). ESP is an osmolarity receptor which increases its binding affinity as the osmolarity increases (Cordingley *et al.,*1996).

The cysts are resistant to chemicals, repeated cycles of freeze-thawing (Neelam and Niederkorn 2017) and chlorinated water (Dawson and Brown 1987). *Acanthamoeba culbertsoni* survives after 3 hours of exposure to concentrations more than 40 µg/mL chlorine in swimming pools (De Jonckheere,1991), however the cyst is killed by moist heat, 3 minutes of microwave irradiation, and 15 minutes cycle of ultraviolet irradiation (De Jonckheere,1991).

The cyst has a double wall structure, the outer layer (ectocyst) contains polysaccharides, and the inner layer (endocyst) is made of cellulose (Weisman 1976, Neff *et al.*, 1964a). At periodic intervals, the endocyst and ectocyst come in contact together forming points called ostioles and the cytoplasm bulges at these points to be closer to the outside of the cyst (Bowers and Korn, 1968). The centre of this specific area is called the operculum (Bowers and Korn, 1968), and *Acanthamoeba* excysts through this pore leaving behind an empty cyst (Stratford and Griffiths, 1978).

In laboratory, encystation process is initiated by using a medium composed of many compounds like NaCl, KCl, MgSO4 ,$NaHCO_3$, $CaCl_2$, and Neff`s constant- pH encystment medium containing magnesium, chloride and amine buffer at pH 8.9-9 (Hughes *et al.,*2001; Khunkitti *et al.,*1998; Neff *et al.,*1964) or through starvation and depletion of bacterial food source by culturing trophozoites on non-nutrient agar (NNA) seeded with *Escherichia Coli*, or in axenic medium for 6 weeks or more (Hughes *et al.,*2001; Buck and Rosenthal 1996; Page 1988).

Acanthamoeba encystment can also be stimulated by taurine or catecholamines including epinephrine and norepinephrine (Srivastava *et al.,*1983, Verma *et al.,*1974). Activation of the encystment process using epinephrine is facilitated by a

receptor that induces cAMP synthesis (Murti,1984) which has the capability of initiating encystment (Raizada and Murti 1972).

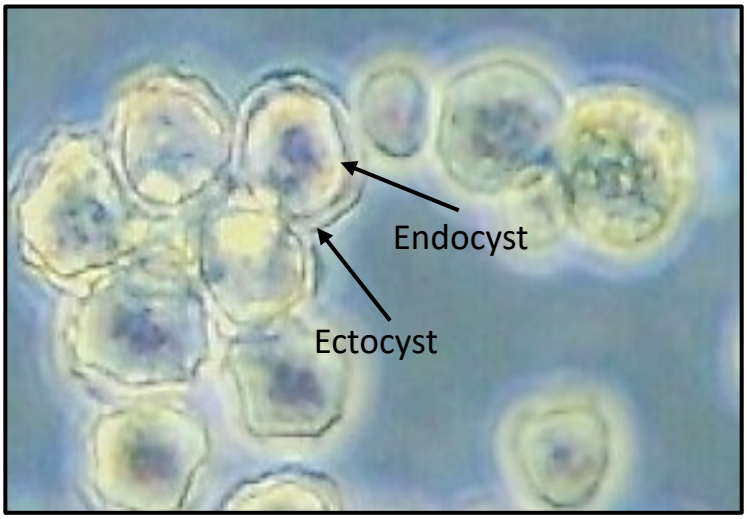

Figure 1.2: Mature cysts of *Acanthamoeba castellanii* demonstrating endocyst and ectosyst at 400X.

1.5 *Acanthamoeba* Feeding

Acanthamoeba feeds through a range of engulfment methods such as pinocytosis and phagocytosis (Allen and Dawidowicz 1990, Alsam 2005). The pinocytosis process is nonspecific and depends on membrane invagination to engulf large amounts of liquid and small particles (Bowers and Olszewski 1972) while phagocytosis is a direct ingestion of large food particles by enveloping them in vacuoles using a receptor dependent process (Khan 2006). *Acanthamoeba* has the ability to distinguish between digestible and nondigestible content by digesting the former and expelling the latter out of the cell (Bowers and Olszewski 1972). Feeding depends primarily on formation of food cup mainly on the posterior end of

Acanthamoeba (Page ,1967). The food cup (Figure 1.3) is part of the cell wall that projects out to take bacteria, yeast, and cellular debris (Marciano-Cabral and Cabral, 2003).

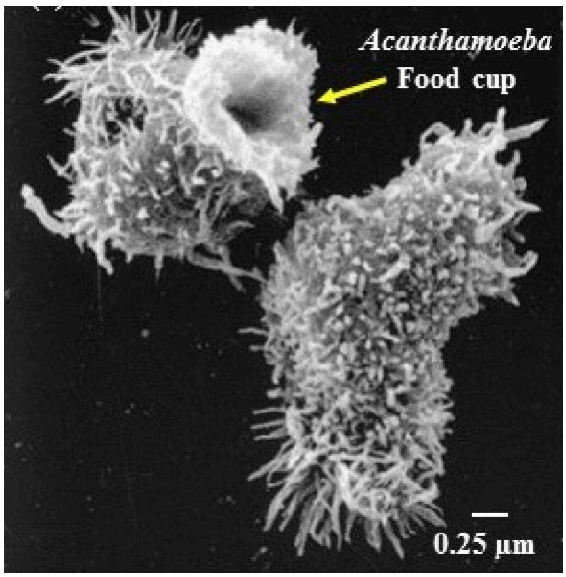

Figure 1.3: Scanning electron microscope of *Acanthamoeba* trophozoites showing the food cup (Banjo, 2018).

1.6 *Acanthamoeba* Distribution

Acanthamoeba is distributed worldwide, as it is considered one of the most prevalent protozoa in the environment which can be found in natural and artificial areas, such as soil, drinking water, water wash bottles, deep ocean bottom, cooling water of nuclear power plants, swimming pools (Carnt *et al.,*2020, Lorenzo-Morales *et al.,*2015, Taravaud,2017), air conditioning units, dental treatments units, dialysis units, contact lenses, lens care products, contamination in tissue culture (Marciano-Cabral and Cabral 2000) hot tubs, ventilation ducts and eye wash stations (Niederkorn *et al.,*1999). *Acanthamoeba* are also frequently isolated from tap water

in houses with a variation between seasons ranging from 27.9% during the winter period to 29.6% over summer (Carnt *et al.,*2020). It is thus obvious that human beings regularly encounter and interact with this organism.

1.7 *Acanthamoeba* Classification

Acanthamoeba is a eukaryote organism of the Protozoa Subkingdom within the Protista kingdom (Martinez and Visvesvara, 1997). It is a member of the Rhizopodia Superclass that contains Genera *Entamoeba*, *Hartmannella*, *Naegleria*, *Vahlkampfia*, and *Balamuthia* (Martinez and Visvesvara,1997). Extensive research has been conducted to study *Acanthamoeba* since its discovery by Castellani in 1930 in a culture of the yeast *Cryptococcus pararoseus* (Castellani 1930) which was initially classified under genus *Hartmannella* and called *Hartmannella Castellanii* (Castellani 1930, Douglas 1930), and this classification was modified one year later when Volkonsky found that the genus *Hartmannella* was in fact a different group of amoebae that has its distinctive features.

In 1931, Volkonsky divided *Hartmannella* into 3 groups: Group 1 was named *Hartmannella* which is characterized by a rounded smooth cyst wall and cylindrical spindle, group 2 named *Glaeseria* characterized by nuclear division in the cyst, and group 3 named *Acanthamoeba* and has double walled cyst with irregular outer layer and pointed spindles during mitosis.

In 1952, Singh stated that it was unreliable to classify amoeba based on morphology and mitotic spindle shape so the genus *Acanthamoeba* was dropped. In 1966, Pussard endorsed the fact that the mitotic spindle shape was not helpful, however he disagreed with the futility of using cyst morphology to differentiate between

various species at the level of genera and thus renowned the genus *Acanthamoeba* which was acknowledged again by Page in 1967 (Pussard and Pons 1977).

In 1976, Page differentiated between *Acanthamoeba castellanii* and *Acanthamoeba polyphaga* based on the degree of contact between the layers of the cyst wall and how smooth or wrinkled the cyst wall is (Stratford and Griffiths 1978). Pussard and Pons divided *Acanthamoeba* into three groups depending on cyst morphology (Table 1.1) identifying 18 different species of *Acanthamoeba*. Group 1 includes: *Acanthamoeba Astronyx*, *Acanthamoeba Comandori*, *Acanthamoeba Echinulata* and *Acanthamoeba Tubiashi*. This group has a cyst diameter of 18-25 μm and both ectocyst and endocyst are wildly separated with a smooth stellate inner layer (Pussard and Pons 1977, Marciani-Cabral and Cabral 2003). Group 2 constitutes the most widespread *Acanthamoeba* and includes: *Acanthamoeba Castellanii*, *Acanthamoeba Polyphaga* and *Acanthamoeba Rhysodes*. The cyst diameter is less than 18 μm and endocyst and ectocyst can either be separated or in close proximity to each other. Group 3 includes: *Acanthamoeba culbertsoni* and *Acanthamoeba Pustulosa*, with a cyst diameter of almost 18 μm and a thin ectocyst. Groups 2 and 3 are pathogenic, while group 1 is nonpathogenic (Pussard and Pons 1977; Gast *et al.,*1996; Walochnik *et al.,*2000b; Walochnik *et al.,*2003).

Sawyer discovered that the ionic strength of the growth medium can change the morphology of cyst walls, which rendered the previous classification uncertain (Stothard *et al.,*1998). In 1978, Stratford and Griffenns stated that cyst morphology is not a reliable classification criterion as it can change depending to the surrounding environmental conditions.

Group I	
A. astronyxis	*A. comantioni*
A. tubiashi	*A. echinulata*
Group II	
A. castellanii	*A. mauritaniensis*
A. polyphaga	*A. lug-dunensis*
A. quina	*A. rhysodes*
A. divionensis	*A. paradivionensis*
A.griffini	*A. triangularis*
A. hatchetti	
Group III	
A. palestinensis	*A. culbertsoni*
A. lenticulata	*A. pustulosa*
A. royreba	

Table 1.1: Classification of *Acanthamoeba* based on morphology (Xuguang Sun *et al.,* 2018)

1.7.1 Genetic Grouping

The genome size of *Acanthamoeba* is around $1X10^8$ base pairs (Byers *et al.,*1990) and it has 24 copies of 18s ribosomal RNA (Yang *et al.,*1994), and the ploidy is between 9 and 25 depending on the stage of the cell cycle and the strain (Matsunaga *et al.,*1998, Rimm *et al.,*1988). This difference may be attributed to the

destruction of part of the DNA during the encystment (Byers *et al.,*1991). In 1996, T-typing classification of *Acanthamoeba* was introduced by Gast *et al.* based on 18s ribosomal RNA sequence, to overcome the restrictions of cyst morphological characteristic classification. Four genotypes were identified based on sequences of nuclear small ribosomal subunits RNA genes and were named T1, T2, T3, T4 (Gast *et al.,*1996). *Acanthamoeba* genotypes vary by less than 5% depending on 18s ribosomal RNA sequence (Stothard *et al.,*1998).

Acanthamoeba is currently classified into 20 different genotypes T1-T20 (Table 1.2) based on ribosomal RNA sequence (Schuster and Visvesvara 2004; Corsaro and Venditti 2010; Horn *et al.,*1999; Magnet *et al.,*2014). A research in 2005 suggested to further subdivide T2 into T2a, T2b to help recognizing and differentiating pathogenic from non-pathogenic genus (Maghsood *et al.,*2005). Groups T3, T4, T6 comprise the majority of pathogenic strains (Stothaed *et al.,*1998; Walochnik *et al.,*2000) as T4 genotype is responsible for 90% of keratitis, granulomatous Acanthamoeba encephalitis and cutaneous infection (Maghsood *et al.,*2005).

Morphology groups	Genotypes
Group I	T7, T8, T9, T17
Group II, III	T1-T6, T10-T16

Table 1.2: Morphology groups and genotypes of *Acanthamoeba* based on 18s ribosomal RNA sequence (Xuguang Sun *et al.,* 2018)

1.8 *Acanthamoeba* as a Reservoir for Other Microorganisms

Some bacteria, viruses and fungi can grow and survive inside the free-living amoeba (Greub and Raoult, 2004). Endosymbiont is a term used when two non-related microorganisms co-exist where one of them lives inside the other (Figure 1.4). *Acanthamoeba* is shown to act as a reservoir for bacteria (Drozanski, 1956) and pathogenic facultative mycobacteria such as *Mycobacterium avium*, *Mycobacterium marinum, Mycobacterium simiae, Mycobacterium phlei, Mycobacterium smegmatis and Mycobacterium fortuitum* (Krishna-Prasad and Gupta, 1978). *Burkholderia cepacia* was seen in different *in vitro* strains of *Acanthamoeba* (Marolda *et al.,*1999), *Legionella* was detected in vesicles of trophozoites and within the cysts of *Acanthamoeba astronyxis* cultured *in vitro* (Marciano-Cabral and Cabral 2000) and it was demonstrated that Mimivirus uses *Acanthamoeba polyphaga* as a natural host to survive (Ghedin and Claverie 2005).

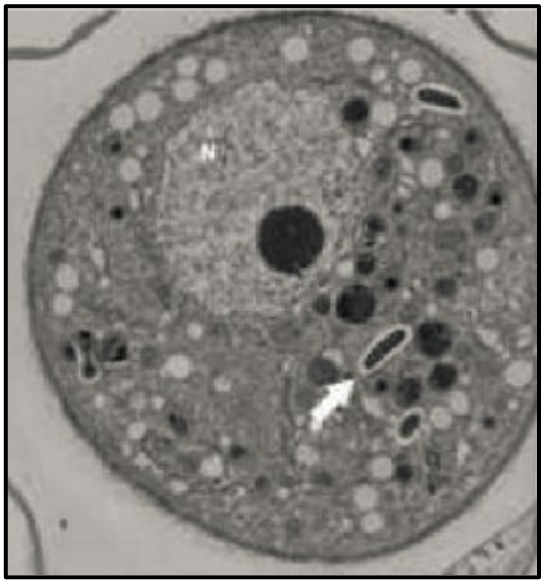

Figure 1.4: Transmission electron microscopy image of *Acanthamoeba* cyst containing *Legionella* (arrow) (Miller *et al.,*2012).

1.9 Pathogenicity of *Acanthamoeba*

The pathogenicity of *Acanthamoeba* is initiated by the adhesion step where the mannose binding proteins on the plasma membrane of the *Acanthamoeba* interact with the carbohydrate mannose residues in the host cell membrane to firmly attach the *Acanthamoeba* to the infected tissue and avoid being cleared during the disease onset (Huth *et al.,*2017). This binding initiates the release of metallo and cysteine proteases that digest extracellular targets (Cao *et al.,*1998) and also stimulates *Acanthamoeba* to secrete a mannose-induced 133 kDa protease (MIP-133) that interacts with the plasma membrane of the target cells leading to activation of cytosolic phospholipase A2 leading to cell damage (Tripathi *et al.,* 2012).

Acanthamoeba binds to target cells by using acanthopodia after the formation of a structure called an amoebastome, then invades the membrane of the target cell, with many studies reporting that *Acanthamoeba* cannot attach to the tissue without acanthopodia demonstrating the critical role of these structures in the pathogenicity of *Acanthamoeba* (Khan *et al.,*2001). The target cells are engulfed by the phagocytosis process which facilitates infection and cause further invasion and damage of the tissue by the proteolytic enzymes leading to apoptosis and necrosis of the infected cells (Niederkorn *et al.,*1999).

1.9.1 Granulomatous Amoebic Encephalitis (GAE)

GAE is a chronic slowly progressive disease of the central nervous system (CNS) mostly caused by *Acanthamoeba* genotype T4 (Walochnik ,2014) which was first identified by Jager and Stamm in 1972 (Willaert *et al.,*1978). It is characterized by granulomatous encephalitis mostly affecting immunocompromised individuals such as patients with malignancies, systemic lupus erythematosus, diabetes mellitus, liver cirrhosis and acquired immunodeficiency syndrome. Granulomatous response is seen in several tissues including skin, liver, kidney, adrenal, pancreas, prostate, lymph nodes and bone marrow (Khan 2006), and may also involve the lungs (Marciano-Cabral and Cabral 2003).

There are many risk factors for GAE such as alcohol dependence, drug abuse, chemotherapy and organ transplant, all of which suppress immunity (Marciano-Cabral and Cabral 2003). GAE is different from amoebic meningeo-encephalitis which is a fast-progressing disease that affects healthy and debleated patients and is caused by the free-living amoeba *Naegleria fowleri* that enters the central nervous system via olfactory neuroepithelium causing hemorrhagic meninigo-encephalitis (Butt, 1966; Valenzela *et al.,*1984).

The entry of *Acanthamoeba* to the human body is by inhalation or via skin lesions then by hematogenous spread (Martinez & Visvesvara, 1997) as shown in Figure 1.5. The disease progresses within weeks or months to exhibit clinical signs and symptoms of headache, nausea, vomiting, fever, neck stiffness, increased intracranial pressure, Seizure, diplopia and coma (Martinez *et al.,*1980). Postmortem examination reveals many pathological findings including necrosis, thrombus formation and inflammation with the majority of lesions found in the basal ganglia, mid-brain, brainstem and cerebral hemispheres (Khan, 2006).

The diagnosis is difficult to establish as it requires ruling out other pathogens like viruses, bacteria and fungi which are more common to cause CNS infections. Cerebrospinal fluid findings include lymphocytosis, increase protein concentration and decrease glucose concentration (Marciano-Cabral and Cabral 2000). Treatment is difficult due to *Acanthamoeba* resistance and the inability of the drug to pass through the blood brain barrier into the CNS. This fatal disease has a mortality rate of more than 90% despite aggressive treatment with different combinations of drugs such as amphotericin B, rifampicin, pentamidine, pyrimethamine, ketoconazole, voriconazole or clotrimazole (Taravaud *et al.,*2017; Siddiqui *et al.,*2016; Ong *et al.,*2017), with amphotericin B being the most widely used medication for treatment of GAE (Siddiqui *et al.,*2016; Ong *et al.,*2017).

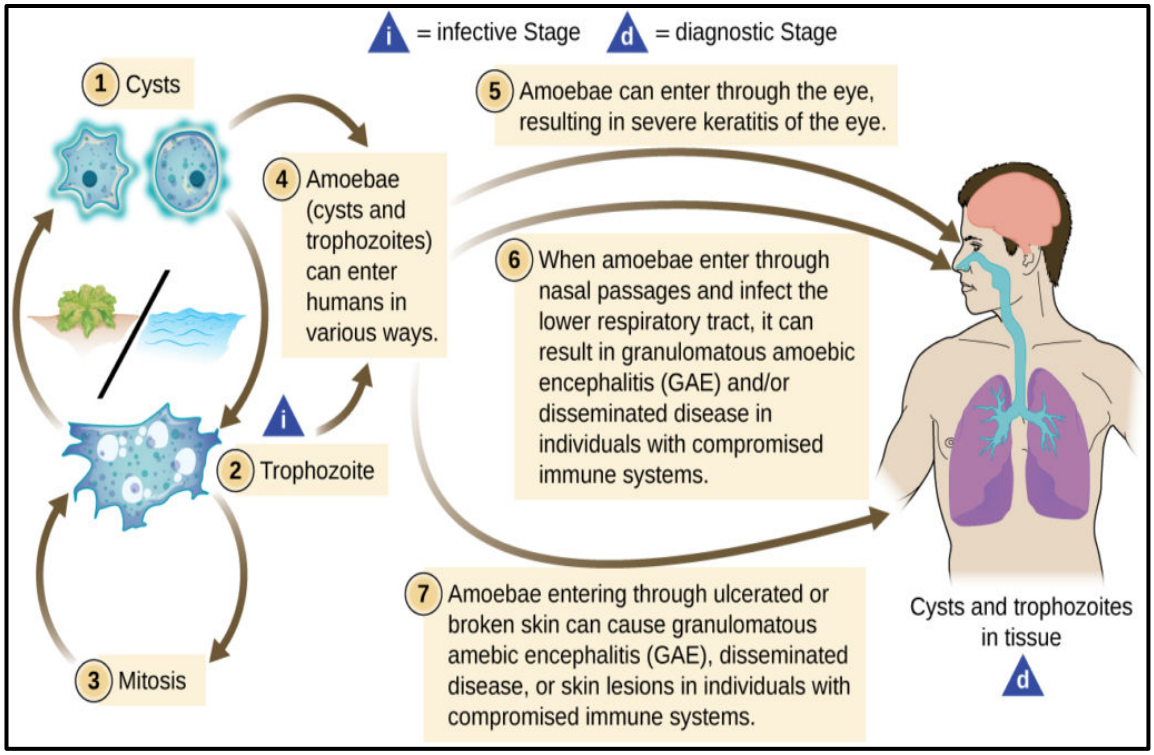

Figure 1.5: Life cycle of *Acanthamoeba* in environment and human body, credit: modification of work by Centers for Disease Control and Prevention.

1.9.2 Acanthamoeba Keratitis (AK)

Acanthamoeba keratitis is a progressive infection caused by pathogenic *Acanthamoeba* strains mostly T4 genotype (Maghsood *et al.,*2005; Walochnik *et al.,*2014) and affects healthy immunocompetent individuals with higher prevalence in males (Niederkorn *et al.,*1999). The first eye infection caused by *Acanthamoeba* was reported in United Kingdom in a healthy young teacher in 1974 (Nagington *et al.,*1974).

Despite being a rare infection, Acanthamoeba keratitis carries serious clinical implications as it causes ulceration of the corneal epithelium, swelling of the stroma and scarring that can result in permanent blindness (Figure 1.6) (Khan, 2006). The infection is usually unilateral but can affect both eyes and the clinical symptoms are similar to herpes simplex keratitis and include eye pain, photophobia and blurred vision (Robaei *et al.,* 2014), and the common signs are ptosis and conjunctival redness without eye discharge (Niederkorn *et al.,*1999). The infection rarely extends beyond the cornea and poor prognosis is anticipated if sclero-keratitis develops or if the infection persists despite treatment (Perez-Santonja *et al.,*2003).

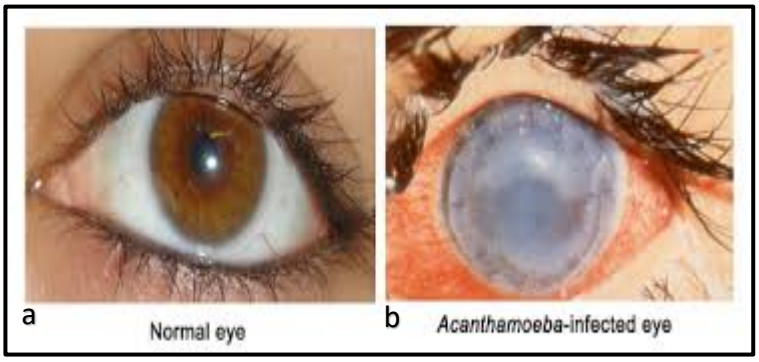

Figure 1.6: (a) Normal eye compared to (b) *Acanthamoeba*-infected eye (Siddiqui and Khan, 2012).

1.9.2.1 Pathogenesis of Acanthamoeba Keratitis

The first step in the pathogenesis of Acanthamoeba keratitis is the attachment of trophozoites to specific mannosylated glycoprotein receptors at the corneal epithelium inducing the release of MIP133 and initiating a cascade of cytolytic processes including the production of proteases leading to destruction to Bowman's membrane and deep penetration and dissolution of corneal structures but rarely beyond the stroma as shown in Figure 1.7 (Clarke and Niederkorn, 2006).

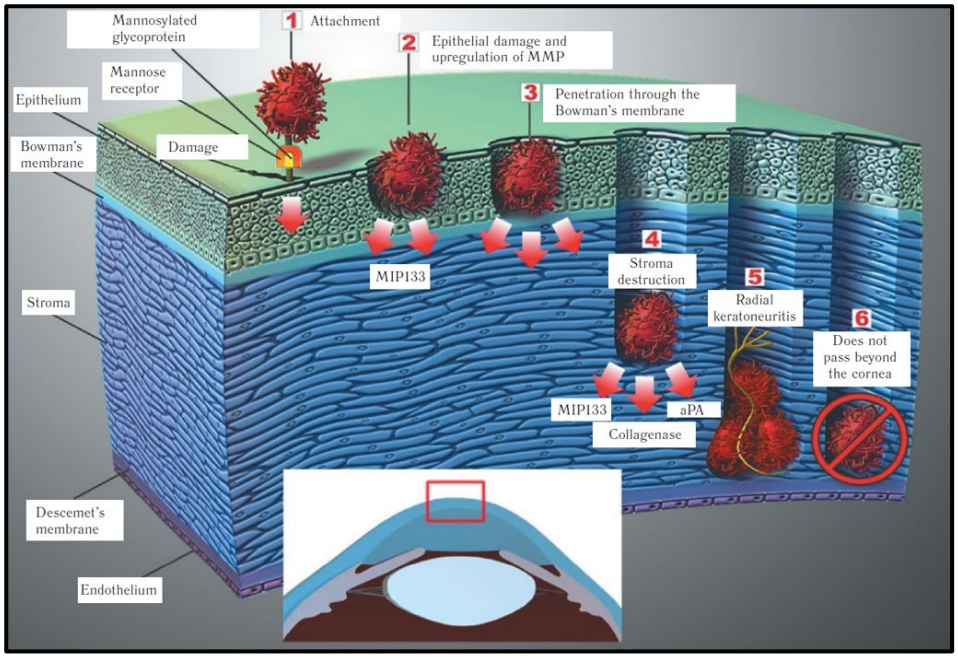

Figure 1.7: The pathogenesis of Acanthamoeba keratitis (Clarke, Niederkorn,2006). Step (1): trophozoites attach to mannosylated glycoproteins at corneal epithelium following abrasion. Step (2): trophozoites induce the release of MIP133 following mannose exposure. Step (3): destruction of Bowman's membrane and trophozoites penetrate stroma. Step (4): trophozoites produce proteases that dissolute corneal stroma. Step (5): trophozoites aggregate around corneal nerves, causing radial keratoneuritis. Step (6): AK rarely progresses beyond the corneal endothelium.

1.9.2.2 Risk Factors

The most common risk factors for developing Acanthamoeba keratitis are the use of contact lenses and poor lens hygiene (Carnt *et al.,*2020),the use of Oxipol disinfection which is an agonist combination of cleaning, disinfecting and lubricating agents, poor hand hygiene and the use of contact lenses while swimming or bathing (Pinna *et al.,*2017; Carnt and Stapelton 2016; Page and Mathers 2013, Carnt *et al.,*2018). *Acanthamoeba* is the most common agent of contact lens-related keratitis in addition to Pseudomonads and Staphylococci (Walochnik *et al.,*2004). The frequent use of contact lenses causes abrasion and microtrauma to the corneal epithelium which is noted more in soft contact lenses as they have more adherent surfaces than hard lenses increasing the probability of the attachment of trophozoites to the corneal epithelium (Maycock and Jayaswal 2016) increasing the incidence of the disease over the past 3 decades as a result of the climbing use of contact lenses.

1.9.2.3 Incidence

The incidence of Acanthamoeba keratitis in developed countries is 1 to 33 cases/1,000,000 contact lens wearer per year, in the United Kingdom it is reported as 1.4 cases/1,000,000 persons per year (Pinna *et al.,*2017). The current surge in cases of Acanthamoeba keratitis started in 2010–2011 with a threefold increase compared to the years 2004–2009 (Carnt *et al.,*2018). A recent study conducted over 12 years took place in a tertiary UK hospital covering 1500 keratitis cases reported an incidence rate for *Acanthamoeba* keratitis of around 2.3% (Tan *et al.,*2017). Acanthamoeba keratitis should be considered as a possible cause of keratitis in all contact lens wearers and any case of corneal trauma (Cohen *al.* 1985),

and effective disinfection of contact lenses is crucial to eliminate the risk of *Acanthamoeba* keratitis (Radford *et al.,*1995).

Since the cyst stage of *Acanthamoeba* can resist unfavourable conditions and drugs, this might lead to a delay in diagnosis and difficulty in treating the illness leading to further complications including severe extra-corneal inflammation (Robaei *et al.,*2014) along with recurrence of infection. In the first stages of the infection, AK can be missed and confused with Herpes simplex keratitis and as the disease advances the infection attains a similar clinical picture of fungal keratitis (Carnt *et al.,*2018) which further delays correct diagnosis and treatment which profoundly impacts the prognosis with poorer visual outcome in these patients and prolonged duration of treatment, increased incidence of corneal perforation and increase in the number of cases requiring penetrating keratoplasty (Carnt *et al.,*2018). Early and accurate diagnosis is fundamental to initiate the most effective therapy, ideally introduced within 3 weeks for a better prognosis (Kovacevic *et al.,*2008; Claerhout *et al.,*2004).

1.9.2.4 Contact Lens Disinfection

Most cases of AK occur in wearers of soft contact lenses, so a good lens hygiene is crucial to prevent the infection (Carnt *et al.,*2020). There are two main groups of lens disinfectants: one group contains hydrogen peroxide and the other group contains polyhexamethylene biguanide (PHMB) or myristamidopropyl dimethylamine (MAPD), however there are no agreed standards of evaluating the efficacy of contact lens solutions (Buck *et al.*, 1998, Hughes *et al.*, 2003b).

1.9.2.5 Diagnosis of *Acanthamoeba* Keratitis

Acanthamoeba keratitis should be suspected in patients with a history of contact lens use with exposure to contaminated water, symptoms of severe pain in the affected eye and negative laboratory cultures for bacterial, viral and fungal especially if there is no clinical improvement following antimicrobial therapy (Moshirfar *et al.,* 2006). There are many laboratory techniques used to diagnose AK such as culture of corneal scraping where samples are obtained by scraping the corneal surface then the sample is cultured in appropriate culture media and examined for growth of *Acanthamoeba*. Another method for diagnosing AK is corneal biopsy which is reliable but invasive (Page and Mathers 2013) and must involve the active edge and base of the corneal ulcer.

After either scraping the cornea or taking a biopsy, the sample is inoculated on *E. coli* on non-nutrient agar or buffered charcoal-yeast extract agar (Hau *et al.,*2010) and the *Acanthamoeba* cyst can be visualized using Gram's and Giemsa stains or Calcofluor white stain with fluorescent microscope. Corneal culture takes 21 days and has low sensitivity of 50% misdiagnosed cases (Rusciano *et al.,* 2013) as the positive culture rate ranges between 31 to 55% (Goh ,2018, Tu, 2008).

In vivo confocal microscopy (IVCM) is used to detect cysts and trophozoites in corneal tissue and the diagnostic criteria of Acanthamoeba keratitis include the recognition of specific cystic and trophozoite-like structures with single file presentation and clustering of cystic objects as a reliable predictor of poor visual outcome (De Craene 2018, Chopra 2020). Confocal microscopy examination is effective in detecting organisms deeply located within the cornea that are difficult to be sampled by scraping and also provides a tool for prognostication based on the confocal microscopy findings as the presence of clusters or chains of cysts is

associated with poor prognosis (Garg *et al.,*2017). Nevertheless, the accuracy of this method is highly dependent on the experience of the observer (Hau *et al.,*2010).

Impression cytology is a non-invasive technique used to diagnose superficial ocular surface infection by applying a cellulose acetate filter to the corneal surface to remove the superficial layers of the epithelium, then performing histological immune-histochemical stains and molecular analysis (Singh *et al.,*2005). Polymerase chain reaction (PCR) is another method used to detect *Acanthamoeba* DNA in corneal scrapping and tears (Mathers *et al.,*2000). PCR is quick, sensitive, and specific compared to corneal culture (Pasricha *et al.,*2003; Zamfir *et al.,*2006; Thompson *et al.,*2008; Niyyati *et al.,*2009), can detect as few as five cells (Khan *et al.,*2001) and can be used without prior culture (Gast ,2001).

1.9.2.6 Treatment of Acanthamoeba Keratitis

There is no licensed pharmacological treatment for Acanthamoeba keratitis, and the current unlicensed therapy is based on individual cases which is a topical therapy of either polyhexamethylene biguanide (PHMB) 0.02% (v/v) or chlorhexidine digluconate 0.02% (v/v) as a single therapy or in combination with propamidine isetionate (Brolene™) 0.1% (w/v) or hexamidine diisethionate (Desomedine®) 0.1% (w/v) (Papa *et al.,*2020).

PHMB is a sterilizing agent for contact lenses that reacts with the cytoplasmic membrane leading to cellular leakage (Ikeda *et al.,*1984) and depression of respiratory enzymes essential for *Acanthamoeba* survival (Broxton *et al.,*1984; Larkin *et al.*1991). It is widely used as a disinfectant and antiseptic agent due to its

effectiveness against multiple pathogens including *Pseudomonas aeruginosa* (Hübner *et al*., 2010), *Enterococcus faecalis*, *Staphylococcus epidermidis* and *Candida albicans* (Medvedec *et al.*, 2018)

Corticosteroids comprise another pharmacological therapy for stromal infiltration at the site of infection (Azuara -Blanco *et al.,*1997) or if there is limbitis, scleritis or uveitis (Bacon *et al.,*1993), However the use of topical steroid as a monotherapy without combination with amoebicidal therapy will lead to proliferation of *Acanthamoeba* trophozoites. This is clinically significant especially when steroids are used as a monotherapy in patients not correctly diagnosed with AK where steroids were prescribed to alleviate corneal inflammation and uveitis which leads to proliferation and disease progression (McClellan *et al.,*2001).

1.9.2.7 Surgical Treatment

A delay in the diagnosis and treatment of *Acanthamoeba* keratitis leads to corneal destruction and progression of the infection which may ultimately require surgical interventions such as penetrating keratoplasty (Figure 1.8) which is a full-thickness removal of the patient's cornea, followed by placement of a full-thickness donor corneal graft (Donaghy *et al.,* 2015).

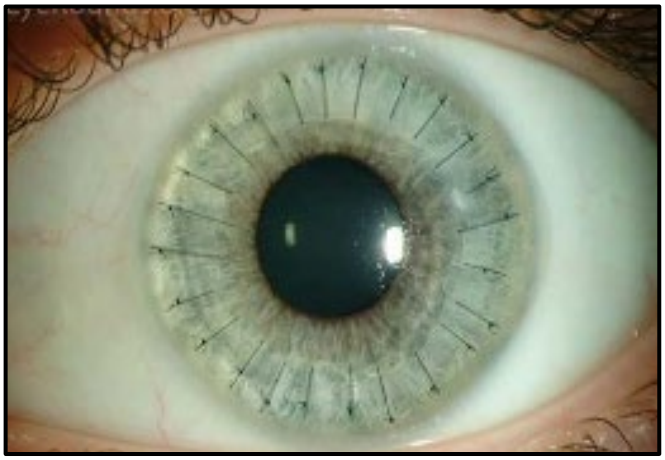

Figure 1.8: Penetrating keratoplasty: full thickness donor graft placed using interrupted sutures in radial distribution (Donaghy *et al.,*2015)

Penetrating keratoplasty is used in special circumstances such as severe scarring, increase in the size of the corneal abscess, severe eye pain, corneal perforation (Zhong *et al.,*2017) and failure of medical treatment (Robaei *et al.,*2014). This procedure includes the excision of all infected tissue to decrease the chance of graft reinfection and the need for subsequent re-grafting of the cornea and should be deferred to a minimum of 6 months from complete healing to reduce any risk of rejection (Donaghy *et al.,*2015).

1.10 Overview of the Immune System

The immune system plays a significant role in protecting the body against endogenous and exogenous toxins and microorganisms including bacteria, viruses and parasites (Foligne *et al.,*2007). The immune system has two response systems: innate and adaptive.

The innate system recognizes pathogens such as bacteria, fungi, viruses and parasites by pattern recognition receptors (PRRs), and this recognition step is vital for the innate system to provide protection against pathogens by recruitment and proliferation of immune cells, secretion of proinflammatory cytokines, and phagocytosis of pathogens (Schroecksnadel *et al.,*2011). The phagocyte system is composed of three major cell types: monocytes, macrophages and dendritic cells. Monocytes and macrophages have a crucial role in innate immunity and response to pathogens by phagocytosis, secretion of reactive oxygen species, cytokines and chemokines while dendritic cells present antigens to the cells of the adaptive immune system (Gordon and Tylor, 2005).

The adaptive system is more specific and has the capacity to recognize prior non self-antigens by creating memory cells for faster immune response in subsequent infections (Cousins *et al.,* 2003, Rogers *et al. ,*2003). The adaptive system has two major cell lineages: B cells which produce antibodies that bind to antigens and neutralize them or cause lysis, and T cells that interact with the pathogen and differentiate into cytotoxic T cells that ultimately lead to destruction or lysis of the pathogen (Mangan and Wahl, 1991).

The Complement system is one component of the immune system that is made of a large number of proteins and enzymes that react with each other to regulate the

production of enzymes and chemotaxins to help fighting infection (Law Ska 1995). There are three pathways to activate the complement system: the classical pathway which is directly activated by antibody or by direct binding between the pathogen surface and complement component C1q, the mannan-binding lectin that binds some encapsulated bacteria and the alternative pathway that is triggered directly on pathogen surfaces (Janeway *et al.,* 2001).

1.11 The Human Eye

The human eye is a unique and well protected organ containing many distinguished structures with specialized physiological functions (Figure 1.9). It is divided into an anterior segment that contains the cornea, limbus, conjunctiva, iris, ciliary body, aqueous humor and lens and a posterior segment composed of sclera, choroid, retina, optic nerve and vitreous humor (Patel *et al.,*2013). The cornea is the outer part of the anterior segment covering 15% of the anterior surface area of the eye (Willoughby *et al.,*2010), and it maintains the structural integrity of the eye globe, protects the eye component from injury and focuses the light into the retina without distorting the light due to its transparent and avascular nature (Willoughby *et al.,*2010).

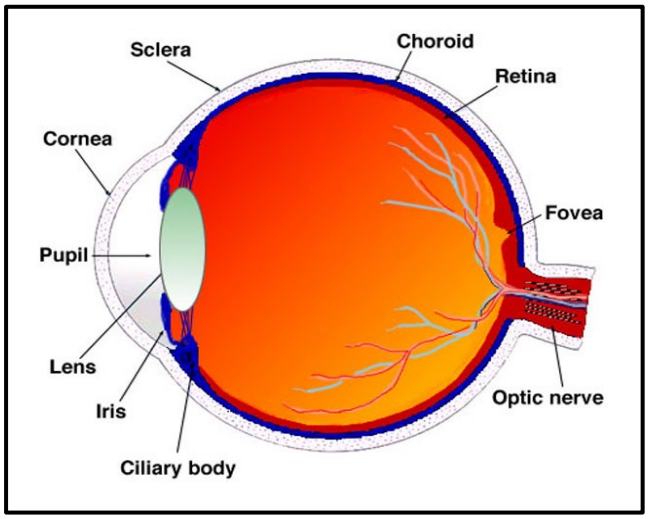

Figure 1.9: Schematic diagram of the human eye (Kolb, 2012).

The limbus is a transitional zone between the cornea and the sclera, and the epithelium of this area bridges the conjunctiva to the corneal epithelium (Snell and Lemp,1998). The limbus is the site where the stem cell niches of the corneal

epithelium are located. The conjunctiva is a translucent mucous membrane divided into palpebral, fornical and bulbar conjunctiva and plays an important function in ocular surface protection and lubrication due to its goblet cells, melanocytes and immune cells (Snell and Lemp,1998, Knop and Knop, 2007).

The cornea is composed of five layers (Figure 1.10) with the stroma being the thickest layer forming 90% of the thickness of the cornea and gives it its transparency and strength. The other layers are the epithelium, Bowmen's layer, Descement's membrane and the endothelium (Rathore and Nema, 2009).

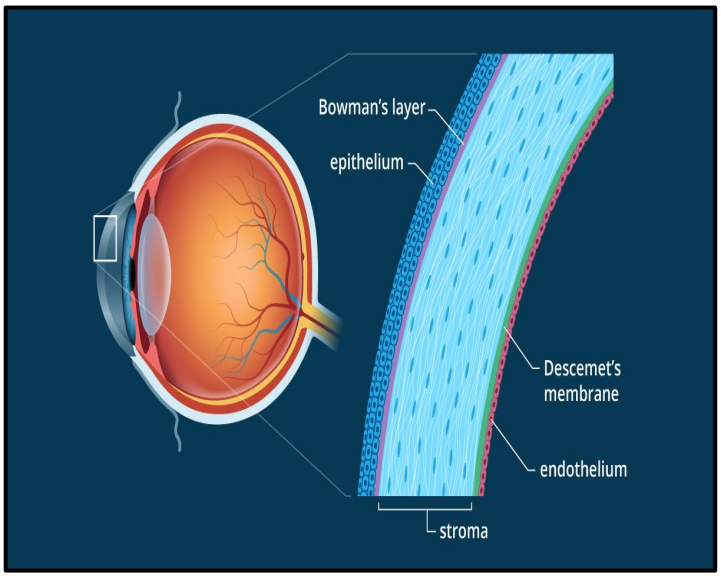

Figure 1.10: Schematic diagram of corneal layers (www.AllAboutVision.com).

1.11.1 Defense Mechanisms

The eye globe is surrounded by strong bony structures that provide external protection from injury (Snell and Lemp,1998), and the cornea is well protected from the external environment and pathogens by several mechanical, chemical and cellular defence mechanisms including blinking, lacrimation, tears enzymes,

epithelium, keratocytes, antimicrobial peptides, antigens, cytokines and inflammatory mediators (Zhou *et al.,*2000, Ruan *et al.,*2002, Choy *et al.,*2009). Corneal nerves transport the sensory stimulation which leads to reflux movement and secretion of neuropeptides that stimulate neutrophils chemotaxis following irritation of ocular surface (Muller *et al.,*1996; Tran *et al.,*2000).

Epithelial cells secrete cytokines such as Interleukin-1 (IL-1) that protect against bacteria, fungi, and enveloped viruses that may invade the cornea from ocular trauma, dust exposure or contact lens use (Mcdermott, 2004).

1.11.1.1 Tear Film

The tear film has a vital role in preventing dryness of cornea while deterring the entrance of antigens by flushing pathogens and foreign bodies from the surface through lid wiping of the tear fluid that contains immunoglobulin A (IgA) and immunoglobulin G beside other antimicrobial proteins such as lactoferrin and lysozymes (Knop and Knop 2007). IgA antibodies prevent the adhesion of *Acanthamoeba* trophozoites to the epithelial layer, however they have limited effect if trophozoites have already penetrated the cornea (Clarke and Niederkorn, 2006). The binding of *Acanthamoeba* to IgA will activate the complement system via the alternative pathway (Ferrante ,1991) which stimulates opsonization and lysis of *Acanthamoeba* (Said *et al.,*2004).

1.11.1.2 Immunological Factors

The cornea has immune privilege as it tolerates the introduction of antigens without generating an inflammatory immune response that would potentially damage its own structure and affect its function (Hong and Kaer, 1999). The cornea has no centrally located antigen presenting cells, however Langerhans cells that are peripherally located can migrate to the centre of cornea upon invasion by non-self antigens and act as antigen presenting cells (Klink *et al.*, 1997).

Acanthamoeba trophozoites are identified by Toll-like receptor-4 (TLR4), activating nuclear factor kappa B (NF-kB) and MAPK/ERK (Mitogen Activated Protein Kinases/ Extracellular Signal-Regulated Kinases) pathway which leads to the production of pro-inflammatory and chemotactic mediators such as interferon- β (IFN-β), interleukin 8 (IL-8) and tumour necrosis factor alpha (TNF-α) attracting macrophages and neutrophils to the site of injury (Ren *et al.,*2009).

The role of cells of innate immunity in protecting the ocular surface from pathogens cannot be overemphasized; Neutrophils are the main acute inflammatory cells that phagocyte pathogens (Trocme and Aldave,1994) and macrophages secrete inflammatory cytokines and have phagocytic ability to kill microbes (Underhill and Ozinsky,2002). Both cell types induce phagocytosis and lysis of *Acanthamoeba* by different mechanisms where macrophages initiate an inflammatory response by secreting macrophage inflammatory protein 2 (MIP-2) (Marciano-Cabral and Toney, 1998), and neutrophils release myeloperoxidase enzymes contained within cytoplasmic granules that once activated can destroy *Acanthamoeba* (Alizadeh *et al.*,1996).

1.12 Aims and Objectives

In this study, we will develop an *ex vivo* model of Acanthamoeba keratitis (AK) to better understand the pathophysiological processes that occur throughout the disease and to study the pathogenesis of *Acanthamoeba* and the role of cells of innate immunity in fighting the infection. The study will also evaluate the phenotypic similarities between *Acanthamoeba* and cells of the innate immune system mainly macrophages. The aims of this study are:

1. Establish an *ex vivo* model for Acanthamoeba keratitis (AK) using porcine corneas.
2. Utilise the model to investigate the pathogenesis, drug treatment and diagnosis of AK.
3. Correlate *ex vivo* confocal microscopy (EVCM) findings with *in vivo* confocal microscopy (IVCM) images from culture positive AK cases.
4. Investigate the phenotypic and functional similarities between *Acanthamoeba* and human macrophages.

1.12.1 Objectives for Aim 1: Developing *ex vivo* model

- Optimisation of methods for maintenance of corneal tissue in the lab.
- Developing different systems of corneal culture models to optimise the model integrity at gross and microscopic levels.
- Mimicking natural conditions like eye blinking using rocking system.

1.12.2 Objectives for Aim 2: Using the model to study Acanthamoeba keratitis (AK)

- Applying *Acanthamoeba* trophozoites and cysts to the corneal model to study the pathogenesis of AK.
- Evaluating the effect of macrophages and neutrophils on the progress of AK.
- Studying *in vitro* and *ex vivo* activity of a number of therapeutic compounds including doxycycline and polyhexamethylene biguanide (PHMB).

1.12.3 Objectives for Aim 3: Correlation between *ex vivo* (EVCM) and *in vivo* confocal microscopy (IVCM) findings

- Preparation of various forms of *Acanthamoeba* live and dead trophozoites and live, dead and empty cysts.
- Inoculation of the model with various forms of *Acanthamoeba*.
- Studying the model using confocal microscopy.
- Comparing EVCM findings with IVCM images of patients with AK.

1.12.4 Objectives for Aim 4: Investigating similarities between *Acanthamoeba* and human macrophages

- Differentiation of human leukemic cell line (THP-1) cell line into macrophages.
- Running a flow cytometry analysis to assess the expression of various membrane-bound antigens on both *Acanthamoeba* and macrophages.

Chapter Two

Materials and Methods

Chapter 2: Materials and Methods

2.1 Chemicals

All chemicals, materials and media used in this study were obtained from the Sigma Chemical Company Ltd and VWR International and Scientific Laboratory Supplies Ltd (UK) unless otherwise stated.

2.2 Test Organisms

The table illustrates the organisms and cell lines used in this study.

Human cell line	Strain
Human epithelial cell type 2 (HEp-2)	ECACC #86030501
THP-1 Cell	ATCC TIB-202
HL-60	ATCC CCL-240
Amoebae	Strain
Acanthamoeba polyphaga	ATCC 30461
Acanthamoeba castellanii	ATCC 50370
Acanthamoeba culbertsoni	ATCC 30171
Gram –ve bacteria	Strain
Escherichia coli (E. coli)	ATCC 8739

Table 2.1: Organisms and cell lines

Acanthamoeba castellanii (ATCC 50370), *A. polyphaga* (ATCC 30461) and *Acanthamoeba culbertsoni* (ATCC 30171) were obtained from the American Type Culture Collection (ATCC) (LGC Standards, Teddington, U.K.). The human cell line was obtained from the European Collection of Cell Cultures (PHE, Salisbury, U.K).

2.3 *Acanthamoeba* Cell Culture

The ingredients for *Acanthamoeba* trophozoites medium (Ac#6 growth medium) were based on a study by Hughes and Kilvington (2001) which is formed of 5g glucose, 0.3g potassium dihydrogen orthophosphate (KH_2PO_4), 15mg L-methionine, 10mg vitamin B_{12} and 20g biosate peptone, all in 900 mL of distilled water. The pH of the medium was modified to pH 6.5-6.6 with 1M Sodium hydroxide (NaOH) and the volume adjusted to 1000ml.The solution was then divided into four bottles with 250 mL in each and autoclaved for 15 minutes at 121°C.

Penicillin-Streptomycin was added to the medium to give a final concentration of 100 U/mL and 0.1 mg/mL respectively. The medium was kept at 25°C to be used within one month. The trophozoites were grown in tissue culture flask at 32°C.

2.4 Cryopreservation of *Acanthamoeba*

The cells were assessed using inverted microscope to confirm the absence of any contamination, then the cells were centrifuged at 500 x *g* for 5 minutes. The pellet was suspended in foetal bovine serum containing 5 % (v/v) dimethyl sulphoxide (DMSO) as freezing media. 1mL was aliquoted in each cryoprotective ampule then placed inside a passive freezer Naglene Mr Frosty filled with Propan-2-ol and placed in a -80°C freezer for 48 hours. The propan-2-ol reduces cell damage by slowing the

rate of temperature drop to 1°C/min. The frozen ampules were taken out from Mr Frosty and kept in the freezer at -80°C.

Recovery of the cryopreserved cells was achieved by taking cells from deep freezer and thawing them quickly in a 37°C water bath, then the aliquots were added to a fresh prewarmed Ac#6 growth medium incubated in small 25 cm^2 culture flasks at a temperature of 32°C. After 6 hours, a fresh media replaced the original one to remove any remnants of DMSO that might cause toxicity. The cells were examined after 24 hours using inverted microscope to detect any contamination and confirm cell growth.

2.5 Preparation of *Acanthamoeba* Food *E. coli* Stock

A tryptic soy agar (TSA) agar plate was prepared for *E.coli* culture and incubated for 24 hours at 37°C to facilitate colony formation. One colony of *E. coli* was placed in 100 mL of tryptic soy broth (TSB) in a 182.5 cm^2 tissue culture flask and incubated overnight at 37°C at 120 revolutions per minute (rpm) in an orbital shaking incubator. The suspension was transferred to two 50 mL polypropylene tubes and centrifuged at 3000 x *g* for 30 minutes to pellet the *E. coli*. The pellet was washed by ¼ strength Ringer's solution twice to prevent further multiplication of the bacteria, then the *E. coli* pellet was suspended in 10mL of ¼ strength Ringer's solution and stored at 4°C for 14 days.

2.6 Preparation of *Acanthamoeba* Mature Cysts in Neff's Medium

The production of cysts was successfully achieved using Neff's encystment medium (NEM) by the method described by Neff in 1964 (Kilvington and Lam,2013, Hughes *et al.,*2003). The trophozoites were cultured in 182.5 cm^2 tissue culture flask (1 x 10^5 cells/mL) of Ac#6 growth medium then were incubated at 32°C for 48 hours. Trophozoites were centrifuged (500 x *g*) for 5 minutes, then washed three times using ¼ strength Ringer's solution. The resulting pellet was suspended again in 50 mL NEM (5 x 10^5 cells/mL) using 75 cm^2 tissue culture flask. The flask was incubated in an orbital shaking incubator at 32°C at 120 rpm for 7 days. On day 8, the cysts were examined using the inverted light microscope which confirmed cysts maturation. The cysts were finally harvested from the flask and the inner side was swabbed to collect any adherent cysts. the resultant cysts were washed three times with a ¼ strength Ringer's solution (1000 x *g* for 10 minutes). Using a modified Fuchs Rosenthal haemocytometer, the final pellet was adjusted to 5 x 10^6 cells/mL and stored at 4-8°C to be used within two weeks.

2.7 The Preparation of *Acanthamoeba* Mature Cysts in NNA Medium

A different approach was used for the preparation of a smaller number of cysts as the non-nutrient agar (NNA) method was prepared by adding 2.5% (w/v) agar (non-nutrient) and 1 tablet of ¼ strength Ringer's solution in 500 mL of deionized water then autoclaved at 121°C for 15 minutes. The plates were poured and allowed to dry overnight at 37°C. The prepared *E. coli* stock were added to each plate by dropping 2-3 drops, then they were spread out and left to dry overnight. *Acanthamoeba* trophozoites were centrifuged (1000 x *g* for 10 minutes), then 2-3 drops *of E. coli*

stock were added to the trophozoites pellet and this suspension was spotted on the prepared plates which were incubated at 32˚C for 7-10 days to complete the encystment process. The plates were checked periodically for any contamination and also to assess the replication of *Acanthamoeba*.

In order to harvest the cysts, 20mL of ¼ strength Ringer's solution were first added to the agar surface, then firm pressure was applied in a circular motion using a sterilised rubber teat and the resulting suspension was centrifuged (1000 x *g* for 10 minutes) and the pellet was washed twice in ¼ strength Ringer's solution to remove any traces of *E.coli*. Following this step, the pellet was suspended by ¼ strength Ringer's solution and the cell density was assessed under the microscope using a modified Fuchs Rosenthal haemocytometer and the cell count was adjusted to 2 × 10^4 cysts/mL and the resultant pellet was stored at 2-8˚C for up to 14 days.

2.8 Human Epithelial Cell Line Culture (HEp-2)

The medium of HEp-2 cells contains Dulbecco's minimum essential medium (DMEM) with 10% (v/v) foetal bovine serum, 2 mM L-glutamine, 15 mM HEPES buffer. Penicillin/Streptomycin were added to the medium of 100 U/mL and 0.1 mg/mL, respectively. Cells were grown in 75cm^2 tissue culture flask at 37˚C and 5 % CO_2. The cells were sub-cultured once they became confluent.

2.9 HEp-2 Cells Sub-culture

The culture medium was removed and discarded, and the cells were rinsed with 10 mL of pre-warmed Dulbecco's phosphate buffered saline (DPBS) to remove all traces of serum that might contain any residual buffer, then 3mL of 0.25 % w/v trypsin solution were added to the flask and gently rocked so that the solution covered the whole surface. The flask was incubated at 37˚C, 5% CO_2 for 5 minutes. 0.3-0.5mL of the trypsinized cell solution was added to the new sterile flask containing 20 mL of complete growth medium and the cell count was kept around 1 x 10^5 cells/flask (75 cm^2) and was sub-cultured every 3-4 days. The culture vessel was kept in 5% CO_2, 37˚C incubator.

2.10 Cryopreservation of HEp-2 Cells

The cells were checked using inverted microscope confirming the absence of any contamination and the adherent cells were brought into suspension using trypsin/EDTA then were suspended in a fresh medium with the same volume as that of trypsin then centrifuged at 500 x *g* for 5 minutes. The pellet was then suspended in foetal bovine serum containing 5% (v/v) Dimethyl Sulphoxide (DMSO) as a freezing media. 1mL was aliquoted in each cryoprotective ampule then placed inside a passive freezer Naglene Mr Frosty which was filled with Propan-2-ol and placed in a -80˚C freezer for 48 hours. The propan-2-ol reduces cell damage by slowing the rate of temperature drop to 1˚C/min. The frozen ampules were taken out from Mr Frosty and kept at -80˚C. Recovery of the cryopreserved cells was achieved by taking the cells from the deep freezer and thawing them quickly in a 37˚C water bath, then the growth medium was added to the melted cells and incubated at 37˚C, 5% CO_2.

2.11 THP-1 and HL-60 Cell Culture

The cell line used for THP-1 is the human monocytic leukaemia cell line (ATCC TIB-202), and the cell line used for HL-60 is the human acute promyelocytic leukaemia cell line (ATCC CCL-240) which predominantly shows neutrophilic morphology, and both cell lines were obtained from the European Collection of Cell Cultures (Centre for Applied Microbiology and Research, Salisbury, UK). The cells were grown in tissue culture flask at 37˚C· incubator, 5% CO_2 in RPMI 1640 growth medium with 2mμ L-glutamine.10% foetal bovine serum and Penicillin/Streptomycin were added to the medium of 100U/mL and 0.1mg/mL respectively. The density of the cells was kept between 1×10^5 cells/mL to 1×10^6 cells/mL because if they got denser, they would stop dividing or even clump. The cells were sub-cultured every 2-3 days by centrifugation and changing the media.

2.12 Cryopreservation of THP-1 and HL-60 Cell

The cells were assessed using inverted microscope which confirmed the absence of any contamination, then were centrifuged at 500 x *g* for 5 minutes. The pellet was then suspended in foetal bovine serum containing 5% (v/v) Dimethyl Sulphoxide (DMSO) as a freezing media. 1mL was aliquoted in each cryoprotective ampule then placed inside passive freezer Naglene Mr Frosty- filled with Propan-2-ol and placed in a -80˚C freezer for 48 hours which controls the rate of freezing to 1 degrre C / min. The frozen ampules were taken out from Mr Frosty and kept at -80˚C freezer and thawing them quickly in a 37˚C water bath, then the growth medium was added to the melted cells and incubated at 37˚C· incubator, 5% CO_2.

2.13 THP-1 Differentiation to Macrophages

The cells were centrifuged at 500 x *g* and suspended in fresh RPMI 1640 media to a concentration of 1×10^6 cells/mL. The PMA (phorbol 12-myristate 13-acetate) was diluted to 100ng/L and added to 1 mL of cell suspension in 24 well plate and allowed to differentiate for 2-3 days at 37°C. incubator, 5% CO_2.

2.14 Excision of Cornea from Porcine Ocular Globe

Porcine eye globes were obtained from freshly slaughtered pigs (Gill slaughterhouse, Wolverhampton, UK). They were collected 10 globes at a time. Excess tissue muscle and fat were removed from the eyes and the corneas were harvested in a Class 2 safety cabinet following these steps adapted from (Parekh *et al.*, 2012):

The corneas were visually inspected for defects such as pigmentation or scratches on the epithelium; those with defects were discarded. The eye globes were immersed in sterile povidone-iodine (I-PVP) 0.5% (w/v) for 2 minutes to decontaminate the ocular globes (Figure 2.1b), then transferred using sterile forceps in sodium thiosulphate 0.1% (w/v) for 1 minute which acts as a reducing agent for the I-PVP, then further transferred to 0.1% (w/v) gentamicin phosphate buffered saline (PBS) solution for 15 minutes to prevent bacterial infection and finally to a bottle containing sterile saline solution (PBS) at room temperature where corneas are kept until processed.

The eye globes were taken out of the bottle within 10 minutes using forceps and hand-held using sterile gloves and sterile gauze maintaining adequate pressure, then forceps and scissors were used to remove the remaining conjunctiva. Following

this step, a scalpel blade was used to perform a scleral incision of 3-4mm from the limbus region (Figure 2.1 c,d).

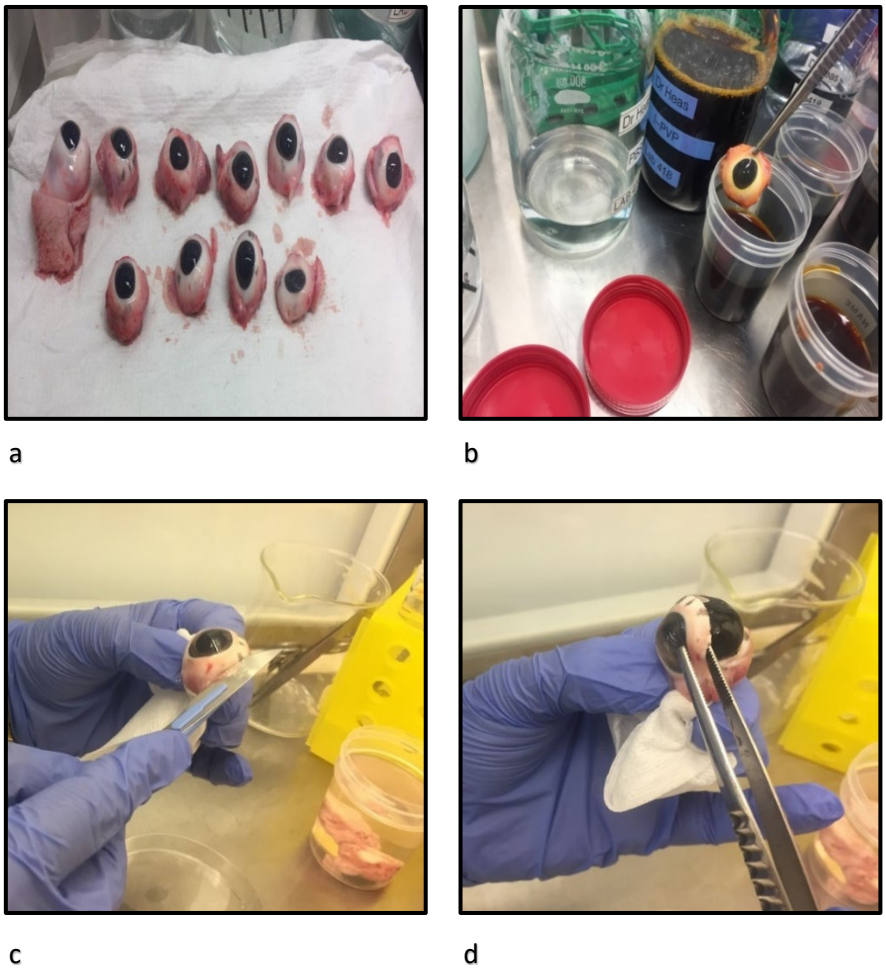

Figure 2.1: Corneal harvesting. **a.** Eye globes. **b.** Initial stage of the sterilization process: eye globes immersed in sterile I-PVP 0.5% for 2 minutes to decontaminate the ocular globes. **c.** Scalpel blade was used to perform a scleral incision of 3-4 mm from the limbus region. **d.** Harvesting cornea from the eye globe.

2.15 Culture of Corneal Tissue

The corneas were cultured in a previously prepared storage medium which is Dulbecco's minimum essential medium (DMEM) (Sigma Aldrich, UK), Ham's F12 medium in a 1:1 ratio plus 10 % (v/v) foetal bovine serum, 2µm L-glutamine and 2 mL pluronic-F68 for deswelling of corneal stroma (Zhao *et al.,* 2008). The above medium was further supplemented with 200µg of gentamicin, Penicillin/Streptomycin of 100U/mL and 0.1mg/mL respectively and 2.5µg/mL amphotericin B and 10ng/mL epidermal growth factor (EGF), 5µg/mL insulin, 2.5µg/mL as the use of EGF and insulin in corneal medium results in a better safety and efficacy profile compared to media without them (Lass *et al.,* 1994) The corneas were cultured at 37˚C in 5% CO_2 environment. The culture techniques were adapted from (Deshpande *et al.,* 2015).

2.16 Histological Techniques

For histological processing of the cornea, the following steps were undertaken:

- Corneas were harvested from the porcine eyes (steps described above).
- Fixation of the cornea in 10% (v/v) formaldehyde for 24-48 hours inside paraffin block to harden the tissue which facilitates the sectioning step (Figure 2.2).

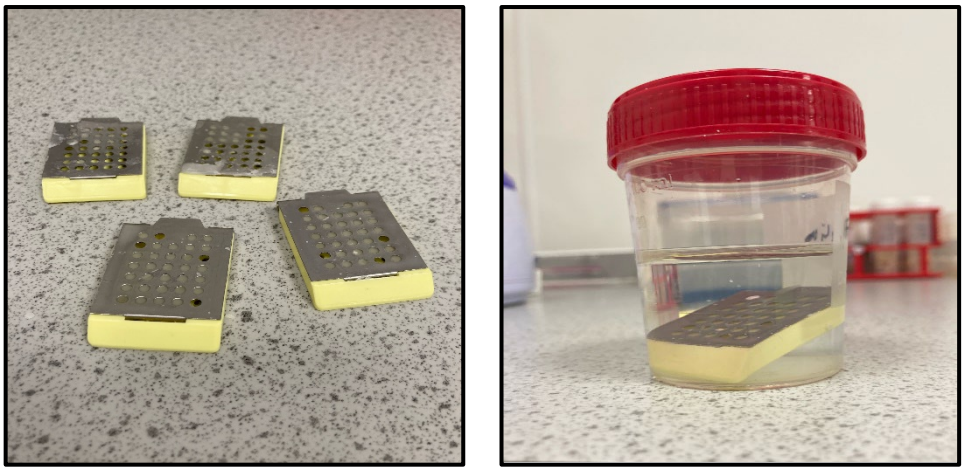

a b

Figure 2.2: Histology processing - fixation process. **a.** Paraffin block. **b.** Fixation of cornea in 10% formaldehyde.

- Dehydration: this is a vital step to remove the water from the tissue. Isopropyl alcohol (IPA) is a favoured reagent because it is miscible in paraffin. The tissue must not be dehydrated rapidly because this will cause distortion of the tissue. Dehydration is carried out in a slow, stepwise approach (Table 2.2) by passing the tissue block through a series of solutions of increasing IPA concentration to ensure the water is fully replaced by IPA (Figure 2.3 a ,b).

Step	Incubation period
70% (v/v) IPA	1 hour
70% (v/v) IPA	1 hour
85% (v/v) IPA	1 hour
95% (v/v) IPA	1 hour
100% (v/v) IPA	1 hour
100% (v/v) IPA	1 hour

Table 2.2: Histology processing - dehydration steps.

a b

Figure 2.3: Dehydration processor (Leica EM TP, Milton Keynes, UK)

- Clearing: the alcohol was then replaced by a clearing agent (xylene) which is an intermediate step before embedding the tissue in paraffin wax which does not mix with alcohol hence the need for the clearing process (Table 2.3).

Step	Incubation period
Xylene	20 minutes
Xylene	20 minutes
Xylene	45 minutes

Table 2.3: Histology processing - clearing steps.

- Infiltration and embedding: prior to sectioning, the tissue block must be infiltrated with a material that acts as a support during the sectioning process. For the method described here, paraffin serves this purpose. During infiltration, the paraffin will eventually equilibrate within the tissue block occupying all the space in the tissue that was originally held by the clearing agent. To achieve this, the blocks were kept in a vial filled with melted paraffin, then the tissue was allowed to equilibrate in an incubator at 58°C (Table 2.4), then the paraffin was poured into the container labelled for paraffin disposal. The newly fresh melted paraffin was used for embedding, and the tissue was left to solidify in a mould, embedded within a small cube of paraffin (Figure 2.4).

Step	Incubation period
Wax	30 minutes
Wax	30 minutes
Wax	45 minutes

Table 2.4: Histology processing - infiltration steps.

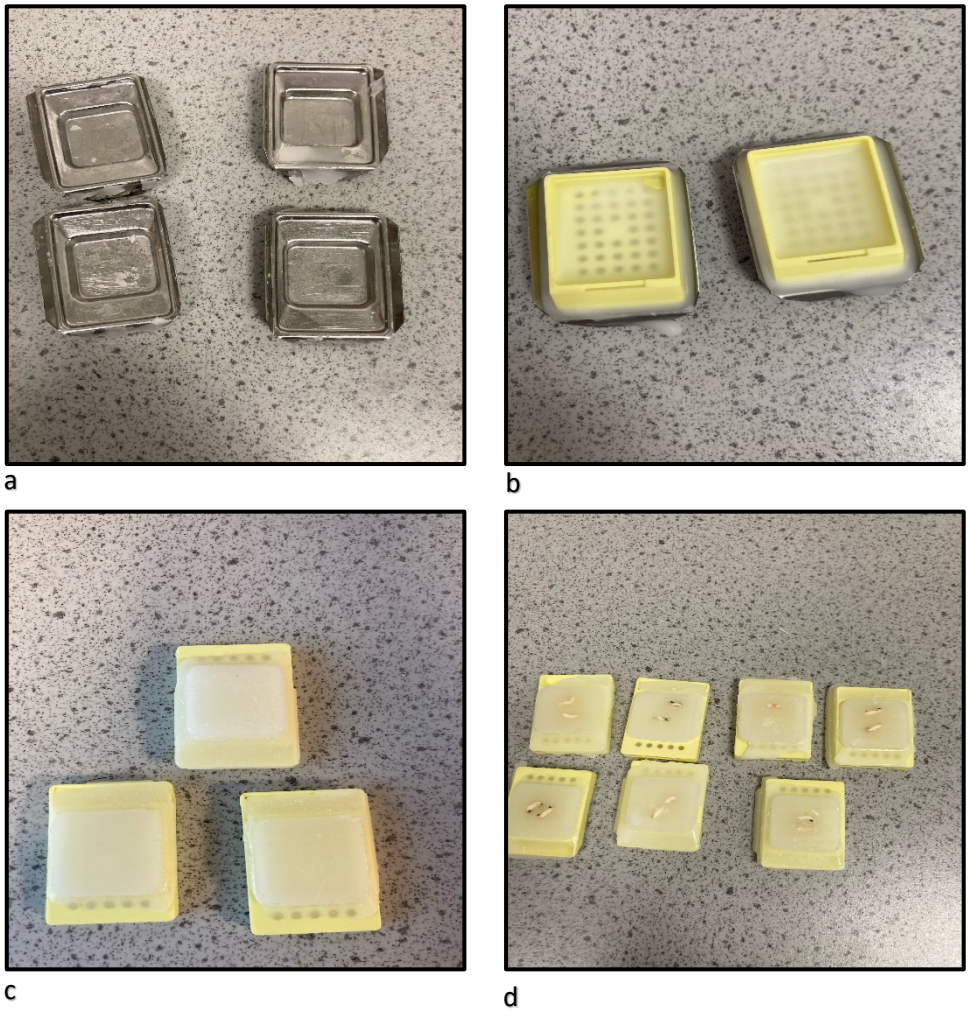

Figure 2.4: Histology processing - embedding process. **a.** Block moulds. **b.** Paraffin blocks placed in moulds with poured paraffin within. **c,d.** Paraffine block after solidification.

- Sectioning: this step was performed by using a cutting device called microtome (Anglia Scientific 0325, UK) to obtain thin sections of very precise thickness about 5-10µm (Figure 2.5).

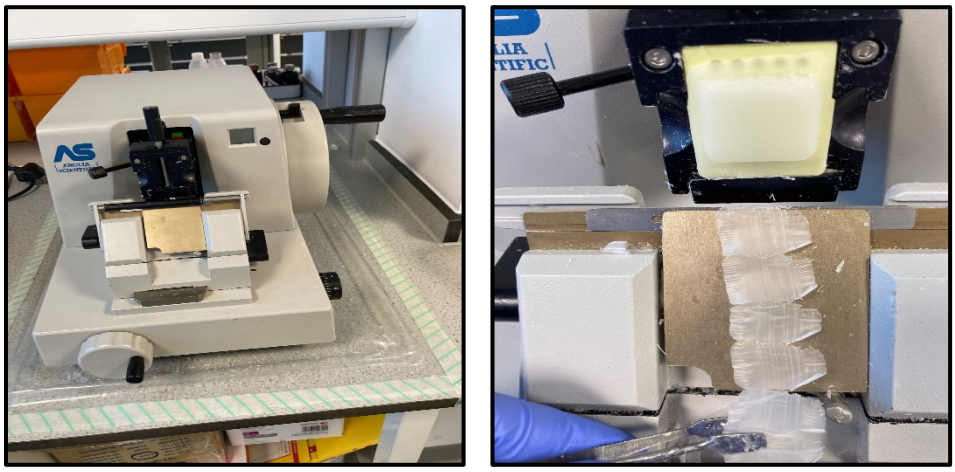

a b

Figure 2.5: Histology processing - sectioning process. **a.** The microtome. **b.** Ribbon of thin sections.

- Mounting of sections on adhesive microscope slides: in this step, the sections were permanently attached to microscope slides by following these steps:
  - The sections were carefully transferred to a 45˚C water bath (Figure 2.6 a). Within a few seconds, the sections were flattened, and the wrinkles disappeared (Figure 2.6 b).
  - A clean microscope slide was dipped in the water bath, and was slowly pulled upward, out of the water, allowing the sections to adhere to the surface (Figure 2.6 c).
  - The slides were left to dry using a hotplate at 60˚C (Figure 2.6 d).

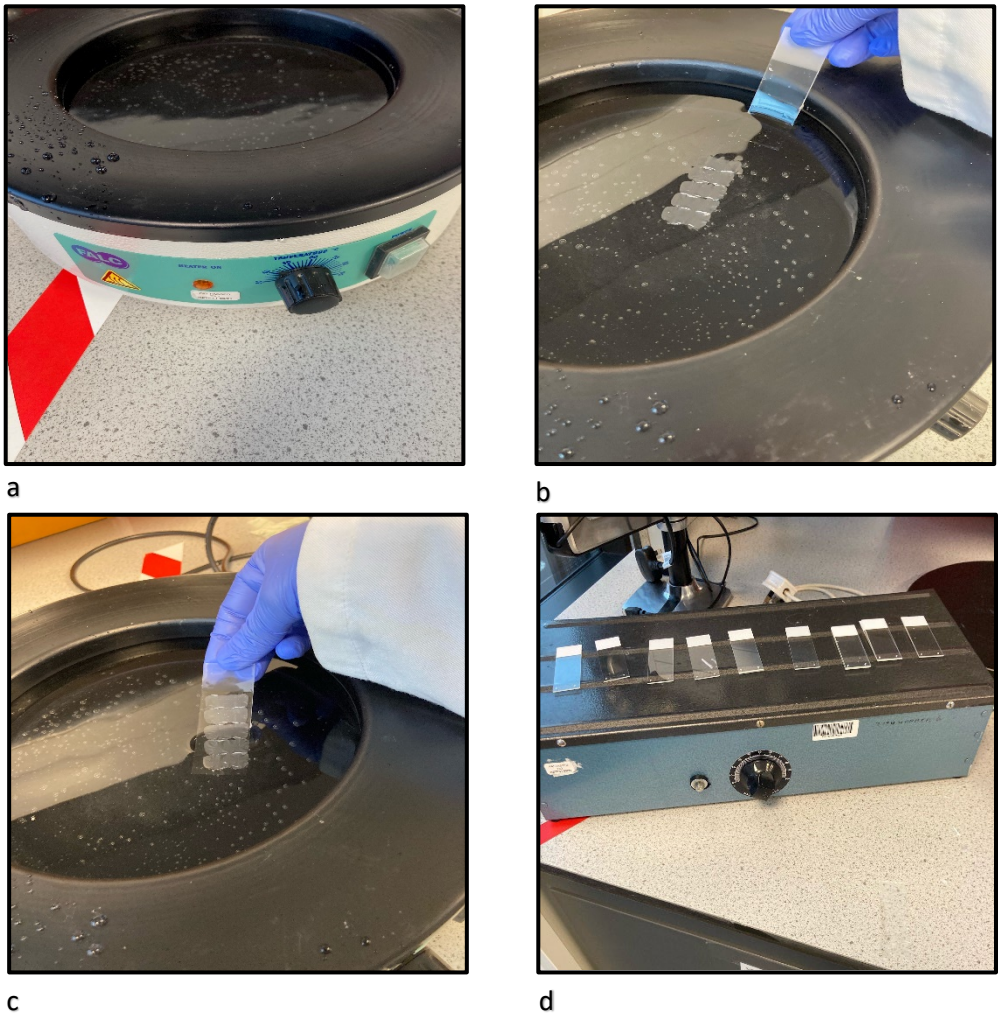

Figure 2.6: Histology processing - mounting process. **a.** The water bath. **b, c.** Slide dipped in water bath, pulled out of water with sections adhering to its surface **d.** The slides were placed on hot plate.

- Rehydration: before a section can be stained, the paraffin must be removed by a clearing rehydration process (Table 2.5). After clearing, only the tissue remains adherent to the slide. Rehydration was done by passing the mounted sections through the solvent clearance that dissolved the paraffin (Figure 2.7).

Step	Incubation period
Clearing agent 1	3 minutes
Clearing agent 2	2 minutes
Clearing agent 3	1 minutes
100% (v/v) IPA	30 seconds
95% (v/v) IPA	30 seconds
70% (v/v) IPA	30 seconds
Tap water	30 seconds

Table 2.5: Histology processing - clearing and rehydration process.

- Staining: this step helps recognizing non distinguishable features under the microscope (Table 2.6), (Figure 2.7). For routine histological stain, two dyes are usually used, one that stains certain components with a bright colour and the other -called the counterstain- stains other cellular structures with a contrasting colour. The two stains are usually haematoxylin and eosin. Haematoxylin stains negatively charged structures such as DNA with a blue colour. Eosin stains most of the other cell components by red colour.

Step	Incubation period
Haematoxylin	2 minutes
Tap water	30 seconds
Scott's solution	1 minute
Tap water	30 seconds
Buffer	1 minute
Tap water	30 seconds
70% (v/v) IPA	1 minute
95% (v/v) IPA	1 minute
Eosin	1 minute
95% (v/v) IPA	2-3 minutes
100% (v/v) IPA	2-3 minutes
Clearing Agent	1 minute
Clearing Agent	1 minute
Clearing Agent	1 minute

Table 2.6: Histology processing - staining process.

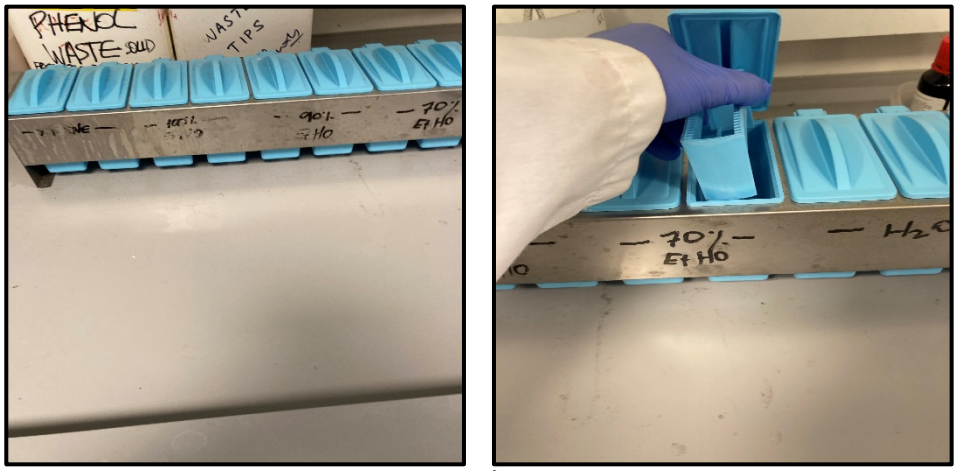

a b

Figure 2.7: Histology processing - rehydration and staining process.

- Preparing permanently mounted sections: the final step in this procedure is to permanently mount the sections under a coverslip (Figure 2.8).

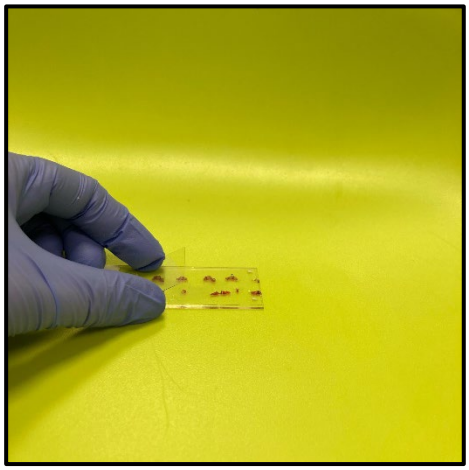

Figure 2.8: Mounting the sections under a coverslip.

- The slides were permanently mounted ready for examination under the light microscope and were stored in storage boxes for subsequent examinations (Figure 2.9).

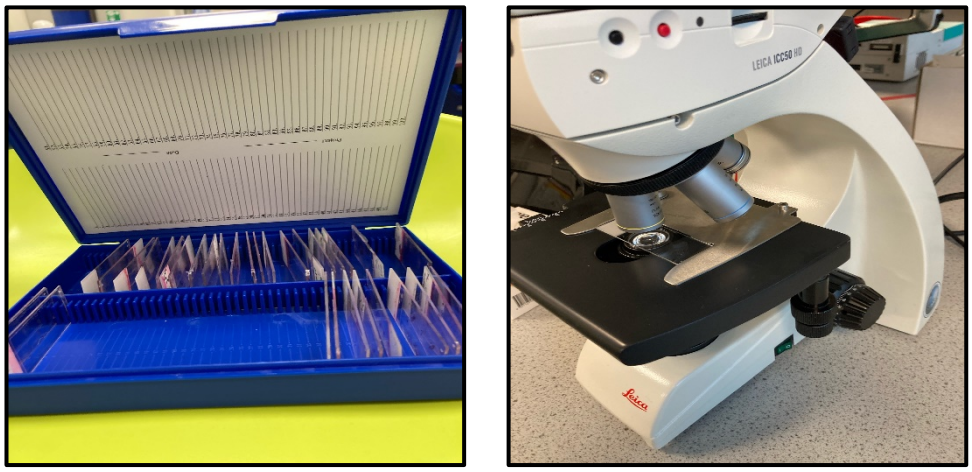

Figure 2.9: Storage of slides and examination **a.** Slides stored in storage boxes **b.** Slides examined under the light microscope.

2.17 Capturing Microscopic Slides

All images of microscopic slides were captured on a Canon EOS M50 digital camera using a Zeiss P95-T2 DSLR 1.6x trinocular microscope adapter.

Chapter Three

Establishing *Ex Vivo* Corneal Model

Chapter 3: Establishing *Ex Vivo* Corneal Model

3.1 Introduction

The human eye is a protected organ consisting of many specialized structures with unique physiological functions (Figure 3.1). It is formed of many structures including the cornea, limbus, conjunctiva, iris, ciliary body, aqueous humor, lens, sclera, choroid, retina and vitreous humor (Patel *et al.,*2013).

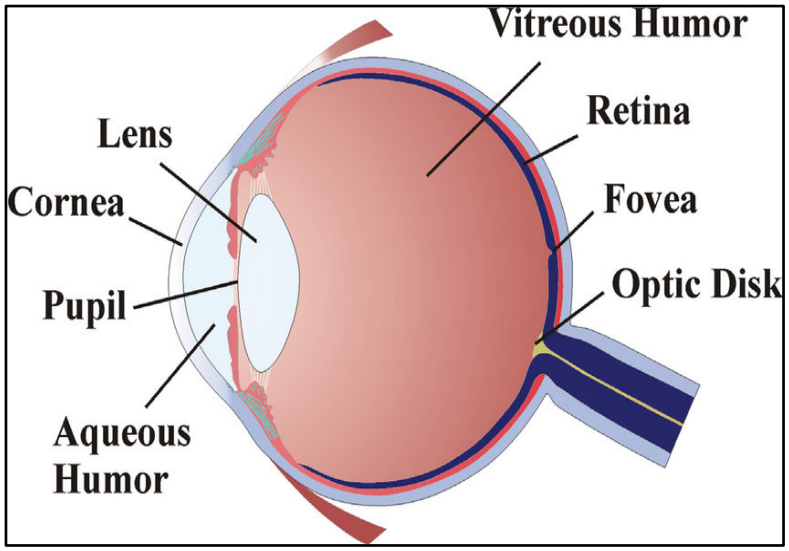

Figure 3.1: Schematic diagram of the human eye (Mauser, 2011)

3.1.1 Cornea

The cornea is the outer part of the eye globe and comprises 15% of the anterior surface area of the eye (Willoughby *et al.,*2010) with the conjunctiva covering the anterior, non-corneal areas of the globe (Shumway *et al.,*2020). The cornea continues posteriorly with the white oblique sclera and plays a vital role in maintaining the structural integrity of the eye globe, protecting the eye components

from injury and focusing the light into the retina which is made possible by the transparent and avascular nature of the cornea (Willoughby *et al.,*2010)

The cornea is composed of 5 layers (Figure 3.2 & 3.3). The stroma is the layer where collagenous lamellae intersect and run parallel to cover the whole of the cornea which gives the cornea its transparency and strength and forms 90% of the corneal surface. The other four layers form the remaining 10% include the epithelium, Bowmen's layer, Descement's membrane and the endothelium (Knop and Knop,2007).

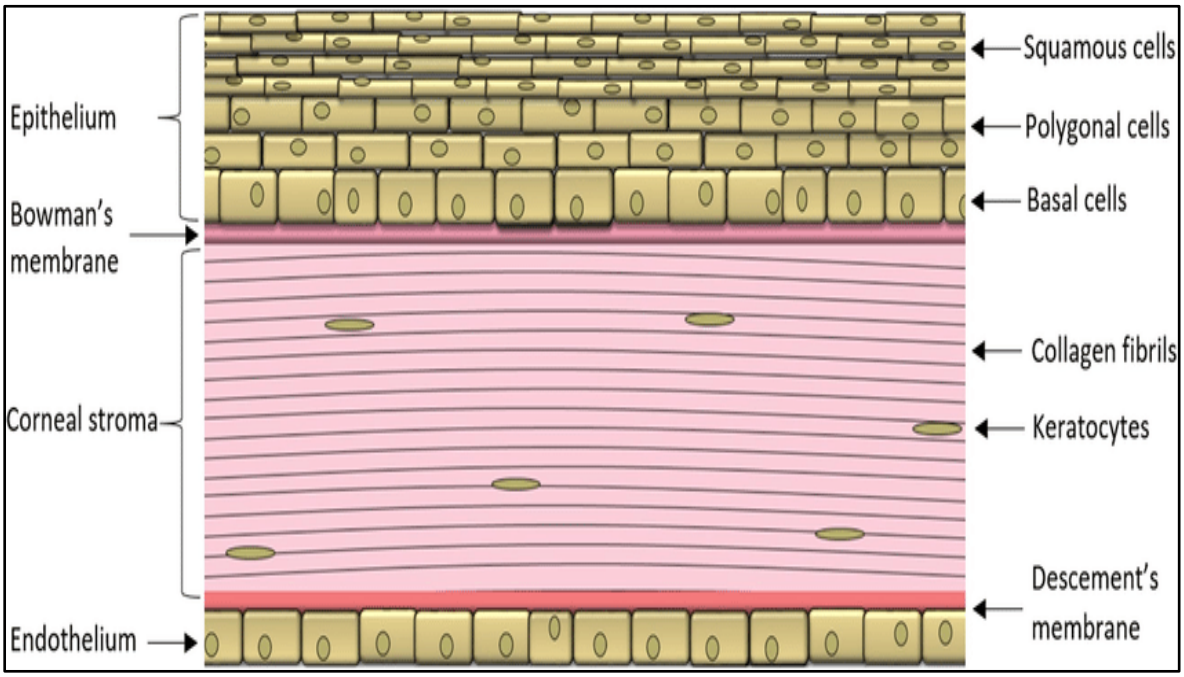

Figure 3.2: Schematic presentation of different layers of the cornea. (Toguri *et al.,*2016)

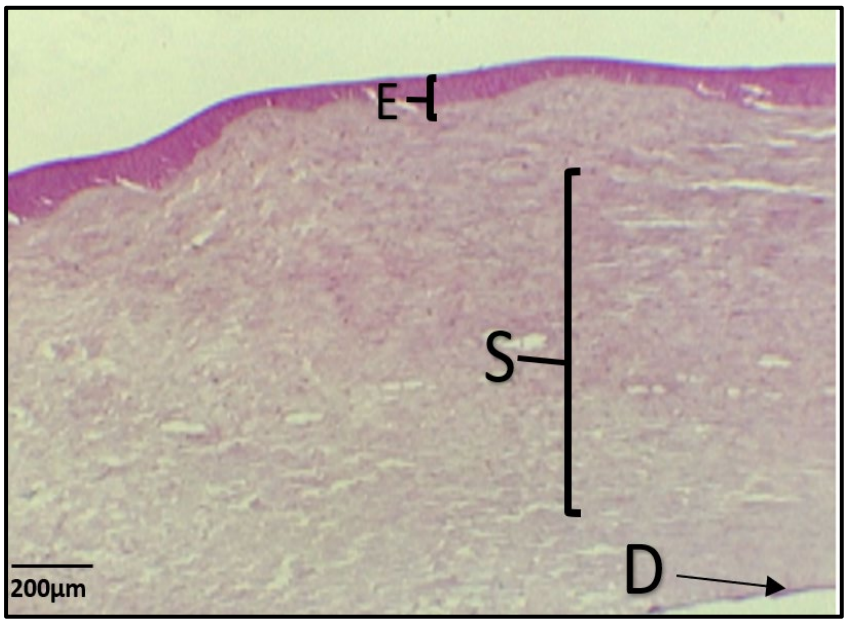

Figure 3.3: Histology section from cornea of pig eye showing parts of the epithelium (E) with five to six layers of squamous cells, stroma (S) with regular parallel collagen fibres and Descemet's membrane (D). (The cornea was harvested and processed in University of Wolverhampton laboratories, UK)

3.1.1.1 The Epithelium

The epithelium (Figure 3.2) is a non-keratinized stratified squamous layer of about 50-90 µm thickness composed of five to six layers of nucleated cells (Knop and Knop,2007). The layers are self-regenerating with high turnover rate and maintain the same thickness overtime (Reinstein *et al.,*2008). The number of epithelial cells is balanced by division at limbus and basal layers and cell sloughing at the surface (Zhou *et al.,*2000). When the old cells slough off into the tear film, the newly formed cells take their place and get exposed to the surface (Zhou *et al.,*2000). The renewal rate takes around a week in normal cornea (Bantseev *et al.,*2007), and this high

turnover rate protects the cornea from adherent pathogens and mechanical stress at the surface (Ladage *et al.,*2003).

The basal layer of the epithelium forms the germinative layer which is the innermost layer from which new cells arise. (Figure 3.2). It is generated by the corneal epithelial stem cells at the limbus (Wolff *et al.,*1997). The horizontal migration from the limbus to the centre of the cornea can take as long as a year (Kaye 1980). The basal lamina is formed of collagen, glycoproteins, and filamentary materials secreted by the deep basal cells (Wolff *et al.,*1997, Snell and Lemp,1998).

3.1.1.2 Bowman's Layer

The Bowman's layer is the acellular part of the anterior stroma and is regarded as a visible indicator of ongoing stromal-epithelial interactions in the human eye (Wilson *et al.,*2000). It is 8-12 μm in thickness and is composed of randomly oriented collagen fibers contributing to its structural strength, however the destruction of this layer can lead to fibrous tissue formation as it is unable to regenerate or divide (Snell and Lemp,1998, Bron *et al.,*1997).

3.1.1.3 The Stroma

The stroma (substantia propria) is 500 μm thick layer that is composed of regularly spaced sheets of collagen bundles produced by keratocytes and lie in proteoglycan ground substance parallel to each other and to the corneal surface (Figure 3.2 & 3.3). The stroma forms 90% of the corneal thickness and has no blood or lymphatic

vessels so that it can maintain corneal transparency to maximize transmission of light to the photoreceptors (Knop and Knop, 2007).

3.1.1.4 Descemet's Membrane and Endothelium

The Descemet's membrane (Figure 3.2 & 3.3) is a true basal lamina produced by underlying endothelial cells and it is formed of type IV collagen and laminin (Bron *et al.,*1997). The endothelium (Figure 3.2) is formed of a single layer of cuboidal flat cells that do not regenerate, it demonstrates an important role in maintaining corneal transparency and regulating the transportation of glucose, amino acids and oxygen to other corneal layers (Bron *et al.,*1997). The endothelium layer keeps the cornea dehydrated and transparent by acting as a pump (Snell and Lemp 1998).

3.1.2 Previous Models

3.1.2.1 *In Vivo* Animal Models

The expansion in research on products that are potentially harmful to the human eye led to an increasing demand on animal models used to evaluate these products. The use of live animals had been established since the early 18th century and continued since (Wilhelmus, 2001). Many models of animal corneas have been established from live animals including rabbits, rats, and hamsters. *In vivo* Models of rabbit corneas are widely used compared to corneas from other animals such as pigs, monkeys, dogs, and cats given the reasonable size of rabbits compared to large animals which facilitates its handling in a laboratory setting while at the same time having the appropriate size of the eye globe compared to smaller animals (Hornof *et al.,*2005).

The animal rights movement which started in the 1950s focused on the ethical aspect of using animals in experimental studies (Stephens and Mak, 2013). One study classified some of these experiments as inhumane based on many factors including degrees of pain and the lasting harm inflicted on the animals being tested (Russell *et al.,*1959). This was the core research upon which the 3R's concept emerged: Replacement, Reduction and Refinement of animals in research (Russell *et al.,*1959). The principle focuses on avoiding or replacing animals as test objects by using technology to design tools and models that can be used for the experiments instead of live animals, appropriately designing and analysing animal experiments to reduce the number of animals used and the amount and duration of the experiments, and finally refining the used methods to minimise the suffering of animals and improve welfare.

The 3R's principle highlights the need to find alternatives to *in vivo* animal testing and to use available resources to establish *in vitro* and *ex vivo* alternatives to the conventional *in vivo* animal studies.

3.1.2.2 *In Vitro* Models

In vitro epithelial models were first developed in the 1960s to be used as an alternative to *in vivo* models using primary and immortalized cell lines of both animal and human origins (Postnikoff *et al.,*2014). The models can be used in the evaluation of different combinations of parameters not easily achievable using *in vivo* animal models (Elliott *et al.,*2011). *In vitro* cell based models are simple, easily constructible, inexpensive and reproducible and offer a clear deterministic explanation of the results (Barar *et al.,*2009).

Rabbit corneal epithelial cells are widely used in research to build cell culture cornea models due to the similarity with the layers and barriers of human cornea (Hornof *et al.,*2005).A publication from 1998 established a rabbit corneal epithelial cells model and tested the potential appropriateness of the model to study drug permeation and metabolism. Rabbit corneal epithelial cells were cultured in DMEM-F12 seeded on Transwell-COL inserts coated with fibronectin to promote cell attachment and spreading, and the integrity of the epithelial layers was evaluated using scanning and transmission electron microscopy 8 days after the seeding step, with the measurement of the permeability of beta-adrenergic antagonist as an indication of transcellular permeability. Upon ultrastructural analysis, the model was shown to be multi-layered containing many cytoplasmic organelles and desmosomes (junctions between the epithelial layers and underlying basement membrane) resembling an intact cornea in structure and permeability (Kawazu *et al.,* 1998).

One of the successes in establishing *in vitro* human cell-based cornea models is the development of 3-dimensional tissue engineering models (Germain *et al.,*2000) as EpiOcular™ (MatTek), SkinEthic™, and Clonetics™ (Lonza). EpiOcular™ is a stratified, squamous epithelial model in which a permeable polycarbonate membrane is used to culture human epidermal cells from neonatal skin (Jung *et al.,*2011) (Figure 3.4). SkinEthic™ model is developed from human epithelium mucosa cells cultured at air–liquid interface that exhibit similar growth and morphological features to *in vivo* environment. (Van Goethem *et al.,*2006). EpiOcular™ and SkinEthic™ are used for eye irritation tests in product development which is a mandatory test for new cosmetic and pharmaceutical agents before licensing them for human use (Mohan *et al.,*2003). This application of the model replaces the conventional Draize test previously adapted as an international

standard assay for acute ocular toxicity (Draize *et al.,*1944). Another application of the model is the assessment of corneal penetration of pharmaceutical ophthalmic preparations and permeability studies (Jung *et al.,*2011).

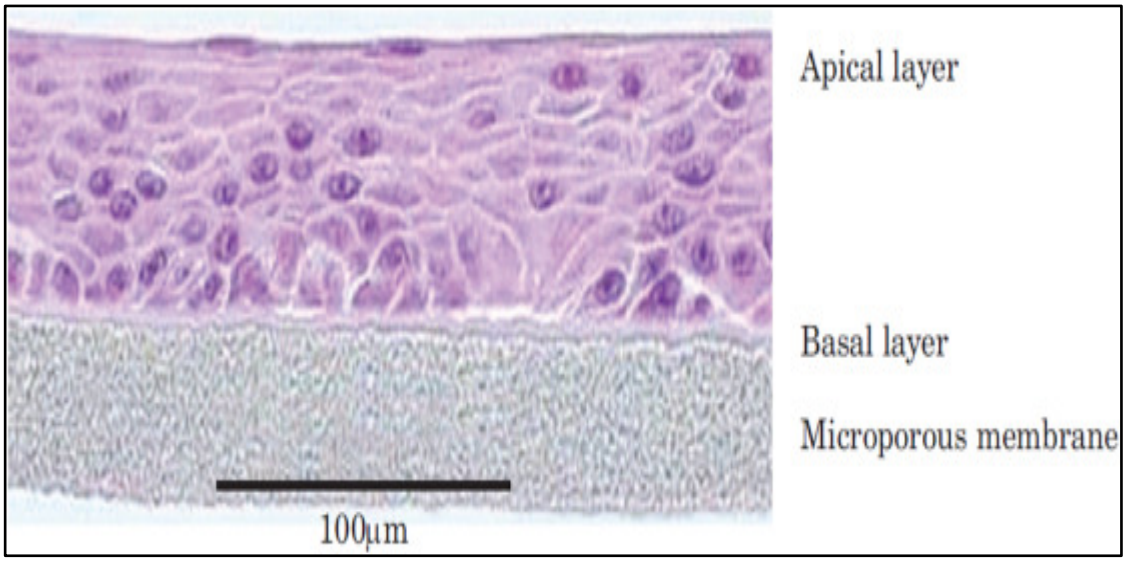

Figure 3.4: Haematoxylin-eosin-stained histological cross-section of the EpiOcular™ tissue model (Kolle *et al.,*2018)

In vitro cell based models from both primary and immortalized cell lines have their own limitations as the primary cells have limited cell division and tend to lose the cell characteristics after few passages, while the immortalized cell lines change their growth behaviour and become aggressive by secreting cell surface markers in abnormal levels and expressing several chromosomal anomalies (Toropainen *et al.,*2007) making *in vitro* based models less reflective of *in vivo* environment. The human cell-based model has similar limitation being developed from noncorneal and immortalized cell lines (Wilson *et al.,*2015) and requires great care when handling the model to prevent cell damage or death (Shafaie *et al.,*2016).

3.1.2.3 *Ex Vivo* Animal Model

To comply with the 3R's principle of animal research, there is an ever growing need to move away from the heavy dependence on *in vivo* animal models by establishing an *ex vivo* corneal model that minimises animal suffering and improves its welfare while at the same time overcoming the limitations of *in vitro* models.

The use of ocular organotypic models started in 1981 (Burton *et al.,*1981) with the introduction of isolated rabbit eyes from animals already processed for the food industry (ICCVAM, 2010). Slaughterhouse waste was explored as a potential tissue source for isolated eyes for bovine and porcine corneas (Prinsen,1996, Reichl and Muller-Goymann,2001).

Researchers use different species including pig, rabbit, cow and chicken tissues to study a variety of ocular diseases, eye irritants, and permeability assays. The isolated rabbit eye test was initially developed to evaluate the damage caused by severe ocular irritants (Brantom *et al.,*1997, Xiang *et al.,*2012) and it was accredited by many regulatory bodies (Wilson *et al.,*2015). The isolated chicken eye test method was developed to mitigate the limitations of the isolated rabbit eye test (Prinsen and Koëter,1993). The model was used to evaluate the toxic responses by measuring surface tissue changes, retention of fluorescein, opacity changes and the effect of swelling on tissue thickness (OECD, 2009). In 1992, bovine cornea opacity and permeability (BCOP) assay was developed (Gautheron *et al.,*1992) and as advised by the scientific advisory committee of the European Centre for the Validation of Alternative Methods (ECVAM), both corneal opacity permeability assay and isolated chicken eye test are scientifically validated to detect severe ocular irritants (Zuang *et al.*, 2015).

The development of porcine cornea opacity permeability (PCOP) assay has several advantages over bovine based assays because it shares similar structure and thickness to the human cornea (Lynch and Ahearne, 2013), there are fewer concerns about bovine spongiform encephalopathy (Van den Berghe *et al.,*2005) and the developed models had already been successful in producing favourable results at lower costs and fewer ethical concerns over animal welfare. Nevertheless, there will always be interspecies anatomical and physiological differences that cannot be overcome, and the models can only be used to investigate the corneal rather than the systemic effects of substances (Shafaie *et al.,*2016).

3.1.2.4 *Ex Vivo* Human Model

Other potential sources for human tissue are expired donor corneas from eye banks, excised corneas from keratoconus patients in addition to corneal remnants following corneal procedures and corneal rim tissues which are corneoscleral rims from human cadaveric eyes not suitable for transplantation. However, the supply is mainly dependant on hospitals and collection after surgery and this uncertainty of supply may hinder the smooth running of experiments.

3.1.3 Rationale

This study adapts the *ex vivo* model that provides the benefit of studying the full corneal structure with its various layers without having to run the experiments on live animals which is more compliant with the 3R's principle for animal welfare by reducing the number of animals used and their suffering. Porcine cornea is used to establish the model given its close resemblance to native human cornea and its availability as slaughterhouse waste compared to bovine which reduces costs and contributes further to minimising the implications on animals.

The establishment of *ex vivo* model will have many applications including the development of Acanthamoeba keratitis and studying the progression of infection in the model without the effect of human immune response in the *in vivo* setting and can also be used to evaluate drug efficacy against this infection which will be further discussed in the subsequent chapters.

3.1.4 Aim and Objectives

The aim of this chapter is to establish an *ex vivo* model of porcine cornea. The objective is to investigate different culture techniques to optimize the survival of cornea and maintain its normal structure with preservation of the transparency of the cornea. The culture techniques are:

- Immersion system
- Air/liquid interface system
- Cornea culture in Petri dish, static with CO_2
- Cornea culture in Petri dish, rocking with and without CO_2

3.2 Methods

3.2.1 Excision of Cornea from Porcine Ocular Globe

Porcine eye globes were obtained from freshly slaughtered pigs (FA Gill Ltd, Wolverhampton, UK). The eye globes were collected 10 at a time (Figure 3.5a). Excess tissue muscle and fat were removed from the eyes and the corneas were harvested in a Class 2 safety cabinet (BioMAT 2) following the same steps described in chapter 2 section 2.14.

3.2.2 Culture of Corneal Tissue

The corneas were cultured in a previously prepared storage medium (DMEM), Ham's F12 medium in a 1:1 ratio plus 10 % (v/v) foetal bovine serum, 2μM L-glutamine and 2 mL pluronic-F68 (x100 stock).The above medium was further supplemented with 200 μg/mL of gentamicin, 100 IU/mL penicillin, 100 μg/mL streptomycin, 2.5 μg/mL amphotericin B, 10 ng/mL, Epidermal growth factor (EGF) and 5 μg/mL insulin. The corneas were cultured at 37°C in 5% CO_2 environment. The culture techniques were adapted from (Deshpande *et al.,*2015) as previously described in chapter 2 section 2.15. The systems studied were immersion system and air/liquid interface system.

3.2.2.1 Immersion System

In this system, corneas were cultured by complete immersion in the above-mentioned medium in a sterile 50 mL tissue culture flat tubes (Figure 3.5) which were kept at 37°C in 5% carbon dioxide (CO_2) environment and the medium was changed every 48hrs.

Figure 3.5: Immersion method**.** Corneas cultured in storage medium in 50 mL tissue culture flat tubes.

3.2.2.2 Air/Liquid Interface System

Cornea culture in Petri dish, static with CO_2:

The endothelial corneal concavity was filled with 500 µl DMEM containing 1% agarose. The gel form of the mixture helps supporting the structure of the cornea. Each cornea was cultured in 13 mL of the above-mentioned medium in 90 mm Petri dish in air–liquid interface (Figure 3.6). The corneas were kept in an incubator at 37°C in 5% CO_2 environment. The medium was changed every 48hrs and the corneas were kept moist by adding 2 drops of the medium on the anterior surface

every day. This static model was simple to set up but did not mimic the *in vivo* conditions in which the corneas are kept intermittently wet through the blinking action of the eyelid that constantly spreads the tear film over the corneal surface.

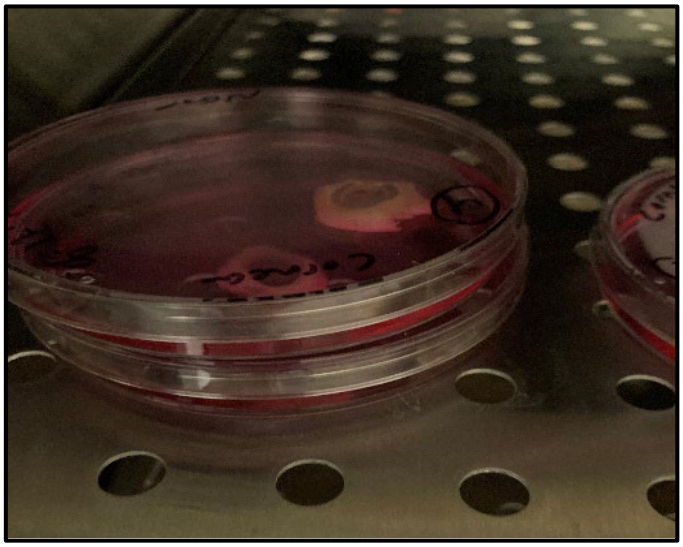

Figure 3.6: Culture in Petri dish, static with CO_2**.** Corneas cultured in storage medium in 90 mm Petri dish.

Cornea culture in Petri dish, rocking with and without CO_2:

The endothelial corneal concavity is filled with 500 µl DMEM containing 1% agarose. The corneas were cultured in 13 mL of the previously described medium in 90 mm Petri dish then placed in an egg incubator (Rcom King Suro Max-20 Incubator, the Incubator Shop, Beverley, UK) at 37°C (Figure 3.7).

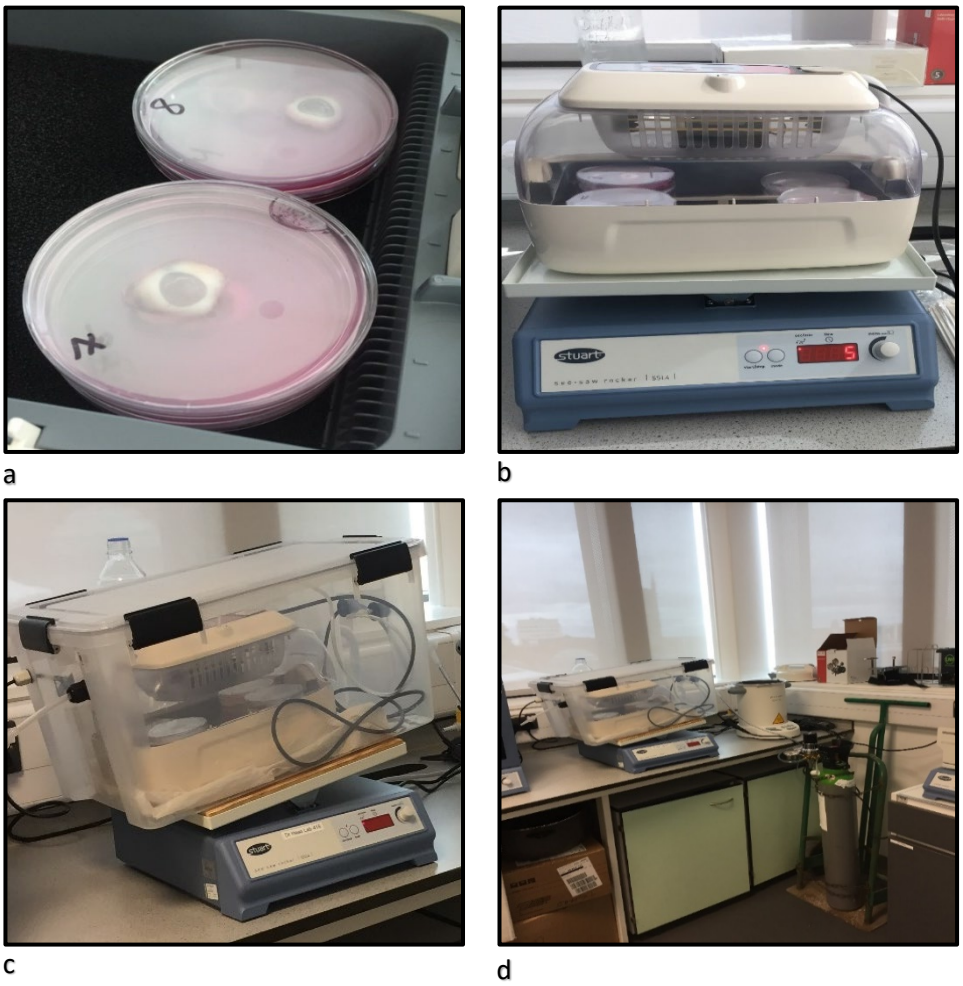

Figure 3.7: Cornea culture in Petri dish, rocking system. **a.** Cultured corneas in Petri dish. **b.** Cultured corneas inside an egg incubator placed on a rocker. **c.** The incubator was placed inside a sealed system box. **d.** Sealed system box supplied with 5% CO_2 by a tube connected to a 5% CO_2 cylinder.

We developed a sealed system using a fully sealed box (Hespapa ,50L Box with Lid and Latching Handles) (Figure 3.7,3.8), by drilling four openings in the sides: two for entry and exit of CO_2, an opening for the power cord for the incubator and one opening for the CO_2 sensor. The openings were secured with airtight glands to prevent any CO_2 leakage. The incubator was placed inside this sealed system box

which was supplied with 5% CO_2 by a tube connected to a 5% CO_2 cylinder (Figure 3.7).

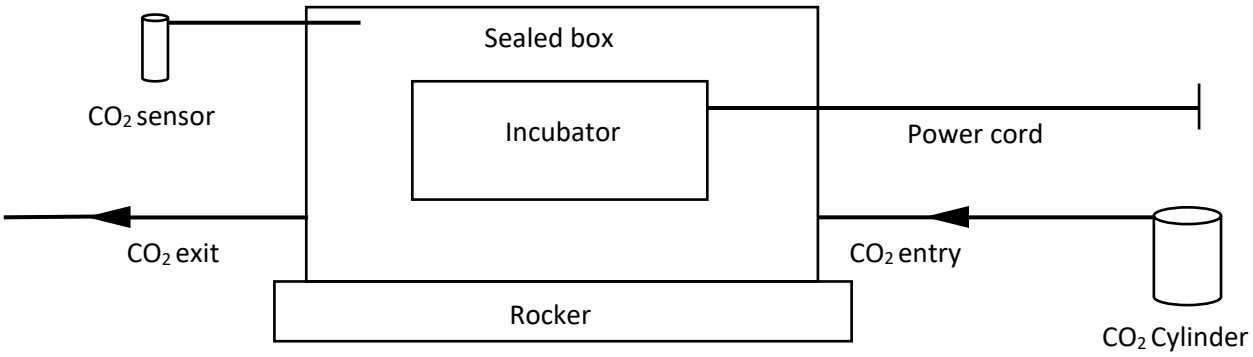

Figure 3.8: Schematic diagram of the box – containing the egg incubator- placed on a platform rocker supplied with 5% CO_2 added through a hole in the sealed box by a tube connected to a 5% CO_2 cylinder. The CO_2 levels were monitored through a CO_2 sensor attached to the system.

A CO_2 sensor (The ExplorIR®-M) was connected to the box to regularly monitor the CO_2 level (Figure 3.9). The sealed system was placed on a platform rocker (Platform Rocker STR6; Stuart, VWR, UK) (Figure 3.9) set at a speed of 10 rpm to keep the medium flowing over the corneal surface mimicking the normal blinking of the eye which would intermittently bath the anterior section of the eye. Up to 16 corneas can be cultured in the incubator at one time and the medium was changed every 48hrs.

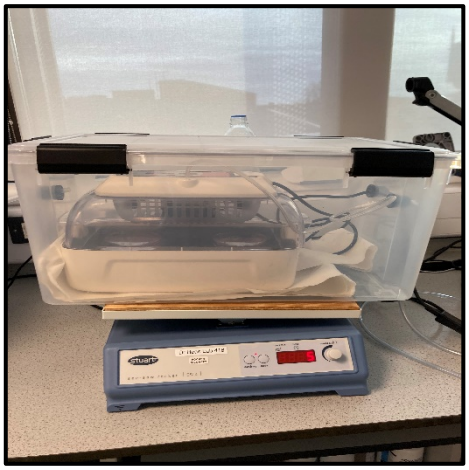

a

b

c

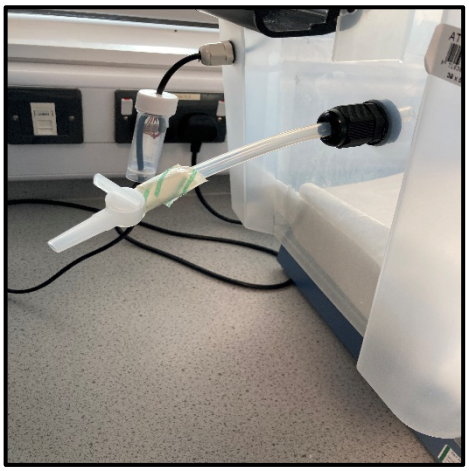

d

e

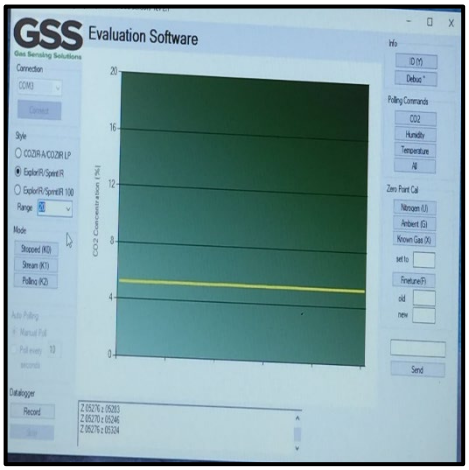
GSS
Evaluation Software
Gas Sensing Solutions
Connection
Style
Mode
Info
Polling Commands
CO2
Humidity
Temperature
All
Zero Point Cal
Nitrogen (U)
Ambient (G)
Known Gas (K)
Send
Datalogger
Record

f

Figure 3.9: Cornea culture in Petri dish, rocking system with 5% CO_2. **a.** The box – containing the egg incubator- placed on a platform rocker. **b.** 5% CO_2 cylinder. **c.** CO_2 added through a hole in the sealed box by a tube connected to the CO_2 cylinder. **d**. CO_2 exit. **e.** CO_2 sensor attached to the box. **f.** CO_2 levels monitoring using a computer software analysing the data from the CO_2 sensor. The graph demonstrates a steady 5% CO_2 concentration within the sealed box.

We studied the rocking model with and without CO_2 administration to compare the effect of CO_2 on the corneal model. For all the above-described systems, the corneas were evaluated daily for gross evidence of contamination and were evaluated histologically at the following intervals: one week, two weeks, and four weeks. The selected corneas were placed in 10% formaldehyde (v/v) for tissue fixation prior to sectioning into histology slides using the method described in chapter 2 section 2.16.

3.2.3 Assessment Methodology

There were two main outcomes assessed for each model: the transparency of the cornea and the maintenance of the integrity of the model through following the preservation of the epithelium and the development of stromal oedema seen under the microscope as mild disruption of the collagen fibres arrangement and swelling of the connective tissue. These outcomes were observed and recorded at the end of week 1, week 2 and week 4.

The transparency of the cornea cultured by different techniques was assessed till the point it became opaque. The transparency was observed by placing the cornea over a letter ‘X’ and reading the letter through the cornea. If the letter ‘X’ was easily visible, the cornea was described as ‘transparent’. If the letter ‘X’ was not visible through the cornea, it was described as ‘opaque’.

The integrity of the model was assessed depending on two main features: how long the model maintained its epithelial lining, and how early stromal oedema emerged. The following grading system was developed to facilitate the comparison between culture techniques and determine the best *ex vivo* corneal model:

- Grade 0: Healthy cornea.
- Grade 1: Superficial loss of the outermost layers of the corneal epithelium, normal stroma.
- Grade 2: Loss of < 50% of the epithelium layers, mild oedema of the stroma.
- Grade 3: Loss of >50% of the epithelium layers, mild oedema of the stroma.
- Grade 4: Total loss of the corneal epithelium, mild oedema of the stroma.

3.3 Results

In this study, corneas were cultured by both full immersion and air-liquid interface techniques with the latter performed through both a static and rocking approach. The rocking function was used to mimic the blinking action of the eyelids that kept the cornea wet. The CO_2 effect was investigated in the rocking technique by running the experiment with and without CO_2. The two main outcomes assessed were corneal transparency and the preservation of epithelial layers with the development of any stromal oedema.

3.3.1 Immersion system

Corneal transparency:

At day 0 (control), the cornea was placed against the letter ‘X’ and it was easily readable through it. The cornea was described as ‘transparent’ (Figure 3.10a).

At week 1, the cornea was further assessed for transparency. The ‘X’ letter was not read through it and the cornea was described as ‘opaque’ (Figure 3.10b). No further assessment regarding transparency was conducted following this stage.

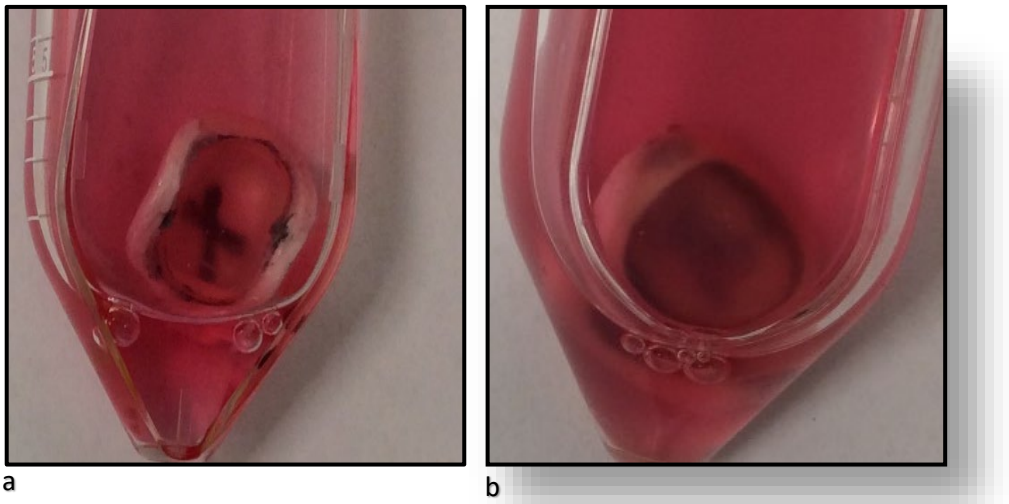

Figure 3.10: Corneal transparency, immersion system. **a.** Day 0 (control): transparent cornea. **b.** Week 1: opaque cornea.

Model integrity:

At day 0 (control), the cornea was examined under the light microscope (Figure 3.11a). It showed normal epithelial lining of healthy five to six non-keratinized, stratified squamous epithelium and normal stroma forming 90% of the thickness of cornea which contained regularly spaced collagen fibres oriented in a uniform parallel direction that maintained transparency. The cornea was labelled as grade 0.

At week 1, the model was examined under the light microscope. There was a total loss of the epithelium with no epithelial layers seen in the section and there was also a mild disruption of the collagen fibres not running parallel to each other which indicated a mild degree of stromal oedema (Figure 3.11b). The cornea was labelled as grade 4 and no further examination was conducted.

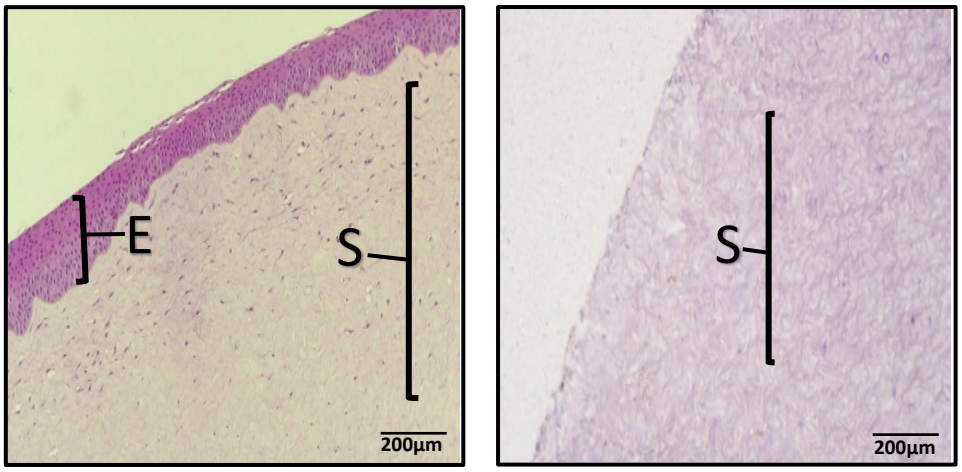

a b

Figure 3.11: Histology sections, immersion system. **a.** Day 0 (control), grade 0: healthy cornea with five to six layers of squamous epithelium (E), normal underlying stroma (S) and regular parallel collagen fibres. **b.** Week 1, grade 4: total loss of the epithelium with mild disruption of the collagen fibres arrangement not running parallel to each other indicating mild degree of stroma oedema.

3.3.2 Air/Liquid Interface System

3.3.2.1 Cornea Culture in Petri Dish, Static with CO_2

Corneal transparency:

At day 0 (control), the cornea was placed against the letter ‘X’ which was easily visible through it (Figure 3.12a). The cornea at this stage was described as ‘transparent’.

At week 1, the cornea was further assessed for transparency and the letter ‘X’ was still readable through it (Figure 3.12b). The cornea was described as ‘transparent’

At week 2, The ‘X’ letter was not visible through the cornea which was described as opaque (Figure 3.12c). No further assessment regarding transparency was conducted following this stage.

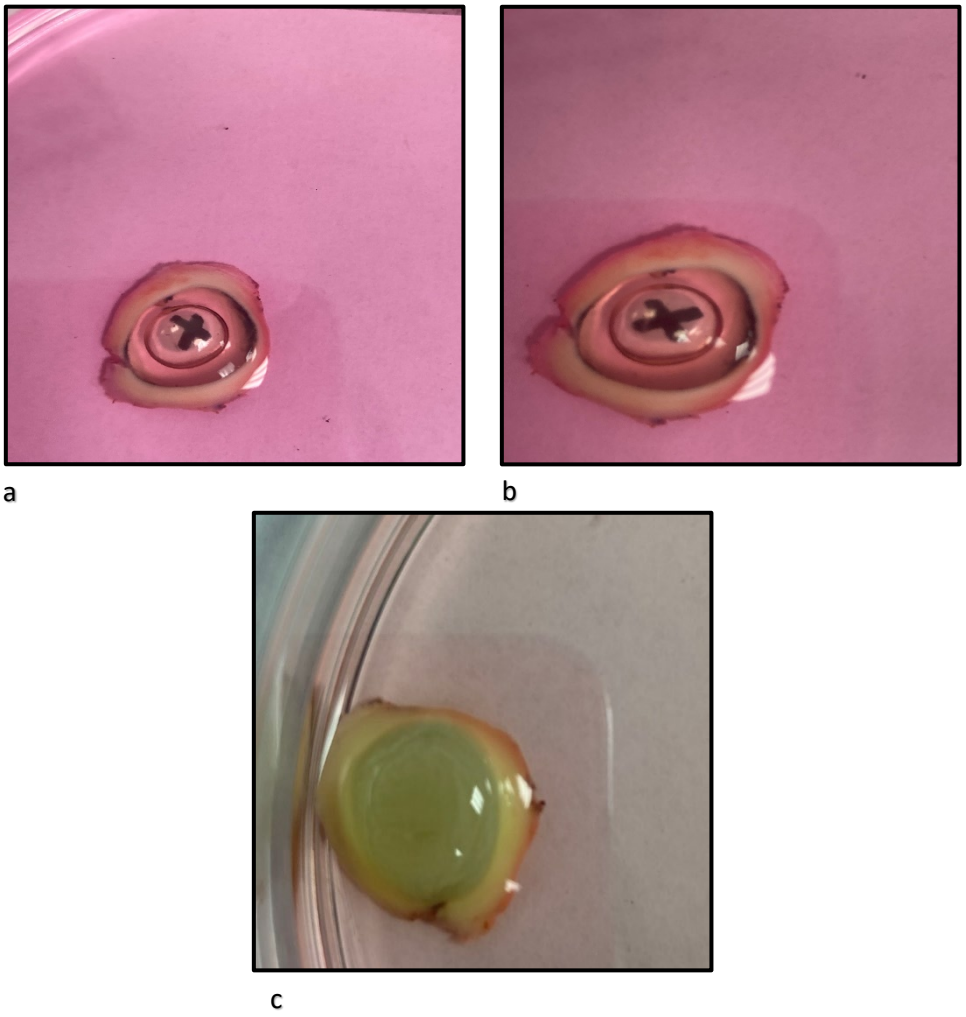

Figure 3.12: Corneal transparency, static with CO_2. **a.** Day 0 (control): transparent cornea. **b.** Week 1: transparent cornea. **c.** Week 2: opaque cornea ‘x’ not visible.

Model integrity:

At day 0 (control), the cornea was examined under the light microscope (Figure 3.13a) and it showed normal epithelial lining of healthy five to six non-keratinized, stratified squamous epithelium and normal stroma which contained regularly spaced collagen fibres oriented in a uniform parallel direction. The cornea was labelled as grade 0.

At week 1, the model was examined under the light microscope. There was loss of the epithelium layers less than 50% of the full thickness where the number of epithelial layers was around 2-3 layers. There was a mild disruption of the collagen fibres indicating mild degree of stromal oedema (Figure 3.13b). The cornea was labelled as grade 2.

At week 2, the model was examined under the light microscope. There was further loss of the epithelium layers of more than 50% of the full thickness with mild disruption of the arrangement of collagen fibres indicating mild degree of stromal oedema (Figure 3.13c). The cornea was labelled as grade 3.

At week 4, the model was examined under the light microscope. There was a complete loss of the epithelium with mild disruption of the arrangement of collagen fibres indicating mild degree of stromal oedema (Figure 3.13d). The cornea was labelled as grade 4 and no further examination was conducted.

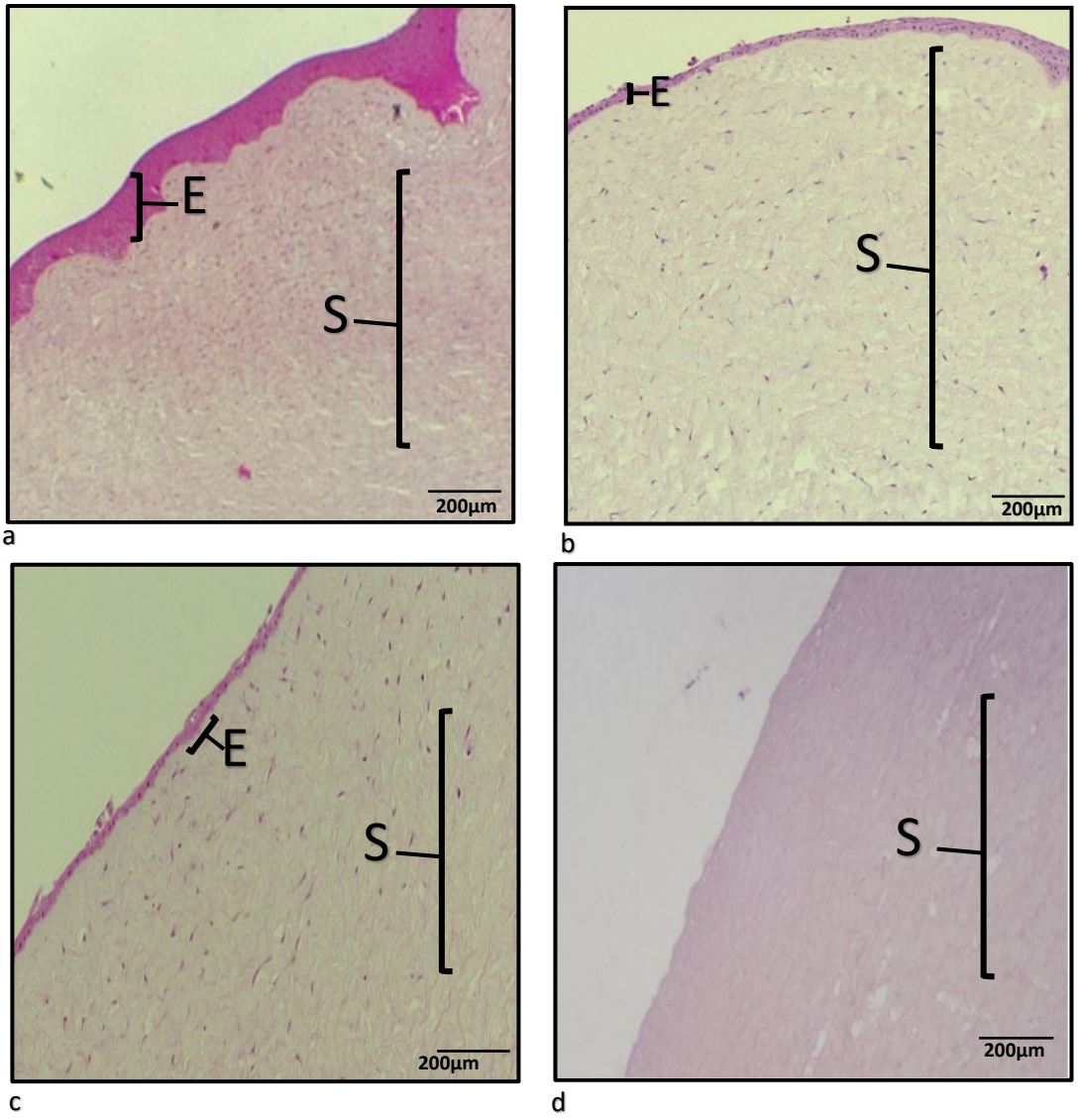

Figure 3.13: Histology sections, static with CO_2. **a.** Day 0 (control), grade 0: normal cornea with five to six layers squamous epithelium (E), normal underlying stroma (S) and regular parallel collagen fibres. **b.** Week 1, grade 2: there is loss of less than 50% of the epithelia thickness, mild disruption of the collagen fibres **c.** Week 2, grade 3: further loss of the epithelium layers of more than 50% of the full thickness with mild disruption of the arrangement of collagen fibres **d.** Week 4, grade 4: complete loss of the epithelium with mild disruption of the arrangement of collagen fibres.

3.3.2.2 Cornea Culture in Petri Dish, Rocking without CO_2

Corneal transparency:

At day 0 (control), the cornea was placed against the letter ‘X’ which was easily visible (Figure 3.14a). The cornea was described as ‘transparent’.

At week 1, the cornea was further assessed for transparency and the letter ‘X’ was still visible (Figure3.14b). The cornea was described as ‘transparent’.

At week 2, The ‘X’ letter was not visible through the cornea which was described as ‘opaque’. (Figure 3.14c). No further assessment regarding transparency was conducted following this stage.

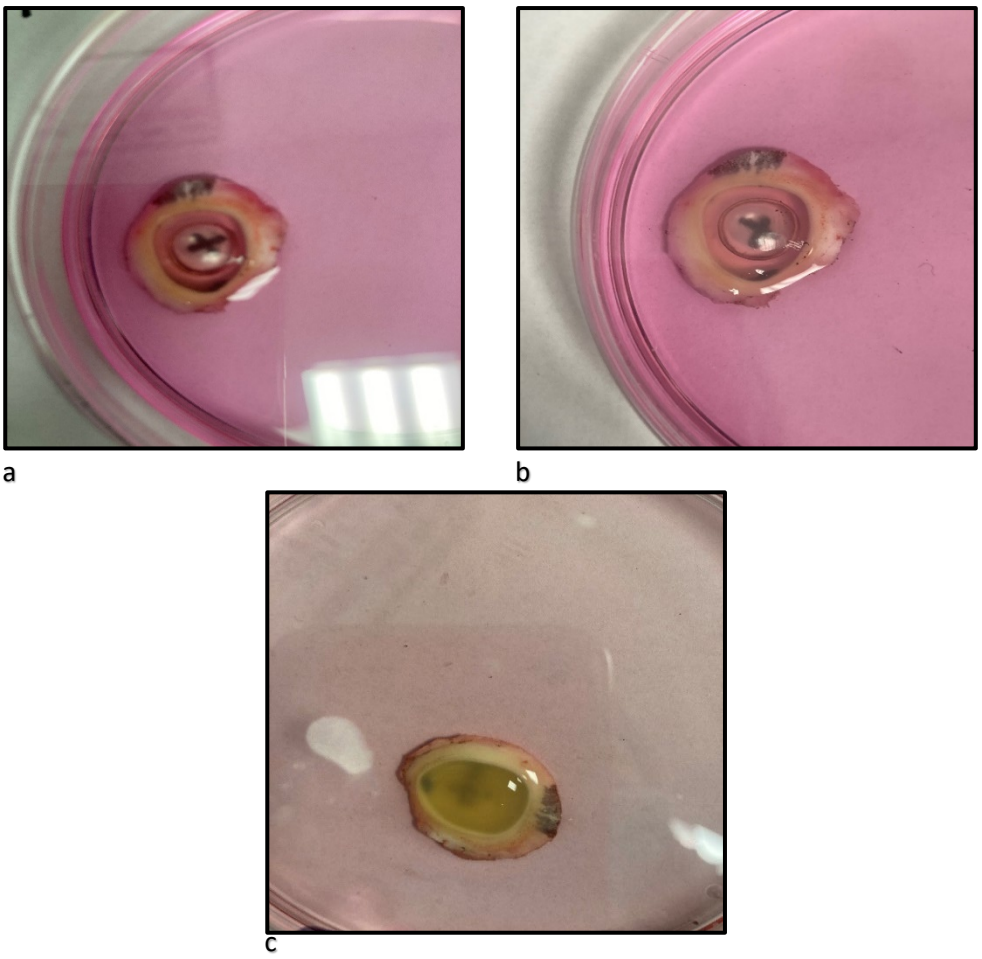

Figure 3.14: Corneal transparency, rocking without CO_2. **a.** Day 0 (control): transparent cornea **b.** Week 1: transparent cornea. **c.** Week 2: opaque cornea.

Model integrity:

At day 0 (control), the cornea was examined under the light microscope. It showed normal epithelial lining of healthy five to six non-keratinized, stratified squamous epithelium and normal stroma which contains regularly spaced collagen fibres oriented in a uniform parallel direction that maintained transparency. The cornea was labelled as grade 0. (Figure 3.15a)

At week 1, the model was examined under the light microscope. There was a superficial loss of the outermost epithelium layers and the number of epithelial layers was 4-5 layers, with normal underlying stroma (Figure 3.15b). The cornea was labelled as grade 1.

At week 2, the model was examined under the light microscope. There was a loss of the epithelium layers less than 50% of the full thickness as the number of epithelial layers was around 2-3 layers in this cornea. There was mild disruption of the arrangement of collagen fibres indicating mild degree of stromal oedema (Figure 3.15c). The cornea was labelled as grade 2.

At week 4, the model was examined under the light microscope. There was further loss of the epithelium layers of more than 50% of the full thickness and the number of epithelial layers is around 1-2 layers. There was mild disruption of the collagen fibres indicating mild degree of stromal oedema. The cornea was labelled as grade 3. (Figure 3.15d)

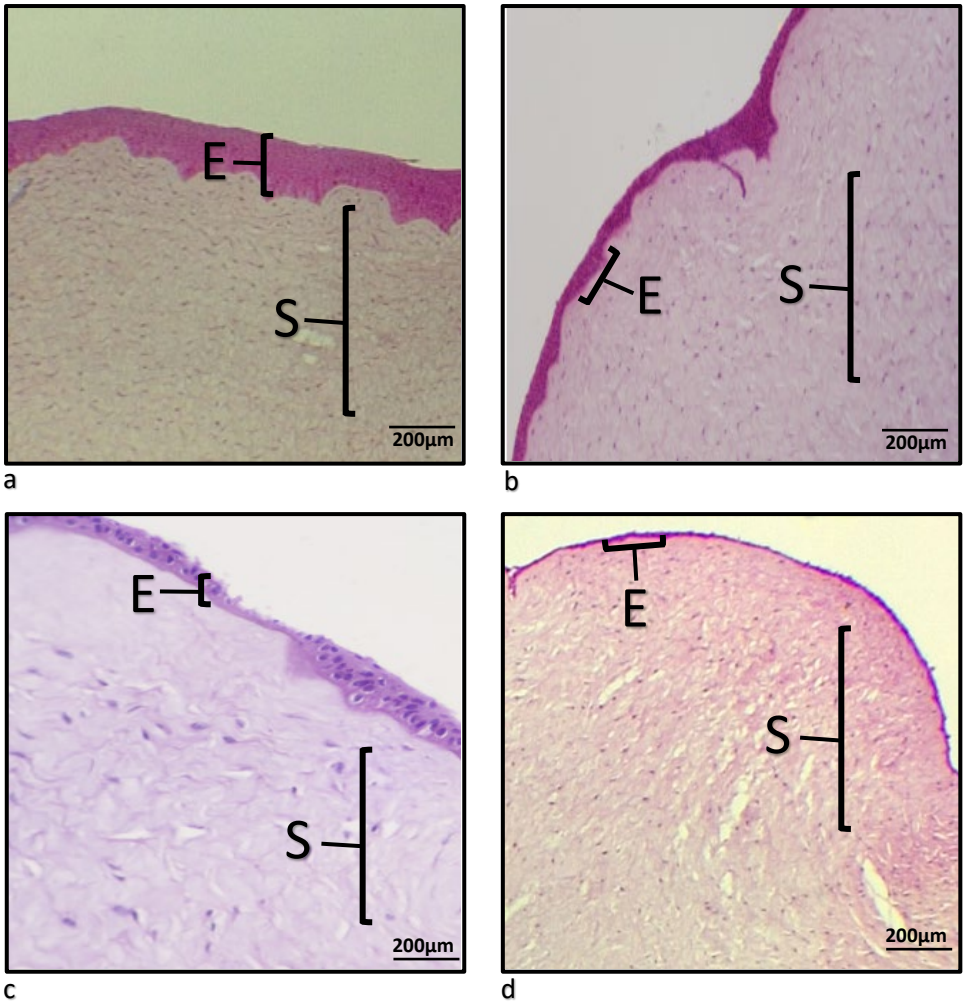

Figure 3.15: Histology sections, rocking without CO_2. **a.** Day 0 (control), grade 0: normal epithelial layers (E) and parallel collagen fibres within the stroma (S). **b.** Week 1, grade 1: superficial loss of the outermost epithelium layers, with normal underlying stroma. **c.** Week 2, grade 2: loss of < 50% of the epithelium layers, with mild disruption of the alignment of collagen fibres. **d.** Week 4, grade 3: loss of >50% of the epithelium layers, with mild disruption of the arrangement of collagen fibres.

3.3.2.3 Cornea Culture in Petri Dish, Rocking with CO_2

Corneal transparency:

At day 0 (control), the cornea was placed against the letter ‘X’ which was easily visible (Figure 3.16a). The cornea was described as ‘transparent’.

At week 1, the cornea was further assessed for transparency and the letter ‘X’ was visible through it (Figure 3.16b). The cornea was described as ‘transparent’.

At week 2, The ‘X’ letter was not visible through the cornea which was described as opaque (Figure 3.16c). No further assessment regarding transparency was conducted following this stage.

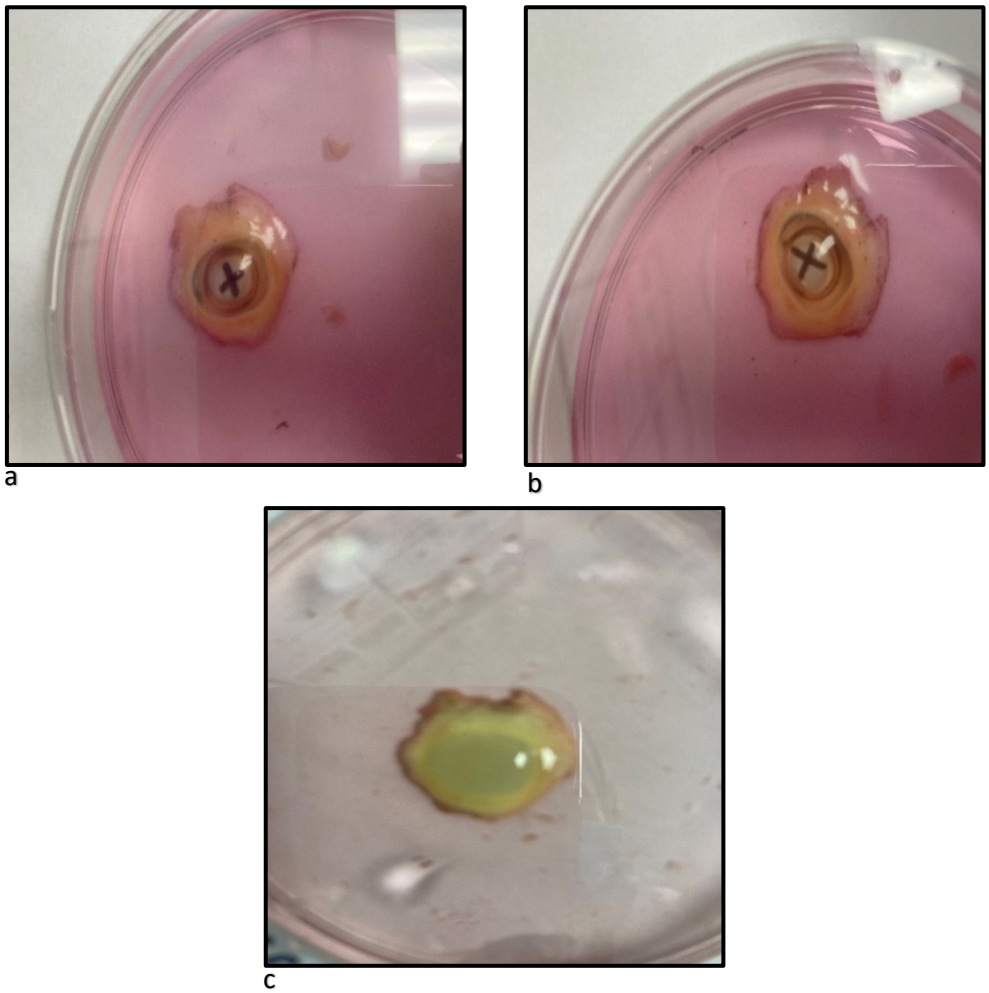

Figure 3.16: Corneal transparency, rocking with CO_2. **a.** Day 0 (control): transparent cornea. **b.** Week 1: transparent cornea. **c.** Week 2: opaque cornea.

Model integrity:

At day 0 (control), the cornea was examined under the light microscope. The cornea demonstrated normal epithelial lining of healthy five to six non-keratinized, stratified squamous epithelium and normal stroma with regularly spaced collagen fibres oriented in a uniform parallel direction that maintained transparency (Figure 3.17a). The cornea was labelled as grade 0 .

At week 1, the cornea was examined under the light microscope. The cornea showed normal epithelial lining and normal underlying stroma (Figure 3.17b). The cornea was labelled as grade 0.

At week 2, the cornea was examined under the light microscope. It showed normal epithelial lining and normal stroma (Figure 3.17c). The cornea was labelled as

grade 0.

At week 4, the model was examined under the light microscope. There was a superficial loss of the outermost epithelium layers as the number of layers is around 4-5 cells with no stromal oedema (Figure 3.17d). The cornea was labelled as grade 1.

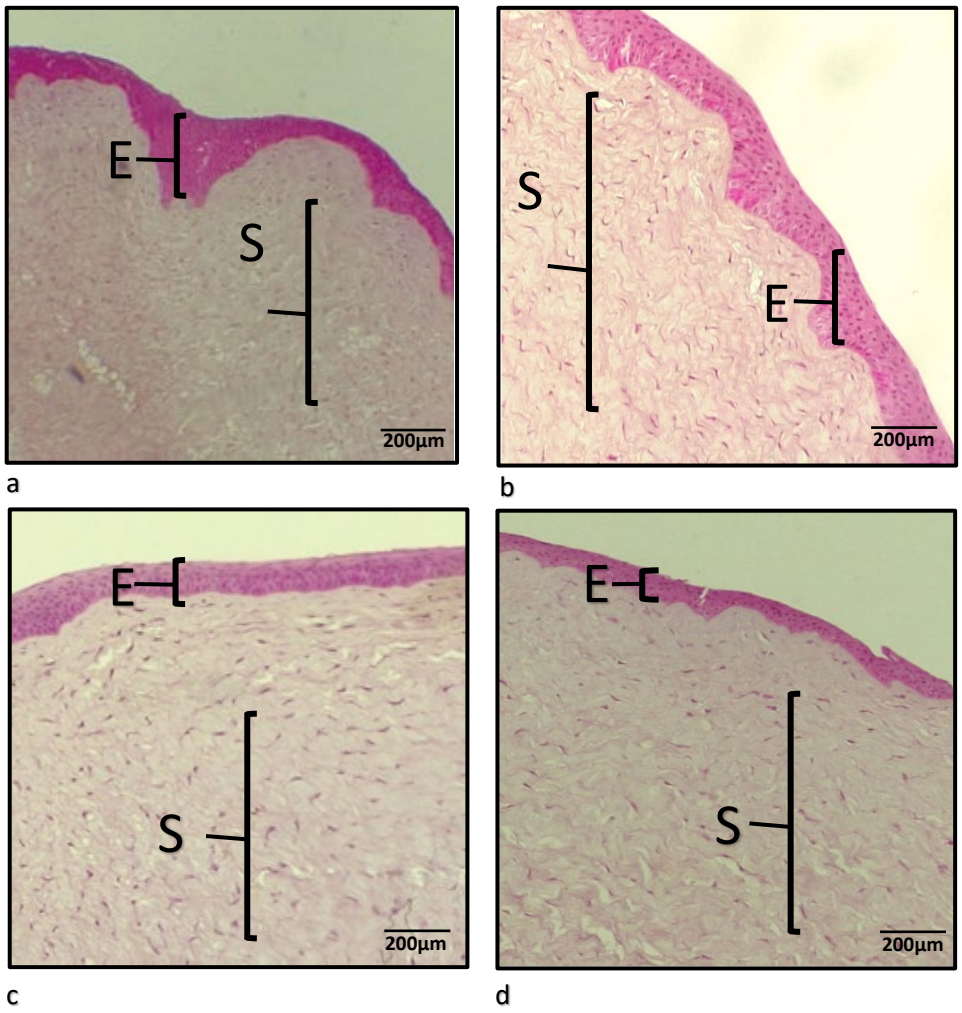

Figure 3.17: Histology sections, rocking with CO_2. **a.** Day 0 (control), grade 0: normal cornea with five to six layers squamous epithelium (E) with normal underlying stroma (S)with regular parallel collagen fibres. **b.** Week 1, grade 0: healthy cornea with normal underlying stroma. **c.** Week 2, grade 0: healthy cornea with normal underlying stroma. **d.** Week 4, grade 1: superficial loss of the outermost epithelium layers and the number of epithelial layers is 4-5 layers, the stroma was normal with parallel collagen fibres.

3.4 Discussion

The *ex vivo* model demonstrated that air-liquid interface model culture system generated better results regarding corneal transparency and the preservation of epithelium for longer period s in comparison to the immersion system. It was also shown that the air-liquid rocking system gave better results from the air-liquid static model. In the air liquid rocking system, the supplement of CO_2 gave superior results to a system without CO_2.

Corneal transparency was maintained for one week only in the immersion system before becoming opaque. The air-liquid interface system preserved corneal transparency one week longer than the immersion system (2 weeks in total) with no difference between the air-liquid static and rocking techniques. This illustrates the significance of attempting to mimic the exact *in vivo* environment when making an *ex vivo* model because the air-liquid interface shares more similarities with the normal eye.

Using the immersion system, the corneal model showed complete loss of all epithelial layers by the end of week 1 with stromal oedema (grade 4). The use of the air-liquid interface system yielded better results compared to the immersion system with a notable difference between the air-liquid static and rocking approaches and even better outcome with the administration of CO_2 in the rocking system .The microscopic examination by the end of week 4 for the air-liquid static model revealed total loss of all epithelial layers and stromal oedema (grade 4), while the air-liquid rocking model without CO_2 showed loss of >50% of the epithelium layers with mild oedema of the stroma (grade 3), and the air-liquid rocking model with CO_2 showed

superficial loss of the outermost layers of the corneal epithelium with normal stroma (grade 1).

The results illustrate the advantages of the air-liquid rocking system and the supplement of CO_2 on the model integrity. In the normal eye, the corneal cells are nourished by the tear film that is continuously provided by the blinking of the eyelid. This is the rationale behind the rocking system which aims to mimic the blinking of the eyelid by ensuring a constant spread of the nutrient rich medium over the cornea at a desired rate resembling the frequent blinking which constantly provides adequate nutrition to the corneal epithelium. The addition of CO_2 helps preserving the model due to its fundamental role in cell growth by keeping the pH around 6.9-7.8 (Ceccarini and Eagle,1971). Carbon dioxide dissolves into culture medium and reacts with water to form carbonic acid that interacts with its conjugate base (the dissolved bicarbonate ions in the medium) and this tightly controlled buffering system ensures a stable physiological pH environment (Bernhardt *et al.,*1988). When pH deviates from neutral, this will negatively affect cell growth and viability, therefore maintaining a tight control of pH around neutral value keeps the equilibrium in the tissue culture medium and prevents the increase in the pH to over 8.5 which is toxic to cells (Zetterberg *et al*.,1981). In a publication from 1974, CO_2 was found to serve as a vital nutrient utilized by cells for growth as the paper reported failure of cell growth using HEPES buffered medium without CO_2 supplement, however the growth drastically improved when CO_2 was added to the same medium (Itagaki *et al.,*1974*)*.

3.4.1 Previous Studies

This current study is adapted from a published research in 2015 that investigated the effect of rocking versus static conditions on the integrity of the corneal epithelium by developing an *ex vivo* model from New Zealand white rabbits (leporine). In the study, the authors investigated the effect of cytokines on wound healing by inducing injury to the epithelial surface. This was achieved by wounding the central area of the cornea using 20% methanol within an 8 mm diameter trephine, then scraping the epithelium using a sclerotome knife. Subsequently, the corneas were placed in a medium that contained interleukins (IL-17A, IL-22) and were cultured using a similar technique compared to our study where corneas were kept in Petri dishes and were placed on an egg incubator at 37°C which was in turn placed on a rocker system at a speed of 10 rpm (Platform Rocker STR6) for 4 weeks and were finally compared with the same model in static condition. They also studied the effect of CO_2 supplement to the rocking system by culturing the model with and without CO_2 administered using a 5% CO_2 cylinder connected to a tube entering the incubator from a hole on the top and documenting their observations at week 2 and week 4 by evaluating corneas using the light microscope (Deshpande *et al.,*2015).

The outcome of their study supported the results of this current study as authors concluded that culturing corneas under static conditions with CO_2 over 2 or 4 weeks resulted in an epithelium only one or two cell layers thick while the rocking system with or without CO_2 resulted in an epithelium five cell layers thick over the same period. Under rocking conditions, there was poor organisation of epithelium in corneas cultured without CO_2 compared to corneas cultured with CO_2 after 2 weeks. At 4 weeks, the epithelium was completely lost in corneas cultured without CO_2

compared to corneas cultured with CO_2 that maintained its organisation showing only loss of superficial cells. They also concluded that wound healing process generated a single layer of epithelium using the static model while approximately 5 layers of new epithelium developed using the rocking system.

In the work presented in this chapter, porcine (pig) corneas were used which share more anatomical similarities to the human eye having similar size, appearance and having no tapetum lucidum layer as rabbit eyes do. Pig eyes are thus a more suitable choice to develop an *ex vivo* model to study Acanthamoeba keratitis and possible treatment modalities. We studied the immersion system in addition to comparing the effect of rocking over static conditions and the effect of CO_2. The outcome was measured at both gross (corneal opacity) and microscopic level (integrity of epithelium and stromal oedema). In this current study, we did not study wound healing or the effect of cytokines.

One major addition in our work was the filling of the corneal concavity with a gel formed of DMEM containing 1% agarose to maintain the convex shape of the cornea and further support the structure of the model during the rocking process. The gel also provides nutrition to the overlying endothelium.

The Petri dishes were placed in an egg incubator at 37°C contained within an air-tight sealed box with the whole system placed on a rocker platform. This is another major modification in our research as we established a fully sealed box supplied with 5% CO_2 and continuously monitored by a CO_2 sensor attached to the box as previously described (section 3.2.2.2). The use of the sealed box has many benefits:

it provides a contamination-free environment to culture corneas in tightly controlled conditions regarding temperature and CO_2 levels, it provides a physical space for a CO_2 sensor to be attached to the apparatus to continuously monitor CO_2 level and finally the consumption of the gas will be significantly minimized compared to 'Deshpande *et al.*' study as the closed system we use conserves the gas within the system.

Regarding the assessment methodology for both studies, 'Deshpande *et al.*' study evaluated the microscopic changes under the light microscope regarding the thickness of the epithelium and its cell organization, but no grading system was implemented and no description of the stromal architecture was reported while we developed a grading system to describe the microscopic features of corneal epithelial layer and the stroma and we used this system for the comparisons made between corneas from various models at different stages of the experiment

The following table illustrates the outcome of both studies.

	Current study	'Deshpande *et al.'* study
Air-liquid static system (week2)	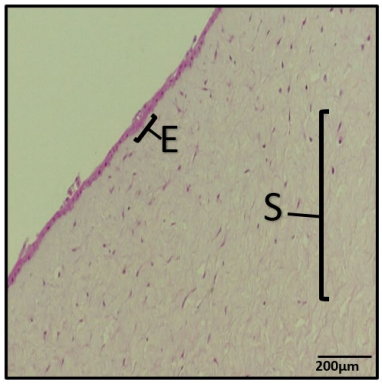 Loss of the epithelium layers of more than 50% of the full thickness with mild stroma oedema (grade 3). E: epithelium, S: stroma.	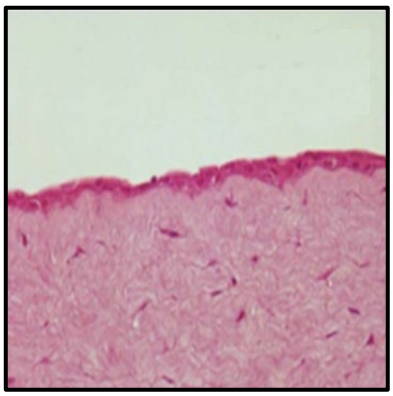 Epithelium one or two cell layers thick.
Air-liquid static system (week4)	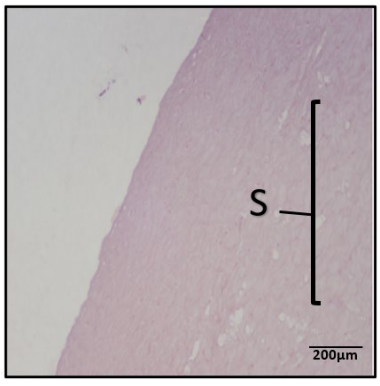 Complete loss of the epithelium with mild stromal oedema (grade 4).	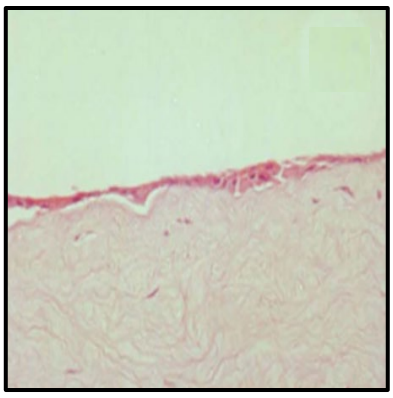 Epithelium one or two cell layers thick.

Air-liquid Rocking system without CO_2 (week 2)	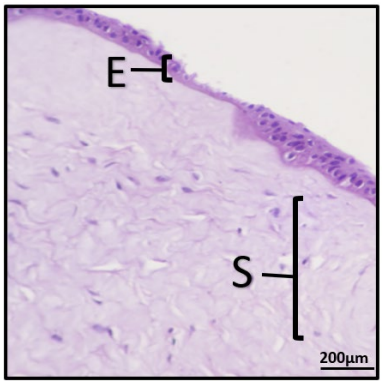 Loss of < 50% of the epithelium layers, with mild stromal oedema (grade 2).	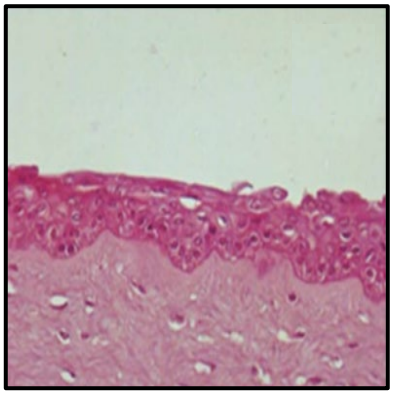 Epithelium of five cell layers thick with poor organisation.
Air-liquid Rocking system without CO_2 (week 4)	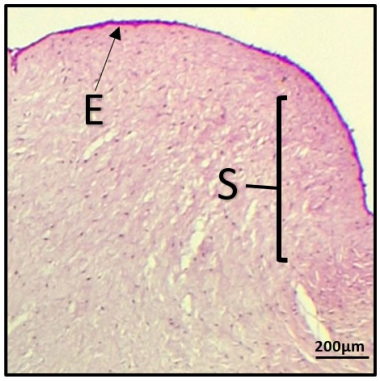 Loss of >50% of the epithelium layers, with mild stromal oedema (grade 3).	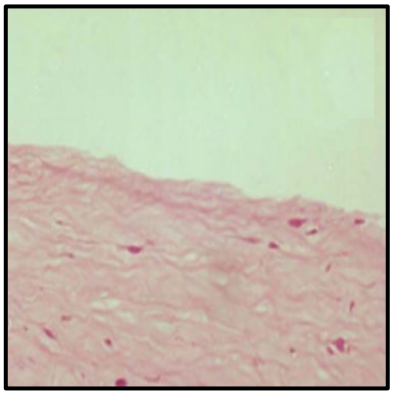 The epithelium is completely lost.
Air-liquid Rocking system with CO_2 (week 2)	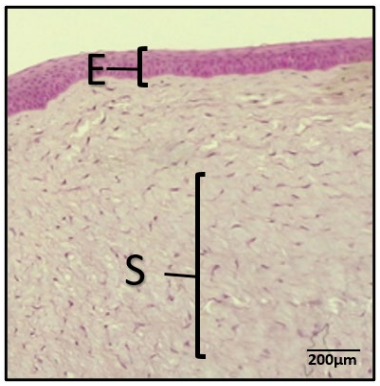 Healthy cornea with normal underlying stroma (grade 0).	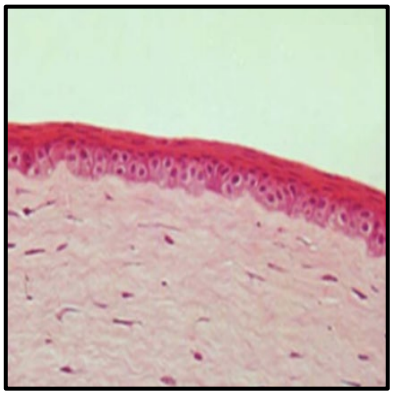 The epithelium is maintained and no effect on the organisation of the layer.

Air-liquid Rocking system with CO_2 (week 4)	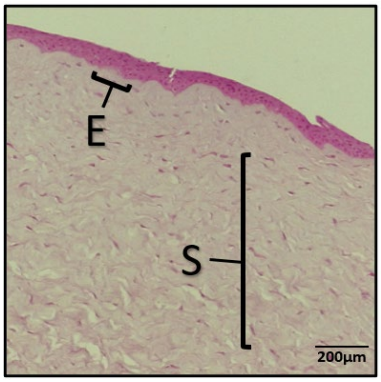 Superficial loss of the outermost epithelium layers with normal underlying stroma (grade 1).	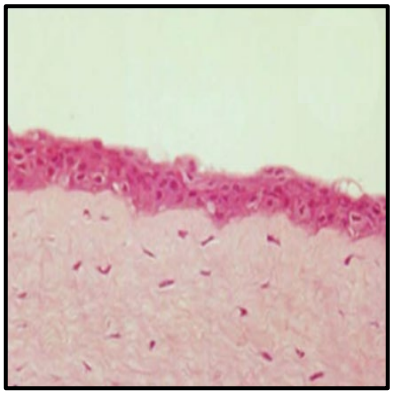 The epithelium appeared to have lost the superficial desquamated cells.

Table 3.1: Outcome of current study and 'Deshpande *et al.'* study

As shown in the table above both studies illustrated the beneficial role of CO_2 in the maintenance and preservation of the epithelium over longer periods of time as the microscopic examination at the end of the 4-week period for both studies demonstrated complete loss of the epithelial layers for corneas cultured without CO_2 and the preservation of the layers with CO_2 administration in rocking conditions with loss of superficial cells only. Both studies demonstrated that when using the air-liquid interface system, the rocking system was better than the static system in preserving epithelial layers. This current study further demonstrated that the air-liquid interface system can better preserve corneal transparency and number of epithelial layers compared to the immersion system and this comparison was not made in 'Deshpande *et al.*' study.

A recent study in 2016 evaluated the differences between immersion and air-liquid interface systems over one week and the outcome was similar to this study demonstrating that air-fluid interface model preserves corneal transparency by the end of the experiment and maintains corneal architecture by preserving the corneal epithelia layers with lesser degrees of stromal oedema. They used horse corneas randomly placed in either immersion condition or air/liquid interface condition for 7 days. The immersion system was developed by completely submerging the cornea in the culture medium while in the air-liquid interface system, the endothelium was totally bathed in the medium leaving only a small area of the cornea exposed to air. All corneas were cultured in tissue culture plates filled with minimum essential medium (MEM) supplemented with 10% (v/v) foetal bovine serum, essential amino acids, penicillin, streptomycin, and MEM vitamins at 37°C in 5% CO_2 for 7 days. The corneas were evaluated daily by gross photography, and on day 7 they performed histological examination, real-time polymerase chain reaction (PCR) and terminal deoxynucleotidyl transferase dUTP nick end labelling (TUNEL) assay (Marlo *et al.,*2016).

The outcome of 'Marlo *et al.*' study supported this current study as they evaluated the corneas both grossly and under the light microscope at day 7 and noticed that corneal transparency was completely lost for corneas cultured under the immersion system in contrast to those cultured under air-liquid interface system that maintained their natural transparency. They generated a grading system for microscopic features where healthy control corneas were classified as grade 0, while corneas with complete loss of the corneal epithelium in addition to breaks in Descemet's membrane and severe corneal oedema were classified as grade 3. They reported that corneas cultured using the immersion system had complete loss of the corneal

architecture with complete loss of epithelium and severe corneal oedema (grade 3), while the corneas cultured using air-liquid interface system had better preservation of architecture as some corneas demonstrates features of healthy corneas (grade 0) and others developed minimal disruption of the corneal epithelium and mild corneal oedema (grade 1).

They also performed real-time (PCR) to evaluate for alpha smooth muscle actin (α-SMA) which is a cellular cytokine that indicates the transformation of corneal fibroblasts to myofibroblasts compared to a control (Fini and Stramer,2005) as an increased detection α-SMA reflects an increase in wound healing processes caused by an increased loss of epithelium. They found a significantly increased α-SMA levels in corneas cultured with immersion system compared to corneas cultured with air-liquid interface system. They also found that α-SMA was seven times higher in corneas cultured using the immersion system compared to healthy control corneas while corneas cultured using air-liquid interface system also had higher levels than control corneas however the latter was not statistically significant.

They also used TUNEL assay which is a well-established method to detect DNA fragments as a reflection of the level of cellular apoptosis. They noticed higher levels of cellular apoptosis in corneas cultured using immersion system compared to control corneas, while there was minimal apoptosis in corneas cultured using air-liquid interface compared to control corneas.

In our study, we ran a longer experiment over 4 weeks, and we used pig (porcine) corneas instead of horse (equine) corneas and the medium used in culture contained other components: DMEM, Ham's F12 medium in a 1:1 ratio supplemented with penicillin, streptomycin, gentamicin, amphotericin B, EGF and insulin. Similar to 'Marlo *et al.*' study, this current study evaluated both immersion and air-liquid interface systems and we further supported the cornea in the latter system by filling the corneal concavity with a gel formed of DMEM containing 1% (w/v) agarose. Both static and rocking settings were evaluated in the air-liquid interface system using an egg incubator and a rocker platform placed inside a sealed box system. The corneas were cultured at 37°C with and without CO_2 and for an extended period for 4 weeks. The model was evaluated by studying corneal transparency, number of epithelial layers and the development of any stromal oedema.

The following table illustrates the outcome of both studies:

	Current study	'Marlo *et al.'* study
Control	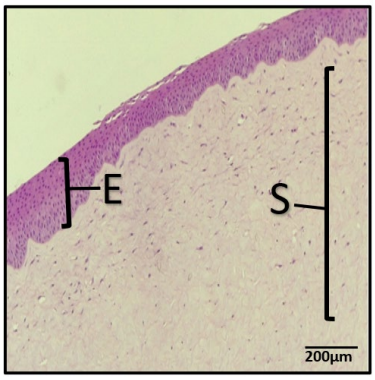 Healthy porcine corneal control (grade 0). E: epithelium, S: stroma.	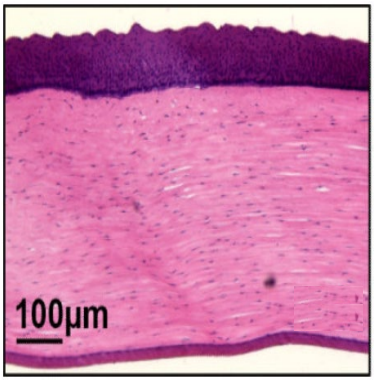 Healthy equine corneal control (grade 0).

Immersion system (week1)	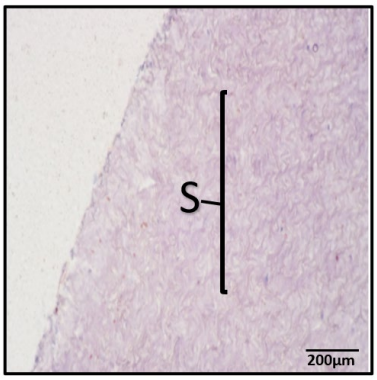 Total loss of the epithelium with mild degree of stromal oedema (grade 4).	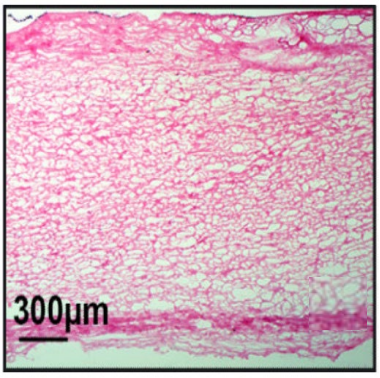 Complete loss of corneal epithelium with severe stromal oedema (grade 3).
Air-liquid static system (week 1)	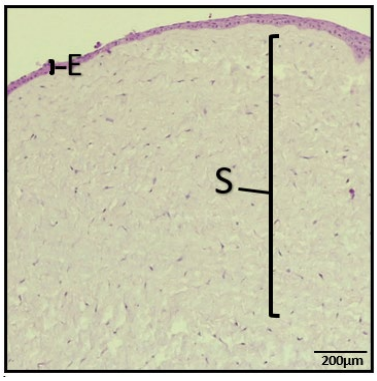 Loss of less than 50% of the epithelial thickness, mild stromal oedema (grade 2).	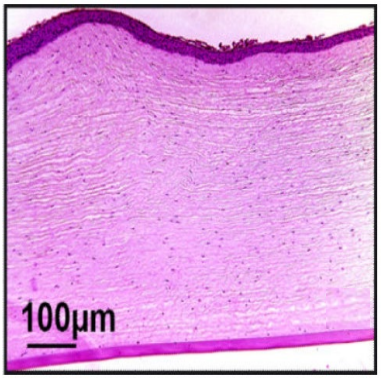 Corneal epithelium is still present, mild to moderate stromal oedema (grade 1).

Table 3.2: Outcome of current study and 'Marlo *et al.'* study.

Our study continued for four weeks and we were able to maintain corneal transparency for one week with corneas cultured in the immersion system and two weeks for corneas cultured in the air-liquid interface system. At week 1, corneas cultured by the immersion system were examined under the light microscope and demonstrated similar results to 'Marlo *et al.'* study with complete loss of epithelial layers however the corneas showed only mild stromal oedema compared to severe oedema in their model and this might be attributed to the difference in the components of the medium used in both studies as stated earlier. In our model, corneas cultured with air-liquid interface system under static conditions demonstrated the presence of epithelial layers with loss of less than 50% of epithelial thickness and mild disruption of the collagen fibres indicating mild oedema while their study reported the presence of epithelial layers without commenting on the thickness and they reported mild to moderate corneal oedema.

Our study demonstrated a notable difference between the static and rocking approaches for corneas cultured in air-liquid interface system and better preservation of the epithelial layer for four weeks with the administration of CO_2 in the rocking system.

3.4.2 Eye Banks- Corneal Storage Techniques

There are several approaches adapted by eye banks for the storage and preservation of corneas and the three main modalities are organ culture (immersion), hypothermia and cryopreservation (Armitage, 2011). Most eye banks in Europe store corneas using organ culture technique due to the prolonged storage time it offers. The media widely used is Eagle's minimum essential medium (MEM) with different banks using up to 8% foetal bovine serum with the addition of penicillin,

streptomycin and amphotericin B (Claerhout *et al*.2010). This prolongs storage times up to 4 weeks (Pels *et al.,*1983) with some banks reporting storage times up to 7 weeks with successful subsequent transplantation (Ehlers *et al.,*1999). Corneas stored using organ culture technique are reported to maintain endothelial and outer epithelial cell layers up to four weeks with cell loss via apoptosis affecting epithelial cell layers more than the endothelial cells (Crewe and Armitage,2001).

Compared to our study, it is noticed that the immersion technique used by eye banks preserves corneal integrity for an extended period of four weeks while we managed to preserve the cornea for one week only using the immersion system, and up to four weeks using the air-liquid interface. There are many factors that might possibly explain this discrepancy as eye banks use human corneas while we use animal corneas which are obviously not identical to human tissue and have more tendency to rapidly swell and lose transparency (Crouzet *et al.,* 2016), and also their handling of corneas takes place in controlled clinical settings at all levels starting from the harvesting step, transport and storage by experts in corneal tissue transplant in a strictly sterile environment compared to laboratory setting. Nevertheless, human corneas are not a reliable source to establish corneal model due to its scarcity therefore the widely available porcine corneas are considered a suitable alternative to develop the *ex vivo* model and use it for many applications.

3.5 Conclusion and Future Work

In developing *ex vivo* corneal model, better preservation of corneal transparency and model integrity was observed under the following conditions:

- Air liquid interface compared to immersion.
- Rocking system compared to static system.
- The supplement of CO_2.

It is thus clear that when establishing an *ex vivo* model, corneal gross and microscopic architecture are better maintained when developing a rocking system that mimics the blinking action of the eyelid and even better results are reported with the supplement of 5% CO_2 that provides vital nutrition to the cells and keeps the pH close to neutral, all of which lead to more resemblance to *in vivo* environment.

Future studies can use corneal rim tissue left over from a transplant and human donor corneas which are not suitable for human transplant (past transplant window or those taken from keratoconus patients) and this can provide a closer similarity to the human *in vivo* model. This requires collaboration between the research team and regional/national organ transplant networks (Bristol or Moorfields eye banks).

Chapter Four

Establishing *Ex Vivo* Acanthamoeba Keratitis Model

Chapter 4: Establishing *Ex Vivo* Acanthamoeba Keratitis Model

4.1 Introduction

4.1.1 *Acanthamoeba*

Acanthamoeba is a small free-living amoeba found in tap water and garden soil (Carnt *et al.,*2020). The organism has a life cycle of a feeding and replicating trophozoite which, in response to adverse conditions including drug treatment can form a dormant highly resistant cyst stage (Kovacs *et al.,*2015). *Acanthamoeba* species are opportunistic pathogens of humans that can cause a fatal granulomatous encephalitis in the immunocompromised patients and a potentially blinding infection of the cornea called Acanthamoeba keratitis (AK) (Carnt *et al.,*2016) in both contact lens wearers and non-contact lens wearers (Lorenzo-Morales *et al.,* 2015).

4.1.2 Acanthamoeba Keratitis

In the United Kingdom, it is estimated that there are approximately 4.1 million people who wear contact lenses (Carnt *et al.*,2020). There are established independent risk factors attributed to the development of Acanthamoeba keratitis in wearers of contact lenses which include: bathing or swimming while wearing the contact lenses (Carnt *et al.,*2020), exposure to house tap water (Carnt *et al.,* 2020) and poor lens hygiene (Stehr-Green *et al.,*1987, Radford *et al.,*2002, Cope *et al.,*2016).

According to one study in the UK, free-living amoeba was isolated from 76% of water samples from bathroom cold taps in houses of patients who developed Acanthamoeba keratitis as water storage tanks increase the level of water colonization by free living amoeba including *Acanthamoeba* (Kilvington *et al.,*2004).

Efficacy issues with certain contact lenses disinfection systems are also linked to previous outbreaks of the disease in the United States and the United Kingdom (Tu *et al.,*2010).

A recent study conducted over a period of 12 years covering 1500 keratitis cases took place in Manchester Royal Eye Hospital and reported an incidence rate for Acanthamoeba keratitis of around 2.3% (Tan *et al.,*2017). Having such a low incidence of AK cases, the disease can be initially misdiagnosed and treated as bacterial, fungal or herpes simplex keratitis (Carnt *et al.,*2018) before a proper yet delayed diagnosis of AK is established. This delay in diagnosis profoundly impacts the prognosis with poorer visual outcome, prolonged duration of treatment, increase incidence of corneal perforation and an increased number of patients requiring penetrating keratoplasty (Carnt *et al.,*2018).

4.1.3 Pathogenesis

The process of keratitis starts by adhesion of trophozoites to the corneal epithelium by specific receptors inducing cytolytic effect to the epithelium that is followed by degradation and penetration to deeper layers however rarely to progress beyond the cornea. Patients are likely to have a poor prognosis if they develop sclero-keratitis or a persistent infection despite the treatment (Perez-Santonja *et al.,*2003).

Acanthamoeba keratitis has three phases: phase 1 infects the corneal epithelium only and has the best prognosis, phase 2 causes one or more corneal epithelial defects, invades the underlying stroma and damages the collagen with severe inflammation leading to stromal or perineural infiltrates which can be demonstrated in up to 63% of cases of AK, while phase 3 forms corneal ring infiltrate highly suggestive of AK and seen in about 50% of the cases , beside one or more features of the second phase (Niederkorn *et al.,*1999; Robaei *et al.,*2014). The late stages of AK are characterized by focal loss of keratocytes and stromal tissue (Awwad *et al.,*2005).

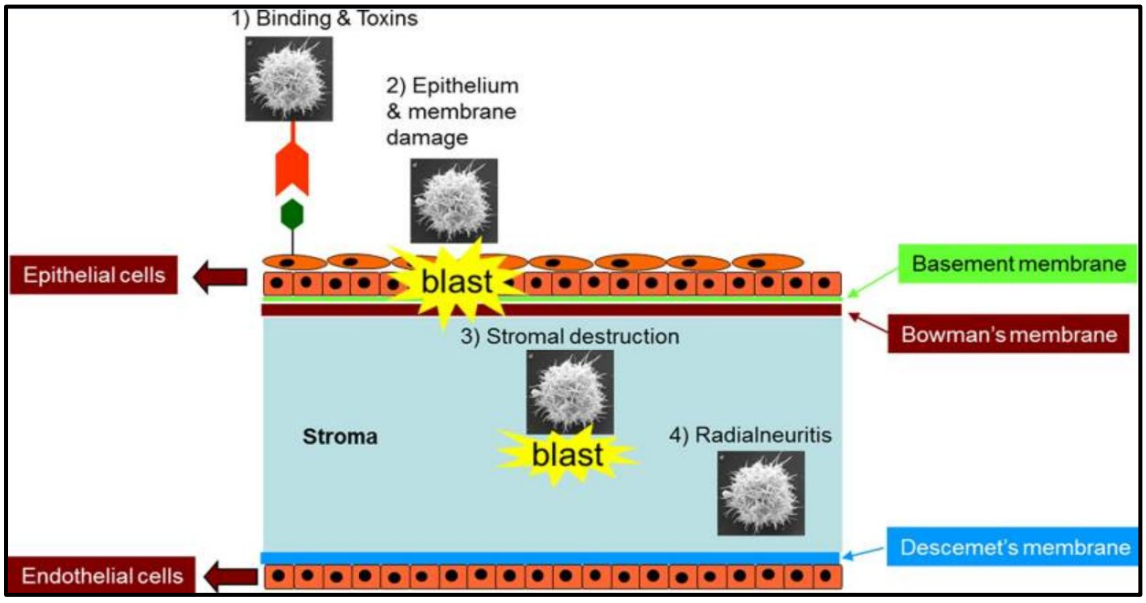

Figure 4.1: The pathogenic cascade of Acanthamoeba keratitis. 1. Acanthamoeba trophozoites adhere to the corneal epithelium. 2. Acanthamoeba trophozoites cause damage to corneal epithelial cells. 3. Trophozoites breach Bowman's membrane and enter the collagenous stroma leading to destruction of the corneal stroma. 4. Trophozoites often cluster around corneal nerves producing radial keratoneuritis (Lorenzo- Morales *et al.,*2015).

The disease affects the corneal epithelium of humans and can cause experimental infection in pigs and hamsters (Neelam and Niederkorn,2017, Clarke and Niederkorn,2006). It is caused by several *Acanthamoeba* species including *Acanthamoeba castellanii, A. culbertsoni, A. polyphaga, A. hatchetti, A. rhysodes, A. lugdunesis, and A. griffini* (Lorenzo-Morales *et al.,*2015).

4.1.4 Pharmacological Treatment

There is no licensed treatment for AK and the current unlicensed therapy is topical preparation of a biguanide which is 0.02% (v/v) polyhexamethylene biguanide (PHMB) or 0.02% (v/v) chlorhexidine used alone or in combination with 0.1% (w/v) hexamidine or 0.1% (w/v) propamidine (Papa *et al.,* 2020).

4.1.5 Previous Models

There is some success in developing an animal model of Acanthamoeba keratitis. Rabbits treated with immunosuppressive drugs were used for the development of Acanthamoeba keratitis models where researchers successfully demonstrated AK by intrastromal injection of *Acanthamoeba* cysts without corticosteroid treatment (Font *et al.,*1982). Another group of researchers developed a model of AK in rabbit eyes that had a better demonstration of the actual process of infection and immune response against *Acanthamoeba* corneal infection in humans (Feng *et al.,* 2015). Developing a porcine model of AK was achieved by using contact lenses already contaminated with *Acanthamoeba* and applying them onto the corneas of pigs, and the induced infection was similar clinically and histologically to human Acanthamoeba keratitis (He *et al.,*1992).

One study compared different methods of developing animal models of AK, and it showed that corneal scratching followed by applying *Acanthamoeba* laden contact

lenses has higher rate of infection than corneal scratching alone, but intrastromal injection yielded the highest rate and most severe form of AK (Ren *et al.,*2009). Other researchers developed AK model using infected contact lenses on rabbit eyes after debridement of corneal epithelium (Ortillés *et al.,*2017).

4.1.6 Rationale

Patients with Acanthamoeba keratitis characteristically develop a stromal “haze” caused by infiltration of host macrophages. The infiltrates are responsible for loss of visual acuity of patients which makes it difficult to follow the progression of the infection in an *in vivo* cornea. Therefore, an *ex vivo* model would offer a unique opportunity to monitor the progression of infection in the absence of host immune response by observing the spread of infection from initial attachment to corneal epithelial cells until invasion of the corneal stroma.

The establishment of an *ex vivo* Acanthamoeba keratitis model may enable it to be used for many applications such as comparing different diagnostic methods for this particular infection (Costa *et al.,*2017), testing different pharmacologic agents and drug resistance (Vasseneix *et al.,*2006), studying the underlying molecular pathways that enhance adhesion of *Acanthamoeba* to corneal epithelium (Panjwani *et al.,*1997) and studying the role of the risk factors associated with AK like the use of contact lenses and trauma (Huth *et al.* 2017).

A substantial consideration in the establishment of this model is the adherence to the 3R principle for animal research (replacement, reduction, and refinement) which minimises the number of animals used per experiment, reducing animal suffering and improving animal welfare.

4.1.7 Aim and Objectives

The aim of this chapter is to establish an *ex vivo* model of Acanthamoeba keratitis using porcine corneas. The objectives are:

- To utilise the *ex vivo* model that has been developed to establish a model of Acanthamoeba keratitis.
- To monitor the progression of infection in the absence of host immune response by gross examination and histological sections using light microscopy.
- To observe the spread of infection from initial attachment to corneal epithelial cells until the invasion of the corneal stroma by studying histological sections under the light microscope.
- To evaluate the role of macrophages and neutrophils in controlling the progress of AK.

4.2 Methods

4.2.1 *Acanthamoeba* Culture

Acanthamoeba polyphaga (ATCC 30461) strain was obtained from the American Type Culture Collection (LGC Standards, Teddington, UK). Trophozoites were maintained in tissue culture flasks using a semi defined axenic medium (Ac#6) as previously described in chapter 2 section 2.3. Cysts were produced using Neff's encystment medium (NEM) method as previously described in chapter 2 section 2.6.

4.2.2 Developing *Acanthamoeba* Passage Cells

In Ac#6 medium, *Acanthamoeba* were fed a semi define axenic medium which caused a phenotypic shift and became less motile and more rounded in appearance because the diet they were fed contained a mixture of amino acids so they could feed by just taking in nutrients by phagocytosis or pinocytosis without having to move within the medium or secrete enzymes or pathogenic factors. This is different from when *Acanthamoeba* feeds on live or whole cells as it needs to undergo certain morphological and functional changes to become highly motile with wider body and large abundant acanthapodia (Omaña-Molina *et al.,*2004) and produces large quantities of enzymes to digest cells that are the same size as it.

To stimulate pathogenicity, *Acanthamoeba polyphaga* were fed on HEp-2 cell monolayers in three-step passage process where it became stretched out instead of rounded and upon feeding demonstrated the presence of large feeding vacuoles that contained the phagocytosed target cells.

4.2.3 Culture of Mammalian Cells

4.2.3.1 THP-1 Cell Culture

The cell lineage used was the human monocytic leukaemia cell line (ATCC TIB-202). The cells were grown as previously described in chapter 2 section 2.11. THP-1 cells were differentiated into macrophages using PMA as described previously in chapter 2 section 2.13.

4.2.3.2 HL-60 Cell Culture

The cell lineage used was the human acute promyelocytic leukaemia cell line (ATCC CCL-240). The cells were grown using the method described in chapter 2 section 2.11.

4.2.3.3 Human Epithelial Cell Line Culture (HEp-2) Cell Culture

HEp-2 (HeLa derivative) human cervix carcinoma cell line (ECACC number 86030501) was obtained from the European Collection of Cell Cultures (Centre for Applied Microbiology and Research, Salisbury, UK). The cells were grown in tissue culture flask at 37°C incubator with 5 % CO_2 in Dulbecco's minimum essential medium (DMEM) with 10% heat-inactivated foetal bovine serum as previously described in chapter 2 section 2.8.

4.2.4 Cornea Culture

Eye globes were collected, disinfected, then corneas were harvested following the same method described in chapter 2 section 2.15. The corneas were cultured using a rocking system with 5% CO_2 as previously described in section 3.2.2.2.

4.2.5 Inducing Infection

A single gentle superficial scratch to the corneal surface (3mm in length) was performed using sterile forceps and scalpel prior to infection with *Acanthamoeba*. The infection was initiated by adding 5µL of 1x 10^5 /mL *Acanthamoeba* trophozoites to the corneal surface. The same method was used to add 5µL of 1 x 10^5 *Acanthamoeba* cysts to the corneal surface using a different set of corneas. Uninfected corneas were maintained as a control along with the infected corneas under the same conditions.

The progression of infection was monitored macroscopically by naked eye for the first two days, then from day 3 onwards they were observed every 5 days up to 28 days by light microscopy. Before microscopic examination, the specimens were fixed in 2% (v/v) buffered paraformaldehyde for 24 hours before sectioning and staining with haematoxylin and eosin stain as per the previously described protocol in section 2.16 . After 28 days, no further assessment was performed, and the model was not used beyond this point.

4.2.6 Adding Macrophages and HL-60

After developing infection following the above-described method, 5µL of 1 x 10^5 /mL macrophages and HL-60 cells were added or injected in the infected corneal surface using a 26-gauge needle.

4.2.7 Assessment Methodology

The corneas were assessed at both gross and microscopic levels. On the gross level, the effect of infection on the transparency of the cornea was evaluated by placing the cornea over the letter 'X' and evaluate if the letter was still apparent through the cornea in both control and infected ones. If the letter 'X' was not clearly seen through the cornea it was reported as opaque.

On the microscopic level, the effect of infection on the integrity of the cornea was assessed based on two main features: the damage to the epithelium and the development of oedema in stroma. The microscopic examination started on day 3 and then every 5 days until day 28 based on the results from chapter 3 as this was the time when the model started to lose its superficial epithelium. The following scoring system was developed to follow the infection:

- Score 0*: healthy cornea, control.
- Score 1*: attachment of *Acanthamoeba* to the corneal epithelium, normal stroma.
- Score 2*: superficial loss of the outermost layers of the epithelium, normal stroma.

- Score 3*: loss of < 50% of the epithelium, normal stroma.
- Score 4*: loss of >50% of the epithelium, mild stromal oedema.
- Score 5*: total loss of the corneal epithelium, invasion of the upper part of the stroma with mild oedema.
- Score 6*: total loss of the corneal epithelium, invasion of the upper and middle layers with stromal oedema.

4.3 Results

In this study, the corneas were cultured using the model established in chapter 3 (air-liquid interface technique, rocking approach with CO_2). Following the establishment of the model, the corneas were scratched and *Acanthamoeba* trophozoites and cysts were added to the medium and were followed over a period of four weeks when the control cornea started to show histological changes. The measured outcomes were corneal transparency and epithelial and stromal changes.

4.3.1 Macroscopic Level

On the macroscopic level, the cornea infected with *Acanthamoeba* demonstrated visible haziness on day 10 compared to control cornea (Figure 4.2). No further assessment was conducted.

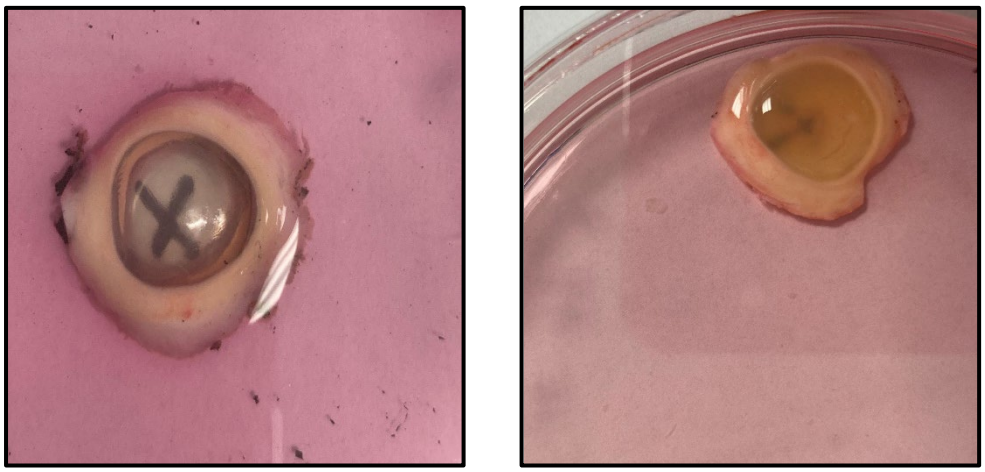

a b

Figure 4.2: Corneal transparency. **a**. Healthy cornea (control): transparent cornea with the letter X visible through the cornea. **b**. Infected cornea: opaque cornea with no clear letter seen through it.

4.3.2 Microscopic Level

4.3.2.1 Day 0 (control)

The control for healthy cornea (Figure 4.3) was examined under the light microscope. It showed normal epithelial lining of healthy five to six layers of non-keratinized, stratified squamous epithelium and normal stroma which contained regularly spaced collagen fibres oriented in a uniform parallel direction.

Score: 0*: Healthy cornea

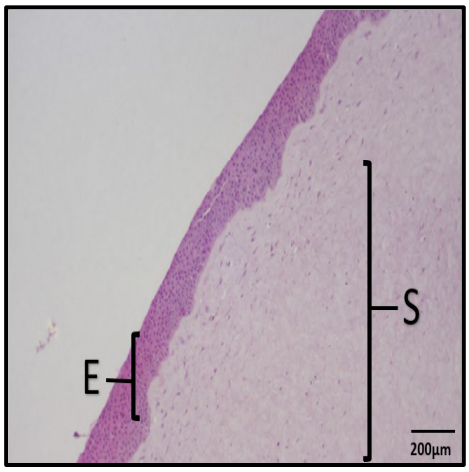

Figure 4.3: Normal cornea at day 0 showing five to six layers squamous epithelium (E) with normal underlying normal stroma (S) and regular parallel collagen fibres, score 0*: healthy cornea.

4.3.2.2 Day 3

Control cornea

The cornea was examined under the light microscope. It showed normal epithelial lining with five to six layers of squamous epithelium with normal underlying stroma with regular parallel collagen fibres (Figure 4.4a). Score 0*: healthy cornea

Infected cornea

The infected cornea was examined under the light microscope and there was an attachment of the *Acanthamoeba* trophozoites to the superficial layer of the corneal epithelium. The stroma had normal appearance formed of parallel layers of collagen fibres (Figure 4.4 b, c).

Score: 1*: Attachment of the *Acanthamoeba* to the corneal epithelium, normal stroma.

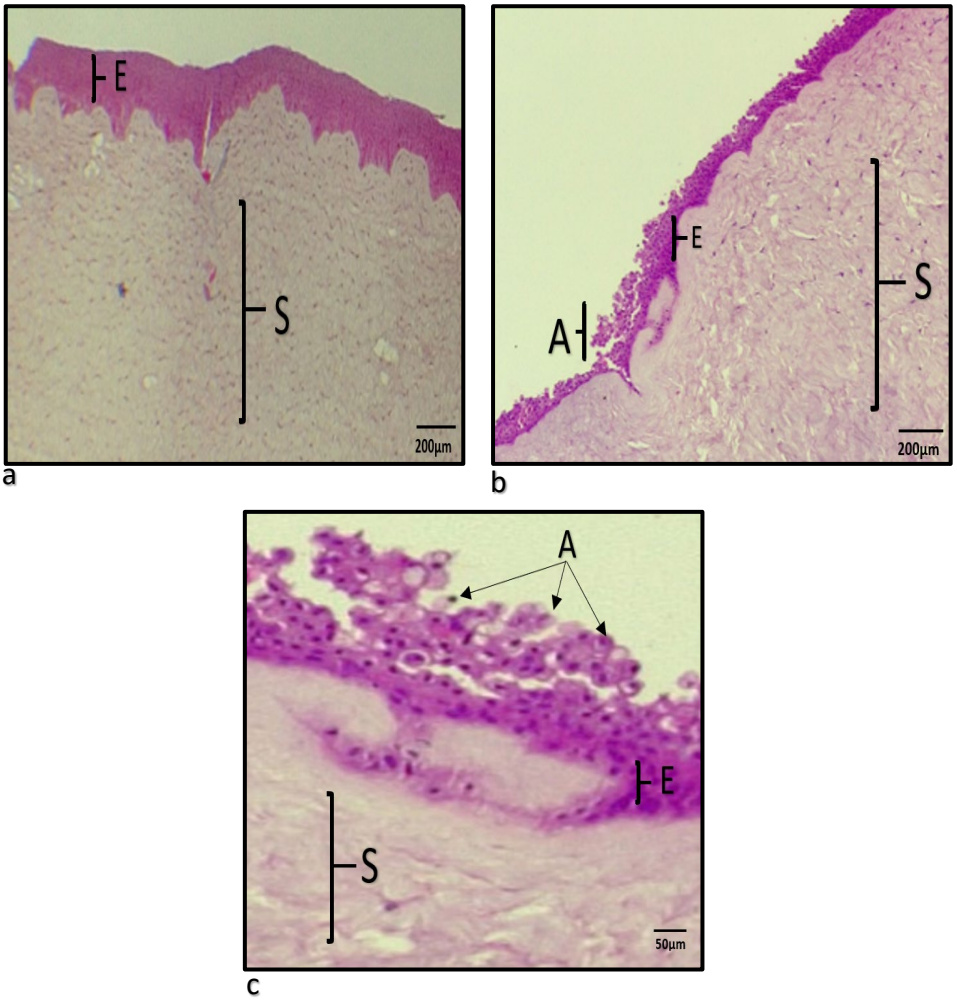

Figure 4.4: Control and infected corneas at day 3. **a**. Control: healthy control cornea with normal five to six layers squamous epithelium (E) with normal underlying stroma (S) and regular parallel collagen fibres, score 0*. **b**. Establishment of infection demonstrated by the attachment of *Acanthamoeba* trophozoites (A) to the superficial layers of the corneal epithelium (E) with normal stroma (S) formed of parallel layers of collagen fibres, score 1*. **c.** Attachment of *Acanthamoeba* (A) to the corneal epithelium. *Acanthamoeba* is recognised by its characteristic foamy cytoplasm containing conspicuous vacuoles.

4.3.2.3 Day 8

Control cornea

The cornea was examined under the light microscope. It showed normal epithelial lining with five to six layers of squamous epithelium with underlying normal stroma with regular parallel collagen fibres (Figure 4.5a). Score: 0*: Healthy cornea.

Infected cornea

The cornea showed attachment of *Acanthamoeba* trophozoites to corneal epithelium with loss of the superficial layers of the epithelium as the number of epithelial layers was around 3-4 layers in contrast to the normal 5-6 epithelial layers in normal cornea, however the appearance of stroma was normal with parallel layers of collagen fibres (Figure.4.5b).

Score 2*:Superficial loss of the outermost layers of the epithelium, normal stroma.

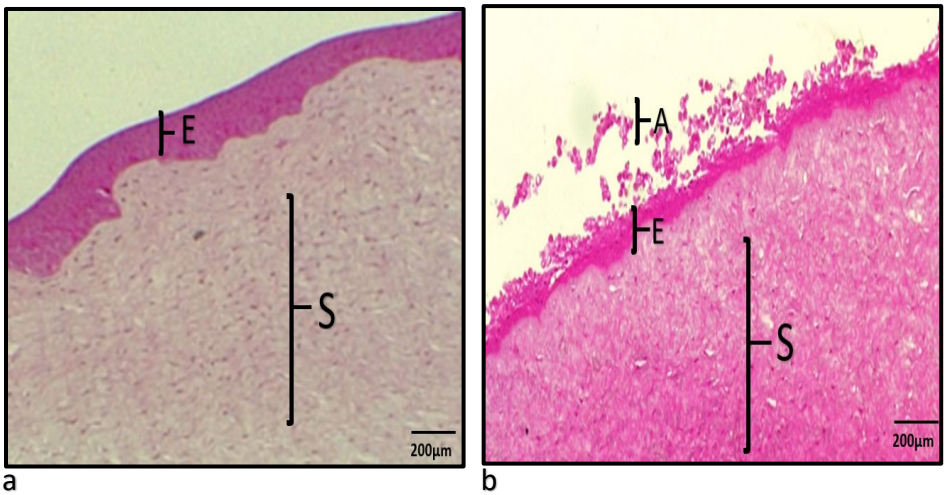

Figure 4.5: Control and infected corneas at day 8. **a**. Healthy control cornea showing normal squamous epithelium (E) with five to six layers with normal underlying stroma (S) and regular parallel collagen fibres, score: 0*. **b**. Attachment of *Acanthamoeba* trophozoites (A) to the corneal epithelium (E) with loss of the superficial layers of epithelium as the number of epithelial layers is around 3-4 layers in this cornea, the stroma (S) is normal, score 2*.

4.3.2.4 Day 13

Control cornea

The cornea was examined under the light microscope. It demonstrated normal epithelial lining with five to six layers of squamous epithelium with underlying normal stroma with regular parallel collagen fibres (Figure 4.6a). Score 0*: healthy cornea.

Infected cornea

The cornea was examined under the light microscope. There was further loss of epithelial lining as the number of epithelial layers was around 2-3 layers with parallel layers of collagen fibres within the normal stroma (Figure 4.6b).

Score: 3*: Loss of < 50% of the epithelium, normal stroma.

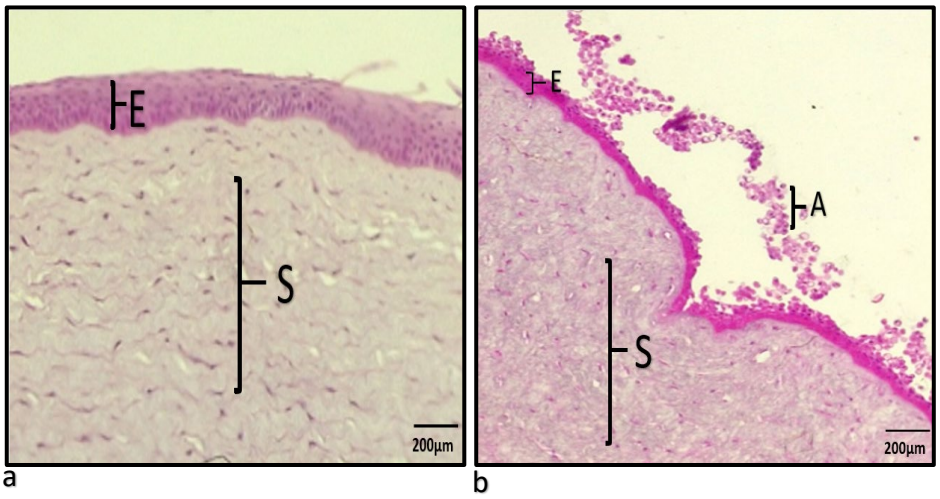

Figure 4.6: Control and infected corneas at day 13. **a**. Healthy cornea showing normal five to six layers of squamous epithelium (E) with normal underlying stroma (S) with regular parallel collagen fibres, score 0*. **b**. Infected cornea showing attachment of *Acanthamoeba* trophozoites (A) to the corneal epithelium (E) composed of 2-3 cell layers with parallel layers of collagen fibres within the normal stroma (S), score 3*.

4.3.2.5 Day 18

Control cornea

The cornea was examined under the light microscope. The epithelial lining was normal with five to six layers of squamous epithelium with normal underlying stroma with regular parallel collagen fibres (Figure 4.7a). Score: 0*: healthy cornea.

Infected cornea

The cornea was examined under the light microscope. *Acanthamoeba* trophozoites were seen invading the whole epithelium with loss of most epithelial layers demonstrated by the loss of >50% of the epithelium, and a mild disruption in the arrangement of the collagen fibres was noticed indicating mild degree of stroma oedema (Figure 4.7b).

Score: 4*: Loss of >50% of the epithelium with mild stromal oedema.

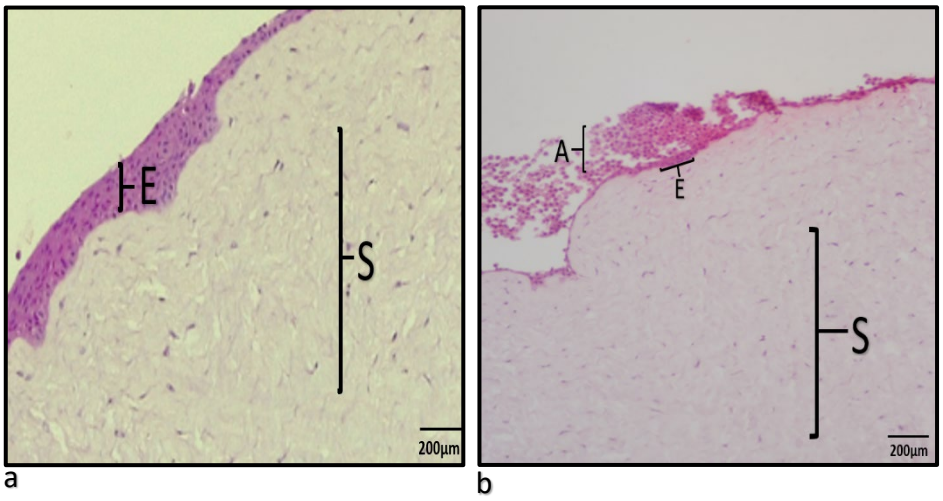

Figure 4.7: Control and infected corneas at day 18. **a**. Healthy control cornea showing normal five to six layers of squamous epithelium (E) with normal underlying stroma (S) with regular parallel collagen fibres. **b**. Infected cornea showing *Acanthamoeba* trophozoites (A) invading the whole epithelium (E) with loss of most epithelial layers, the stroma was also noticed to show mild disruption of the collagen fibres arrangement indicating a mild degree of stroma oedema, score 4*.

4.3.2.6 Day 23

Control cornea

The cornea was examined under the light microscope. It showed normal five to six layers of squamous epithelium and mild disruption of the collagen fibres arrangement indicating mild degree of stroma oedema (Figure 4.8a).

Infected cornea

The cornea was examined under the light microscope. There was total loss of the corneal epithelium and invasion of the upper part of the stroma with mild disruption of the collagen fibres arrangement indicating mild degree of stroma oedema (Figure 4.8b).

Score: 5*: Total loss of the corneal epithelium, stromal invasion in the upper part and mild stromal oedema.

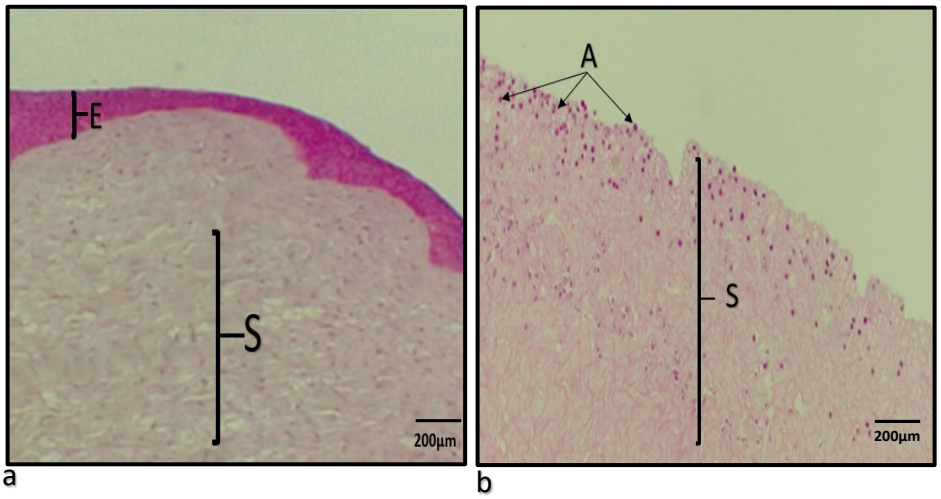

Figure 4.8: Control and infected corneas at day 23.**a.** Normal with five to six layers of squamous epithelium (E) with mild disruption of the collagen fibres arrangement indicating mild degree of stroma oedema (S). **b.** Infected cornea demonstrating total loss of the corneal epithelium with invasion of the upper part of stroma (S) by *Acanthamoeba* (A) with mild distribution of the collagen fibres arrangement indicating mild degree of stroma oedema, score 5*.

4.3.2.7 Day 28

Control cornea

The cornea was examined under the light microscope. There was a superficial loss of the outermost epithelium layers as the number of epithelial layers is around 3-4 layers in this cornea with mild disruption of the collagen fibres arrangement indicating mild degree of stroma oedema (Figure 4.9a).

Infected cornea

The cornea was examined under the light microscope. There was total loss of the corneal epithelium with stromal invasion in the upper and mid layers and mild disruption of the collagen fibres arrangement indicating mild degree of stroma oedema (Figure 4.9b).

Score: 6*: Total loss of the corneal epithelium, invasion of upper and mid layers, mild stromal oedema.

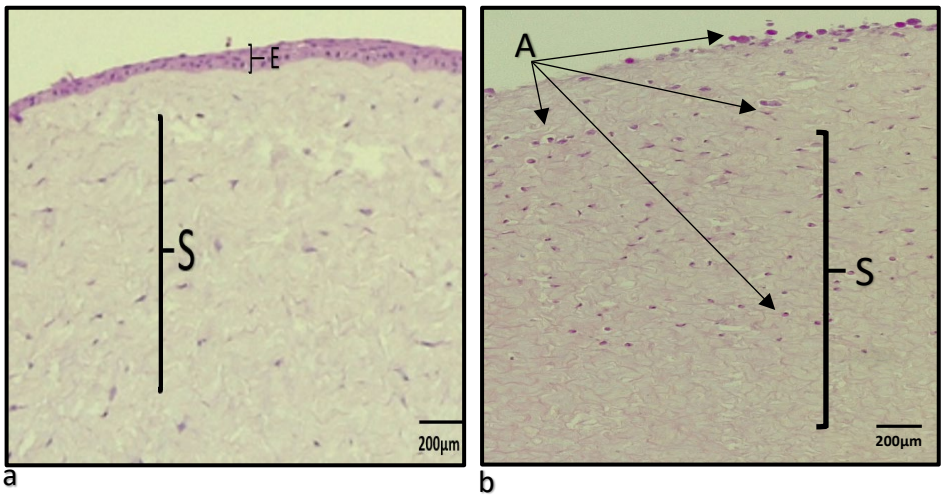

Figure 4.9: Control and infected corneas at day 28. **a.** Control cornea showing 3-4 layers of epithelium indicating lo ss of the outermost epithelial layers (E) with mild disruption of the collagen fibres arrangement indicating mild degree of stromal (S) oedema. **b.** Infected cornea demonstrating a total loss of the corneal epithelium and stromal (S) invasion in the upper and mid layers by *Acanthamoeba* trophozoites (A) with mild disruption of the collagen fibres arrangement indicating mild degree of stromal oedema, score 6*.

4.3.3 Outcome of Adding *Acanthamoeba* Cysts to Cornea

Acanthamoeba cysts were added to the medium over the corneal surface, and upon microscopic inspection on day 3, many cysts had already hatched into trophozoites and continued the same infectious process described above.

4.3.4 Outcome of Adding or Injecting Macrophages and HL-60 Cells to the Infected Cornea

The addition of macrophages and HL-60 (neutrophils) to the already infected cornea did not alter or limit the process of infection as the *Acanthamoeba* phagocytosed them (Figure 4.10).

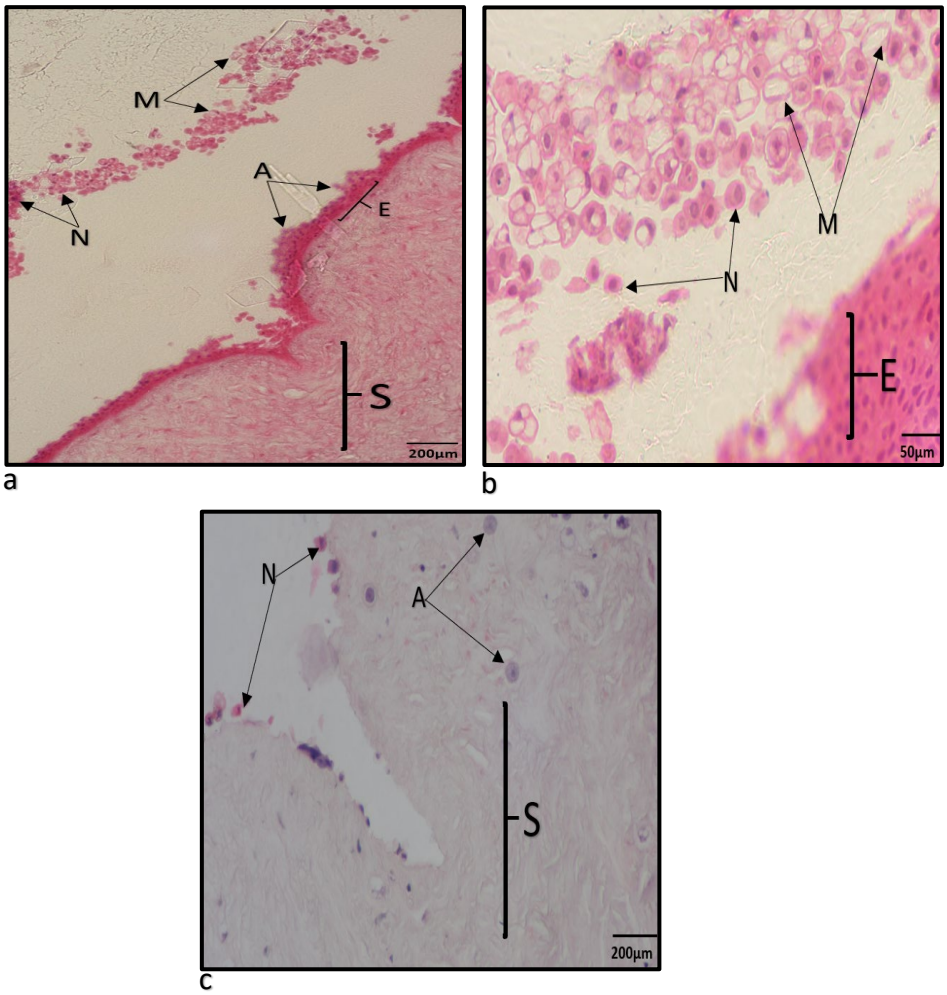

Figure 4.10: The addition of macrophages and HL-60 to the infected cornea. **a.** *Acanthamoeba* trophozoites (A) were attached to the epithelial surface (E) of the cornea with macrophages (M) and HL-60 (neutrophils) (N) seen in the slide. **b.** Macrophages demonstrated as rounded cells with abundant clear, vacuolated, cytoplasm and HL-60 cells (N) with eosinophilic (pink) cytoplasm. **c.** Total loss of the corneal epithelium and invasion of the upper part of stroma (S) by *Acanthamoeba* trophozoites (A) with mild disruption of the collagen fibres arrangement indicating mild degree of stroma oedema with scattered HL-60 cells (N).

4.4 Discussion

In this study, we used the previously established air-liquid interface rocking with CO_2 model to induce Acanthamoeba keratitis by scratching the corneal surface and introducing *Acanthamoeba* trophozoites and cysts over a period of four weeks with histological examination starting on day 3 and every 5 days afterwards. The main outcomes assessed were corneal transparency and damage to epithelium and stroma on the microscopic level.

4.4.1 Summary of Results

On the gross level, the transparency of cornea became obviously opaque on day 10, and on the microscopic examination, the attachment of trophozoites to the epithelium started on day 3 (score 1*), the earliest observed loss of the superficial epithelial layers started on day 8 (score 2*) and on day 13, less than 50% of epithelial layers were lost (score 3*). On day 18, the stroma started to demonstrate mild oedema with loss of more than 50% of epithelium (score 4*), and by day 23 the model showed complete loss of epithelial layers and mild stromal oedema with trophozoites invading the upper part of the stroma (score 5*) which further invaded the middle parts of the stroma by day 28 (score 6*).

The results demonstrate the usability of the *ex vivo* model to induce Acanthamoeba keratitis and monitor the progression of the infection in the absence of host immune response by observing the spread of infection from initial attachment to corneal epithelial cells until the invasion of corneal stroma. To our knowledge, this is the first *ex vivo* model developed to study the disease progress of Acanthamoeba keratitis for an extended period of 4 weeks.

When culturing corneas with *Acanthamoeba* cysts, most of these cysts hatched into trophozoites following the adhesion to the epithelium which served a source of nutrition beside the nutrient medium. It is well demonstrated across literature that the presence of the carbohydrate mannose in the membrane of the host cell is fundamental for pathogenic *Acanthamoeba* to adhere to cells by the interaction between the mannose on the corneal cell with the mannose-binding proteins (MBP) in the membrane of the amoebae which is reported to exert one of the strongest pathogenic mechanisms of *Acanthamoeba* (Huth *et al.,*2017).

4.4.2 Inducing the Infection

In this current study, we introduced *Acanthamoeba* to the model after inducing injury to the cornea by scratching its surface. The interactions between corneas and microbes were extensively studied in previous research (*in vivo, in vitro* or *ex vivo*) explaining how bacteria and fungi are introduced into corneas and the two main methods described were corneal scratching (Blaylock *et al.,*1990, Kwong *et al.,*2007) and intrastromal injection (Butler *et al.,*2001, Barequet *et al.,* 2012).

A study in 2017 supported the results of this current study where researchers evaluated infections of single versus mixed species of *Staphylococcus aureus*, *Pseudomonas aeruginosa*, *Candida albicans* and *Fusarium solani* in both human and rabbit corneas by both scratching and injection methods and they endorsed scratching method to better mimic the mechanism of clinical infection of the human eye that is usually initiated by a mechanical abrasion to the corneal surface (Pinnock *et al.,2017)*. Different to their study, our work is exclusively focused on studying *Acanthamoeba* which was not part of the microorganisms they used in

their research, and our model was developed using pig corneas while they used human and rabbit corneas.

In ‘ Pinnock *et al.’* study they scratched the cornea with a scalpel, and a metal ring was placed on the centre of the cornea to create a watertight seal then they inoculated 1 x 10^8 of the above-mentioned microorganisms were either added or injected in the cornea using a 26-gauge needle. In our study we used a scalpel to induce the epithelial injury before adding 5µL of 1x 10^5 /mL *Acanthamoeba* trophozoites or cysts without using metal rings or using the injection method.

In ‘Pinnock *et al.*’ study, the duration of the experiment was short (24 hours – 48 hours) which is very brief however they were able to demonstrate corneal haziness caused by the infection and the histological sections demonstrated infiltration of *Staphylococcus aureus, Pseudomonas aeruginosa, Candida albicans* and *Fusarium solani* within the corneal layers with variable degrees of infiltration. In this current study, we were able to follow the progression of infection in the *ex vivo* model for four weeks and were equally able to demonstrate the effect of the infection evident by corneal haziness and histological sections showing invasion of the microorganism into corneal layers. The long duration upon which this current study was performed, hugely facilitates the study of disease pathogenicity, host-pathogen interaction and facilitates investigating and trialling different treatment options.

4.4.3 Pathogenesis and Previous Studies

The first step we observed under the light microscope was the attachment of the originally cultured trophozoites and the ones stemming from cysts to the corneal epithelium. The cyst stage helps *Acanthamoeba* to survive in extreme conditions until excystation process starts in more favourable conditions with the presence of glutamic acid and other amino acids (Krishna *et al.,*1984) which were available to the cysts after they were added to the cornea and nutrient medium.

The attachment process was observed on day 3 of this experiment under the light microscope as shown in Figure 4.4 and it is considered a critical step in inducing infection (Panjwani,2010) that was extensively studied by many researchers (Jaison *et al.,*1998, Kenett *et al.,*1992, Yang *et al.,*1997). The carbohydrate mannose proteins in the membrane of the cornea stimulates *Acanthamoeba* to secrete a mannose-induced 133 kDa protease (MIP133), which in turn interacts with phospholipids on plasma membrane of the corneal cells and activates the cytosolic phospholipase A_2 that plays an integral role in apoptosis by activating proinflammatory cytokines from the corneal cells facilitating the crossing of biological barriers and destruction of the host cell (Tripathi *et al.,* 2012, Lorenzo-Morales *et al.,* 2015).

The second step we observed under the light microscope following the attachment was the destruction of the epithelium. The destruction starts from superficial layers down to the basal layers and is facilitated by the phagocytosis mechanism that engulfs epithelial cells which ultimately leads to further invasion, tissue damage and cytolysis by proteolytic enzymes such as metallo and cysteine proteases which degrade and digest extracellular targets (Niederkorn *et al.,*1999).

A study from 2004 supported our observations regarding the attachment and tissue destruction process where the authors monitored the early steps within the first 12 hours of the interaction of *Acanthamoeba* trophozoites with corneas harvested from hamsters by using both light and scanning electron microscope (SEM) (Omaña-Molina *et al.,*2004). Using light microscopy, they observed adherence of trophozoites to the surface of corneal epithelium at hour 1, further advancement between the superficial epithelial cell layers at hour 2, extended damage to the middle layers at hour 4, and after prolonged periods at 8 and 12 hours the basal cell layer was completely disorganised but no *Acanthamoeba* was seen to extend beyond the basal layer into the stroma however in our study we were able to observe the invasion of the stroma from day 23 as shown in Figures 4.8 and 4.9.

In 'Omaña-Molina *et al.*' study, they used SEM to study the morphological changes during the infection process and they reported that *Acanthamoeba* showed amebostome-like structures once became in contact with host cells, suggesting that phagocytosis of the target cells is vital to the pathogenesis process. They also noticed morphological differences between the trophozoites incubated with corneas and the trophozoites kept in medium culture only as the former demonstrated wide body with large abundant acanthapodia and the latter showed a flattened appearance with short acanthapodia. The work presented in this chapter was based on light microscopy findings and no SEM was used.

A similar study (Moore *et al.,1991)* also supported our observations regarding the attachment and tissue destruction process in which *Acanthamoeba castellanii* trophozoites were added to the medium and cultured for 12 hours in corneas obtained from humans, and it was demonstrated through their work that the

attachment of the trophozoites is followed by destruction of the epithelium mainly at the periphery of the cornea.

The outcome of our study is consistent with the above discussed studies 'Omaña-Molina *et al.,* 2004, Moore *et al.,1991'* in the observations regarding the *ex vivo* progression of Acanthamoeba keratitis starting by *Acanthamoeba* adhesion, epithelial destruction and tissue invasion. The main differences between their work and this current study are that their observations were limited to the first 12 hours while our study continued for 28 days. The corneas they used were from hamster and human eyes while this current study used pig corneas. The authors also used both light and electron microscopes to evaluate the progression of infection while we used light microscopy only . In their studies, the adhesion of the trophozoites to the corneal epithelium started within hours in contrast to our study where it took days for the *Acanthamoeba* to succeed in adhesion step. This is likely due to the use of the rocking model in our study that mimics the blinking of the eyelid as a defensive mechanism against pathogens that perhaps washes *Acanthamoeba* leading to less bonding to the receptors hence less production of MIP133 which might in turn be further washed by the rocking effect.

4.4.4 Previous Studies on Macrophages

In this current study, we investigated the effect of adding and injecting macrophages and HL-60 cells (neutrophils) to the *ex vivo* infected corneas given the fact that this *ex vivo* model lacks these naturally existing immune cells that normally migrate from blood stream to the site of infection. Macrophages are the first line of defence against most infectious diseases where monocytes migrate from blood stream to the site of infection then differentiate into macrophages (Auffray *et al.,*2009). Macrophages are present in high numbers in corneas with Acanthamoeba keratitis highlighting its importance in controlling and resisting *Acanthamoeba* infection (Klink, *et al.,*1996) beside other phagocytic cells like neutrophils (Ferrante,1991) which are chemotactically attracted to *Acanthamoeba* and can kill trophozoites (Marciano-Cabral *et al.,*1998, G.L. Stewart *et al.,*1992).

Our study shows no alteration or limitation to the process of infection as the added cells might have been phagocytosed or destroyed by the *Acanthamoeba*. A previous study conducted on 1998 supports this observation as they cultured different *Acanthamoeba* strains (*Acanthamoeba culbertsoni, Acanthamoeba castellanii*, and *Acanthamoeba polyphaga*) with macrophages obtained from eight-week-old mice and stated that the highly pathogenic *Acanthamoeba* strains (*Acanthamoeba culbertsoni*) resisted the amoebicidal activity of macrophages and destroyed them compared to less pathogenic strains (*Acanthamoeba castellanii* and *Acanthamoeba polyphaga*) (Marciano-Cabral *et al.,* 1998). Considering the above, *Acanthamoeba* strains used in our study were fed on HEp-2 cells in three-step passage process as discussed in section 4.2.2 which ultimately boosted the pathogenicity of *Acanthamoeba,* and this potentially explains how *Acanthamoeba* might have been able to destroy the added macrophages and HL-60 cells in the

established *ex vivo* model similar to the above-mentioned study (Marciano-Cabral et al., 1998) that demonstrated the destruction of macrophages by highly pathogenic *Acanthamoeba* strains compared to less pathogenic ones.

4.5 Conclusion and Future Work

It is demonstrated through the work in this chapter that we were able to establish an *ex vivo* model for Acanthamoeba keratitis for a period of four weeks that is reproducible and mimics the natural human infection. This model can be further used for many applications including: diagnostic approaches, treatment options and investigating risk factors linked to Acanthamoeba keratitis.

Chapter Five

Application of the Porcine *Ex Vivo* Model: Drugs

Chapter 5: Application of the Porcine *Ex Vivo* Model: Drugs

5.1 Introduction

5.1.1 Acanthamoeba Keratitis

Acanthamoeba is a virtually ubiquitous free-living amoeba with two stages in its life cycle; the active trophozoites stage and the dormant cyst stage (Kovacs *et al.*,2015). It infects healthy immunocompetent individuals causing a potentially blinding infection of the eye called Acanthamoeba keratitis (AK) mainly among contact lens wearers.

5.1.2 Treatment- PHMB

There is no licensed treatment for AK; however, the current unlicensed therapy is available on a named patient-based approach and consists of topical therapy of either polyhexamethylene biguanide (PHMB) 0.02% (v/v) or chlorhexidine digluconate 0.02% (v/v) alone or in combination with propamidine isethionate (Brolene™) 0.1% (w/v) or hexamidine diisethionate (Desomedine®) 0.1% (w/v) (Papa *et al.,*2020). PHMB (Figure 5.1) is a synthetic cationic polymer that is formed of repeating basic units of biguanide that are interconnected by hexamethylene hydrocarbon chains (Chindera *et al.,*2016).

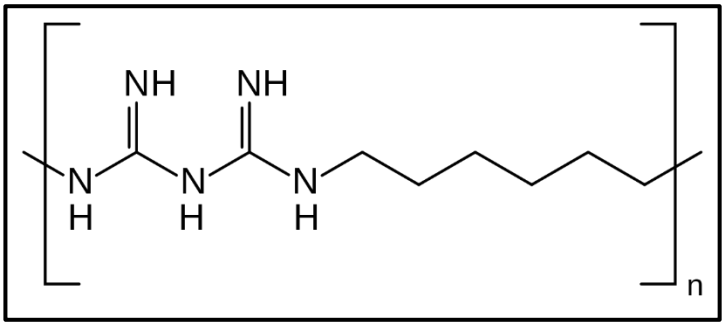

Figure 5.1: Molecular structure of PHMB (Ansorg *et al.,*2003)

The duration of treatment ranges between 6 months to 29 months (Lorenzo-Morales *et al.,*2015). Despite this therapy, many patients remain persistently culture positive, 30% lose some degree of their vision, 11% require repeated corneal transplantation and up to 5% have the eye surgically removed (Dart *et al.,*2009).

5.1.3 Treatment- Doxycycline

Doxycycline is a drug frequently used for the treatment of ocular surface diseases, especially recurrent epithelial cell erosions where spontaneous breakdown of corneal epithelium occurs repeatedly due to many factors like minor mechanical trauma, diabetes mellitus, ocular rosacea and corneal dystrophies (Durson *et al.,*2001). Doxycycline acquires its therapeutic effect by its effectiveness at inhibiting matrix metalloproteinase (MMP) activity of corneal epithelial cells (Golub *et al.,*1995).

Doxycycline is a broad-spectrum antibiotic well recognised for its effectiveness against a multitude of bacterial and parasitic infection including bacterial pneumonia, chlamydia, Lyme's disease, Typhus, Syphilis and Cholera (Navarro-Triviño *et al.,*2019) and doxycycline is also used as a prophylaxis for malaria, (Gaillard *et al.,*2018).

5.1.4 Rationale

Many researchers investigated the efficacy of commonly used drugs in treating Acanthamoeba keratitis by studying the effect on the viability of the parasite and the potential toxicity to the keratocytes. However, up to our knowledge, no previous studies were performed on an *ex vivo* model like the Acanthamoeba keratitis model established in this study and so in this chapter we will use the model to study the drug effect against *Acanthamoeba*.

5.1.5 Aim and Objectives

The model will be utilized to test two pharmacological agents in terms of activity against *Acanthamoeba* and toxicity against the corneal epithelial layer. The objectives are:

- Study *ex vivo* activity of polyhexamethylene biguanide (PHMB) against *Acanthamoeba* to investigate its efficacy in controlling the progression of Acanthamoeba keratitis and to study the toxicity against the epithelial layer of the cornea.

- Study *ex vivo* activity of doxycycline against *Acanthamoeba* to investigate its efficacy in controlling the progression of Acanthamoeba keratitis and to study the toxicity against the epithelial layer of the cornea.

5.2 Methods

PHMB (Cosmocil CQ 20% (w/v), Lonza, U.K) and doxycycline (Scientific Laboratory Supplies Ltd, Nottingham, U.K) were screened to evaluate their efficacy against *Acanthamoeba castellanii* and *Acanthamoeba polyphaga* using both amoebicidal and cysticidal assays and were tested also against HEp-2 cells to detect possible toxicity. This step took place before applying the drugs on the *ex vivo* model.

5.2.1 Test Organism Strains and Culture

The strains used in this study were *A. castellanii* (ATCC 50370) and *A. polyphaga* (ATCC 30461) (LGC Standards, Teddington, UK). Trophozoites culture and cysts production are described in detail in chapter 2 section 2.3, 2.6 and 2.7.

5.2.2 Drug Sensitivity Testing

5.2.2.1 Amoebicidal Assay

To test potential antimicrobial activity of the test compounds, the plate was prepared by adding 200 µl of 1000µg/mL solution of test compound to column 1 row A-H of the 96 well microtiter plate, and the other wells were filled with 100µl of ¼ strength Ringer's solution, then serial 2-fold dilution was done through the plate from column 1-11 to achieve final drug concentrations in the range 500 to 0.49 µg/mL. Column 12 contained only ¼ strength Ringer's to act as a control (Figure 5.2).

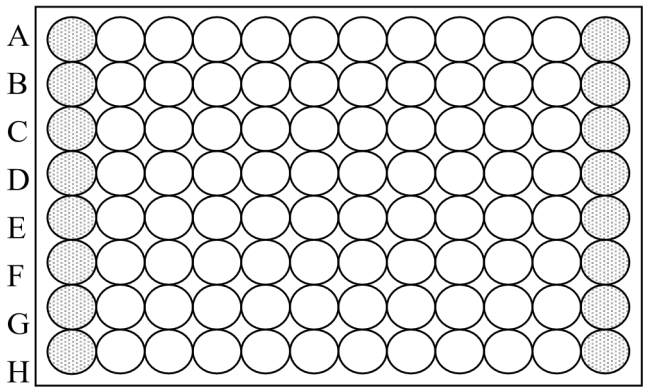

Figure 5.2: The layout of the microtiter plate for the sensitivity testing.

Trophozoites were suspended in their growth medium (Ac#6) and cysts were suspended in ¼ strength Ringer's then added to the wells to give a final concentration of 1×10^4 cells/mL to achieve the requisite concentration.

The wells were checked after 24 hours for contamination. At 48 hours, the wells were checked again under inverted microscope at x 10 objective and x 20 objective to compare the test wells to the control to determine the:

- Minimum trophozoite inhibitory concentration (MTIC) that means 50% inhibition of *Acanthamoeba* trophozoites.
- Minimum Trophozoite Amoebicidal Concentration (MTAC) which means all trophozoites are non-motile and or lysed.

5.2.2.2 Cysticidal Assay

For the cyst assay, the plate was kept for 48 hours in the incubator at 32°C. Following that, the liquid was expelled from the 96 wells plate by inverting them sharply leaving the cysts attached to the bottom of the wells. ¼ strength Ringer's was filled in the wells and left for 15 minutes to allow the cysts to reattach and then the liquid was removed as before. This process was repeated 3 times to fully remove the drug. *E. coli* was added to each well and the plates were incubated at 32°C and checked daily for up to 7 days to see if the alive cyst excysted and the trophozoites replicated, and to determine the minimum cysticidal concentration (MCC) which means the lowest concentration of test solution that results in no excystation and no trophozoites replication.

5.2.3 Toxicology Assay

This method is used to determine the toxic effect of compounds to human cells. 96 microtiter plate was seeded with 2×10^4 cells/mL of the HEp-2 (HeLa derivative) human cervix carcinoma cell line (ECACC number 86030501) obtained from the European Collection of Cell Cultures (Centre for Applied Microbiology and Research, Salisbury, UK). Cells were incubated at 37°C, 5% CO_2 for 48 hours to allow the cells to achieve 80-90% confluence. After that, the test compound was diluted to two-fold serial dilution across the plate achieving a range of concentration in the range 500-0.49 µg/mL.

To determine the toxic effects of the test compounds, a colorimetric method called CellTiter 96® AQuous One Solution Cell Proliferation Assay (Promega, Southampton, U.K.) was used. This method uses the tetrazolium MTS compound

[3-(4, 5-dimethylthiazol-2-yl)-5-(3-carboxy methoxyphenyl)-2-(4-sulfophenyl)-2H-tetrazolium salt] with PES (Phenazine ethosulfate) which is an electron coupling agent. In active cells, the MTS is reduced by NADPH (Nicotinamide adenine dinucleotide phosphate hydrogen) producing a coloured formazan product. 5 µl of cell titter 96 assay was added to each well in the plate and then incubated for 1-2 hours at 37°C, 5% (v/v) CO_2. The amount of the coloured product was then measured in a multiplate reader at 595 nm.

As a confirmation step to support the CellTiter 96 assay, the toxicity was also checked visually using a light microscope (x10 eye piece, x20 objective) to determine:

- Minimum Inhibitory Concentration (MIC) at which inhibition of cell division and localised detachment of the cells occurred compared to the control well.
- Minimum Cytotoxic Concentration (MCT) at which all Hela cells were rounded and lysed with general detachment.

5.2.4 Applying the Drugs on The *Ex Vivo* Model

PHMB was used in the same concentration used in clinical practice (0.02% v/v), and doxycycline was used as recommended in the literature (0.1% w/v). *Acanthamoeba* trophozoites and cysts were added to the corneas as described in chapter 4 section 4.2.5 and were left for four days to initiate the infection process. Following this step, 5µL of each drug were added to the respective corneas directly to the surface using a pipette to mimic the application of eye drops to the eyes of patients with Acanthamoeba keratitis (Figure 5.3).

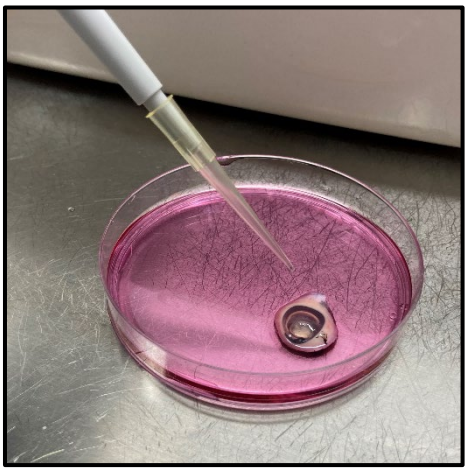

Figure 5.3: Adding the drug to the corneal surface.

The process was repeated daily, and every 3-4 days a histological section was taken looking for any changes under the light microscope. Histological changes were compared to the control corneas that were divided into two control groups: healthy corneas with no induced infection or added drugs and healthy corneas with added drugs but no induced infection.

5.3 Results

5.3.1 Drug Assays

PHMB and doxycycline were used to evaluate their efficacy against *Acanthamoeba castellanii* and *Acanthamoeba polyphaga* using both amoebicidal and cysticidal assays. The toxicity of these drugs against HEp-2 cells was also evaluated. The results are shown in the table below.

	A. castellanii (50370)			*A. polyphaga (*30461)			HEp-2
Drug	MTIC*	MTAC**	MCC***	MTIC*	MTAC**	MCC***	MCT
PHMB	1	3.9	15.6	1	7.8	7.8	31.3
Doxycycline	625	1250	2500	625	1250	2500	625

*Minimum trophozoite inhibitory concentration, **Minimum trophozoite amoebicidal concentration, *** Minimum cysticidal concentration, MCT Minimum cytotoxic concentration.

Table 5.1: Activities of tested drugs against the trophozoites and cysts of *A. castellanii* (ATCC 50370) and *A. polyphaga* (ATCC 30461) and their toxicity against HEp-2 cells.

Regarding PHMB, the trophozoite assay showed that the MTIC is 1µg/mL for both species and the MTAC activity is 3.9 µg/mL for A. *castellanii* and 7.8 for A. *polyphaga*, while the MCC activity is 15.6 for A. *castellanii* and 7.8 µg/mL for A. *polyphaga*, with HEp-2 toxicity assay of 31.3 µg/mL.

Doxycycline does not exert any major antimicrobial effect on the viability of *Acanthamoeba* in comparison with PHMB as it achieved a MTIC of 625 µg/mL and MTAC of 1250 µg/mL, respectively. Doxycycline showed very low toxicity against human cells in the 625µg/mL range.

5.3.2 Histological Sections - PHMB

5.3.2.1 Day 3, Control

The control for healthy cornea (Figure 5.4a) was examined under the light microscope. It showed normal epithelial lining of healthy five to six non-keratinized, stratified squamous epithelium and normal stroma which contained regularly spaced collagen oriented in a uniform parallel direction to maintain transparency.

The control for infected cornea at day 3 (Figure 5.4b) was examined under the light microscope and there was an attachment of the *Acanthamoeba* trophozoites to the superficial layer of the corneal epithelium. The stroma was normal and formed of parallel layers of collagen fibres.

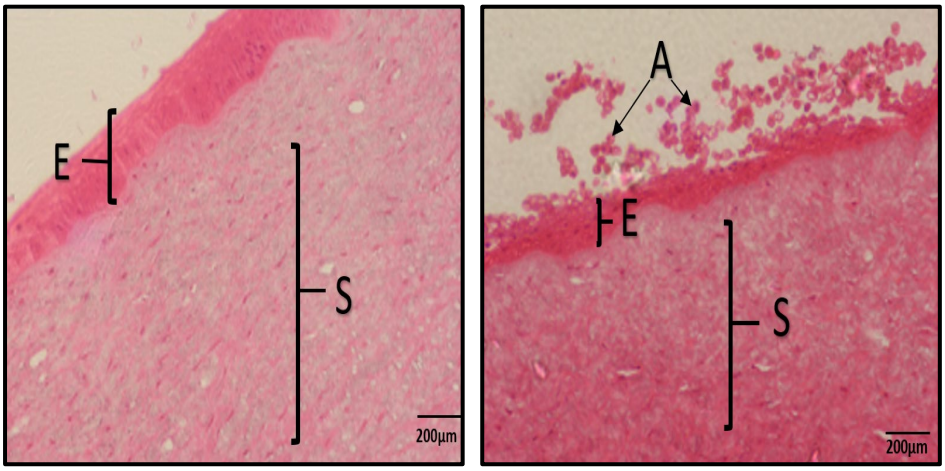

Figure 5.4: Histology sections, control versus infected cornea, day 3. **a**. Normal cornea with five to six layers squamous epithelium (E) with underlying normal stroma (S) with regular parallel collagen fibres. **b**. Establishment of infection demonstrated by the attachment of *Acanthamoeba* trophozoites (A) to the superficial layers of the corneal epithelium.

5.3.2.2 Day 7 – Control and Test Corneas

The healthy cornea with added PHMB was examined under the light microscope and it showed normal epithelial lining of healthy five to six non-keratinized, stratified squamous epithelium and normal stroma with parallel layers of collagen fibres (Figure 5.5b).

In the infected cornea with no added PHMB (Figure 5.5c), the *Acanthamoeba* trophozoites were seen attached to the corneal epithelium to start the invasion process, however the stroma was normal. In the Infected cornea with added PHMB (Figure 5.5 c), light microscopy examination showed dead trophozoites at the stage of attachment to the superficial layers of the epithelium. The cells were reported as dead because of the loss of the integrity of its plasma membrane and some of these cells showing complete fragmentation into discrete bodies (apoptotic bodies). The basal epithelial layers were still preserved, and the stroma was normal (Figure 5.5 d,e).

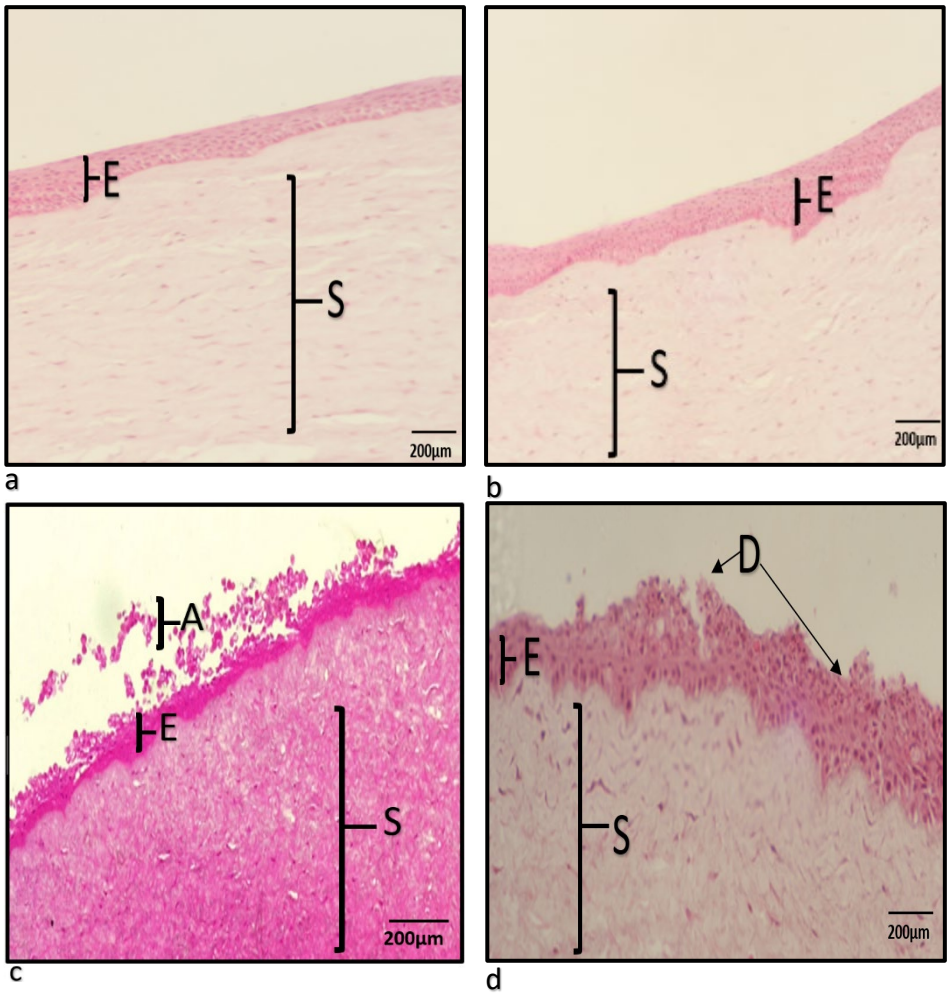
E
S
200µm
a
E
S
200µm
b
A
E
S
200µm
c
D
E
S
200µm
d
D
S
E
100µm
e

Figure 5.5: Histology sections, healthy versus infected cornea, day 7, added PHMB. **a.** Control cornea with healthy five to six non-keratinized, stratified squamous epithelium(E) and normal stroma (S) with parallel layers of collagen fibres. **b.** Healthy cornea with added PHMB showing five to six non-keratinized, stratified squamous epithelium (E) and normal stroma (S) with parallel layers of collagen fibres. **c.** *Acanthamoeba* trophozoites were attached to the corneal epithelium starting the invasion process. **d.** Infected cornea with added PHMB showing dead trophozoites (D) at the stage of attachment to the superficial epithelial layers. **e.** Higher magnification of image d.

5.3.2.3 Day 10 – Control and Test Corneas

The healthy cornea (with added PHMB) was examined under the light microscope. It showed loss of the superficial layers of epithelium as the number of epithelial layers is around 3-4 layers in this cornea contrast to the normal cornea with healthy five to six non-keratinized, stratified squamous epithelium, however the stromal layers are normal with parallel layers of collagen fibres (Figure 5.6b).

Examination of the infected cornea with no added PHMB shows *Acanthamoeba* trophozoites invading the epithelium with loss of the superficial layers of the epithelium, however there was normal appearance of the stroma (Figure 5.6c).

The infected cornea with added PHMB showed dead trophozoites and shedding of the epithelium with normal stroma (Figure 5.6 d).

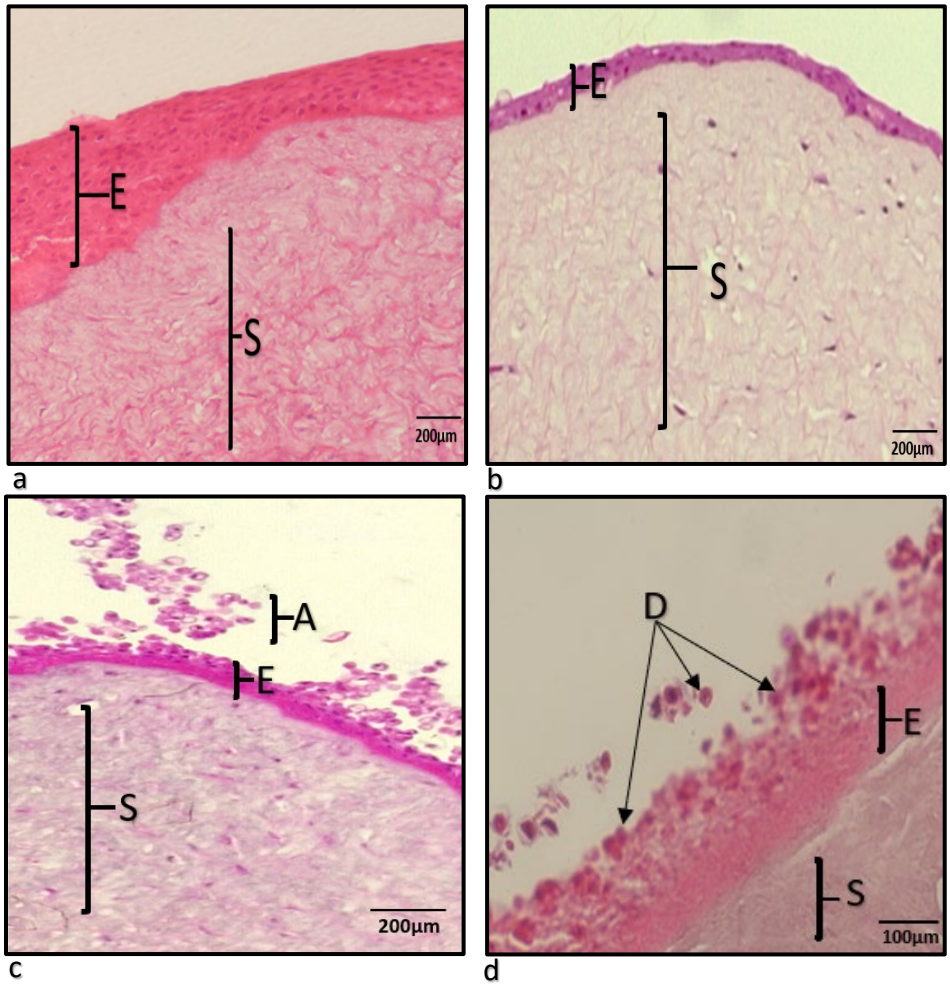

Figure 5.6: Histology sections, healthy versus infected cornea, day 10, added PHMB. **a.** Control cornea with healthy five to six non-keratinized, stratified squamous epithelium(E) and normal stroma (S) with parallel layers of collagen fibres. **b.** Cornea with added PHMB: loss of the superficial layers of epithelium as the number of epithelial layers is around 3-4 layers in this cornea and normal stromal. **c.** Infected cornea with no added PHMB showed *Acanthamoeba* trophozoites invading the epithelium with loss of the superficial layers of the epithelium. **d.** Infected cornea with added PHMB day 10: dead trophozoites (D) with shedding of the epithelium with normal stroma.

5.3.2.4 Day 14- Control and Test Corneas

The healthy cornea with added PHMB was examined under the light microscope. It showed further loss of the epithelial layers which was around 2-3 layers with parallel layers of collagen fibres within the normal stroma (Figure 5.7b).

The infected cornea with no added PHMB showed *Acanthamoeba* trophozoites invading the epithelium with loss of many layers of the epithelium; however, the stroma was still normal (Figure 5.7c).

Examination of the infected cornea with added PHMB demonstrated fragmented cells with apoptotic bodies and shadows of dead cells where only the outline of the cell could be seen. The stroma was normal (Figure 5.7d).

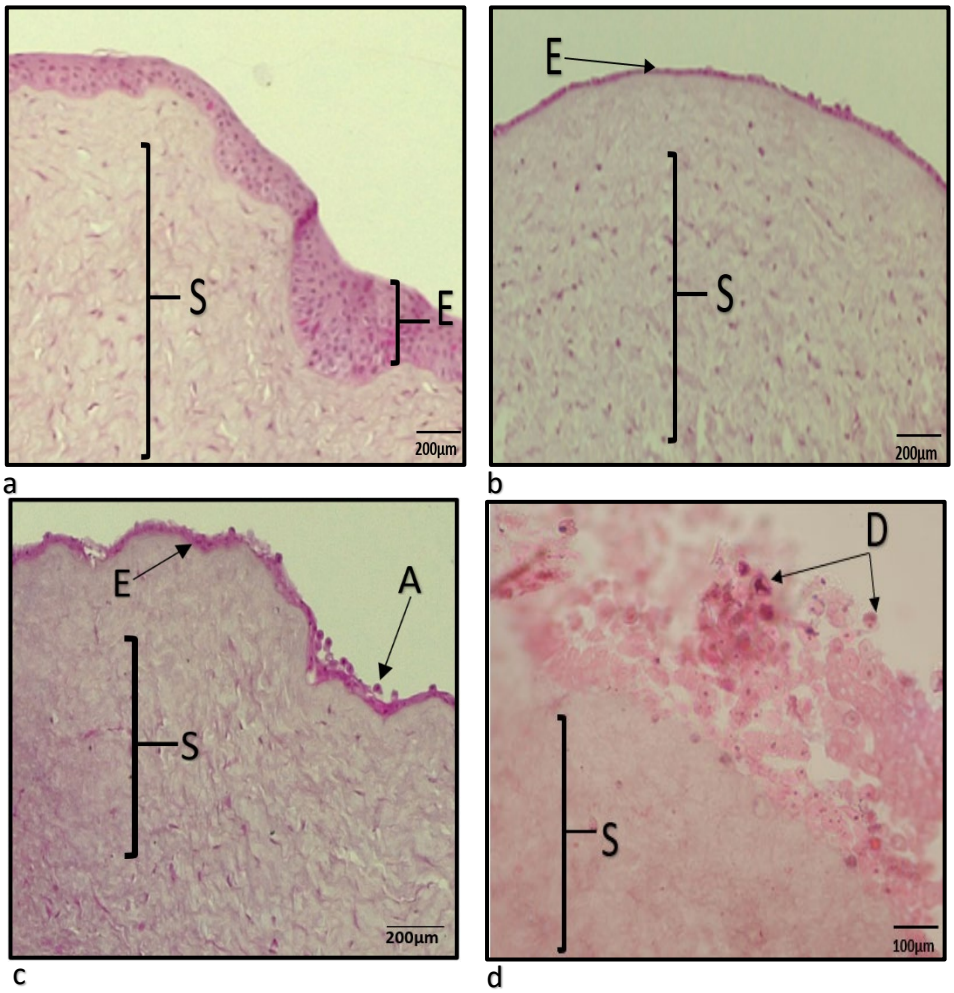

Figure 5.7: Histology sections, healthy versus infected cornea, day 14, added PHMB. **a.** Control cornea with healthy five to six non-keratinized, stratified squamous epithelium (E) and normal stroma (S). **b.** Cornea with added PHMB: further loss of epithelial lining as the number of epithelial layers is around 2-3 layers in this cornea with normal stroma. **c.** Infected cornea with no added PHMB showing *Acanthamoeba* trophozoites (A) invading the epithelium (E) with loss of many layers of the epithelium. **d.** Infected cornea with added PHMB day 14: fragmented cells with apoptotic bodies and shadows of dead cells (D) with normal stroma.

5.3.3 Histological Sections - Doxycycline

5.3.3.1 Day 3, Controls

The control cornea was examined under the light microscope, and -as stated earlier- it showed normal epithelial lining of healthy five to six non-keratinized, stratified squamous epithelium and normal stroma which contained regularly spaced collagen fibres oriented in a uniform parallel direction (Figure 5.8a).

The control for infected cornea was examined under the light microscope and there was an attachment of the *Acanthamoeba* trophozoites to the superficial layer of the corneal epithelium and the stroma was normal (Figure 5.8b).

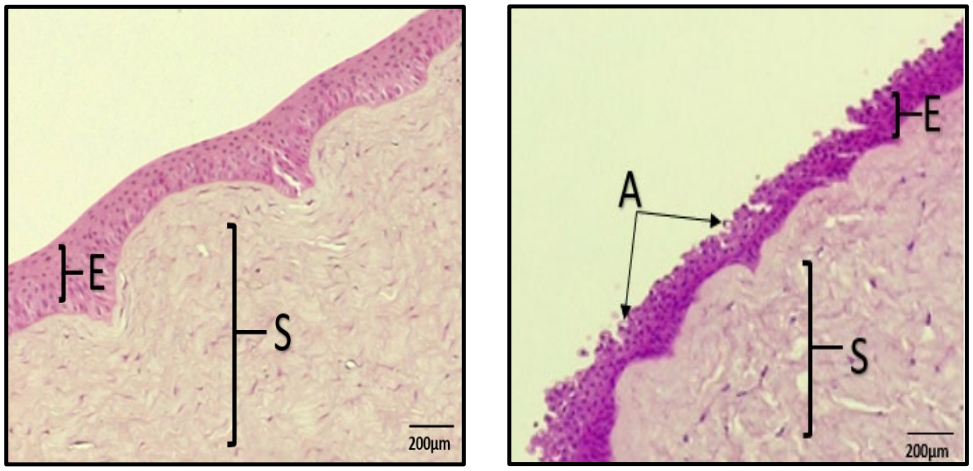

Figure 5.8: Histology sections, control versus infected cornea, day 3. **a.** Normal cornea with healthy five to six non-keratinized, stratified squamous epithelium (E) and normal stroma (S) with parallel layers of collagen fibres. **b.** Attachment of the *Acanthamoeba* trophozoites (A) to the superficial layer of the corneal epithelium.

5.3.3.2 Day 7, Control and Test Corneas

The healthy Cornea with added doxycycline was examined under the light microscope. It showed normal epithelial lining with healthy five to six non-keratinized, stratified squamous epithelium and normal stroma with parallel layers of collagen fibres (Figure 5.9b).

Examination of the infected cornea with no added doxycycline showed *Acanthamoeba* trophozoites attached to the corneal epithelium to start the invasion process and the stroma was normal (Figure 5.9c). The Infected cornea with added doxycycline was examined under the light microscope. The *Acanthamoeba* trophozoites were viable and attached to the corneal epithelium to start the invasion process, normal stroma (Figure 5.9d).

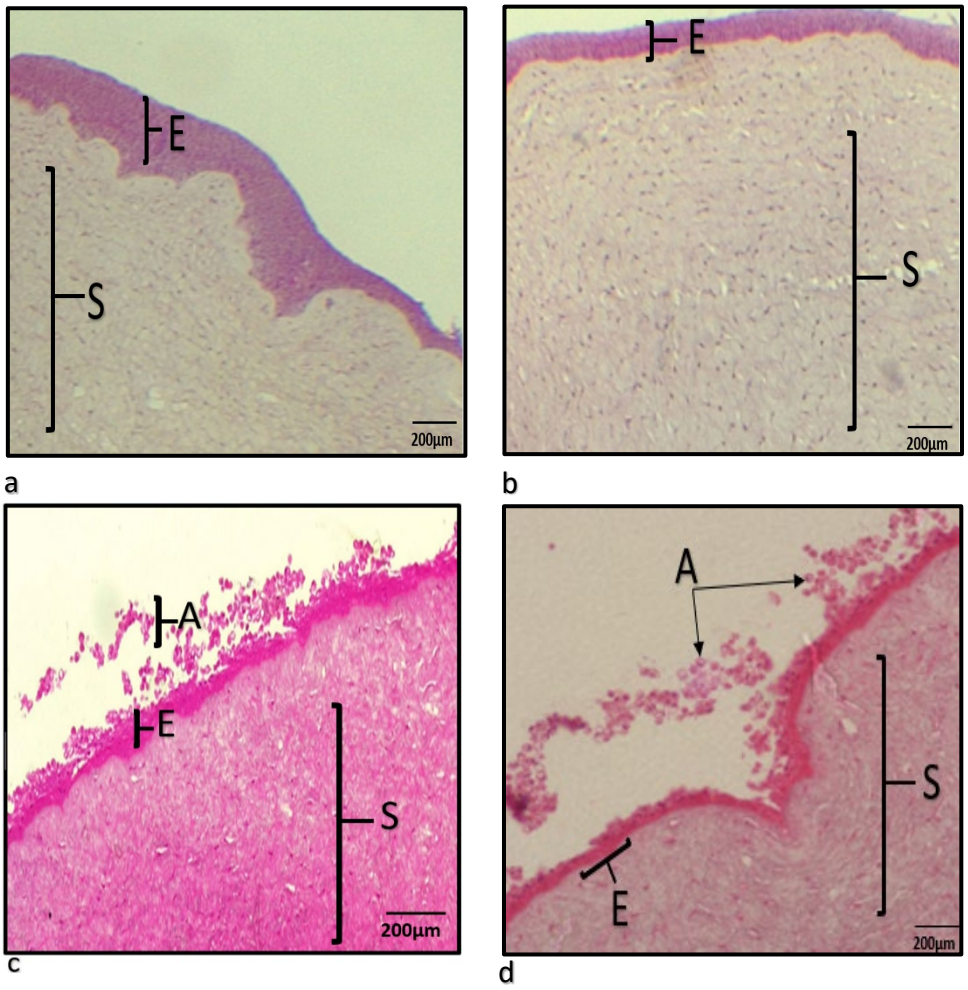

Figure 5.9: Histology sections, healthy versus infected cornea, day 7, added doxycycline. **a.** Control cornea with healthy five to six non-keratinized, stratified squamous epithelium (E) and normal stroma (S). **b.** Cornea with added doxycycline: normal cornea with healthy five to six non-keratinized, stratified squamous epithelium (E) and normal stroma (S). **c.** Infected cornea with no added doxycycline: attachment of *Acanthamoeba* trophozoites (A) to the epithelium. **d.** Infected cornea with added doxycycline: Viable *Acanthamoeba* trophozoites (A) invading the epithelial layers of this cornea, normal stroma.

5.3.3.3 Day 10, Control and Test Corneas

The healthy cornea with added doxycycline- was examined under the light microscope. It showed normal epithelial lining with healthy five to six non-keratinized, stratified squamous epithelium and normal stroma with parallel layers of collagen fibres (Figure 5.10b).

Examination of the Infected cornea with no added doxycycline- showed *Acanthamoeba* trophozoites invading the epithelium with loss of the superficial layers of the epithelium and the stroma was normal (Figure 5.10c).The Infected cornea with added doxycycline was examined under the light microscope. It showed viable *Acanthamoeba* trophozoites invading the epithelium with loss of the superficial layers of the epithelium with normal stroma (Figure 5.10d).

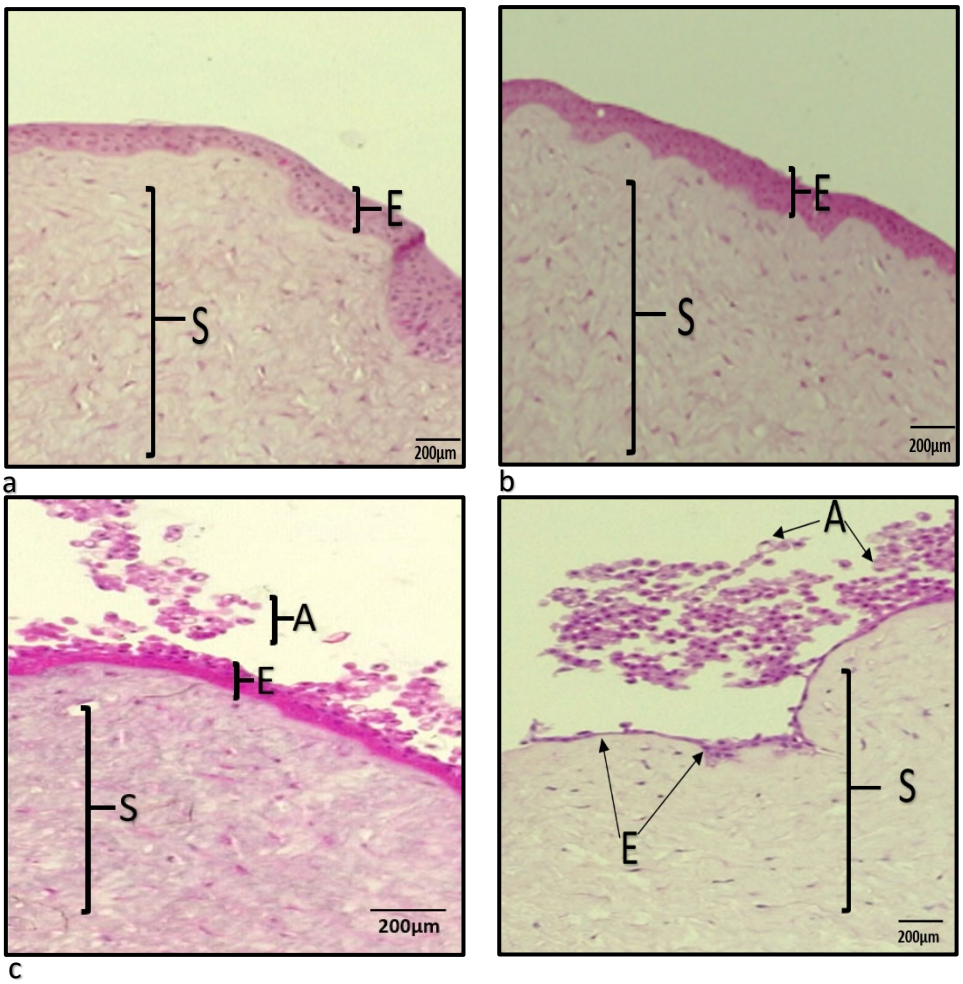

Figure 5.10: Histology sections, healthy versus infected cornea, day 10, added doxycycline. **a.** Control cornea with healthy five to six non-keratinized, stratified squamous epithelium (E) and normal stroma (S) with parallel layers of collagen fibres. **b.** Cornea with added doxycycline: normal cornea with healthy five to six non-keratinized, stratified squamous epithelium (E) and normal stroma (S). **c.** Infected cornea with no added doxycycline: attachment of *Acanthamoeba* trophozoites (A) to the epithelium with loss of the superficial layers of the epithelium. **d.** Infected cornea with added doxycycline: Viable *Acanthamoeba* trophozoites (A) invading the epithelium with loss of the superficial layers of the epithelium of this cornea, normal stroma (S).

5.3.3.4 Day 14, Control and Test Corneas

The healthy cornea with added doxycycline was examined under the light microscope. It showed normal epithelial lining with healthy five to six non-keratinized, stratified squamous epithelium and normal stroma with parallel layers of collagen fibres (Figure 5.11b)

Examination of the infected cornea with no added doxycycline showed *Acanthamoeba* trophozoites invading the epithelium with loss of many layers of the epithelium and the stroma was normal (Figure 5.11c).

The Infected cornea with added doxycycline was examined under the light microscope. It showed viable *Acanthamoeba* trophozoites invading the epithelium with loss of many layers of the epithelium with a normal stroma (Figure 5.11d).

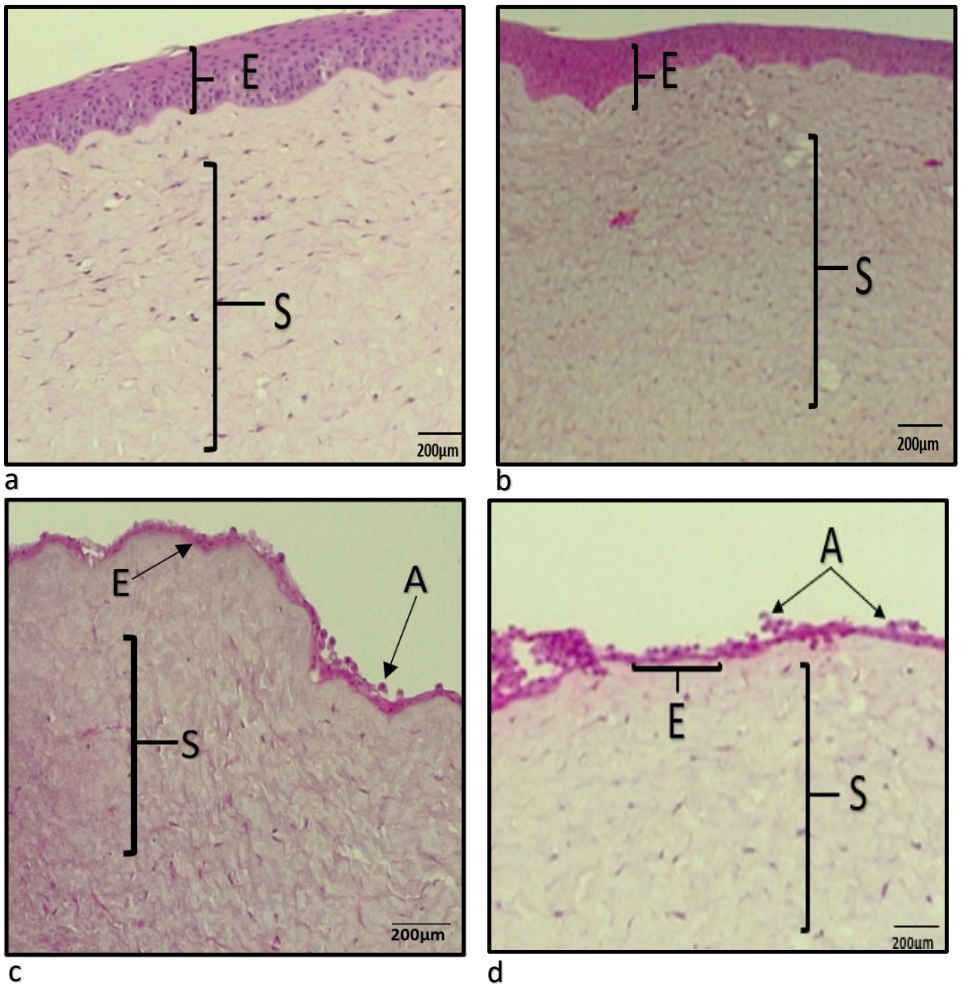

Figure 5.11: Histology sections, healthy versus infected cornea, day 14, added doxycycline. **a.** Control cornea with healthy five to six non-keratinized, stratified squamous epithelium (E) and normal stroma (S) with parallel layers of collagen fibres. **b.** Cornea with added doxycycline: normal cornea with healthy five to six non-keratinized, stratified squamous epithelium (E) and normal stroma (S). **c.** Infected cornea with no added doxycycline shows *Acanthamoeba* trophozoites (A) invading the epithelium with loss of many layers of the epithelium. **d.** Infected cornea with added doxycycline: viable *Acanthamoeba* trophozoites (A) invading the epithelium with loss of many layers of the epithelium in this cornea with normal stroma (S).

5.3.3.5 Day 18, Control and Test Corneas

The healthy cornea with added doxycycline was examined under the light microscope. It showed loss of the superficial layers of epithelium as the number of epithelial layers was around 3-4 layers in this cornea and the stroma was normal (Figure 5.12 b).

Examination of the infected cornea with no added doxycycline showed *Acanthamoeba* trophozoites invading the whole epithelium and part of the stroma with loss of most epithelial layers (Figure5.12c). The infected cornea with added doxycycline was examined under the light microscope. It showed viable *Acanthamoeba* trophozoites invading the whole epithelium and part of the stroma with loss of most epithelial layers (Figure 5.12d).

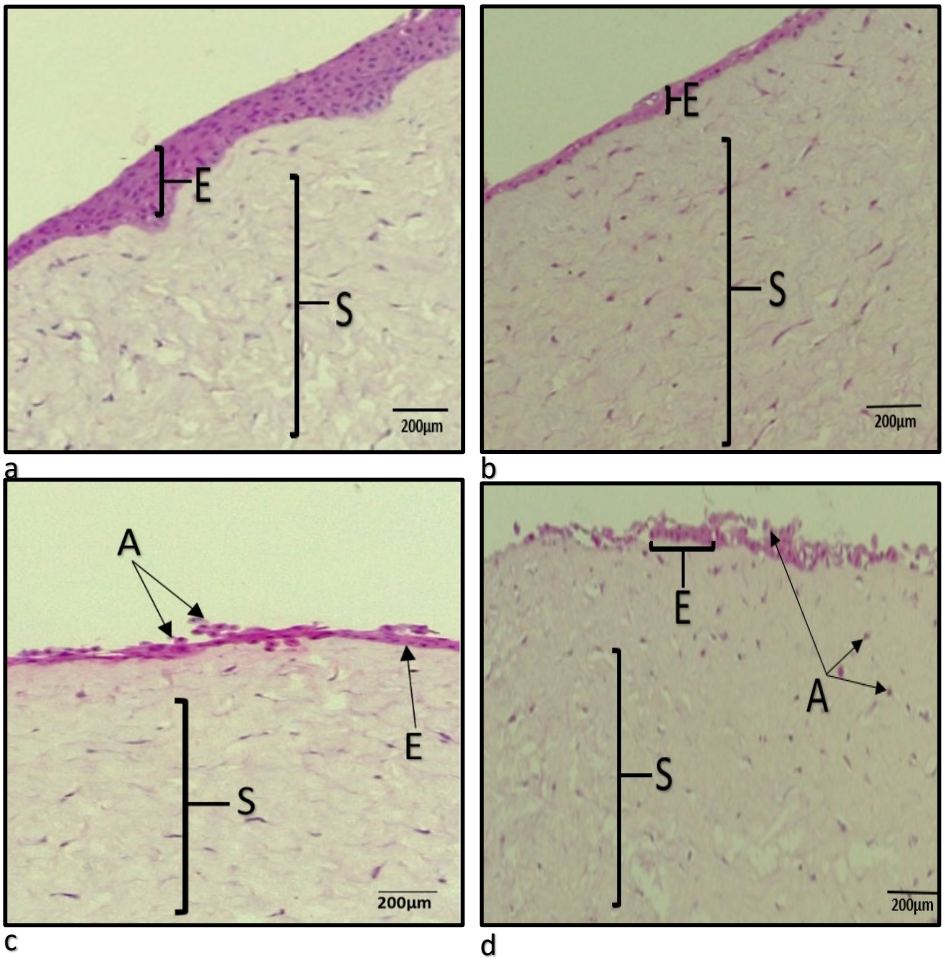

Figure 5.12: Histology sections, healthy versus infected cornea, day 18, added doxycycline. **a.** Control cornea with healthy five to six non-keratinized, stratified squamous epithelium (E) and normal stroma (S) with parallel layers of collagen fibres. **b.** Cornea with added doxycycline: loss of the superficial layers of epithelium as the number of epithelial layers is around 3-4 layers in this cornea, normal stroma. **c.** Infected cornea with no added doxycycline shows *Acanthamoeba* trophozoites (A) invading the whole epithelium and part of the stroma with loss of most epithelial layers. **d.** Viable *Acanthamoeba* trophozoites (A) invading the whole epithelium and part of the stroma with loss of most of the epithelial layers.

5.3.3.6 Day 22, Control and Test Corneas

The healthy cornea with added doxycycline is examined under the light microscope. It showed further loss of the epithelial lining as the number of epithelial layers was around 2-3 layers and the stroma was normal (Figure 5.13b).

Examination of the infected cornea -with no added doxycycline- showed *Acanthamoeba* trophozoites invading the stroma and there was total loss of the epithelium (Figure 5.13c). The infected cornea with added doxycycline was examined under the light microscope. It showed a viable *Acanthamoeba* invading the stroma and there was total loss of the epithelium (Figure 5.13d).

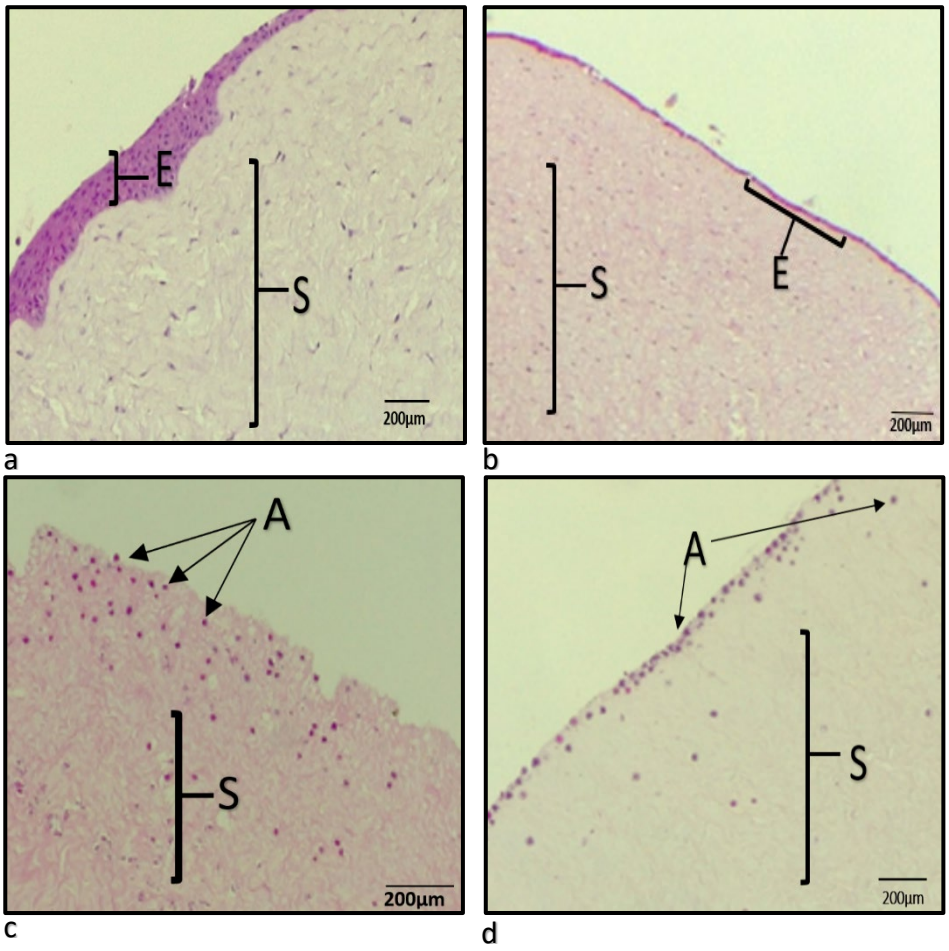

Figure 5.13: Histology sections, healthy versus infected cornea, day 22, added doxycycline. **a.** control cornea with healthy five to six non-keratinized, stratified squamous epithelium (E) and normal stroma (S) with parallel layers of collagen fibres. **b.** Cornea with added doxycycline: further loss of the epithelial lining as the number of epithelial layers was around 2-3 layers in this cornea, normal stroma. **c.** Infected cornea with no added doxycycline shows *Acanthamoeba* trophozoites (A) invading the stroma. There was total loss of the epithelium. **d.** Infected cornea with added doxycycline: viable *Acanthamoeba* trophozoites (A) invading the stroma with total loss of the epithelium.

5.4 Discussion

Drug assays were used to investigate the efficacy of PHMB and doxycycline against *Acanthamoeba* trophozoites and cysts and their toxicity against human cells. The established *ex vivo* model was also used to test the therapeutic effect of both PHMB and doxycycline against Acanthamoeba keratitis in addition to studying any potential toxicity against the corneal epithelium.

5.4.1 PHMB- Assay Results

The results showed that the inhibitory activity is 1 µg/mL for both *A. castellanii* and *A. polyphaga,* and the amoebicidal activity was 3.9 µg/mL for *A. castellanii* and 7.8 µg/mL for *A. polyphaga*, and the HEp-2 toxicity assay was 31.3 µg/mL.

The results of PHMB amoebicidal activity were consistent with previously published studies (Kilvington *et al.,*2002, Heaselgrave *et al.,*2019) in which they used the same amoebicidal assays we used in this study and the same concentration of PHMB (0.02% v/v). They reported the MCC mean for different clinical isolates of *Acanthamoeba* to be 3.2 µg/mL in one study (Kilvington *et al.,*2002), and 15.6 for A. *castellanii* and 7.8 µg/mL for A. *polyphaga* in the other study (Heaselgrave *et al.,*2019).

5.4.2 PHMB- Light Microscope Results

The effect of drugs was also investigated using the light microscope to study the histology sections of the corneas. On day 7 of adding PHMB to the infected cornea, most of the *Acanthamoeba* trophozoites that were at the stage of attachment with the superficial layers of the epithelium were dead. On day 10, further dead

trophozoites were noticed and the shedding of the epithelial layers was more obvious. On day 14, fragmented dead cells and apoptotic bodies were seen as dead cells showed loss of the integrity of the plasma membrane whereas apoptotic cells demonstrated complete fragmentation into discrete bodies. These findings were compared against healthy corneas with added PHMB. The superficial epithelial layers in the corneas without infection started to shed on day 10 with further loss on day 14.

The histological findings were consistent with the drug assay results and confirmed the ability of PHMB to inactivate the trophozoites however there was a mild toxic effect against corneal epithelial cells, and despite the MCT assay results demonstrating PHMB toxicity to human monolayer cells, the actual effect on the model was of less amplitude as the model was based on a whole cornea with its distinctive layers compared to a monolayer in the MCT assay and also due to the extra protection offered by the rocking mechanism. The toxic effect noticed in the *ex vivo* model is of less degree in the human eye which has multiple protective mechanisms compared to the *ex vivo model.* The eye globe is enclosed in the orbit socket which is part of the skull bones forming a four-sided pyramid , and the corneal surface is protected by the eyelid (Davson and Perkins,2020) all of which further diminish any potential toxic effect of the drug on the human eye.

5.4.3 PHMB- Previous Studies

Rabbit Eye Model

The observed limited toxicity of PHMB against corneal epithelial cells in the *ex vivo* model developed in this current study is supported by the outcome of a recent study where the authors evaluated the toxic effect of PHMB on the cornea by injecting the drug to the corneal stroma of white rabbits. They injected the cornea with (0.01% or 0.02% v/v) PHMB, then on day 7 post injection the rabbits were euthanized, and the corneas were harvested for evaluation. They noticed that the injection of 0.02% PHMB led to erosion in the corneal epithelial layer, oedema and neovascularization, while 0.01% PHMB did not lead to any obvious corneal toxicity (Lim, 2020).

There are differences between their study and this current study; they injected the drug to the corneas of rabbits *in vivo,* while in this study we added the drug topically to the surface of *ex vivo* porcine corneas similar to the way patients administer the drug to the eye.

Another difference is that Lim's study evaluated the toxic effect of PHMB on day 7, while this study followed the toxicity from day 4 till day 14 and so we were able to run the experiment longer with still limited toxicity shown. Furthermore, they noticed mild corneal damage in terms of epithelial erosion, corneal oedema and neovascularization while in this study the main observed toxicity was epithelial loss given the fact that this study was done in *ex vivo* conditions that lack the other contributors of the body immune system like the attraction of immune and inflammatory cells at the site of infection leading to inflammation, angiogenesis and further tissue destruction (Chaplin,2010). Both studies are similar in using the 0.02% concentration of PHMB and both show mild toxic effect of PHMB on the epithelial layers over 7-14 days.

PHMB Penetration of Corneal Epithelium Study

Another study from 2015 was conducted on antiseptic compounds commonly used in treating Acanthamoeba keratitis including PHMB to investigate the ability to penetrate the corneal epithelium and any effect on the epithelium, and the outcome supported our observation in showing the mild toxic effect of PHMB on the corneal epithelium (Vontobel *et al.,*2015). The corneas were harvested from albino rabbits and were mounted in artificial anterior chamber. The study showed that PHMB is unable to reach the anterior chamber through penetration of the cornea, which may explain why treatment of Acanthamoeba keratitis requires several months of continuous topical drug treatment. A small degree of damage to the corneal epithelium was also reported.

The differences between their study and this study includes their use of rabbit corneas while in this study porcine corneas were used; the aim of their study was focused on the penetration ability of the drug while we aimed to follow the therapeutic effect of PHMB and its toxic effects on the corneal cells. They added the drug as drops on the surface of the cornea every 30 minutes up to 8 hours while in this study we added the drug to the corneal surface once a day for 14 days. The therapeutic application of PHMB requires the administration of one application every hour day and night for 72 hours then hourly daytime for 48 hours followed by a 6-month period of administering the drug 6 times daily. In this current study, this is unapplicable as PHMB would accumulate in the medium whereas patients' eyes frequently wash out the excess through eye blinking. There are some similarities between both studies as both were run in *ex vivo* environment, both administered the drugs as drops on the surface of the cornea and both demonstrated a toxic effect of the drug to the epithelial layers.

PHMB and Chlorhexidine Study

Another research supporting our results was conducted to evaluate the effect of PHMB and chlorohexidine on *Acanthamoeba* cysts viability and its toxic effect on cultured human corneal cells (Lee *et al.,*2007). They used PHMB (0.02% v/v) which is similar to our study and chlorhexidine (0.02% v/v) and followed the same cysticidal assay to determine the MCC. They also administered PHMB (0.02% v/v) and chlorohexidine (0.02% v/v) to the cultured corneal cells to observe the survival rate. They noticed a strong and similar cysticidal effect for both drugs, however PHMB was more toxic to corneal cells compared to chlorohexidine and the level of cell death increased with increasing disinfectant concentration and exposure time.

There are some differences between both studies as they used cultured human keratocytes and we used the *ex vivo* model and although both studies demonstrated the PHMB toxicity to cell monolayers, the *ex vivo* model suffered less damage due to the extra protective mechanisms the model possesses. Furthermore, they used inverted light microscope and electron microscope to evaluate the morphological changes while we used the inverted light microscope only, and they used *Acanthamoeba castellanii* and *A. lugdunesis*, while we used *A. castellanii and A. polyphaga.*

The outcome of both studies is similar as they reported that the cysticidal activity against *Acanthamoeba castellanii* was 13.21 µg/mL and it was (15.6 µg/mL) in this current study. Moreover, both studies demonstrated a toxic effect of PHMB on corneal cells.

5.4.4 Doxycycline- Assay and Histology Results

Amoebicidal and cysticidal assays did not show any major antimicrobial effect of doxycycline on the viability of *Acanthamoeba* in comparison with PHMB as it achieved a MTIC of 625 µg/mL and MTAC of 1250 µg/mL, respectively. Doxycycline showed very low toxicity against human cells in the 625ug/mL range. Under histology examination, doxycycline showed no effect on the viability of trophozoites as the invasion and spread of *Acanthamoeba* infection progressed until the total loss of corneal epithelium and invasion of stroma. When doxycycline was applied to healthy corneas, the toxic effect of the drug against the epithelial layers started at day 18 with shedding of the superficial layers of the epithelium and further loss at day 22 compared to the control.

5.4.5 Doxycycline- Previous Studies

A study in 2017 investigated the effect of the coinfection of *Acanthamoeba* bacterial endosymbiont on human corneal cells, and any role of doxycycline and azythromycin in treating Acanthamoeba keratitis (Purssell *et al.,*2017) and the outcome of their study supports our observations that doxycycline has no effect on the corneal tissue as *Acanthamoeba* remained viable after administration of the drug, however they reported that doxycycline can decrease the virulence effect of the bacterial endosymbionts which means that it can be potentially used as an adjuvant therapy for Acanthamoeba keratitis beside the standard treatment.

They infected EpiCorneal cells (a three-dimensional human corneal tissue model) with *Acanthamoeba*-endosymbiont then treated this model with a medium containing 4 µg/mL azithromycin and 2 µg/mL doxycycline. The conclusion was that both drugs can effectively target the bacterial endosymbionts hence why it can be

used as a supportive therapy for Acanthamoeba keratitis. They also noticed that neither doxycycline nor azithromycin exert any toxic effect on the EpiCorneal tissue and that *Acanthamoeba* remained viable after the administration of antibiotics. The differences between their study and this study are their use of the EpiCorneal cells while we used the *ex vivo* model, they aimed to study the effect of the antibiotic in treating Acanthamoeba keratitis by inhibiting the endosymbiont effect while in this current study we applied doxycycline on the *ex vivo* model to study any therapeutic effect of the antibiotic on Acanthamoeba keratitis and any toxic effect on corneal cells. They noticed no toxic effect on the EpiCorneal cells while in this current study slight changes to the epithelial layers were observed on day 18. In a similar study, the researchers also noticed that *Acanthamoeba* remained viable for at least 7 days after the addition of azithromycin and doxycycline (Goy and Greub, 2009).

5.5 Conclusion and Future Work

The histological findings are consistent with the drug assay results and confirm the ability of PHMB to inactivate *Acanthamoeba* trophozoites with a mild toxic effect of the drug on *ex vivo* corneal epithelial cells despite high level of *in vitro* toxicity to human cells.

Regarding doxycycline, no major antimicrobial effect was demonstrated on the viability of *Acanthamoeba* by histological findings and drug assays. A minimal toxic effect of doxycycline was demonstrated against *ex vivo* corneal epithelial cells and *in vitro* human cells.

The above results show that the *ex vivo* model can be used to investigate drugs against *Acanthamoeba* in terms of the ability of the drug of interest to stop the keratitis and any potential toxicity it might exert on corneal cells. The model can be used in the future to study further drugs with various concentrations in terms of efficacy and toxicity.

Chapter Six

Correlation of *Ex Vivo* and *In Vivo* Confocal Microscopy Imaging of *Acanthamoeba*

Chapter 6: Correlation of *Ex Vivo* and *In Vivo* Confocal Microscopy Imaging of *Acanthamoeba*

6.1 Introduction

Acanthamoeba species are opportunistic human pathogens that cause Acanthamoeba keratitis (Carnt *et al.,*2016) with its early stages resembling other forms of infective keratitis making it difficult to initially identify *Acanthamoeba* as the pathogen behind the infection causing delay in diagnosis and management with poor visual outcome (Robaei *et al.,* 2016, Carnt *et al.,*2018).

In the United Kingdom, there is no commercially available method for the diagnosis of AK and the diagnosis is based on individual protocols developed locally by different hospitals and clinics (Alexander *et al.,*2015). The diagnosis is often delayed because there is currently no rapid diagnostic test available and the most widely used laboratory technique to help in the diagnosis of AK is the culture method. Corneal samples are commonly obtained by scraping the corneal surface under local anaesthesia then inoculating the sample on 2.5% (w/v) non-nutrient agar overlaid with a lawn of *Escherichia coli*, and this corneal culture method requires up to 10 days to demonstrate results and has very low sensitivity ranging from 0 to 50% which means that many negative cultures are in fact for patients who have the infection (Alexander *et al.,*2015). Polymerase chain reaction (PCR) is another method for the detection of DNA of *Acanthamoeba* in corneal scrapping and tears (Mathers *et al.,*2000). In comparison to corneal culture, it is faster (Pasricha *et*

*al.,*2003), gives results within hours with sensitivity reported as 66.7% to 75% (Goh *et al.,*2018).

In vivo confocal microscopy (IVCM) is a non-invasive technique used to diagnose AK through *in vivo* examination of corneal cells and can differentiate between *Acanthamoeba* and other pathogens by identifying the unique morphological features between pathogens (Matsumoto *et al.,*2007). Previous studies correlated IVCM findings with *ex vivo* imaging of the organism grown on cultured plates obtained from corneal scrape or contact lens solution of same patients (Matsumoto *et al.*2007, Kobayashi 2008, Shiraishi *et al.,*2010) or from directly examining a suspension of cultured *Acanthamoeba* trophozoites (Yamazaki *et al.,*2012). IVCM has a sensitivity as high as 90.6% to 92.9% and a specificity of 77.3% to 100% (Goh *et al.,*2018) but is largely operator dependant based on their experience. The high sensitivity of IVCM helps in detecting *Acanthamoeba* cysts in deep corneal infiltrates that are usually difficult to yield by scraping, and the diagnostic sensitivity varies between different methods of diagnosis. In one study, the sensitivity of culture was reported as 33.3%, while the sensitivity for PCR and IVCM were reported as 74.1% and 100% respectively (Goh *et al.,*2018).

6.2 Aim and Objectives

This chapter will focus on studying the different morphological appearances of *Acanthamoeba* trophozoites and cysts using confocal microscopy by performing the following:

- Preparation of various forms of *Acanthamoeba:* live trophozoites, live, dead and empty cysts.
- Inoculation of the model with the different forms of *Acanthamoeba*.

After achieving the above, confocal microscope will be used to study the different models and correlate the findings of *ex vivo* confocal microscopy (EVCM) with imaging findings from culture positive AK cases on IVCM to investigate any potential similarities that can be used to facilitate the interpretation of *in vivo* findings in light of *ex vivo* images.

6.3 Methods

6.3.1 *Acanthamoeba* Strains and Culture

The strains used in this study were *A. castellanii* (ATCC 50370). Trophozoites were maintained in tissue culture flasks using a semi defined axenic medium (Ac#6) as previously described in chapter 2 section 2.3. Cysts were produced using Neff's encystment medium (NEM) method described in chapter 2 section 2.6.

6.3.2 Preparation of Dead *Acanthamoeba* Cysts

Dead *Acanthamoeba* cysts were prepared by exposure to 0.02% (v/v) polyhexamethylene biguanide (PHMB) for one hour. After incubation, the cells were examined by phase contrast microscopy (x100) to confirm the activity of PHMB. Cysts and trophozoites were again inoculated into growth media and confirmed to be inactivated and non-viable, the cells were then pelleted by centrifugation at 500 x *g* for 5 minutes. Dead organisms are defined as follow:

- Dead trophozoites : smaller and rounded in comparison to live trophozoites with reduced cytoplasm due to damage to the plasma membrane.
- Dead cysts : darker and less refractile compared to live cysts due to shrinkage of the plasma membrane of the encysted trophozoite from the inner wall of the cyst.

6.3.3 Preparation of *Acanthamoeba* Empty Cysts

Cysts were inoculated into Ac#6 medium for 4 hours to permit maximal excystation (>90%) then the resultant trophozoites were exposed to N-lauryl-sarcosine 0.5% (w/v) to lyse them. The remaining cyst walls were unaffected by N-lauryl-sarcosine and were pelleted by centrifugation at 1000 x *g* for 5 minutes. Using phase contrast microscopy, cysts were examined to confirm >90% empty cyst compared to mature un-excysted cysts and cells were then pelleted by centrifugation at 1000 x *g* for 5 minutes. Cysts are identified as empty once trophozoites emerge out of them through the ostioles.

6.3.4 Preparation of Eye Globes

Porcine eye globes were collected from freshly slaughtered pigs from a local slaughterhouse and excess tissues were removed in Class 2 safety cabinet. The globes were processed (previously described in chapter 2, section 2.14) by visually inspecting corneas for defects such as pigmentation or gross epithelial defects, and corneas with such defects were discarded. Eye globes were sterilized in Povidone-iodine (PVP-I) 0.5% (w/v) for 2 minutes and then transferred to sodium thiosulphate 0.1% (w/v) for 1 minute to neutralise the PVP-I followed by transfer to 0.1% (w/v) gentamicin-phosphate-buffered saline (PBS) solution for 15 minutes to remove any residual bacterial contamination. The globes were finally transferred to sterile Dulbecco's Phosphate Buffered Saline (DPBS) solution and were kept at room temperature ready for use.

6.3.5 Inoculation of *Acanthamoeba*

Infection was induced by inoculating a small volume of *Acanthamoeba* at a concentration of 1 X 10^5 cells / mL using a sterile 26-gauge needle. The needle was inserted tangentially into the middle layers of the cornea without applying pressure to the syringe to avoid the formation of pockets of liquid within the stroma. The needle was then withdrawn slowly, and samples were inoculated into the needle path by capillary action. The following forms of *Acanthamoeba* were injected into different eye globes*:* live trophozoites, dead, live and empty cysts.

6.3.6 *Ex vivo* Confocal Microscopy (EVCM)

EVCM studies were conducted using the Heidelberg Retina Tomograph II with the Rostock Corneal Module (HRT II/RCM, Heidelberg Engineering, Dossenheim, Germany). A sterile TomoCap (Heidelberg Engineering) was mounted over the lens objective of the microscope and a coupling agent ‘GelTears’ (0.2% w/w carbomer 980, Bausch & Lomb, UK) was used between the disposable cap and the lens objective. One drop of 1% Carmellose sodium (Celluvisc 1% w/v, Allergan, UK) was added on the corneal surface previously inoculated with *Acanthamoeba* and the whole eye globe was held on a standard retort stand by a 3-prong clamp (Figure 6.1).

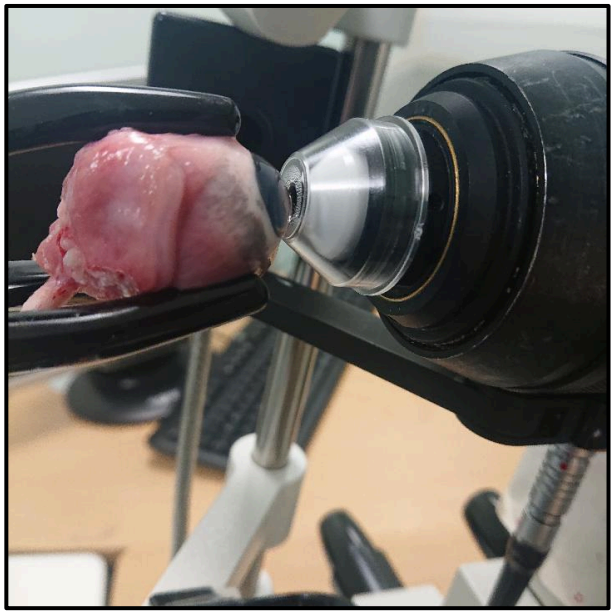

Figure 6.1: Eye globe held in place using a three-pronged clamp attached to a retort stand with the cornea in contact with the TomoCap during the *ex vivo* scanning process.

The microscope was then brought into close contact to the area of the cornea where the *Acanthamoeba* were inoculated and then a series of 40 images were acquired using multiple volumes over 80μm depth starting from the superficial epithelium down to the deep stroma. A total of 10 to 15 volumes scans were recorded for each porcine eye. Each *en face* image has a resolution of 384 x 384 pixels covering an area of 400 μm x 400 μm, with a transverse resolution of approximately 1-2 μm.

6.3.7 EVCM and IVCM Image Comparison

In this study, *Acanthamoeba* morphologies which were already identified using EVCM were used to validate the various cyst and trophozoite-like features seen on IVCM. All available EVCM images were reviewed by experienced observer (Moorfields Eye Hospital NHS Foundation Trust). In total, this equated to approximately 500 images reviewed for each porcine cornea in an anteroposterior approach from the epithelium down to deep stroma. EVCM images from each *Acanthamoeba* form were assessed qualitatively and the observed structures were classified according to previous publications on *Acanthamoeba* morphological structures seen on IVCM as per table 6.1 below:

Acanthamoeba Morphology	Size
Round/ovoid hyper-reflective objects without double wall	10-25 µm
Round/ovoid hyper-reflective objects with double wall	10-25 µm
Target sign - round/ovoid hyper-reflective central object with surrounding halo	10-25 µm
Signet ring - round hyper-reflective outer ring with a grey/dark centre	10-25 µm
Trophozoite-like hyper-reflective objects with spindle shape projection from its surface suggestive of acanthopodia	25-40 µm

Table 6.1: *Acanthamoeba* morphological structures on IVCM (Kobayashi *et al.,*2013, Huang *et al.,*2017, Wang *et al.,*2019, De Craene *et al.,*2018, Chopra *et al.,*2020).

A single most optimal image corresponding to each *Acanthamoeba* form was used as a reference for validating structures observed on IVCM images. IVCM images were taken from an image database of a cohort of *Acanthamoeba* cultured positive cases already categorised into one of the above *Acanthamoeba* morphological features and published in a previous study (Chopra *et al.,*2020). From this database of images, the best images matching EVCM images were identified and compared. In addition, phase contrast images of different forms of *Acanthamoeba* were produced and compared to both EVCM and IVCM images.

6.3.8 Phase Contrast Images

Phase contrast images were generated from the same cell suspensions prepared earlier for the inoculation of corneal tissue. Samples of each morphology were placed onto microscope slides and were mounted with a glass coverslip. The cells were viewed at a magnification of x400 using a Zeiss Primovert inverted microscope (Zeiss, Cambridge, UK) and the images were captured on a Canon EOS M50 digital camera using a Zeiss P95-T2 DSLR 1.6x trinocular microscope adapter.

6.4 Results

In this study, different forms of *Acanthamoeba* (live trophozoites, live, dead and empty cysts,) were injected in different eyes and evaluated using EVCM and the images were correlated with imaging of various cyst and trophozoite-like features from culture positive Acanthamoeba keratitis cases on IVCM. Phase contrast images of each form were also produced and compared with EVCM and IVCM images. Control corneas were examined using the same imaging modalities.

6.4.1 Control Cornea

The cornea of the control porcine eye was evaluated using the HRTII/RCM demonstrated intact corneal epithelium (Figure 6.2a) with part of the stroma containing a corneal nerve within its layers (Figure 6.2b). After introducing a tangential incision to the epithelium and stroma, another image was taken (Figure 6.2c) demonstrating the incision at the microscopic level with increased refractility around the incision site (Figure 6.2d).

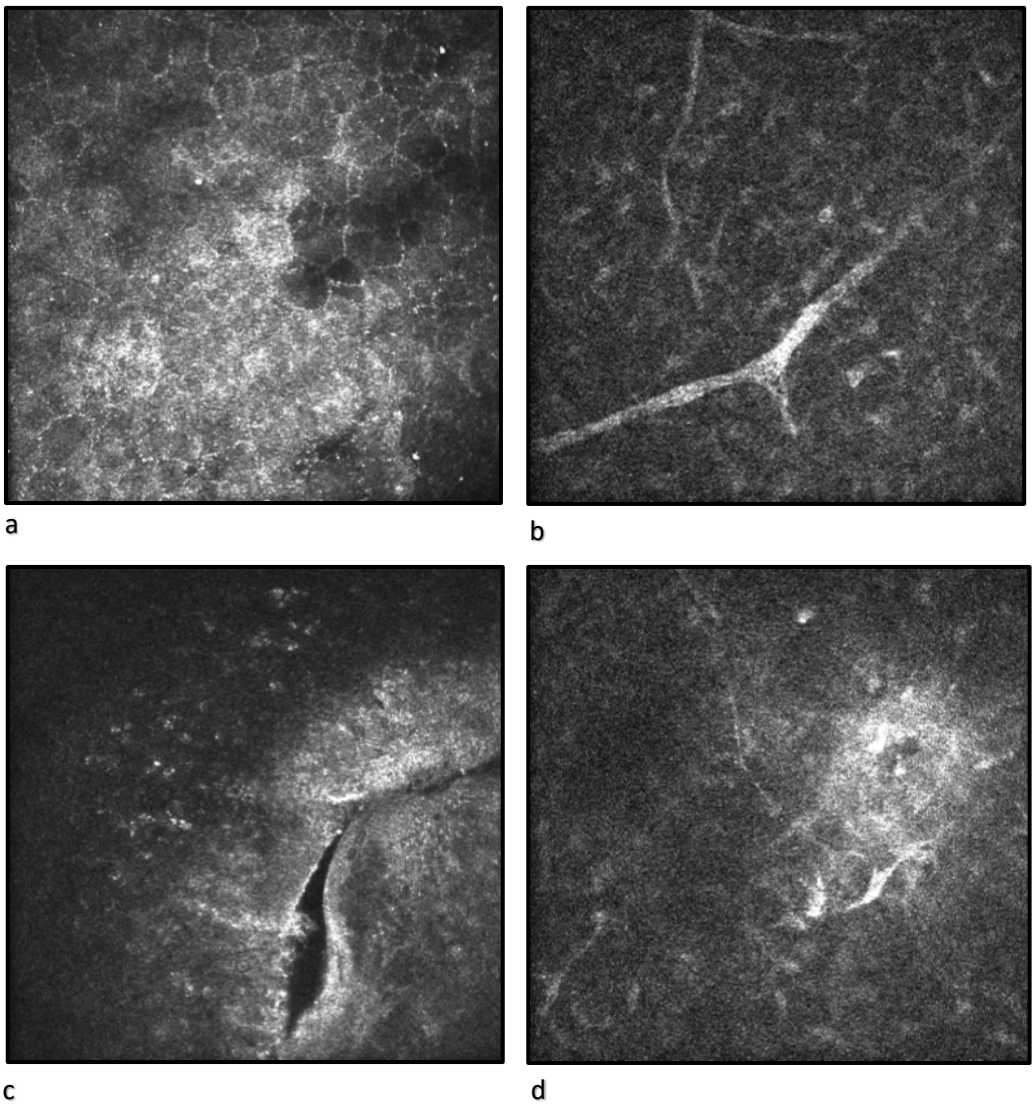

Figure 6.2: EVCM images of control cornea. **a**. *Ex vivo* image of control cornea with intact corneal epithelium **b**. *Ex vivo* image demonstrating corneal nerve within the stroma. **c**. *Ex vivo* image following the stab incision. **d**. *Ex vivo* image showing increase hyper-reflectivity around the stab incision.

6.4.2 Live *Acanthamoeba* cysts

Live *Acanthamoeba* cysts were inoculated in the cornea by introducing the incision tangentially into the epithelium and stromal layers and then withdrawing the needle to deposit the live cyst preparation into the corneal stroma. Using EVCM, the cyst demonstrated a rounded appearance with refractile cyst wall and the trophozoites were visible inside the cysts with bright vacuoles present (Figure 6.3a). The same cyst preparation was viewed under phase contrast microscopy at x400 (Figure 6.3b) and the cyst wall was refractile with a clearly visible double wall. The trophozoites were seen inside the cyst wall but the visible vacuoles were non-refractile under phase contrast. These images closely resembled those from *in vivo* confocal images acquired from Acanthamoeba keratitis patients using HRT II (Figure 6.3 c,d) as both models demonstrated the cysts to be bright and refractile with cyst wall clearly visible.

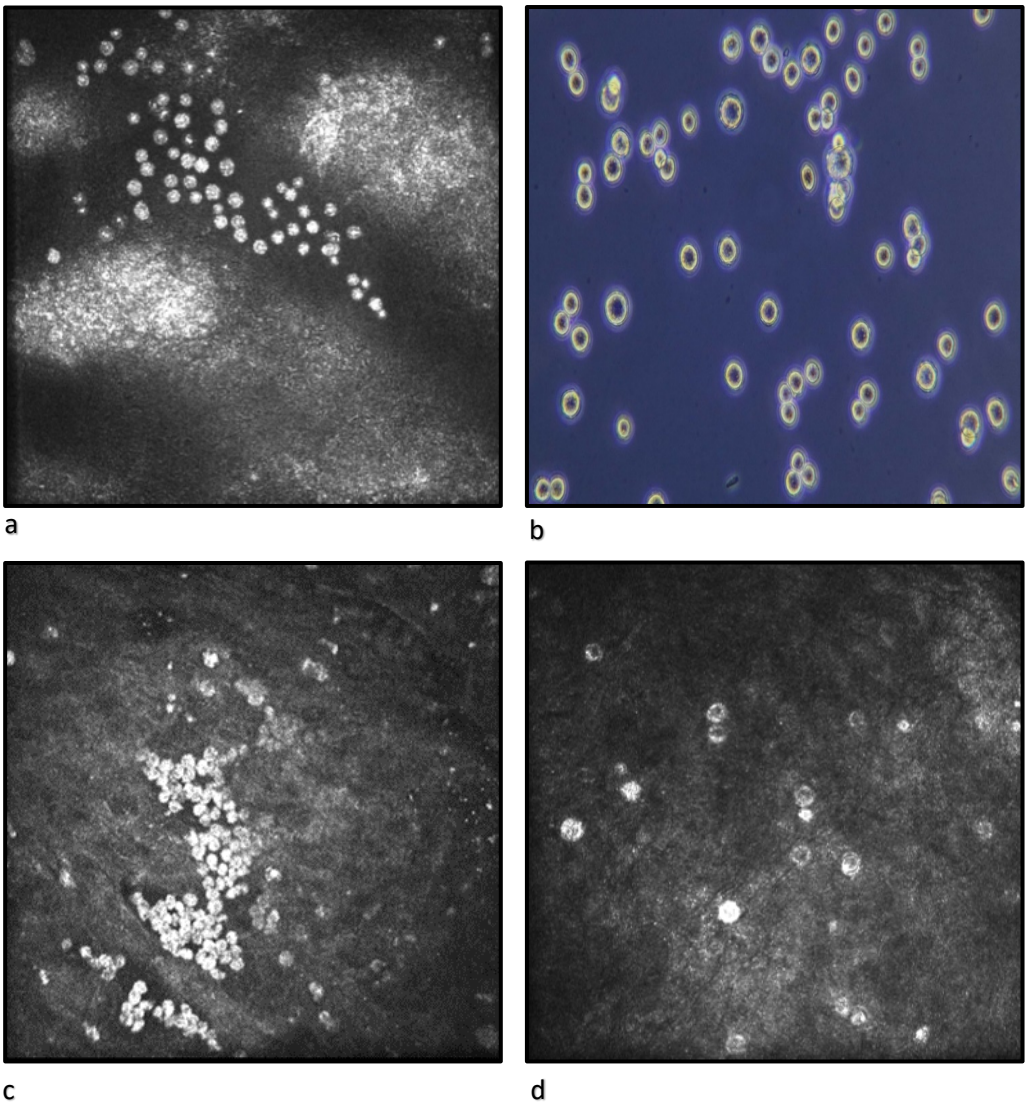

Figure 6.3: EVCM, IVCM and phase contrast images of live cysts. **a**. *Ex vivo* image with mixed morphological appearances: rounded, refractile with trophozoites present inside cysts. **b**. *In vitro* phase contrast image x400, showing refractile cysts with double wall. **c, d**. *In vivo* image from patients with AK showing similar morphological features to EVCM images.

6.4.3 Dead *Acanthamoeba* cysts

Inoculation of dead cysts was also evaluated using the same method in which dead *Acanthamoeba* cysts were inoculated in the epithelium and stromal layers. Under EVCM, the cyst demonstrated a visible non-refractile outer wall and the remainder of the trophozoites within the dead cysts appeared as small refractile dots inside the cysts (Figure 6.4a). The dead cyst preparation was studied under phase contrast microscopy at x400 and showed the same findings of a visible non-refractile outer cell wall and the trophozoites inside the cysts had a ruptured cell membrane leading to leakage of the cytoplasm and the shrinking of the cells with a small refractile dots inside the cysts demonstrating the remainder of the trophozoites (Figure 6.4b). Similar appearance was demonstrated by IVCM for different patients with Acanthamoeba keratitis (Figure 6.4 c,d).

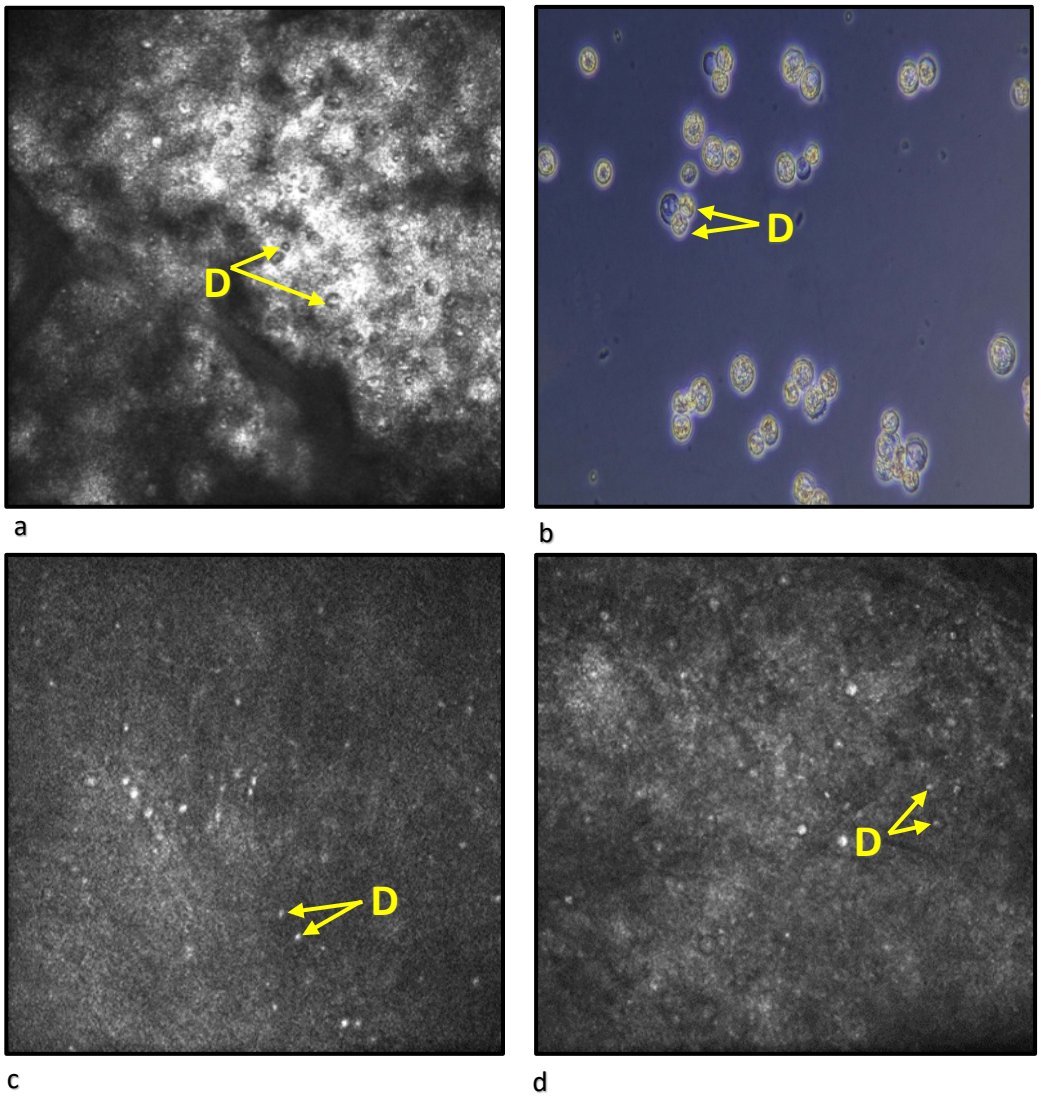

Figure 6.4: EVCM, IVCM and phase contrast images of dead *Acanthamoeba* cysts. **a**. *Ex vivo* image of dead cysts (D) showing non-refractile outer cyst wall with a small refractile dots within the cysts representing non-viable trophozoites. **b**. *In vitro* phase contrast image x400, dead cysts showing non refractile wall. **c,d**. *In vivo* image from patients with AK showing similar morphological features to EVCM images.

6.4.4 Empty *Acanthamoeba* cysts

Empty cysts were inoculated into the cornea using the same method described earlier. Using EVCM, the outer cyst wall was visible, non-refractile with a rounded appearance with a small refractile dot inside the cyst representing the remaining cellular material of the trophozoite (Figure 6.5a). Phase contrast image showed visible non-refractile cyst wall with a small amount of cellular material which was left behind inside the cyst by the excysting trophozoite (Figure 6.5b). IVCM images from different patients with Acanthamoeba keratitis had a similar appearance (Figure 6.5 c,d).

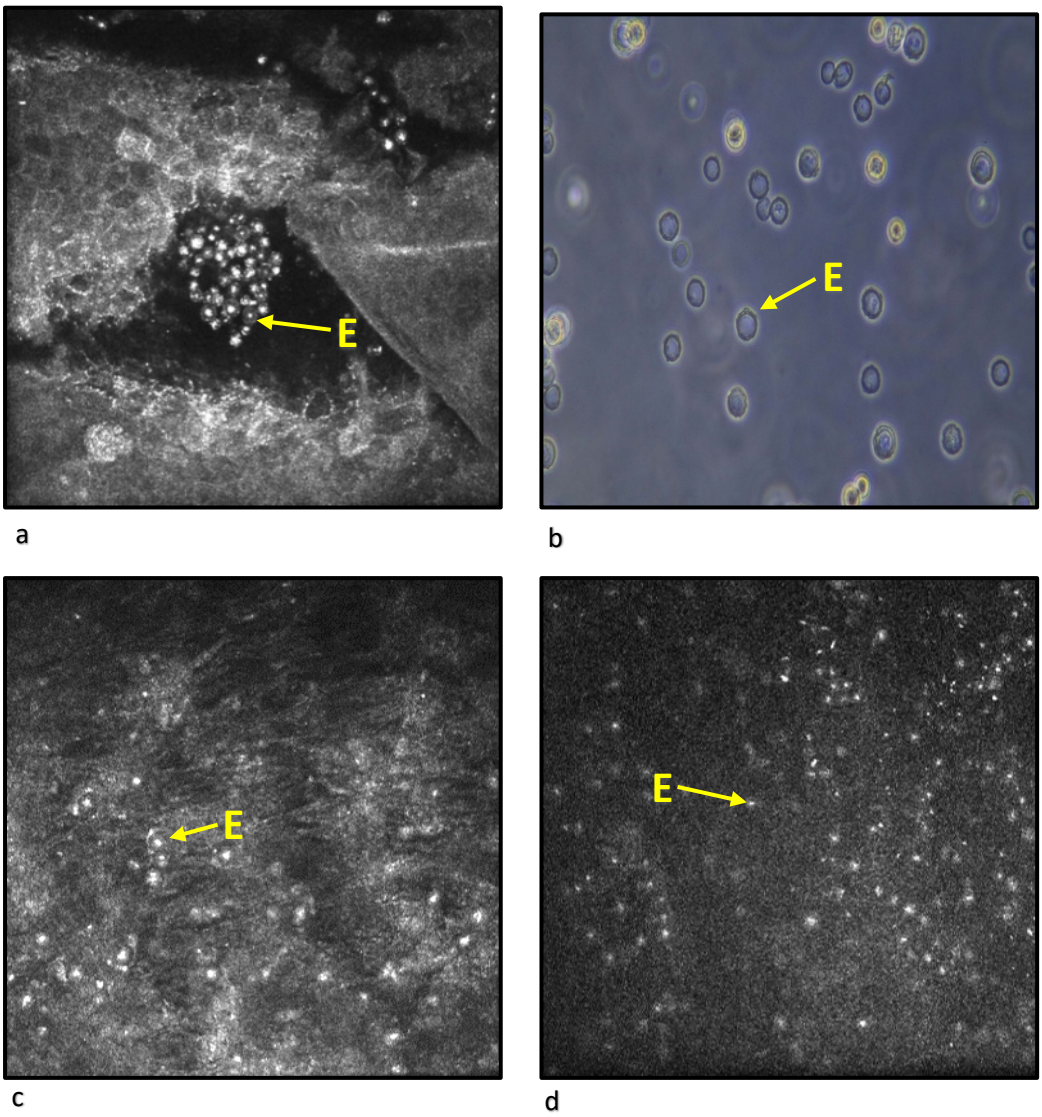

Figure 6.5: EVCM, IVCM and phase contrast images of empty *Acanthamoeba* cysts. **a**. *Ex vivo* image of empty cysts (E) showing non refractile rounded cysts. **b**. *In vitro* phase contrast image x400, demonstrating visible non-refractile cyst walls with remnants of cellular material of trophozoites post excystation. **c,d.** *In vivo* image from patients with AK showing similar morphological features to EVCM images.

6.4.5 Live *Acanthamoeba* Trophozoites

Inoculation of live trophozoites into the *ex vivo* model was also evaluated. Under EVCM, Individual cells were not visualised but an aggregation of trophozoites appeared as a coarse speckled area of refractile material, and the plasma membrane of individual trophozoites was non-refractile and therefore not visible (Figure 6.6a). The phase contrast image demonstrated live trophozoites that were amoeboid in shape with intact non-refractile cell membrane and the cytoplasm was full of refractile food vacuoles (Figure 6.6b). The appearance was similar to the findings of the IVCM (Figure 6.6 c,d).

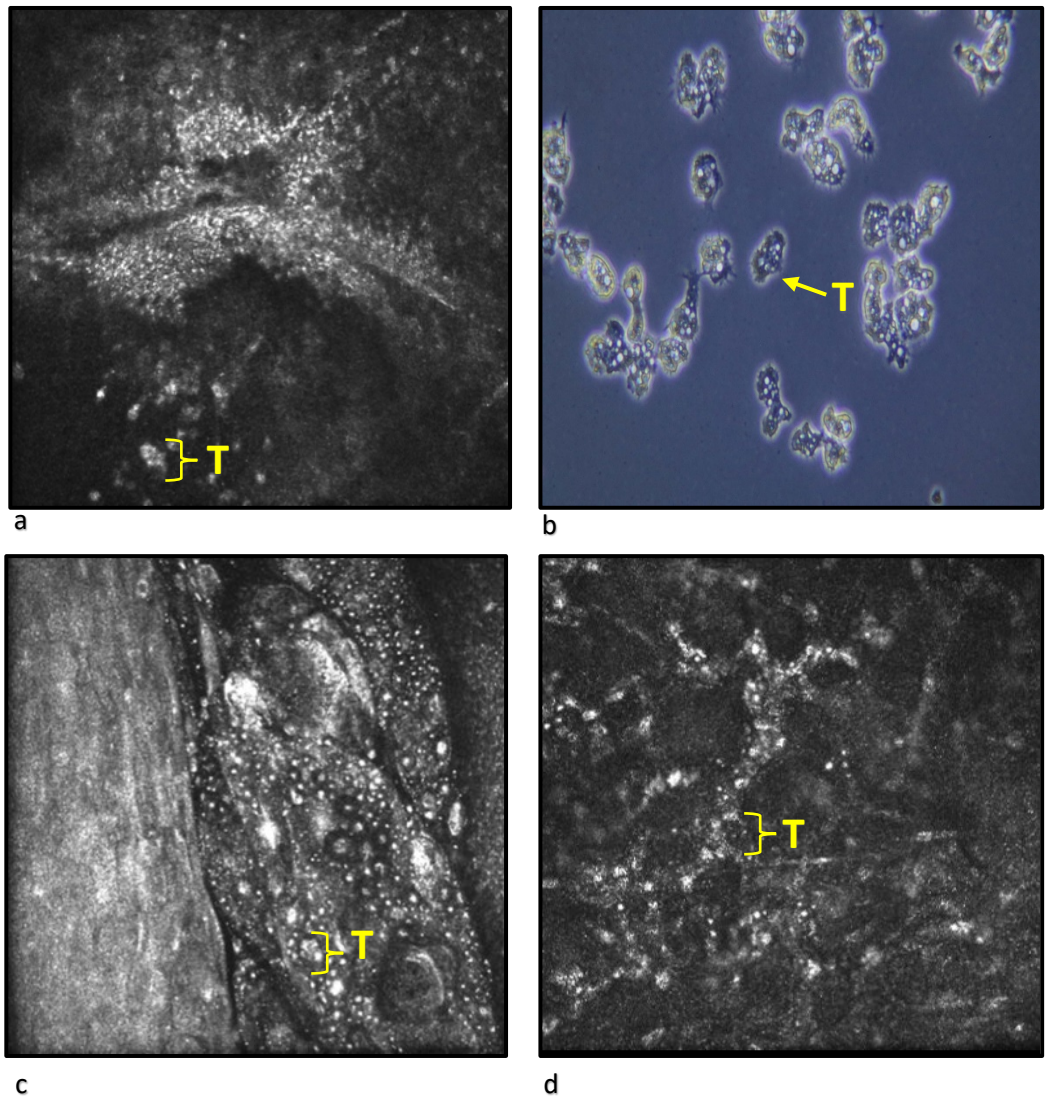

Figure 6.6: EVCM, IVCM and phase contrast images of live *Acanthamoeba* trophozoites. **a**. *Ex vivo* image demonstrating coarse speckled areas representing clusters of trophozoites (T). **b**. *In vitro* phase contrast image x400, showing amoeboid trophozoites with intact cell membrane and many food vacuoles within the cytoplasm. **c,d**. *In vivo* image from patients with AK showing similar morphological features to EVCM images.

6.5 Discussion

In this study, various forms of *Acanthamoeba* morphologies were identified using *ex vivo* confocal microscopy and were correlated with the imaging of various cyst and trophozoite-like features from culture positive Acanthamoeba keratitis cases on IVCM. Furthermore, phase contrast images of these forms were produced and compared with both EVCM and IVCM images.

The evaluation of live cysts inoculation into the *ex vivo* model under EVCM demonstrated a typical rounded appearance with visible cyst wall due to its refractility, and the trophozoite was easily seen inside the cyst alongside refractile bright vacuoles. This appearance was similar to *in vivo* confocal images showing the refractile cyst wall within. The phase contrast microscopy at x400 also showed the refractile double cyst wall with the trophozoite within it. Dead and empty cysts where also studied under EVCM and phase contrast microscopy and the findings were compared to IVCM images taken from corneas of patients confirmed to have Acanthamoeba keratitis and the results were similar in terms of morphology and refractility with both dead and empty cyst demonstrating visible non refractile cyst wall with a small refractile dot inside the cyst representing the remainder of trophozoites.

Researchers studied *Acanthamoeba* cysts and trophozoites morphologies using confocal microscopy on *ex vivo* and *in vivo* models, and their findings were in consistence with the outcome of this current study. One study published in 2013 used IVCM and demonstrated that *Acanthamoeba* cysts were rounded in shape and highly reflective in all examined cases which led to rapid confirmation of the clinical

diagnosis of Acanthamoeba keratitis (Kobayashi *et al.,*2013). They also studied the *ex vivo* cultured samples using EVCM which showed round and stellate reflective particles consistent with cyst morphology. In another study, researchers used HRT II/RCM to study *Acanthamoeba* cysts and reported a rounded, double walled morphology of *Acanthamoeba* cysts with various sizes and shapes which is consistent with the findings of this current study (Matsumoto *et al.,*2007).

One research about diagnosis and management of infectious keratitis used IVCM to study cyst morphologies which were found to be hyper-reflective, rounded, spherical, ovoid, with occasional double walled appearance (Labbé *et al.,*2009). Another research demonstrated hyper-reflective particles with further morphologies including signet ring, coffee bean, rod, stellate, rounded and ovoid shapes that have single or double walls (De Craene *et al.,*2018). Cysts have various morphologies as they can be triangular, 5 pointed or 7 pointed depending on the species of *Acanthamoeba* being examined, or due to the uncertainty of the structure under evaluation as the cornea may contain other micro-organisms including bacterial and fungal spores which are much smaller in size varying between 1-6μm compared to the *Acanthamoeba* cyst size ranging between 25-35μm.

In this study, live *Acanthamoeba* trophozoites were evaluated using EVCM and phase contrast microscopy and the images were compared to IVCM findings from confirmed cases of Acanthamoeba keratitis. Individual cells were not visualised using EVCM and IVCM which only showed the aggregation of trophozoites as a coarse speckled area of refractile material. Phase contrast microscopy images

showed amoeboid trophozoites with non-refractile membrane with refractile food vacuoles in the cytoplasm.

A paper published in 2012 used EVCM to study *Acanthamoeba* trophozoites cultured from patients with confirmed Acanthamoeba keratitis and they reported the trophozoites to be highly reflective, high contrast without cell wall (Yamazaki *et al.,*2012). Another paper used HRT II/RCM to study trophozoites which appeared homogenous, highly reflective intense and multiform in shape (Matsumoto *et al.,*2007). Nevertheless, the demonstration of *Acanthamoeba* trophozoites still poses a challenge as a previous study detected *Acanthamoeba* trophozoites in only one in nine cases of patients with confirmed Acanthamoeba keratitis using HRT II-RCM (Shiraishi *et al.,*2010).

6.6 Conclusion and Future Work

Images generated using HRT II- RCM in both EVCM and IVCM showed rounded, double walled structures representing *Acanthamoeba* cysts, however, the visualization of trophozoites was difficult to achieve. Up to our knowledge, this is the first study to perform this type of *ex vivo* work to comprehensively demonstrate the different morphologies of *Acanthamoeba* in both EVCM and IVCM and the matching in the outcome makes EVCM images a reliable diagnostic aid to validate IVCM findings where the study of *Acanthamoeba* cyst under EVCM facilitates the interpretation of *in vivo* findings in light of *ex vivo* images.

Further studies can follow for other strains of *Acanthamoeba* to create a library of images for all morphological appearances to be used as a reference to facilitate early diagnosis of Acanthamoeba keratitis in the human eye.

Chapter Seven

Phenotypic Similarities between *Acanthamoeba* and Macrophages Using Flow Cytometry

Chapter 7: Phenotypic Similarities between *Acanthamoeba* and Macrophages Using Flow Cytometry

7.1 Introduction

7.1.1 Macrophages

Macrophages are phagocytes that play a crucial role in innate immunity. They form one of the initial defense mechanisms against pathogens and have a major role in maintaining immunological homeostasis (Tarique *et al.,*2015). They are large tissue resident myeloid cells characterized by the presence of pseudopodia that give them the stellate appearance and they contain many vacuoles and granules which give them the foamy appearance (Flannagan *et al.,*2009). Other names for macrophages are based on the tissues within which they reside and include: Kupffer cells in the liver, microglia in the brain, Langerhans cells in the skin, osteoclasts in the bone and alveolar macrophages in the lungs (Yona *et al.,*2013).

7.1.2 Function

The main function of macrophages is phagocytosis which is the ingestion and engulfment of microbes and apoptotic cells by initiating a rapid and extensive cytoskeletal rearrangement of macrophages to facilitate the engulfment of the phagocytosed bodies 'phagosomes' (Flannagan *et al.,*2009). This process is followed by exchange of the components of phagosomes with lysosomes forming the final stage of phagosome maturation which results in the killing and degradation of the lumen content which demarcates one of the most critical steps in macrophages function (Flannagan *et al.,*2009, Silva,2010).

Macrophages recognize changes in tissue such as stress, infection, or injury, and initiate inflammation which will be followed by tissue remodeling (Italiani and Boraschi,2015). They express many receptors such as Toll-like receptors (TLRs), retinoic acid-inducible gene-I-like receptors (RLRs), and cytosolic nucleotide-binding domain leucine-rich repeat-containing proteins (NLRS) receptors (Price and Vance,2014, Takeuchi and Akira,2010), and they are activated when these receptors are ligated.

Macrophages are classified into classically activated macrophages (M1) and alternatively activated macrophages (M2) (Figure 7.1) depending on the surface receptor (cluster of Differentiation-CD), and inflammatory mediators (Tarique *et al.,*2015).

7.1.3 History

Macrophages were first identified by their phagocytic nature in the 19th century by Metchinkoff (Cavaillon,2011). In 1884, Metchinkoff demonstrated that macrophages help in tissue integrity and immunological homeostasis, and he reported that these cells can identify microbes and distinguish between self and non-self cells (Cavaillon,2011). This concept formed the basis of innate immunity that awarded him the Nobel Prize in 1908. The name macrophages came from the Greek word “makros” which means “large” and “phagein” which means “eat” (Das *et al.,*2015).

7.1.4 Activation of Macrophages

The function of macrophages depends on the stimuli they receive from the surrounding micro-environment (Mills *et al.,*2012) (Figure 7.1). The activation of macrophages is mediated by ligation of TLRs and cytokine receptors that results in the expression of specific genes and proteins (Gordon & Taylor 2005). After the discovery of interferon γ (IFN-γ) in the early 1990s and with better understanding of its cellular activity, it is now well established that IFN-γ produced by type 1 T helper cell (TH-1) stimulates macrophages and activates their antimicrobial effect (Mosmann *et al.,*1986, Nathan *et al.,*1983, Pace *et al.,*1983).

M1 macrophages are classically activated as a result of stimulation by IFN-γ and once activated will secrete proinflammatory cytokines like tumour necrosis factor (TNF), IL-1β, IL-6, IL-12 (Shao and Lin 2008, Ziegler-Heitbrock *et al.,*1994). A study in 1960s by Mackness and colleagues showed that macrophages can also be activated by bacterial products, and they reported an activation and enhancement of the anti-microbial activity of macrophages in mice infected with *Mycobacterium bovis* bacillus Calmette-Guerin (BCG) and *Listeria monocytogens* (Mackaness ,1964). M1 macrophages play an important role in host defenses against microorganisms and in tumor suppression and regression (Italiani and Boraschi,2015).

Macrophages that are activated by IL-4, IL-10, IL-13 are referred to as alternatively activated macrophages or M2 macrophages (Nishizuka 1992, McCarthy *et al.,*2012, Qin 2012). They are involved in tissue repair, wound healing (Wynn 2004, Bouhlel *et al.,*2007, Sica *et al.,*2008), resolution of parasite infection, tissue remodeling, immunoregulation and tumor progression (Ziegler-Heitbrock *et al.,*1988, Friedland *et al.,*1993).

Many researchers reported that the concept of macrophage activation (polarization) into M1, M2 states is probably over-simplistic and that these states represent two extreme ends of the polarization journey, with many macrophage phenotypes falling in between (Mosser and Edwards,2008). For example, M2-like macrophages called regulatory macrophages have some of the characteristics of both M1 and M2 states. Regulatory macrophages express CD206, CD163 while also producing high levels of IL-10 and low levels of TNF-α and IL -12 similar to M2 macrophages (Biswas and Mantovani,2010).

Macrophages can be differentiated from the human leukemic cell line (THP-1), which was established by Tsuchiya *et al.*in 1980 from the peripheral blood of a one-year-old male human with acute monocytic leukemia (Takashiba *et al.,*1999). After exposure to phorbol-12-myristate-13-acetate (PMA), THP-1 cells in the monocytic state start to attach to the culture flask and take on a macrophage-like morphology by becoming amoeboid in shape and acquiring a well-developed Golgi apparatus, rough endoplasmic reticulum and large numbers of ribosomes in the cytoplasm (Auwerx,1991). Vitamin D3 (1 alpha, 25-dihydroxyvitamin D3) is another reagent used to differentiate monocytic cells into a macrophage state. PMA works by recruiting protein kinase C leading to a more mature phenotype with higher level of adherence and phagocytic ability and high levels of cell surface CD11b and CD14 (Gordon and Taylor,2005) in comparison to vitamin D3, which recruits MAPK phosphatase -1 (MKP-1) pathways that facilitate monocytic differentiation (Gocek *et al.,*2015).

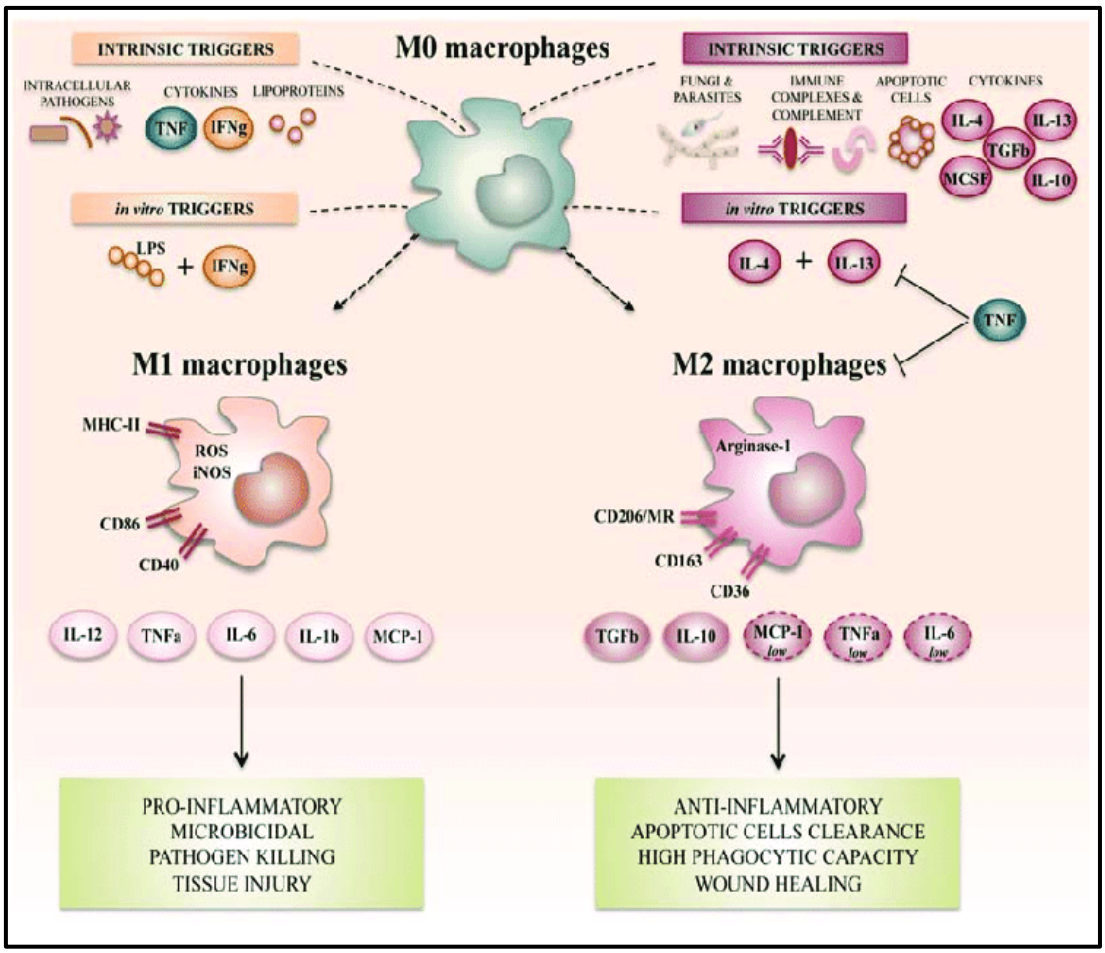

Figure 7.1: Schematic diagram showing different stimuli and signaling pathways in activation and polarization of macrophages from M0 to M1 or M2 and the various roles of the activated macrophages with their surface receptors (CD) and inflammatory mediators. TGF: transforming growth factor; MR: mannose receptor; TNF: tumour necrosis factor; MCP: monocyte chemoattractant protein; IFNg: interferon gamma; IL: interleukin; LPS: lipopolysaccharide (Atri *et al.,*2018).

7.1.5 *Acanthamoeba* and Macrophages

Acanthamoeba and macrophages share many phenotypic and functional properties related to their structure (Figure 7.2), movement, physiology, phagocytic processes and interaction with microorganisms (Greub *et al.,*2003, Wynn *et al.,*2013). Both *Acanthamoeba* and macrophages engulf microbes by an actin-dependent process that leads to pseudopod formation (Siddiqui and Khan,2012). Both hosts exhibit features that allow bacteria to survive within them as for example, *Legionella pneumophila* grows inside them by expressing genes such as ICMT, ICMR, ICMQ, ICMB which play a role in intracellular growth and multiplication in both hosts, (Segal and Shuman 1999), with a similar life cycle in both hosts (Escoll *et al.,*2013). In addition, *Pseudomonas aeruginosa, Yersinia spp., Bacillus anthracis* (Price and Vance,2014), *Parachlamydia intracellular and Listeria monocytogens* had been reported to survive in both hosts (Greub *et al.,*2003). It was established that bacteria which can survive in amoeba can adapt to replicate in macrophages and become human pathogens (Price and Vance,2014).

Both *Acanthamoeba* and macrophages have interchangeable states of cytoplasm, namely endoplasm and ectoplasm. The endoplasm is liquid and can be found in the cell centre while the ectoplasm is gelatinous and is usually located beneath the cell membrane (Siddiqui and Khan,2012), and they both demonstrate an increase in the number of mitochondria in their active stage (Cohn and Benson 1966; Cohn *et al.,*1965). Another similarity is that both Acanthamoeba and macrophages use NADPH oxidase to kill bacteria (Anderson *et al.,*2005). NADPH is essential for the function of phagocytic cells that form the innate immune system such as neutrophils, eosinophils, monocytes and macrophages (Cross *et al.,*2004).

Tissue resident macrophages recognize microbes by receptors such as Toll-like receptors which are transmembrane proteins that recognise pathogen-associated molecular patterns (PAMPs) derived from various microbes and subsequently synthesise pro-inflammatory cytokines and chemokines (Vaure and Liu,2014). Similarly, *Acanthamoeba* carries specific molecules on its surface that are recognized by TLR4 inducing innate immunological response (Cano *et al.,*2017). A previous study reported that the plasma membrane of *Acanthamoeba castellanii* has 31% of its mass composed of lipophosphoglycans (LPG) (Korn *et al.,*1974) which are considered *Acanthamoeba*-associated molecular patterns (Karaś *et al.,*2013) that stimulate TLR expression on macrophages and induce IL12 and IL16 (Cano *et al.,*2017).

There are some differences between *Acanthamoeba* and macrophages, mainly the ability of *Acanthamoeba* to live independently in the environment and its ability to protect itself by entering a dormant cyst stage during its life cycle (Siddiqui and Khan,2012).

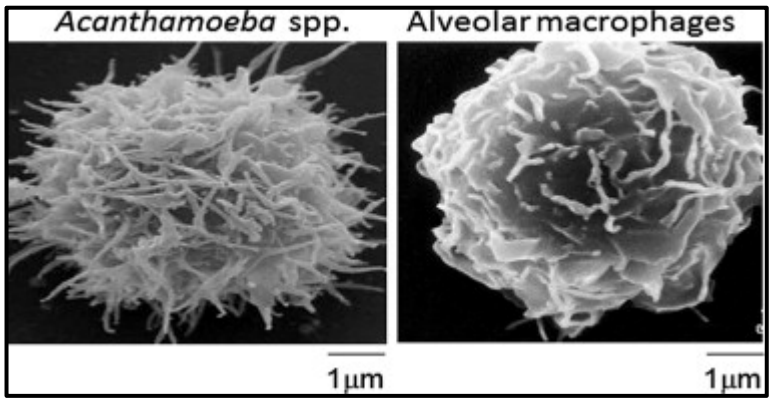

Figure 7.2: Transmission electron microscope images showing similar appearance of *Acanthamoeba castellanii* (left) and alveolar macrophage (right) (Siddiqui and Khan 2012)

7.1.6 Rationale

The similarities between *Acanthamoeba* and macrophages have been investigated throughout literature. Nevertheless, there is a paucity of research performed on studying amoebic cell surface in comparison to that of macrophages. Assessing the expression of various membrane-bound antigens on amoebic cell surface in comparison to macrophages and finding any similarities between *Acanthamoeba* and macrophages will improve the understanding of how *Acanthamoeba* interacts with human immune system during infection which will help to identify novel therapeutic approaches in any future work.

7.1.7 Aim and Objectives

The work of this chapter aims to investigate the similarities between *Acanthamoeba* and human macrophages. The objectives are:

- Investigate structural similarities between *Acanthamoeba* and macrophages that may reflect functional similarities by using the flow cytometry panel to assess the expression of different membrane-bound antigens to screen amoebic cell surface.
- Evaluate the possibility of using anti-human leukocytes antibodies to screen amoebic cells surface to investigate further structural similarities between amoeba and macrophages.

7.2 Methods

7.2.1 Organisms

The following table shows cell lines and organisms used in this study.

Human cell line	Strain
THP-1	ATCC – TIB-202
Microorganism	Strain
Acanthamoeba polyphaga	ATCC 30461
Acanthamoeba castellanii	ATCC 50370
Naegleria gruberi	ATCC 30133
*Acanthamoeba –clinical isolate**	----------
Acanthamoeba culbertsoni	ATCC 30171

*Obtained from Moorfields Eye Hospital NHS Foundation Trust

Table 7.1: Organisms and cells used for flow cytometry analysis.

7.2.2 Culture

7.2.2.1 THP-1 Cells

Cells were maintained at 37 C^o and 5% CO_2 in RPMI 1640 growth medium and were successfully differentiated into macrophages as previously described in chapter 2 section 2.13.

7.2.2.2 Microorganisms

Acanthamoeba castellanii (ATCC 30011), *Acanthamoeba polyphaga* (ATCC 30461) and *Acanthamoeba culbertsoni* (ATCC 30171) were maintained in tissue culture flasks using a semi defined axenic medium (AC#6) as previously described in chapter 2 section 2.3, and the same culture method was followed for both *Naegleria gruberi* (ATCC 30133) and *Acanthamoeba* – clinical isolate.

7.2.3 Flow Cytometry

Organisms and macrophages were processed using the following steps: the culture medium was removed from tissue culture flasks, and adherent cells were washed twice with staining buffer consisting of phosphate buffered saline (PBS), then 2% paraformaldehyde in PBS was added to the cells that were subsequently kept at room temperature for 10 minutes. The cells were then removed by gentle scraping with cell scraper and transferred to a 50 mL tube and centrifuged to form a cell pellet. The supernatant was removed, and cell pellets were re-suspended in 10 mL fresh buffer of PBS. The cells were centrifuged again under the same conditions. The cell pellets were again suspended in 1.5 mL buffer and transferred to 12 mm x 75 mm

tubes for counting. The cells were counted and then the count was adjusted to 1x 10^6 cells/mL.

The monoclonal antibodies (mAb) used in this study were CD11b, CD36, CD14, CD45, and MHC-II, all of which are anti-human. The antibodies used for flow cytometry analysis were obtained from Thermo Fisher Scientific, UK (table7.2). The negative controls consisted of IgG were derived from normal mouse serum conjugated with either PE or FITC fluorophores. Sample tubes with 100 µL of adjusted cell suspension received 5µL of anti-CD45, CD11b, CD36, CD 14, MHC-II, or isotype control antibody according to manufacturer instructions of the antibodies. Cell control tubes received 5 µL of buffer to be used for assessing endogenous auto fluorescence. The tubes were incubated in the dark for 10 minutes at room temperature. All tubes received 3 mL of buffer of BPS, then were centrifuged at 4°C for 10 minutes at 250 x *g*, and the supernatant was removed.

Cell pellets were re-suspended in 3 mL of buffer and centrifuged under the same conditions. The supernatant was then removed, and the cell pellets were further re-suspended in 1 mL buffer. The tubes were kept for 10 minutes in dark area at room temperature before analysis. All samples and corresponding controls were analysed on a BD Accuri™ C6 (BD Biosciences, US) with an excitation wavelength of 488 nm.

Antibody	Clone(s)	Isotype	Label	Supplier
CD14	61D3	IgG 1κ	PE	Thermo Fisher Scientific
CD36	eBioNL07 (NL07)	IgM	FITC	Thermo Fisher Scientific
CD11b	ICRF44	IgG 1κ	PE	Thermo Fisher Scientific
CD45	HI30	IgG 1κ	PE	Thermo Fisher Scientific
MHC Class II	M5/114.15.2	IgG2b κ	APC	Thermo Fisher Scientific

Table 7.2: Anti-human leukocyte monoclonal antibodies used in flow cytometry analysis of amoebic cell surface.

7.3 Results

Flow cytometry (FCM) analysis showed a strong reactivity in macrophages with CD11b, CD36, CD14, MHC-II, CD45 antibodies. Results showed negative staining in all tested amoeba strains except for a positive staining of *Naegleria gruberi* with CD45 compared to its respective isotype control, and potential weak positivity with CD36, CD45 and CD11b in *Acanthamoeba castellanii*.

7.3.1 Macrophages

Flow cytometry analysis showed a positive reactivity in macrophages with the following antibodies: MHC-II (Figure 7.3a), CD 14(Figure 7.3b), CD36 (Figure 7.3c), CD45 (Figure7.3d), CD11b (Figure 7.3e).

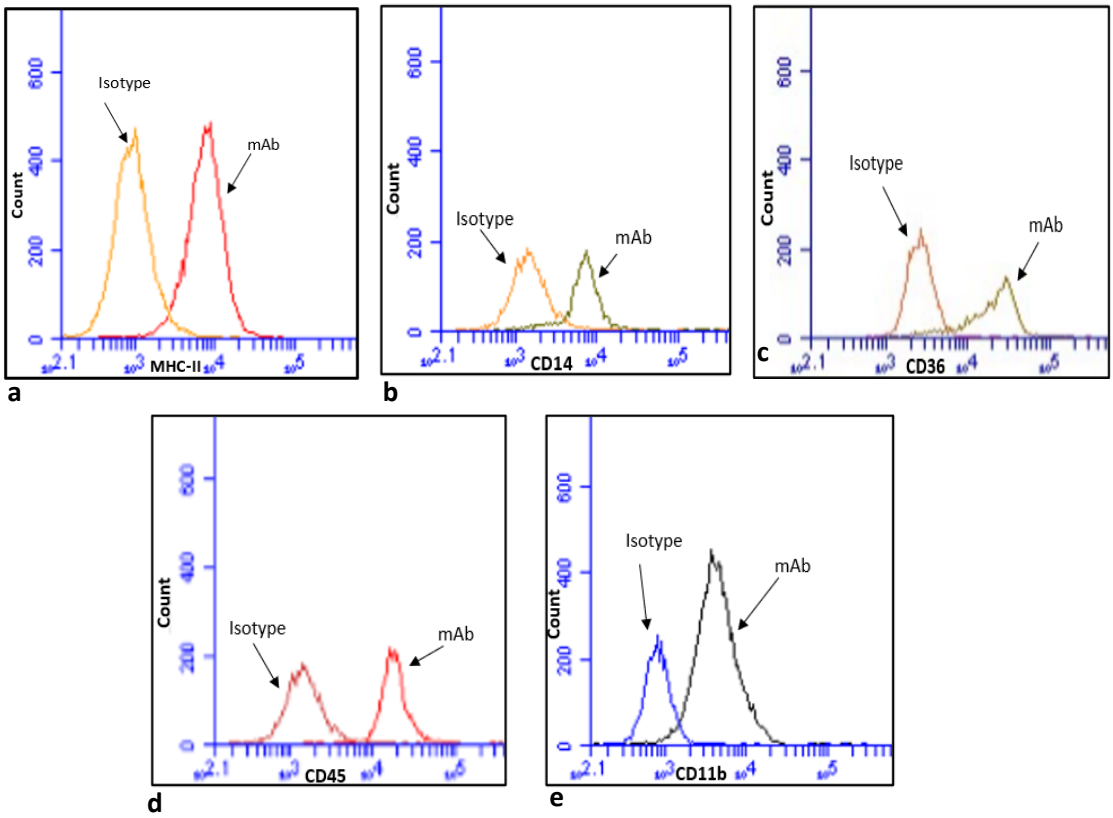

Figure 7.3: Flow cytometry results for macrophages stained with anti-human mAbs. The X-axis represents fluorescent signal intensity, the Y-axis represents the number of detected events. All screened antibodies (mAb) showed positive staining in macrophages compared to the negative control (isotype). **a**. mAb: MHC-II, isotype: IgG2b κ; **b**. mAb: CD14, isotype: IgG 1κ; **c**. mAb: CD36, isotype: IgM; **d**. mAb: CD45, isotype: IgG 1κ; **e**. mAb: CD11b, isotype: IgG 1κ.

7.3.2 *Acanthamoeba castellanii*

Flow cytometry analysis showed a negative reactivity in *Acanthamoeba castellanii* with MHC-II (Figure 7.4a) and CD14 (Figure 7.4b) and weak positivity with CD36 (Figure 7.4c), CD45 (Figure 7.4d) and CD11b (Figure 7.4e).

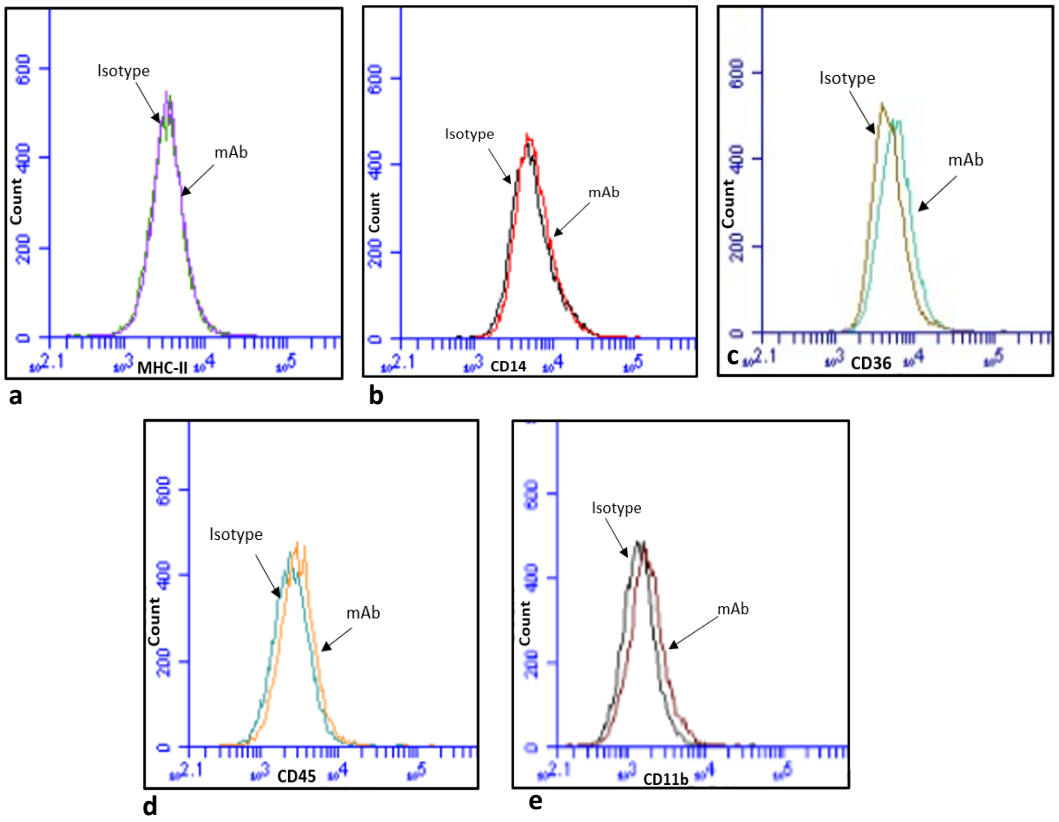

Figure 7.4: Flow cytometry result for *Acanthamoeba castellanii* stained with anti-human mAbs. The X-axis represents fluorescent signal intensity, the Y-axis represents the number of detected events. All controls isotypes were negative. **a**. mAb: MHC-II, negative, isotype: IgG2b κ; **b**. mAb: CD14, negative, isotype:

IgG 1κ; **c**. mAb: CD36, weakly positive, isotype: IgM; **d**. mAb: CD45, weakly positive, isotype: IgG 1κ; **e**. mAb: CD11b, weakly positive, isotype: IgG 1κ.

7.3.3 *Naegleria gruberi*

Flow cytometry analysis showed a negative reactivity in *Naegleria gruberi* with the following antibodies: MHC-II (Figure 7.5a), CD 14(Figure 7.5b), CD36 (Figure 7.5c), and CD11b (Figure 7.5e). However, a positive staining *of Naegleria gruberi* with CD45 antibody (Figure 7.5d) was detected compared to its respective isotype control.

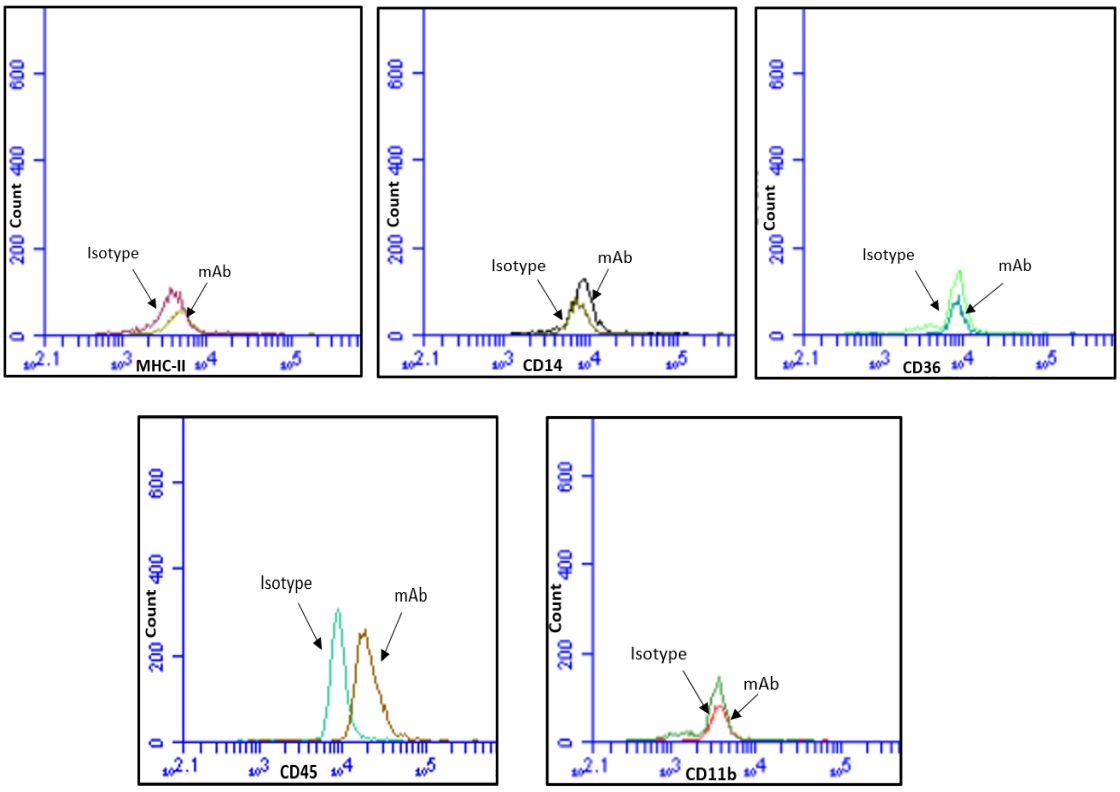

Figure 7.5: Flow cytometry result for *Naegleria gruberi* stained with anti-human mAbs. The X-axis represents fluorescent signal intensity, the Y-axis represents the number of detected events. All controls isotypes were negative. **a**. mAb: MHC-II, negative, isotype: IgG2b κ; **b**. mAb: CD14, negative, isotype: IgG 1κ; **c**. mAb: CD36, negative, isotype: IgM; **d**. mAb: CD45, positive, isotype: IgG 1κ; **e**. mAb: CD11b, negative, isotype: IgG 1κ.

7.3.4 *Acanthamoeba* (clinical isolate)

Flow cytometry analysis showed a negative reactivity in *Acanthamoeba* (clinical isolate) with the following antibodies: MHC-II (Figure 7.6a), CD14 (Figure 7.6b), CD36 (Figure 7.6c), CD45 (Figure 7.6d), CD11b (Figure 7.6e).

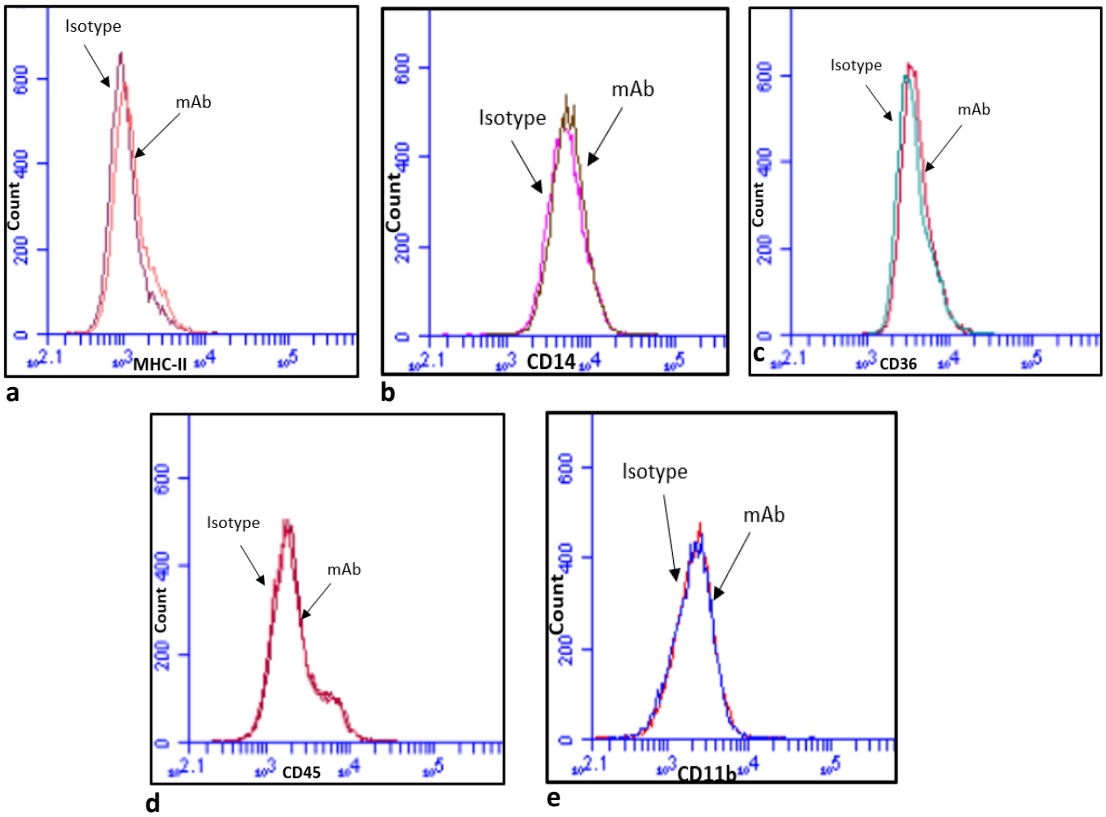

Figure 7.6: Flow cytometry result for *Acanthamoeba* (clinical isolate) stained with anti-human mAbs. The X-axis represents fluorescent signal intensity, the Y-axis represents the number of detected events. All screened antibodies (mAb) showed negative staining in *Acanthamoeba* (clinical isolate) similar to the negative control (isotype).

a. mAb: MHC-II, isotype: IgG2b κ; **b**. mAb: CD14, isotype: IgG 1κ; **c**. mAb: CD36, isotype: IgM; **d**. mAb: CD45, isotype: IgG 1κ; **e**. mAb: CD11b, isotype: IgG 1κ.

7.3.5 *Acanthamoeba polyphaga*

Flow cytometry analysis showed a negative reactivity in *Acanthamoeba polyphaga* with the following antibodies: MHC-II (Figure 7.7a), CD14 (Figure 7.7b), CD36 (fig 7.7c), CD45 (Figure 7.7d), CD11b (Figure 7.7e).

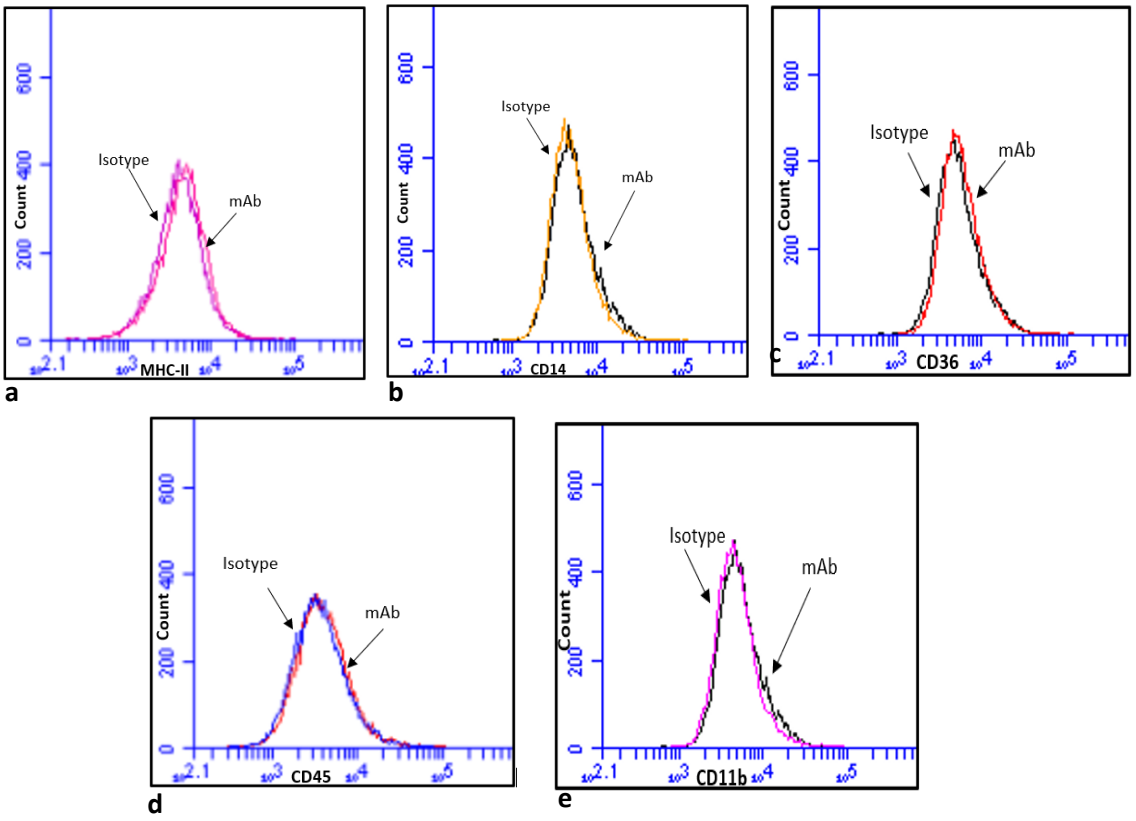

Figure 7.7: Flow cytometry result for *Acanthamoeba polyphaga* stained with anti-human mAbs. The X-axis represents fluorescent signal intensity, the Y-axis represents the number of detected events. All screened antibodies (mAb) showed negative staining in *Acanthamoeba polyphaga* similar to the negative control (isotype).

a. mAb: MHC-II, isotype: IgG2b κ; **b**. mAb: CD14, isotype: IgG 1κ; **c**. mAb: CD36, isotype: IgM; **d**. mAb: CD45, isotype: IgG 1κ; **e**. mAb: CD11b, isotype: IgG 1κ.

7.3.6 *Acanthamoeba culbertsoni*

Flow cytometry analysis showed a negative reactivity in *Acanthamoeba culbertsoni* with the following antibodies: MHC-II (Figure 7.8a), CD 14(Figure 7.8b), CD36 (Figure 7.8c), CD45 (Figure 7.8d) , CD11b (Figure 7.8e).

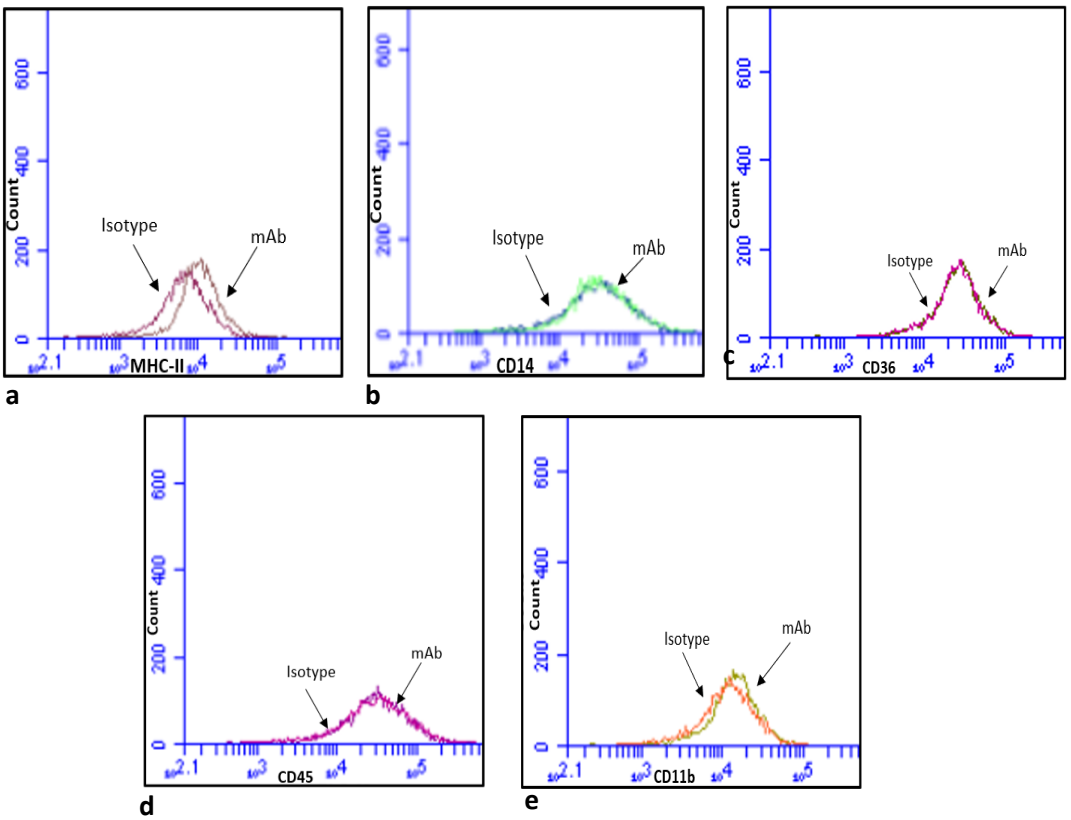

Figure 7.8: Flow cytometry result for *Acanthamoeba culbertsoni* stained with anti-human mAbs. The X-axis represents fluorescent signal intensity whereas the Y-axis represents the number of detected events. All screened antibodies (mAb) showed negative staining in *Acanthamoeba culbertsoni* similar to the negative control (isotype).

a. mAb: MHC-II, isotype: IgG2b κ; **b**. mAb: CD14, isotype: IgG 1κ; **c**. mAb: CD36, isotype: IgM; **d**. mAb: CD45, isotype: IgG 1κ; **e**. mAb: CD11b, isotype: IgG 1κ.

7.4 Discussion

In this study, four species of *Acanthamoeba* alongside *Naegleria gruberi* were incubated with different anti-human leukocyte monoclonal antibodies (mAb) to find any similarities between macrophages and amoebic proteins and to investigate the utility of these anti-human leukocyte antibodies to screen amoebic cell surfaces. Similar to *Acanthamoeba*, *Naegleria* gruberi is a widespread free-living freshwater amoeba which is classified as a free-living protist and its reproductive form is a 15-μm amoeba which feeds on bacteria (Jonckheere,2002). The monoclonal antibodies (mAb) used in this study are well-recognised macrophage markers and they have different established functions: major histocompatibility complex (MHC-II), phagocyte activation (CD14, CD45), surface adhesion (CD11b), and metabolism-mediated receptor (CD36).

The results obtained by the flow cytometry analysis showed a strong reactivity in macrophages with CD11b, CD36, CD14, MHC-II, CD45 antibodies. Results showed negative staining in all tested amoeba strains except for the detection of positive staining of *Naegleria gruberi* with CD45 compared to its respective isotype control, and potential weak positivity with CD36, CD45 and CD11b in *Acanthamoeba castellanii.* The positive staining suggests similarities in protein surfaces and their functions mainly with the positive reactivity of *Naegleria* to CD45 which might indicate the ability of *Naegleria* to synthesize similar proteins on its surface to perform similar functions to CD45 on the surface of macrophages.

There are limited studies on the roles of CD45, however it was recently shown to be involved in several aspects of macrophages activation mainly C5a activated monocytes and epithelium-lining macrophages (Werfel *et al.,*1991). The evidence

suggests a role of CD45 in monocyte adherence (Lorenz *et al.,*1993) and respiratory burst (Liles *et al.*1995, Jean *et al.,*2000). CD45 is also referred to as protein tyrosine phosphatase receptor type C (PTPRC) which plays an important role in regulating human leukocyte activity making it a panleukocytic marker highly expressed in all hemopoietic cell lines (Dahlke *et al.,*2004).

There are possible similarities between surface proteins and their functions between *Acanthamoeba castellanii* and macrophages given the potential weak positivity with CD11b, CD36 and CD45. Regarding CD11b, it is also referred to as macrophage-1 antigen or complement receptor 3 and is expressed on the surface of a number of leukocytes that play a role in innate immunity as macrophages, neutrophils and monocytes (Solovjov *et al.,*2005). CD11b facilitates inflammation by its role in the regulation of adhesion and migration of leukocytes and is also involved in vital immune processes including phagocytosis and attraction of the immune cell to the site of inflammation or injury by a process called chemotaxis (Solovjov *et al.,* 2005). CD36, also known as fatty acid translocase, is found on many cell surfaces and aids in importing fatty acids inside cells and has many ligands as collagen (Tandon et al.,1989), native lipoproteins (Calvo *et al.,*1998) and long chain fatty acids (Baillie *et al.,*1996).

7.4.1 Previous Studies

A similar research was conducted in 2010 to investigate whether anti-human leukocytes antibodies can be used to screen amoebic cell surface to find similar proteins (Ravine *et al.,*2010) and the results of which supported the outcome of this current study. In their research, they incubated *Naegleria* and *Acanthamoeba* with anti-human antibodies such as CD14, CD45, CD206 and CD59, and they found that both *Naegleria fowleri* and *Naegleria gruberi* demonstrated strong reactivity for CD45 antibody and a dimmed positive staining of *N. fowleri* with CD59 antibody, while *N. gruberi* revealed a negative result for CD59 antibody. Negative staining results were obtained in all other tested *Acanthamoeba* species. The differences between their study and this study is that they used *Acanthamoeba castellanii, Acanthamoeba culbertsoni, Naegleria fowleri* and *Naegleria gruberi* where this study did not include *Naegleria fowleri* but included further species of *Acanthamoeba* such *as A. polyphaga* and *Acanthamoeba* (clinical isolates).Their selection of CD markers (CD14, CD45, CD206, CD59) was based on their role in phagocyte activation while the CD markers used in this study have different roles like adhesion (CD11b), metabolism (CD36), phagocytosis (CD14,CD45) and major histocompatibility complex (MHC-II). Both studies showed positive reactivity of *Naegleria* to CD45 antibody and negative staining for the rest of the antibodies however in our study we also observed potential weak positivity with CD36, CD45 and CD11b in *Acanthamoeba castellanii*.

Another research supported this current study by demonstrating the potential to use anti-human leukocytes antibodies to screen amoebic cells surface (Fritzinger *et al.,*2006). They reported that *Naegleria fowleri* expresses CD59 like molecule on its surface, but this molecule was not detected on the surface of non-pathogenic

Naegleria gruberi amebae. They used Southern blot, Western immunoblot, and immunofluorescence analysis to identify any reactivity of *Naegleria fowleri* membrane with anti-human CD59 antibody. Southern blot analysis showed one gene in *Naegleria fowleri* that encodes CD59, while Western immunoblot revealed a protein that is reactive with human CD59 monoclonal antibodies in the membrane of *Naegleria fowleri*. Furthermore, immunofluorescence analysis demonstrated the presence of CD59 on the membrane of *Naegleria fowleri*. They concluded that the expression of this protein may be associated with a protective role for amoeba (Fritzinger *et al.,*2006).

CD59 (protectin) is a membrane inhibitor of reactive lysis that attaches to host cells by a glycophosphatidylinositol anchor and can prevent the formation of the complement membrane attack complex (Huang *et al.,*2006). Some viruses such as human immunodeficiency virus and human cytomegalovirus incorporate CD59 of the host cell into their envelope to prevent being lysed by the complement system (Bohana-Kashtan *et al.,*2004).

The differences between their study and this current study are that they mainly studied *N.fowleri* and *N .gruberi*, while in this current work *N. fowleri* was not included but four species of *Acanthamoeba* were studied in addition to *N*. *gruberi*, they used CD59 only while this work investigated different CD markers antibodies, and another difference is that for this study we only used flow cytometry technique as a method of analysis.

7.5 Conclusion and Future Work

The results obtained demonstrate various degrees of positive reactivity of amoebic cell surface to a limited number of anti-human monoclonal antibodies. This positivity suggests some similarities in protein surfaces and their functions between amoeba and macrophages and while this limited reactivity can potentially offer a tool for screening, it is still difficult to use it to screen amoebic cell surface using anti-human monoclonal antibodies.

Future work may include further studies on positive results using immuno-histochemical analysis, electron microscope and Immunofluorescence in conjunction with our method in addition to using comparative genomic analysis techniques.

The surface receptors shown to have positive reactivity in this study can be further investigated with regards to the ligands that bind to them in aim of finding potential similarities between these ligands and the ones that bind to *Acanthamoeba* receptors. Finally, more antibodies can be investigated to detect further similarities between macrophages and amoeba which can potentially carry diagnostic and clinical significance.

Chapter Eight

General Conclusions

Chapter 8: General Conclusions

Acanthamoeba is a virtually ubiquitous, small free-living amoeba found in the environment and has a life cycle of an active trophozoite and a dormant highly resistant cyst stage. *Acanthamoeba* species are opportunistic pathogens of humans that can cause different diseases including a blinding keratitis.

This chapter summarises the work in this thesis starting by the developing an *ex vivo* corneal model of Acanthamoeba keratitis (AK) and using this model for different applications including reaching a better understanding of the pathophysiological processes that occur throughout the disease, investigating the role of cells of innate immunity in fighting the infection, testing the efficacy of different pharmaceutical compounds in treating AK, correlating morphological findings of *Acanthamoeba* between *in vivo* samples of confirmed cases of AK and the *ex vivo* model using confocal microscopy, and finally evaluating the phenotypic similarities between *Acanthamoeba* and cells of the innate immune system mainly macrophages using flow cytometric analysis.

Several approaches were used to develop and maintain the *ex vivo* model, and the outcome was evaluated at both gross and microscopic levels. We developed a grading system to quantify the integrity of the model starting from grade 0 for healthy cornea up to grade 4 where there is a total loss of corneal epithelium and the presence of stromal oedema. The models were evaluated using the grading system to facilitate comparison between the different techniques used to develop the model.

Using the immersion system, we were able to maintain the corneal transparency and epithelium for one week after which the cornea became opaque and lost all of its epithelium (grade 4). Using the air liquid interface, the static model with CO_2 maintained corneal transparency for two weeks with loss of more than 50% epithelium (grade 3), and a total loss of epithelium at week four (grade 4). The air- liquid interface was also evaluated using a rocking system with and without CO_2 which showed superior results with the addition of CO_2 as we were able to maintain the epithelium up to four weeks with only superficial loss of the outermost epithelium layers (grade1) and no stromal oedema. Both rocking models (with and without CO_2) lost corneal transparency after 2 weeks. These results signify the superiority of using the air-liquid interface using a rocking system with better outcome with the supplement of CO_2 where the rocking system mimics the natural blinking of the eye lid and CO_2 serves as a vital nutrient to cells and maintains the pH close to neutral which is more resembling to an *in vivo* environment.

Acanthamoeba keratitis model was developed using the air- liquid interface rocking system with CO_2 for the reasons described above. A scoring system was developed to describe the infection process starting from the attachment of *Acanthamoeba* trophozoites to corneal epithelium (score 1*) and the progression of the disease was followed up till the invasion of trophozoites to the stroma with total loss of epithelium (score 6*). The infection was induced by adding the trophozoites to the corneal surface after inducing epithelial injury by scratching the surface of cornea and the model was subsequently examined microscopically on day 3 and every 5 days afterwards for a total of four weeks. The attachment of trophozoites started on day 3 (score 1*), and the earliest changes to the epithelium were noted on day 8 with

superficial loss of epithelial layers (score 2*). The progression of the disease was studied, and the findings were documented until there was a complete loss of all epithelial layers with invasion of the trophozoites to the middle parts of the stroma on day 28 (score 6*). These observations demonstrated the usability of the *ex vivo* model to induce infection and monitor the progression of the disease in the absence of host immune response. To our knowledge, this is the first *ex vivo* model successfully developed to study Acanthamoeba keratitis for an extended period of four weeks.

The established ex vivo model was utilized to test the therapeutic effect of doxycycline and PHMB against Acanthamoeba keratitis and to study any potential toxicity against the corneal epithelium. Furthermore, drug assay was performed to Investigate the efficacy of PHMB and doxycycline against *Acanthamoeba* trophozoites and cysts and any toxic effect against human cells.

Both histological findings and drug assay results confirmed the ability of PHMB to inactivate *Acanthamoeba* trophozoites, however despite the AK model demonstrating mild toxic effect of PHMB against corneal epithelial cells, drug assay results show high level of *in vitro* toxicity to human cells which is explained by the extra protection mechanisms the *ex vivo* model acquires compared to the *in vitro* setting used in the drug assay. Doxycycline showed no major antimicrobial effect on *Acanthamoeba* with minimal toxic effect on human cells. The findings demonstrate the usability of the *ex vivo* model to test the efficacy of different drugs against

Acanthamoeba and detect any potential toxic effects drugs might exert of corneal epithelial cells.

The model was also used in confocal microscopy and phase contrast studies to correlate morphologies of various forms of *Acanthamoeba* in both *ex vivo* and *in vivo* settings. We inoculated the model with different forms of *Acanthamoeba* (live trophozoites, live, dead and empty cysts) and compared confocal microscopy and phase contrast images to those from *in vivo* images from patients diagnosed with AK. The morphology of *Acanthamoeba* cysts using *ex vivo* confocal microscopy (EVCM) was consistent with phase contrast and *in vivo* contrast microscopy (IVCM) images showing rounded, double walled structures. The visualization of individual trophozoites was difficult to achieve in both EVCM and IVCM as the aggregation of trophozoites was only demonstrated as a coarse speckled area of refractile material. Phase contrast microscopy images showed amoeboid trophozoites with non-refractile membrane and refractile food vacuoles within the cytoplasm. This is the first study to perform this type of *ex vivo* work which will help in early diagnosis of Acanthamoeba keratitis by facilitating the interpretation of IVCM findings in light of *ex vivo* images.

To better understand how *Acanthamoeba* interacts with human immune system during infection, a flow cytometric analysis was conducted to detect any similarities between amoeba and macrophages by investigating the expression of various membrane-bound antigens on amoebic cell surface in comparison to macrophages

using several anti-human monoclonal antibodies, namely CD11b, CD36, CD14, MHC-II and CD45.

The results of the analysis demonstrated a strong reactivity in macrophages with MHC-II, CD14, CD36, CD45 and CD11b antibodies and negative staining in all tested amoeba strains except for a positive staining of *Naegleria gruberi* with CD45 compared to its respective isotype control, and a potential weak positivity with CD36, CD45 and CD11b in *Acanthamoeba castellanii.*

The positive reactivity suggested some structural and functional similarities in protein surfaces between amoeba and macrophages. Despite having the potential to offer a tool for screening, it is still difficult to screen for amoebic cell surface proteins using anti-human monoclonal antibodies.

References

List of References

Alexander, C. L., Coyne, M., Jones, B., & Anijeet, D. (2015). Acanthamoeba keratitis: Improving the scottish diagnostic service for the rapid molecular detection of Acanthamoeba species. *Journal of Medical Microbiology*, *64*(7), 682–687.

Alizadeh, H., J. Y. Niederkorn, and J. P. McCulley. 1996. Acanthamoeba keratitis, p. 1062–1071. In J. S. Pepose, G. N. Holland, and K. R. Wilhelmus (ed.), *Ocular infection and immunity.*

All About Vision (2020). Cornea of the eye. Available at:

http:// www.allaboutvision.com/resources/cornea.htm

Allen, P. G., & Dawidowicz, E. A. (1990). Phagocytosis in Acanthamoeba: I. A mannose receptor is responsible for the binding and phagocytosis of yeast. *Journal of Cellular Physiology*, *145*(3), 508–513.

Alsam, S., Sissons, J., Dudley, R., & Khan, N. A. (2005). Mechanisms associated with Acanthamoeba castellanii (T4) phagocytosis. *Parasitology Research*, *96*(6), 402–409.

Anderson, I. J., Watkins, R. F., Samuelson, J., Spencer, D. F., Majoros, W. H., Gray, M. W., & Loftus, B. J. (2005). Gene discovery in the Acanthamoeba castellanii genome. *Protist*, *156*(2), 203–214.

Ansorg, R., Rath, P. M., & Fabry, W. (2003). Inhibition of the anti-staphylococcal activity of the antiseptic polihexanide by mucin. *Arzneimittel-Forschung/Drug Research*, *53*(5), 368–371.

Armitage, W. J. (2011). Assessment of corneal quality by eye banks. *Journal of Ophthalmic and Vision Research*, *6;1*, 3–4.

Atri, C., Guerfali, F. Z., & Laouini, D. (2018). Role of human macrophage polarization in inflammation during infectious diseases. *International Journal of Molecular Sciences*, *19*(6), 1801.

Auffray, C., Sieweke, M. H., & Geissmann, F. (2009). Blood monocytes: Development, heterogeneity, and relationship with dendritic cells. *Annual Review of Immunology* (Vol. 27, pp. 669–692). *Annu Rev Immunol.*

Auwerx, J. (1991). The human leukemia cell line, THP-1: A multifacetted model for the study of monocyte-macrophage differentiation. *Experientia* (Vol. 47, Issue 1, pp. 22–31).

Awwad, S. T., Parmar, D. N., Heilman, M., Bowman, R. W., McCulley, J. P., & Cavanagh, H. D. (2005). Results of penetrating keratoplasty for visual rehabilitation after Acanthamoeba keratitis. *American Journal of Ophthalmology*, *140*(6).

Azuara-Blanco, A., Sadiq, A. S., Hussain, M., Lloyd, J. H., & Dua, H. S. (1997). Successful medical treatment of Acanthamoeba keratitis. *International Ophthalmology*, *21*(4), 223–227.

Bacon, A. S., Frazer, D. G., Dart, J. K. G., Matheson, A. S., Ficker, L. A., & Wright, P. (1993). A review of 72 consecutive cases of acanthamoeba keratitis, 1984-1992. *Eye (Basingstoke)*, *7*(6), 719–725.

Baillie, A. G. S., Coburn, C. T., & Abumrad, N. A. (1996). Reversible binding of long-chain patty acids to purified FAT, the adipose CD36 homolog. *Journal of Membrane Biology*, *153*(1), 75–81.

Banjo, T.A. (2018). Acanthamoeba Mannose-Binding Protein: Structural and functional characterisation of a therapeutic target for Acanthamoeba keratitis. University of Leicester

Bantseev, V., McCanna, D. J., Driot, J. Y., Ward, K. W., & Sivak, J. G. (2007). Biocompatibility of contact lens solutions using confocal laser scanning microscopy and the in vitro bovine cornea. *Eye and Contact Lens*, *33*, 308–316.

Barar, J., Javadzadeh, A. R., & Omidi, Y. (2008). Ocular novel drug delivery: Impacts of membranes and barriers. *Expert Opinion on Drug Delivery* (Vol. 5, Issue 5, pp. 567–581).

Barequet, I. S., Bourla, N., Pessach, Y. N., Safrin, M., Yankovich, D., Ohman, D. E., Rosner, M., & Kessler, E. (2012). Staphylolysin is an effective therapeutic agent for Staphylococcus aureus experimental keratitis. *Graefe's Archive for Clinical and Experimental Ophthalmology*, *250*(2), 223–229.

Bernhardt, G., Distèche, A., Jaenicke, R., Koch, B., Lüdemann, H. D., & Stetter, K. O. (1988). Effect of carbon dioxide and hydrostatic pressure on the pH of culture media and the growth of methanogens at elevated temperature. *Applied Microbiology and Biotechnology*, *28*(2), 176–181.

Biswas, S. K., & Mantovani, A. (2010). Macrophage plasticity and interaction with lymphocyte subsets: Cancer as a paradigm. *Nature Immunology* (Vol. 11, Issue 10, pp. 889–896).

Blaylock, W. K., Yue, B. Y., & Robin, J. B. (1990). The use of concanavalin A to competitively inhibit Pseudomonas aeruginosa adherence to rabbit corneal epithelium. *The CLAO journal : official publication of the Contact Lens Association of Ophthalmologists, Inc*, *16*(3), 223–227.

Bohana-Kashtan, O., Ziporen, L., Donin, N., Kraus, S., & Fishelson, Z. (2004). Cell signals transduced by complement. *Molecular Immunology*, *41*(6–7), 583–597.

Bouhlel, M. A., Derudas, B., Rigamonti, E., Dièvart, R., Brozek, J., Haulon, S., Zawadzki, C., Jude, B., Torpier, G., Marx, N., Staels, B., & Chinetti-Gbaguidi, G. (2007). PPARγ Activation Primes Human Monocytes into Alternative M2 Macrophages with Anti-inflammatory Properties. *Cell Metabolism*, *6*(2), 137–143.

Bowers, B., & Korn, E. D. (1969). The fine structure of Acanthamoeba castellanii (Neff strain). II. Encystment. *The Journal of cell biology* (Vol. 41, Issue 3, pp. 786–805).

Bowers, B., & Olszewski, T. E. (1972). Pinocytosis in Acanthamoeba castellanii: Kinetics and morphology. *Journal of Cell Biology*, *53*(3), 681–694.

Brantom, P. G., Bruner, L. H., Chamberlain, M., Silva, O. De, Dupuis, J., Earl, L. K., Lovell, D. P., Pape, W. J. W., Uttley, M., Bagley, D. M., Baker, F. W., Bracher, M., Courtellemont, P., Declercq, L., Freeman, S., Steiling, W., Walker, A. P., Carr, G. J., Dami, N., … Stern, M. (1997). A summary report of the COLIPA international validation study on alternatives to the draize rabbit eye irritation test. *Toxicology in Vitro*, *11*(1–2), 141–179.

Broxton, P., Woodcock, P. M., Heatley, F., & Gilbert, P. (1984). Interaction of some polyhexamethylene biguanides and membrane phospholipids in Escherichia coli. *Journal of Applied Bacteriology*, *57*(1), 115–124.

Buck, S. L., & Rosenthal, R. A. (1996). A quantitative method to evaluate neutralizer toxicity against Acanthamoeba castellanii. *Applied and Environmental Microbiology*, *62*(9), 3521–3526.

Buck, S. L., Rosenthal, R. A., & Abshire, R. L. (1998). Amoebicidal activity of a preserved contact lens multipurpose disinfecting solution compared to a disinfection/neutralisation peroxide system. *Contact Lens and Anterior Eye*, *21*(3), 81–84.

Burton, A. B. G., York, M., Food, R. S. L.-, cosmetics toxicology, & undefined 1981. (n.d.). The in vitro assessment of severe eye irritants. *Elsevier*.

Butler, T. K. H., Dua, H. S., Edwards, R., & Lowe, J. S. (2001). In vitro model of infectious crystalline keratopathy: Tissue architecture determines pattern of microbial spread. *Investigative Ophthalmology and Visual Science*, *42*(6), 1243–1246.

Butt, C. G. (1966). Primary amebic meningoencephalitis. *The New England Journal of Medicine*, *274*(26), 1473–1476.

Byers, T. J., Akins, R. A., Maynard, B. J., Lefken, R. A., & Martin, S. M. (1980). Rapid Growth of Acanthamoeba In Defined Media; Induction of Encystment By Glucose-Acetate Starvation. *The Journal of Protozoology*, *27*(2), 216–219.

Byers, T. J., Hugo, E. R., & Stewart, V. J. (1990). Genes of Acanthamoeba: DNA, RNA and Protein Sequences (A Review). *The Journal of Protozoology*, *37*(4), 17s-25s.

Byers, T. J., Hugo, E. R., King, L. E., & King, L. E. (1991). Molecular aspects of the cell cycle and encystment of acanthamoeba. *Reviews of Infectious Diseases*, *13*, S373–S384.

Calvo, D., Gómez-Coronado, D., Suárez, Y., Lasunción, M. A., & Vega, M. A. (1998). Human CD36 is a high affinity receptor for the native lipoproteins HDL, LDL, and VLDL. *Journal of Lipid Research*, *39*(4), 777–788.

Cano, A., Mattana, A., Woods, S., Henriquez, F. L., Alexander, J., & Roberts, C. W. (2017). Acanthamoeba Activates Macrophages Predominantly through Toll-Like Receptor 4- and MyD88-Dependent Mechanisms To Induce Interleukin-12 (IL-12) and IL-6. *Infection and Immunity*, *85*(6).

Carnt, N. A., Subedi, D., Lim, A. W., Lee, R., Mistry, P., Badenoch, P. R., Kilvington, S., & Dutta, D. (2020). Prevalence and seasonal variation of Acanthamoeba in domestic tap water in greater Sydney, Australia. *Clinical and Experimental Optometry*, *103*(6), 782–786.

Carnt, N., & Stapleton, F. (2016). Strategies for the prevention of contact lens-related Acanthamoeba keratitis: A review. *Ophthalmic and Physiological Optics* (Vol. 36, Issue 2, pp. 77–92).

Carnt, N., Hoffman, J. J., Verma, S., Hau, S., Radford, C. F., Minassian, D. C., & Dart, J. K. G. (2018). Acanthamoeba keratitis: Confirmation of the UK outbreak and a prospective case-control study identifying contributing risk factors. *British Journal of Ophthalmology*, *102*(12), 1621–1628.

Carnt, N., Robaei, D., Minassian, D. C., & Dart, J. K. G. (2018). Acanthamoeba keratitis in 194 patients: Risk factors for bad outcomes and severe inflammatory complications. *British Journal of Ophthalmology*, *102*(10), 1431–1435.

Carnt, N., Robaei, D., Watson, S. L., Minassian, D. C., & Dart, J. K. G. (2016). The Impact of Topical Corticosteroids Used in Conjunction with Antiamoebic Therapy on the Outcome of Acanthamoeba Keratitis. *Ophthalmology*, *123*(5), 984–990.

Castellani, A. (1930). An amoeba found in cultures of a yeast Preliminary note-Third note-An amoeba growing in cultures of a yeast Second note-Fourth note. *Journal of Tropical Medicine London*, *33*, 160.

Cavaillon, J.-M. (2011). The historical milestones in the understanding of leukocyte biology initiated by Elie Metchnikoff. *Journal of Leukocyte Biology*, *90*(3), 413–424.

Ceccarini, C., & Eagle, H. (1971). pH as a determinant of cellular growth and contact inhibition. *Proceedings of the National Academy of Sciences of the United States of America*, *68*(1), 229–233.

Chindera, K., Mahato, M., Sharma, A. K., Horsley, H., Kloc-Muniak, K., Kamaruzzaman, N. F., Kumar, S., McFarlane, A., Stach, J., Bentin, T., & Good, L. (2016). The antimicrobial polymer PHMB enters cells and selectively condenses bacterial chromosomes. *Scientific Reports*, *6*.

Chopra, R., Mulholland, P. J., & Hau, S. C. (2020). In Vivo Confocal Microscopy Morphologic Features and Cyst Density in Acanthamoeba Keratitis. *American Journal of Ophthalmology*, *217*, 38–48.

Choy, E. P. Y., To, T. S. S., Cho, P., Benzie, I. F. F., & Choy, C. K. M. (2004). Viability of porcine corneal epithelium ex vivo and effect of exposure to air: A pilot study for a dry eye model. *Cornea*, *23*(7), 715–719.

Claerhout, I., Goegebuer, A., Van Den Broecke, C., & Kestelyn, P. (2004). Delay in diagnosis and outcome of Acanthamoeba keratitis. *Graefe's Archive for Clinical and Experimental Ophthalmology*, *242*(8), 648–653.

Clarke, D. W., & Niederkorn, J. Y. (2006). The pathophysiology of Acanthamoeba keratitis. *Trends in Parasitology* (Vol. 22, Issue 4, pp. 175–180).

Cohen, E. J., Buchanan, H. W., Laughrea, P. A., Adams, C. P., Galentine, P. G., Visvesvara, G. S., Folberg, R., Arentsen, J. J., & Laibson, P. R. (1985). Diagnosis and Management of Acanthamoeba Keratitis. *American Journal of Ophthalmology*, *100*(3), 389–395.

Cohen, N. D., Martin, L. J., Simpson, R. B., Wallis, D. E., & Neibergs, H. L. (1996). Comparison of polymerase chain reaction and microbiological culture for detection of salmonellae in equine feces and environmental samples. *American Journal of Veterinary Research* (Vol. 57, Issue 6, pp. 780–786).

Cohn, Z. A., & Benson, B. (1965). the Differentiation of Mononuclear Phagocytes. Morphology, Cytochemistry, and Biochemistry. *The Journal of Experimental Medicine*, *121*(1), 153–170.

Cohn, Z. A., Hirsch, J. G., & Fedorko, M. E. (1966). The in vitro differentiation of mononuclear phagocytes. IV. The ultrastructure of macrophage differentiation in the peritoneal cavity and in culture. *The Journal of Experimental Medicine*, *123*(4), 747–756.

Cordingley, J. S., Wills, R. A., & Villemez, C. L. (1996). Osmolarity is an independent trigger of Acanthamoeba castellanli differentiation. *Journal of Cellular Biochemistry*, *61*(2), 167–171.

Corsaro, D., & Venditti, D. (2010). Phylogenetic evidence for a new genotype of Acanthamoeba (Amoebozoa, Acanthamoebida). *Parasitology Research*, *107*(1), 233–238.

Costa, A. O., Furst, C., Rocha, L. O., Cirelli, C., Cardoso, C. N., Neiva, F. S., Possamai, C. O., de Assis Santos, D., & Thomaz-Soccol, V. (2017). Molecular diagnosis of Acanthamoeba keratitis: evaluation in rat model and application in suspected human cases. *Parasitology Research*, *116*(4), 1339–1344.

Cousins, R. J., Blanchard, R. K., Popp, M. P., Liu, L., Cao, J., Moore, J. B., & Green, C. L. (2003). A global view of the selectivity of zinc deprivation and excess on genes expressed in human THP-1 mononuclear cells. *Proceedings of the National Academy of Sciences of the United States of America*, *100*(12), 6952–6957.

Craene, S. De, Knoeri, J., Georgeon, C., Kestelyn, P., & Borderie, V. M. (2018). Assessment of Confocal Microscopy for the Diagnosis of Polymerase Chain Reaction–Positive Acanthamoeba Keratitis: A Case-Control Study. *Ophthalmology*, *125*(2), 161–168.

Crewe, J. M., & Armitage, W. J. (2001). Integrity of epithelium and endothelium in organ-cultured human corneas. *Investigative Ophthalmology and Visual Science*, *42*(8), 1757–1761.

Cross, A. R., & Segal, A. W. (2004). The NADPH oxidase of professional phagocytes - Prototype of the NOX electron transport chain systems. *Biochimica et Biophysica Acta - Bioenergetics* (Vol. 1657, Issue 1, pp. 1–22). Europe PMC Funders.

Crouzet, Emmanuel & Guindolet, Damien & He, Zhiguo & Perrache, Chantal & Forest, Fabien & Herbepin, Pascal & Gain, P. & Gabison, Eric & Thuret, Gilles. (2016). Ex-vivo porcine corneal storage using an innovative bioreactor. *Acta Ophthalmologica*. 94.

Culbertson, C. G., Smith, J. W., & Minner, J. R. (1958). Acanthamoeba: Observations on animal pathogenicity. *Science*, *127*(3313), 1506.

Dahlke, M. H., Larsen, S. R., Rasko, J. E. J., & Schlitt, H. J. (2004). The biology of CD45 and its use as a therapeutic target. *Leukemia and Lymphoma* (Vol. 45, Issue 2, pp. 229–236).

Das, A., Sinha, M., Datta, S., Abas, M., Chaffee, S., Sen, C. K., & Roy, S. (2015). Monocyte and Macrophage Plasticity in Tissue Repair and Regeneration. *American Journal of Pathology*, *185*(10), 2596–2606.

Davson, H. and Perkins, Edward S. (2020, August 7). Human eye. *Encyclopedia Britannica*.

Dawson, M. W., & Brown, T. J. (1987). The effect of chlorine and chlorine dioxide on pathogenic free-living amoebae (PFLA) in simulated natural conditions: The presence of bacteria and organic matter. *New Zealand Journal of Marine and Freshwater Research*, *21*(1), 117–123.

De Jonckheere, J. F. (1991). Ecology of acanthamoeba. *Reviews of Infectious Diseases*, *13*, S385–S387.

Deshpande, P., Ortega, Ì., Sefat, F., Sangwan, V. S., Green, N., Claeyssens, F., & MacNeil, S. (2015). Rocking media over ex vivo corneas improves this model and allows the study of the effect of proinflammatory cytokines on wound healing. *Investigative Ophthalmology and Visual Science*, *56*(3), 1553–1561.

Donaghy CL, Vislisel JM, Greiner MA (2015). An Introduction to Corneal Transplantation.

Douglas, M. (1930). Notes on the classification of the amoeba found by Castellani in cultures of a yeast-like fungus', *J Trop Med London,* 33(33), 258-259.

Draize, J. H., Woodard, G., & Calvery, H. O. (1944). Methods for the study of irritation and toxicity of substances applied topically to the skin and mucous membranes. *Journal of Pharmacology and Experimental Therapeutics*, *82*(3), 377–390.

Drozanski, W. (1956). Fatal bacterial infection in soil amoebae. *Acta Microbiologica Polonica*, *5*(3–4), 315–317.

Dursun, D., Kim, M. C., Solomon, A., & Pflugfelder, S. C. (2001). Treatment of recalcitrant recurrent corneal erosions with inhibitors of matrix metalloproteinase-9, doxycycline and corticosteroids. *American Journal of Ophthalmology*,*132*(1), 8–13.

Ehlers, H., Ehlers, N., & Hjortdal, J. (1999). Corneal transplantation with donor tissue kept in organ culture for 7 weeks. *Acta Ophthalmologica Scandinavica*, *77*(3), 277–278.

Elliott, N. T., & Yuan, F. (2011). A review of three-dimensional in vitro tissue models for drug discovery and transport studies. *Journal of Pharmaceutical Sciences* (Vol. 100, Issue 1, pp. 59–74).

Escoll, P., Rolando, M., Gomez-Valero, L., & Buchrieser, C. (2013). *From Amoeba to Macrophages: Exploring the Molecular Mechanisms of Legionella pneumophila Infection in Both Hosts* (pp. 1–34).

Feng, X., Zheng, W., Wang, Y., Zhao, D., Jiang, X., & Lv, S. (2015). A Rabbit Model of Acanthamoeba Keratitis That Better Reflects the Natural Human Infection. *Anatomical Record*, *298*(8), 1509–1517.

Ferrante, A. (1991). Immunity to acanthamoeba. *Reviews of Infectious Diseases*, *13*, S403–S409.

Ferrante, A., & Abell, T. J. (1986). Conditioned medium from stimulated mononuclear leukocytes augments human neutrophil-mediated killing of a virulent Acanthamoeba sp. *Infection and Immunity*, *51*(2), 607–617.

Fini, M. E., & Stramer, B. M. (2005). How the cornea heals: cornea-specific repair mechanisms affecting surgical outcomes. *Cornea*, *24*(8 Suppl), S2–S11.

Flannagan, R. S., Cosío, G., & Grinstein, S. (2009). Antimicrobial mechanisms of phagocytes and bacterial evasion strategies. *Nature Reviews Microbiology* (Vol. 7, Issue 5, pp. 355–366).

Foligne, B., Nutten, S., Grangette, C., Dennin, V., Goudercourt, D., Poiret, S., Dewulf, J., Brassart, D., Mercenier, A., & Pot, B. (2007). Correlation between in vitro and in vivo immunomodulatory properties of lactic acid bacteria. *World Journal of Gastroenterology*, *13*(2), 236–243.

Font, R. L., M. J. Tapert, N. M. Robinson, G. Visvesvara, D. Murphy, and M. S. Osato. (1982). An animal model of Acanthamoeba keratitis. Further studies with emphasis on the early destruction of trophozoites. *Investig. Ophthalmol. Visual Sci*. 22:S163.

Friedland, J. S., Shattock, R. J., & Griffin, G. E. (1993). Phagocytosis of mycobacterium tuberculosis or particulate stimuli by human monocytic cells induces equivalent monocyte chemotactic protein-1 gene expression. *Cytokine*, *5*(2), 150–156.

Fritzinger, A. E., Toney, D. M., MacLean, R. C., & Marciano-Cabral, F. (2006). Identification of a Naegleria fowleri membrane protein reactive with anti-human CD59 antibody. *Infection and immunity*, *74*(2), 1189–1195.

Gaillard, T., Boxberger, M., Madamet, M., & Pradines, B. (2018). Has doxycycline, in combination with anti-malarial drugs, a role to play in intermittent preventive treatment of Plasmodium falciparum malaria infection in pregnant women in Africa? *Malaria Journal*, *17*(1).

Garg, P., Kalra, P., & Joseph, J. (2017). Non-contact lens related Acanthamoeba keratitis. *Indian Journal of Ophthalmology* (Vol. 65, Issue 11, pp. 1079–1086). Medknow Publications.

Gast, R. J. (2001). Development of an Acanthamoeba-specific reverse dot-blot and the discovery of a new ribotype. *Journal of Eukaryotic Microbiology*, *48*(6), 609–615.

Gast, R. J., Ledee, D. R., Fuerst, P. A., & Byers, T. J. (1996). Subgenus systematics of Acanthamoeba: Four nuclear 18S rDNA sequence types. *Journal of Eukaryotic Microbiology*, *43*(6), 498–504.

Gautheron, P., Dukik, M., Alix, D., Sciences, J. F. S.-T., & undefined 1992. (n.d.). Bovine Corneal Opacity and Permeability Test: An in Vitro Assay of Ocular Irritancy. *Academic.Oup.Com*.

Germain, L., Carrier, P., Auger, F. A., Salesse, C., & Guérin, S. L. (2000). Can we produce a human corneal equivalent by tissue engineering?. *Progress in Retinal and Eye Research* (Vol. 19, Issue 5, pp. 497–527).

Ghedin, E., & Claverie, J. M. (2005). Mimivirus relatives in the Sargasso sea. *Virology Journal*, *2*(1), 62.

Gocek, E., & Studzinski, G. (2015). The Potential of Vitamin D-Regulated Intracellular Signaling Pathways as Targets for Myeloid Leukemia Therapy. *Journal of Clinical Medicine*, *4*(4), 504–534.

Goethem, F. Van, Adriaens, E., Alépée, N., Straube, F., Wever, B. De, Cappadoro, M., Catoire, S., Hansen, E., Wolf, A., & Vanparys, P. (2006). Prevalidation of a new in vitro reconstituted human cornea model to assess the eye irritating potential of chemicals. *Toxicology in Vitro*, *20*(1), 1–17.

Goh, J. W. Y., Harrison, R., Hau, S., Alexander, C. L., Tole, D. M., & Avadhanam, V. S. (2018). Comparison of In Vivo Confocal Microscopy, PCR and Culture of Corneal Scrapes in the Diagnosis of Acanthamoeba Keratitis. *Cornea*, *37*(4), 480–485.

Golub, L. M., Sorsa, T., Lee, H. -M, Ciancio, S., Sorbi, D., Ramamurthy, N. S., Gruber, B., Salo, T., & Konttinen, Y. T. (1995). Doxycycline inhibits neutrophil (PMN)-type matrix metalloproteinases in human adult periodontitis gingiva. *Journal of Clinical Periodontology*, *22*(2), 100–109.

Gordon, S., & Taylor, P. R. (2005). Monocyte and macrophage heterogeneity. *Nature Reviews Immunology* (Vol. 5, Issue 12, pp. 953–964).

Goy, G., & Greub, G. (2009). Antibiotic susceptibility of Waddlia chondrophila in Acanthamoeba castellanii amoebae. *Antimicrobial Agents and Chemotherapy*, *53*(6), 2663–2666.

Greub, G., & Raoult, D. (2003). Morphology of Legionella pneumophila according to their location within Hartmanella vermiformis. *Research in Microbiology*, *154*(9), 619–621.

Greub, G., & Raoult, D. (2004). Microorganisms Resistant to Free-Living Amoebae Microorganisms Resistant to Free-Living Amoebae. *Clinical Microbiology Reviews*, *17*(2), 413–433.

Guo, X., Yang, X. F., Yang, Y., Hans, R., Cai, J. H., Xue, J. Y., Tan, X. H., Xie, X. P., Xiong, X. K., & Huang, J. M. (2012). Prediction of ocular irritancy of 26 chemicals and 26 cosmetic products with isolated rabbit eye (IRE) test. *Biomedical and Environmental Sciences*, *25*(3), 359–366.

Hau, S. C., Dart, J. K. G., Vesaluoma, M., Parmar, D. N., Claerhout, I., Bibi, K., & Larkin, D. F. P. (2010). Diagnostic accuracy of microbial keratitis with in vivo scanning laser confocal microscopy. *British Journal of Ophthalmology*, *94*(8), 982–987.

He, Y., McCulley, J. P., Alizadeh, H., Pidherney, M., Mellon, J., Ubelaker, J. E., Stewart, G. L., Silvany, R. E., & Niederkorn, J. Y. (1992). A pig model of Acanthamoeba keratitis: Transmission via contaminated contact lenses. *Investigative Ophthalmology and Visual Science*, *33*(1), 126–133.

Heaselgrave, W., Hamad, A., Coles, S., & Hau, S. (2019). In vitro evaluation of the inhibitory effect of topical ophthalmic agents on acanthamoeba viability. *Translational Vision Science and Technology*, *8*(5), 17.

Helga Kolb. (2012). *Gross Anatomy of The Eye*. Available at: https://webvision.med.utah.edu/book/part-i-foundations/gross-anatomy-of-the-ey/

Henriquez, F. L. (2009). Review of “Acanthamoeba: Biology and Pathogenesis” by Naveed Ahmed Khan. *Parasites & Vectors*, *2*(1), 16.

Hong, S., & Kaer, L. Van. (1999). Immune privilege: Keeping an eye on natural killer T cells. *Journal of Experimental Medicine* (Vol. 190, Issue 9, pp. 1197–1200). IA-Verlag.

Horn, M., Fritsche, T. R., Gautom, R. K., Schleifer, K.-H., & Wagner, M. (1999). Novel bacterial endosymbionts of Acanthamoeba spp. related to the Paramecium caudatum symbiont Caedibacter caryophilus. *Environmental Microbiology*, *1*(4), 357–367.

Hornof, M., Toropainen, E., & Urtti, A. (2005). Cell culture models of the ocular barriers. *European Journal of Pharmaceutics and Biopharmaceutics*, *60*(2), 207–225.

Huang, P., Tepelus, T., Vickers, L. A., Baghdasaryan, E., Huang, J., Irvine, J. A., Hsu, H. Y., Sadda, S., & Lee, O. L. (2017). Quantitative Analysis of Depth, Distribution, and Density of Cysts in Acanthamoeba Keratitis Using Confocal Microscopy. *Cornea*, *36*(8), 927–932.

Huang, Y., Qiao, F., Abagyan, R., Hazard, S., & Tomlinson, S. (2006). Defining the CD59-C9 binding interaction. *Journal of Biological Chemistry*, *281*(37), 27398–27404.

Hübner, N. O., Matthes, R., Koban, I., Rändler, C., Müller, G., Bender, C., Kindel, E., Kocher, T., & Kramer, A. (2010). Efficacy of chlorhexidine, polihexanide and tissue-tolerable plasma against Pseudomonas aeruginosa biofilms grown on polystyrene and silicone materials. *Skin pharmacology and physiology*, *23 Suppl*, 28–34.

Hughes, R., & Kilvington, S. (2001). Comparison of hydrogen peroxide contact lens disinfection systems and solutions against Acanthamoeba polyphaga. *Antimicrobial Agents and Chemotherapy*, *45*(7), 2038–2043.

Hughes, R., Heaselgrave, W., & Kilvington, S. (2003). Acanthamoeba polyphaga strain age and method of cyst production influence the observed efficacy of therapeutic agents and contact lens disinfectants. *Antimicrobial Agents and Chemotherapy*, *47*(10), 3080–3084.

Huth, S., Reverey, J. F., Leippe, M., & Selhuber-Unkel, C. (2017). Adhesion forces and mechanics in mannose-mediated acanthamoeba interactions. *PLoS ONE*, *12*(5), e0176207.

ICCVAM. 2010. ICCVAM Test Method Evaluation Report: Recommendations for Routine Use of Topical Anesthetics, Systemic Analgesics, and Humane Endpoints to Avoid or Minimize Pain and Distress in Ocular Safety Testing. *National Institute of Environmental Health Sciences.* NIH Publication No. 10-7514.

Ikeda, T., Ledwith, A., Bamford, C. H., & Hann, R. A. (1984). Interaction of a polymeric biguanide biocide with phospholipid membranes. *BBA - Biomembranes*, *769*(1), 57–66.

Itagaki, A., & Kimura, G. (1974). TES and HEPES buffers in mammalian cell cultures and viral studies: Problem of carbon dioxide requirement. *Experimental Cell Research*, *83*(2), 351–361.

Italiani, P., & Boraschi, D. (2015). New Insights Into Tissue Macrophages: From Their Origin to the Development of Memory. *Immune Network*, *15*(4), 167.

Jaison, P. L., Cao, Z., & Panjwani, N. (1998). Binding of Acanthamoeba to mannose-glycoproteins of corneal epithelium: effect of injury. *Curr. Eye Res*, *17*(770–776), 161–169.

Janeway, J. C. A., Travers, P., Walport, M., & Shlomchik, M. J. (2001). *The complement system and innate immunity*.

Jung, K. M., Lee, S. H., Ryu, Y. H., Jang, W. H., Jung, H. S., Han, J. H., Seok, S. H., Park, J. H., Son, Y., Park, Y. H., & Lim, K. M. (2011). A new 3D reconstituted human corneal epithelium model as an alternative method for the eye irritation test. *Toxicology in Vitro*, *25*(1), 403–410.

Kaneshiro, E. S., Marciano-Cabral, F., & Moura, H. (2015). Govinda S. Visvesvara: A Tribute. *Journal of Eukaryotic Microbiology*, *62*(1), 1–2.

Karaå, M. A., & Russa, R. (2013). New long chain bases in lipophosphonoglycan of Acanthamoeba castellanii. *Lipids*, *48*(6), 639–650.

Kawazu, K., Shiono, H., Tanioka, H., Ota, A., Ikuse, T., Takashina, H., & Kawashima, Y. (1998). Beta adrenergic antagonist permeation across cultured rabbit corneal epithelial cells grown on permeable supports. *Current Eye Research*, *17*(2), 125–131.

Kaye, D. B. (1980). Epithelial response in penetrating keratoplasty. *American Journal of Ophthalmology*, *89*(3), 381–387.

Kennett, M. J., Hook, R. R., Franklin, C. L., & Riley, L. K. (1999). Acanthamoeba castellanii: Characterization of an adhesin molecule. *Experimental Parasitology*, *92*(3), 161–169.

Khan, N. A. (2006). Acanthamoeba: Biology and increasing importance in human health. *FEMS Microbiology Reviews*, *30*(4), 564–595.

Khan, N. A., Jarroll, E. L., & Paget, T. A. (2001). Acanthamoeba can be differentiated by the polymerase chain reaction and simple plating assays. *Current Microbiology*, *43*(3), 204–208.

Khunkitti, W., Lloyd, D., Furr, J. R., & Russell, A. D. (1998). Acanthamoeba castellanii: Growth, encystment, excystment and biocide susceptibility. *Journal of Infection*, *36*(1), 43–48.

Kilvington, S. (1990). Activity of water biocide chemicals and contact lens disinfectants on pathogenic free-living amoebae. *International Biodeterioration*, *26*(2–4), 127–138.

Kilvington, S., & Lam, A. (2013). Development of standardized methods for assessing biocidal efficacy of contact lens care solutions against Acanthamoeba trophozoites and cysts. *Invest Ophthalmol Vis Sci*, *54*, 4527.

Kilvington, S., Gray, T., Dart, J., Morlet, N., Beeching, J. R., Frazer, D. G., & Matheson, M. (2004). Acanthamoeba Keratitis: The Role of Domestic Tap Water Contamination in the United Kingdom. *Investigative Ophthalmology and Visual Science*, *45*(1), 165–169.

Kilvington, S., Hughes, R., Byas, J., & Dart, J. (2002). Activities of therapeutic agents and myristamidopropyl dimethylamine against Acanthamoeba isolates. *Antimicrobial Agents and Chemotherapy*, *46*(6), 2007–2009.

Klink, F. Van, Taylor, W. M., Alizadeh, H., Jager, M. J., Rooijen, N. Van, & Niederkorn, J. Y. (1996). The role of macrophages in Acanthamoeba keratitis. *Investigative Ophthalmology and Visual Science*, *37*(7), 1271–1281.

Knop, E., & Knop, N. (2007). Anatomy and immunology of the ocular surface. *Chemical Immunology and Allergy*, *92*, 36–49.

Kobayashi, A., Ishibashi, Y., Oikawa, Y., Yokogawa, H., & Sugiyama, K. (2008). In vivo and ex vivo laser confocal microscopy findings in patients with early-stage Acanthamoeba keratitis. *Cornea*, *27*(4), 439–445.

Kolle, S. N., Kandárová, H., Wareing, B., van Ravenzwaay, B., & Landsiedel, R. (2011). In-house Validation of the EpiOcularTM Eye Irritation Test and its Combination with the Bovine Corneal Opacity and Permeability Test for the Assessment of Ocular Irritation. *Alternatives to Laboratory Animals*, 39(4), 365–387.

Korn, Edward & Dearborn, Dorr & Wright, Paddy. (1974). Lipophosphonoglycan of the plasma membrane of Acanthamoeba castellanii. Isolation from whole amoeba and identification of the water-soluble products of acid hydrolysis. *The Journal of biological chemistry. 249. 3335-41.*

Kovacevic, D., Misljenovic, T., Misljenovic, N., Mikulicic, M., & Dabeska-Novkovski, D. (2008). Acanthamoeba keratitis--importance of the early diagnosis. *Coll Antropol*, *32 Suppl 2*, 221–224.

Kovacs, C. J., Lynch, S. C., Rah, M. J., Millard, K. A., & Morris, T. W. (2015). Acanthamoeba encystment: Multifactorial effects of buffers, biocides, and demulcents present in contact lens care solutions. *Clinical Ophthalmology*, *9*, 1905–1913.

Krishna Murti, C. *R., Shukla, O.P. Differentiation of Pathogenic Amoebae: Encystation and Excystation Of Acanthamoeba Culbertsoni Model*, *6*, 475.

Krishna Prasad, B., & Gupta, S. (1978). Preliminary report on engulfment and retention of mycobacteria by trophozoites of axenically grown Acanthamoeba castellanii Douglas, 1930. *Current Science* (Vol. 47, Issue 7, pp. 245–247).

Kwong, M. S. F., Evans, D. J., Ni, M., Cowell, B. A., & Fleiszig, S. M. J. (2007). Human tear fluid protects against Pseudomonas aeruginosa keratitis in a murine experimental model. *Infection and Immunity*, *75*(5), 2325–2332.

Labbé, A., Khammari, C., Dupas, B., Gabison, E., Brasnu, E., Labetoulle, M., & Baudouin, C. (2009). Contribution of in vivo confocal microscopy to the diagnosis and management of infectious keratitis. *Ocular Surface*, *7*(1), 41–52.

Ladage, P. M., Jester, J. V., Petroll, M., Bergmanson, J. P. G., & Cavanagh, H. D. (2003). Vertical movement of epithelial basal cells toward the corneal surface during use of extended-wear contact lenses. *Investigative Ophthalmology and Visual Science*, *44*(3), 1056–1063.

Lane, N. (2015). The unseen World: Reflections on Leeuwenhoek (1677) 'Concerning little animals.' In *Philosophical Transactions of the Royal Society B: Biological Sciences* (Vol. 370, Issue 1666, p. 20140344).

Larkin, D. F. P., & Easty, D. L. (1991). Experimental Acanthamoeba keratitis: II. Immunohistochemical evaluation. *British Journal of Ophthalmology*, *75*(7), 421–424.

Lass, J. H., Musch, D. C., Gordon, J. F., Laing, R. A., Bruner, W. E., Reinhart, W. J., Price, F. W., Whitson, W. E., Krachmer, J. H., Macsai, M. S., Varley, G. A., Eiferman, R. A., Meyer, R. F., Kaz Soong, H., Sugar, A., Keates, R. H., Lembach, R. G., & Cowden, J. W. (1994). Epidermal Growth Factor and Insulin Use in Corneal Preservation: Results of a Multi-center Trial. *Ophthalmology*, *101*(2), 352–359.

Law, S. K, & Reid, K. B (1995). Complement. *Oxford University Press*.

Lee, J. E., Oum, B. S., Choi, H. Y., Yu, H. S., & Lee, J. S. (2007). Cysticidal effect on Acanthamoeba and toxicity on human keratocytes by polyhexamethylene biguanide and chlorhexidine. *Cornea*, *26*(6), 736–741.

Lesh F. A. (1975). Massive development of amebas in the large intestine. Fedor Aleksandrovich Lesh (Lösch). *The American journal of tropical medicine and hygiene*, *24*(3), 383–392.

Liles, W. C., Ledbetter, J. A., Waltersdorph, A. W., & Klebanoff, S. J. (1995). Cross-linking of CD18 primes human neutrophils for activation of the respiratory burst in response to specific stimuli: Implications for adhesion-dependent physiological responses in neutrophils. *Journal of Leukocyte Biology*, *58*(6), 690–697.

Lim, C. C., Peng, I. C., & Huang, Y. H. (2020). Safety of intrastromal injection of polyhexamethylene biguanide and propamidine isethionate in a rabbit model. *Journal of Advanced Research*, *22*, 1–6.

Lorenz, H. M., Harrer, T., Lagoo, A. S., Baur, A., Eger, G., & Kalden, J. R. (1993). CD45 mAb Induces Cell Adhesion in Peripheral Blood Mononuclear Cells via Lymphocyte Function-Associated Antigen-1 (LFA-1) and Intercellular Cell Adhesion Molecule 1 (ICAM-1). *Cellular Immunology*, *147*(1), 110–128.

Lorenzo-Morales, J., Khan, N. A., & Walochnik, J. (2015). An update on *Acanthamoeba* keratitis: diagnosis, pathogenesis and treatment. *Parasite*, *22*, 10.

Mackaness, G. B. (1964). the Immunological Basis of Acquired Cellular Resistance. *The Journal of Experimental Medicine*, *120*, 105–120.

Maghsood, A. H., Sissons, J., Rezaian, M., Holder, D., Warhurst, D., & Khan, N. A. (2005). Acanthamoeba genotype T4 from the UK and Iran and isolation of the T2 genotype from clinical isolates. *Journal of Medical Microbiology*, *54*(8), 755–759.

Magnet, A., Henriques-Gil, N., Galván-Diaz, A. L., Izquiedo, F., Fenoy, S., & Del Aguila, C. (2014). Novel Acanthamoeba 18S rRNA gene sequence type from an environmental isolate. *Parasitology Research*, *113*(8), 2845–2850.

Mangan, D. F., & Wahl, S. M. (1991). Differential regulation of human monocyte programmed cell death (apoptosis) by chemotactic factors and pro-inflammatory cytokines. *Journal of Immunology*, *147*(10), 3408–3412.

Marciano-Cabral, F., & Cabral, G. (2003). Acanthamoeba spp. as agents of disease in humans.*Clinical Microbiology Reviews* (Vol. 16, Issue 2, pp. 273–307).

Marciano-Cabral, F., & Toney, D. M. (1998). The interaction of Acanthamoeba spp. with activated macrophages and with macrophage cell lines. *Journal of Eukaryotic Microbiology*, *45*(4), 452–458.

Marciano-Cabral, F., Puffenbarger, R., & Cabral, G. A. (2000). The increasing importance of Acanthamoeba infections. *Journal of Eukaryotic Microbiology*, *47*(1), 29–36.

Marlo, T. L., Giuliano, E. A., Sharma, A., & Mohan, R. R. (2017). Development of a novel ex vivo equine corneal model. *Veterinary Ophthalmology*, *20*(4), 288–293.

Marolda, C. L., Hauröder, B., John, M. A., Michel, R., & Valvano, M. A. (1999). Intracellular survival and saprophytic growth of isolates from the Burkholderia cepacia complex in free-living amoebae. *Microbiology*, *145*(7), 1509–1517.

Martinez, A. J., & Visvesvara, G. S. (1997). Free-living, amphizoic and opportunistic amebas. *Brain Pathology* (Vol. 7, Issue 1, pp. 583–598).

Martínez, A. J., García, C. A., Halks-Miller, M., & Arce-Vela, R. (1980). Granulomatous Amebic Encephalitis presenting as a cerebral mass lesion. *Acta Neuropathologica*, *51*(2), 85–91.

Mathers, W. D., Nelson, S. E., Lane, J. L., Wilson, M. E., Allen, R. C., & Folberg, R. (2000). Confirmation of confocal microscopy diagnosis of Acanthamoeba keratitis using polymerase chain reaction analysis. *Archives of Ophthalmology*, *118*(2), 178–183.

Matsumoto, Y., Dogru, M., Sato, E. A., Katono, Y., Uchino, Y., Shimmura, S., & Tsubota, K. (2007). The application of in vivo confocal scanning laser microscopy in the management of Acanthamoeba keratitis. *Molecular vision*, *13*, 1319–1326.

Matsunaga, S., Endo, T., Yagita, K., Hirukawa, Y., Tomino, S., Matsugo, S., & Tsuruhara, T. (1998). Chromosome size polymorphisms in the genus Acanthamoeba electrokaryotype by pulsed-field gel electrophoresis. *Protist*, *149*(4), 323–340.

Maycock, N. J. R., & Jayaswal, R. (2016). Update on Acanthamoeba Keratitis: Diagnosis, Treatment, and Outcomes. *Cornea*, *35*(5), 713–720.

McCarthy, A. L., O'Callaghan, Y. C., Connolly, A., Piggott, C. O., Fitzgerald, R. J., & O'Brien, N. M. (2012). Phenolic extracts of brewers' spent grain (BSG) as functional ingredients - Assessment of their DNA protective effect against oxidant-induced DNA single strand breaks in U937 cells. *Food Chemistry*, *134*(2), 641–646.

McClellan, K., Howard, K., Niederkorn, J. Y., & Alizadeh, H. (2001). Effect of steroids on Acanthamoeba cysts and trophozoites. *Investigative Ophthalmology and Visual Science*, *42*(12), 2885–2893.

McDermott, A. M. (2004). Defensins and other antimicrobial peptides at the ocular surface. *Ocular Surface*, *2*(4), 229–247.

Medvedec Mikić, I., Cigić, L., Kero, D., Kalibović Govorko, D., Prpić Mehičić, G., Tambić Andrašević, A., & Simeon, P. (2018). Antimicrobial effectiveness of polyhexamethylene biguanide on Enterococcus faecalis, Staphylococcus epidermidis and Candida albicans. *Medicinski glasnik : official publication of the Medical Association of Zenica-Doboj Canton, Bosnia and Herzegovina*, *15*(2), 132–138.

Meiyu, R., & Xinyi, W. (2010). Evaluation of three different methods to establish animal models of Acanthamoeba keratitis. *Yonsei Medical Journal*, *51*(1), 121–127.

Miller, D., Maestre-Mesa, J., Diaz, M., Perez, E., Shestopalov, V., Gelder, R. Van, & Alfonso, E. C. (2012). Acanthamoeba Associated Microbial Communities. *Investigative Ophthalmology & Visual Science*, *53*(14), 6145.

Mills, C. D. (2012). M1 and M2 macrophages: Oracles of health and disease. *Critical Reviews in Immunology*, *32*(6), 463–488.

Mohan, R. R., Possin, D. E., Mohan, R. R., Sinha, S., & Wilson, S. E. (2003). Development of genetically engineered tet HPV16-E6/E7 transduced human corneal epithelial clones having tight regulation of proliferation and normal differentiation. *Experimental Eye Research*, *77*(4), 395–407.

Molnar, C., & Jane, G. (2013). *Concepts of Biology-1St Canadian Edition Concepts of Biology-1St Canadian Edition* (pp. 1–893).

Moore, M. B., Ubelaker, J. E., Martin, J. H., Silvany, R., Dougherty, J. M., Meyer, D. R., & McCulley, J. P. (1991). In vitro penetration of human corneal epithelium by Acanthamoeba castellanii: A scanning and transmission electron microscopy study. *Cornea*, *10*(4), 291–298.

Moshirfar, M., Mirzaian, G., Feiz, V., & Kang, P. C. (2006). Fourth-generation fluoroquinolone-resistant bacterial keratitis after refractive surgery. *Journal of Cataract and Refractive Surgery*, *32*(3), 515–518.

Mosmann, T. R., Cherwinski, H., Bond, M. W., Giedlin, M. A., & Coffman, R. L. (1986). Two types of murine helper T cell clone. I. Definition according to profiles of lymphokine activities and secreted proteins. *Journal of Immunology (Baltimore, Md.: 1950)*, *136*(7), 2348–2357.

Mosser, D. M., & Edwards, J. P. (2008). Exploring the full spectrum of macrophage activation. *Nature Reviews Immunology* (Vol. 8, Issue 12, pp. 958–969).

Müller, L. J., Pels, L., & Vrensen, G. F. (1996). 22. Ultrastructural organization of human corneal nerves. *Investigative Ophthalmology & Visual Science*, *37*(4), 476–488.

Murat, D., Byrne, M., & Komeili, A. (2010). Cell biology of prokaryotic organelles. *Cold Spring Harbor perspectives in biology* (Vol. 2, Issue 10).

Nagington, J., Watson, P. G., Playfair, T. J., Mcgill, J., Jones, B. R., & Steele, A. D. M. G. (1974). Infection of the eye. *The Lancet*, *304*(7896), 1537–1540.

Nathan, C. F. (1983). Identification of interferon-gamma as the lymphokine that activates human macrophage oxidative metabolism and antimicrobial activity. *Journal of Experimental Medicine*, *158*(3), 670–689.

Navarro-Triviño, F. J., Pérez-López, I., & Ruiz-Villaverde, R. (2020). Doxycycline, an Antibiotic or an Anti-Inflammatory Agent? The Most Common Uses in Dermatology. *Actas Dermo-Sifiliograficas*, *111*(7), 561–566.

Neelam, S., & Niederkorn, J. Y. (2017). Pathobiology and immunobiology of Acanthamoeba keratitis: Insights from animal models. *Yale Journal of Biology and Medicine*, *90*(2), 261–268.

Neff, R. J. (1957). Purification, Axenic Cultivation, and Description of a Soil Amoeba, Acanthamoeba sp. *The Journal of Protozoology*, *4*(3), 176–182.

Neff, R. J., Ray, S. A., Benton, W. F., & Wilborn, M. (1964). Chapter 4 Induction of Synchronous Encystment (Differentiation) in Acanthamoeba sp. *Methods in Cell Biology*, *1*(C), 55–83.

Niederkorn, J. Y., Alizadeh, H., Leher, H., & McCulley, J. P. (1999). The pathogenesis of Acanthamoeba keratitis. *Microbes and Infection*, *1*(6), 437–443.

Niederkorn, J. Y., Ross, J. R., & He, Y. (1992). Effect of donor Langerhans cells on corneal graft rejection. *Journal of Investigative Dermatology*, *99*(5), 104–106.

Nishizuka, Y. (1992). Intracellular signaling by hydrolysis of phospholipids and activation of protein kinase C. *Science*, *258*(5082), 607–614.

Niyyati, M., Lorenzo-Morales, J., Rezaie, S., Rahimi, F., Martín-Navarro, C. M., Mohebali, M., Maghsood, A. H., Farnia, S., Valladares, B., & Rezaeian, M. (2010). First report of a mixed infection due to Acanthamoeba genotype T3 and Vahlkampfia in a cosmetic soft contact lens wearer in Iran. *Experimental Parasitology*, *126*(1), 89–90.

OECD (2009), *Test No. 438: Isolated Chicken Eye Test Method for Identifying Ocular Corrosives and Severe Irritants*, OECD Publishing, Paris.

Omaña-Molina, M., Navarro-García, F., González-Robles, A., De Jesús Serrano-Luna, J., Campos-Rodríguez, R., Martínez-Palomo, A., Tsutsumi, V., & Shibayama, M. (2004). Induction of morphological and electrophysiological changes in hamster cornea after in vitro interaction with trophozoites of Acanthamoeba spp. *Infection and Immunity*, *72*(6), 3245–3251.

Ong, T. Y. Y., Khan, N. A., & Siddiqui, R. (2017). Brain-eating amoebae: Predilection sites in the brain and disease outcome. *Journal of Clinical Microbiology*, *55*(7), 1989–1997.

Ortillés, Á., Goñi, P., Rubio, E., Sierra, M., Gámez, E., Fernández, M. T., Benito, M., Cristóbal, J., & Calvo, B. (2017). A rabbit model of Acanthamoeba keratitis: Use of infected soft contact lenses after corneal epithelium debridement with a diamond burr. *Investigative Ophthalmology and Visual Science*, *58*(2), 1218–1227.

Pace, J. L., Russell, S. W., Schreiber, R. D., Altman, A., & Katz, D. H. (1983). Macrophage activation: priming activity from a T-cell hybridoma is attributable to interferon-gamma. *Proceedings of the National Academy of Sciences of the United States of America*, *80*(12), 3782–3786.

Page, F. C. (1988). *A new key to freshwater and soil Gymnamoebae: With instructions for culture*. Ambleside: Freshwater Biological Association.

Page, M. A., & Mathers, W. D. (2013). Acanthamoeba keratitis: A 12-Year experience covering a wide spectrum of presentations, diagnoses, and outcomes. *Journal of Ophthalmology*, *2013*, 1–6.

Panjwani, N. (2010). Pathogenesis of Acanthamoeba keratitis. *Ocular Surface* (Vol. 8, Issue 2, pp. 70–79).

Panjwani, N., Zhao, Z., Baum, J., Hazlett, L. D., & Yang, Z. (1997). Acanthamoebae bind to rabbit corneal epithelium in vitro. *Investigative Ophthalmology and Visual Science*, *38*(9), 1858–1864.

Papa, V., Rama, P., Radford, C., Minassian, D. C., & Dart, J. K. G. (2020). Acanthamoeba keratitis therapy: Time to cure and visual outcome analysis for different antiamoebic therapies in 227 cases. *British Journal of Ophthalmology*, *104*(4), 575–581.

Parekh, M., Ferrari, S., Iorio, E. Di, Barbaro, V., Camposampiero, D., Karali, M., Ponzin, D., & Salvalaio, G. (2012). A simplified technique for in situ excision of cornea and evisceration of retinal tissue from human ocular globe. *Journal of Visualized Experiments*, *64*, 1.

Pasricha, G., Sharma, S., Garg, P., & Aggarwal, R. K. (2003). Use of 18S rRNA gene-based PCR assay for diagnosis of Acanthamoeba keratitis in non-contact lens wearers in India. *Journal of Clinical Microbiology*, *41*(7), 3206–3211.

Patel, A. (2013). Ocular drug delivery systems: An overview. *World Journal of Pharmacology*, *2*(2), 47.

Pels, E., & Schuchard, Y. (1983). Organ-culture preservation of human corneas. *Documenta Ophthalmologica*, *56*(1–2), 147–153.

Pérez-Samonja, J. J., Kilvington, S., Hughes, R., Tufail, A., Matheson, M., & Dart, J. K. G. (2003). Persistently culture positive Acanthamoeba keratitis: In vivo resistance and in vitro sensitivity. *Ophthalmology*, *110*(8), 1593–1600.

Pfau, J. C., Walker, E., & Card, G. L. (2000). Monoclonal antibodies to CD45 modify LPS-induced arachidonic acid metabolism in macrophages. *Biochimica et Biophysica Acta - Molecular Cell Research*, *1495*(3), 212–222.

Pinna, A., Porcu, T., Boscia, F., Cano, A., Erre, G., & Mattana, A. (2017). Free-Living Amoebae Keratitis. *Cornea*, *36*(7), 785–790.

Pinnock, A., Shivshetty, N., Roy, S., Rimmer, S., Douglas, I., MacNeil, S., & Garg, P. (2017). Ex vivo rabbit and human corneas as models for bacterial and fungal keratitis. *Graefe's Archive for Clinical and Experimental Ophthalmology*, *255*(2), 333–342.

Postnikoff, C. K., Pintwala, R., Williams, S., Wright, A. M., Hileeto, D., & Gorbet, M. B. (2014). Development of a curved, stratified, in vitro model to assess ocular biocompatibility. *PLoS ONE*, *9*(5).

Price, J. V., & Vance, R. E. (2014). The Macrophage Paradox. *Immunity*, *41*(5), 685–693.

Purssell, A., Lau, R., & Boggild, A. K. (2017). Azithromycin and doxycycline attenuation of Acanthamoeba virulence in a human corneal tissue model. *Journal of Infectious Diseases*, *215*(8), 1303–1311.

Pussard, M. and Pons, R. (1977). Morphologies of the cystic wall and taxonomy of the genus Acanthamoeba (Protozoa, Amoebida)', *Protistologica (Paris),* 13, pp. 557-610.

Qin, Z. (2012). The use of THP-1 cells as a model for mimicking the function and regulation of monocytes and macrophages in the vasculature. *Atherosclerosis* (Vol. 221, Issue 1, pp. 2–11).

Radford, C. F., Bacon, A. S., Dart, J. K. G., & Minassian, D. C. (1995). Risk factors for acanthamoeba keratitis in contact lens users: A Case-control study. *BMJ*, *310*(6994), 1567.

Raizada, M. K., & Krishna Murti, C. R. (1972). Transformation of trophic hartmannella culbertsoni into viable cysts by cyclic 3',5'-adenosine monophosphate. *Journal of Cell Biology* (Vol. 52, Issue 3, pp. 743–748).

Rathore, K. S., & Nema, R. K. (2009). Medical management of glaucoma: An overview. *International Journal of PharmTech Research* (Vol. 1, Issue 3, pp. 863–869).

Ravine, T. J., Polski, J. M., & Jenkins, J. (2010). Recognition of *Naegleriae* ameba surface protein epitopes by anti-human CD45 antibodies. *Cytometry Part A*, *77A*(4), 305–309.

Reichl, S., & Müller-Goymann, C. C. (2001). Entwicklung eines organotypischen Korneakonstruktes als ein In-vitro-Modell für Permeationsstudien [Development of an organotypic corneal construction as an in vitro model for permeability studies]. *Der Ophthalmologe: Zeitschrift der Deutschen Ophthalmologischen Gesellschaft*, *98*(9), 853–858.

Reinstein, D. Z., Archer, T. J., Gobbe, M., Silverman, R. H., & Coleman, D. J. (2008). Epithelial thickness in the normal cornea: three-dimensional display with very high frequency ultrasound. *Journal of Refractive Surgery*, *24*(6), 571–581.

Rimm, D. L., Pollard, T. D., & Hieter, P. (1988). Resolution of Acanthamoeba castellanii chromosomes by pulsed field gel electrophoresis and construction of the initial linkage map. *Chromosoma*, *97*(3), 219–223.

Robaei, D., Carnt, N., Minassian, D. C., & Dart, J. K. G. (2014). The impact of topical corticosteroid use before diagnosis on the outcome of Acanthamoeba keratitis. *Ophthalmology*, *121*(7), 1383–1388.

Robaei, D., Carnt, N., Minassian, D. C., & Dart, J. K. G. (2015). Therapeutic and optical keratoplasty in the management of Acanthamoeba keratitis: Risk factors, outcomes, and summary of the literature. *Ophthalmology*, *122*(1), 17–24.

Rogers, P. D., Thornton, J., Barker, K. S., McDaniel, D. O., Sacks, G. S., Swiatlo, E., & McDaniel, L. S. (2003). Pneumolysin-dependent and -independent gene expression identified by cDNA microarray analysis of THP-1 human mononuclear cells stimulated by Streptococcus pneumoniae. *Infection and Immunity*, *71*(4), 2087–2094.

Ruan, X., Chodosh, J., Callegan, M. C., Booth, M. C., Lee, T. D., Kumar, P., Gilmore, M. S., & Pereira, H. A. (2002). Corneal expression of the inflammatory mediator CAP37. *Investigative Ophthalmology and Visual Science*, *43*(5), 1414–1421.

Ruggiero, M. A., Gordon, D. P., Orrell, T. M., Bailly, N., Bourgoin, T., Brusca, R. C., Cavalier-Smith, T., Guiry, M. D., & Kirk, P. M. (2015). A higher level classification of all living organisms. *PLoS ONE*, *10*(4), 1–60.

Rusciano, G., Capriglione, P., Pesce, G., Del Prete, S., Cennamo, G., Di Cave, D., Cerulli, L., & Sasso, A. (2013). Raman Microspectroscopy Analysis in the Treatment of Acanthamoeba Keratitis. *PLoS ONE*, *8*(8), e72127.

Said, N. A., Shoeir, A. T., Panjwani, N., Garate, M., & Cao, Z. (2004). Local and systemic humoral immune response during acute and chronic Acanthamoeba keratitis in rabbits. *Current Eye Research*, *29*(6), 429–439.

Schroecksnadel, S., Jenny, M., & Fuchs, D. (2011). Myelomonocytic THP-1 cells for in vitro testing of immunomodulatory properties of nanoparticles. *Journal of Biomedical Nanotechnology*, *7*(1), 209–210.

Schuster, F. L., & Visvesvara, G. S. (2004). Free-living amoebae as opportunistic and non-opportunistic pathogens of humans and animals. *International Journal for Parasitology*, *34*(9), 1001–1027.

Segal, G., & Shuman, H. A. (1999). Legionella pneumophila utilizes the same genes to multiply within Acanthamoeba castellanii and human macrophages. *Infection and Immunity*, *67*(5), 2117–2124.

Shafaie, S., Hutter, V., Cook, M. T., Brown, M. B., & Chau, D. Y. S. (2016). In Vitro Cell Models for Ophthalmic Drug Development Applications. *BioResearch Open Access* (Vol. 5, Issue 1, pp. 94–108).

Shao, D. Z., & Lin, M. (2008). Platonin inhibits LPS-induced NF-κB by preventing activation of Akt and IKKβ in human PBMC. *Inflammation Research*, *57*(12), 601–606.

Shiraishi, A., Uno, T., Oka, N., Hara, Y., Yamaguchi, M., & Ohashi, Y. (2010). In vivo and in vitro laser confocal microscopy to diagnose acanthamoeba keratitis. *Cornea*, *29*(8), 861–865.

Shumway, C. L., Motlagh, M., & Wade, M. (2020). Anatomy, Head and Neck, Eye Conjunctiva. *StatPearls*.

Sica, A., Larghi, P., Mancino, A., Rubino, L., Porta, C., Totaro, M. G., Rimoldi, M., Biswas, S. K., Allavena, P., & Mantovani, A. (2008). Macrophage polarization in tumour progression. *Seminars in Cancer Biology* (Vol. 18, Issue 5, pp. 349–355).

Siddiqui, R., & Khan, N. A. (2012). Biology and pathogenesis of Acanthamoeba. *Parasites & Vectors*, *5*(1), 6.

Siddiqui, R., Aqeel, Y., & Khan, N. A. (2016). The Development of Drugs against Acanthamoeba Infections. *Antimicrobial Agents and Chemotherapy*, *60*(11), 6441–6450.

Singh, B. N., & Das, S. R. (1970). Studies on pathogenic and non-pathogenic small free-living amoebae and the bearing of nuclear division on the classification of the order amoebida. *Philosophical Transactions of the Royal Society of London. Series B, Biological Sciences*, *259*(832), 435–476.

Singh, R., Joseph, A., Umapathy, T., Tint, N. L., & Dua, H. S. (2005). Impression cytology of the ocular surface. *British Journal of Ophthalmology*, *89*(12), 1655–1659.

Singleton, P., and D. Sainsbury*. 2006. Dictionary of Microbiology & Molecular Biology.* John Wiley & Sons, Chichester, UK. 908 pp.

Snell, R.S., Lemp, M.A., 1998. *Clinical Anatomy of the Eye.* Blackwell Scientific Publications, Boston.

Solovjov, D. A., Pluskota, E., & Plow, E. F. (2005). Distinct roles for the α and β subunits in the functions of integrin αMβ2. *Journal of Biological Chemistry*, *280*(2), 1336–1345.

Srivastava, D. K., & Shukla, O. P. (1983). Encystment of Acanthamoeba culbertsoni in non-nutrient inorganic media. *Indian Journal of Experimental Biology*, *21*(8), 440–443.

Stehr-Green, J. K., Bailey, T. M., Brandt, F. H., Carr, J. H., Bond, W. W., & GS., V. (2010). Acanthamoeba keratitis in soft contact lens wearers. *A Case-Control Study*, *1987*, 258.

Stewart, G. L., Kim, I., Shupe, K., Alizadeh, H., Silvany, R., McCulley, J. P., & Niederkorn, J. Y. (1992). Chemotactic response of macrophages to Acanthamoeba castellanii antigen and antibody-dependent macrophage-mediated killing of the parasite. *Journal of Parasitology*, *78*(5), 849–855.

Stothard, D. R., Schroeder-Diedrich, J. M., Awwad, M. H., Gast, R. J., Ledee, D. R., Rodriguez-Zaragoza, S., Dean, C. L., Fuerst, P. A., & Byers, T. J. (1998). The evolutionary history of the genus Acanthamoeba and the identification of eight new 18S rRNA gene sequence types. *Journal of Eukaryotic Microbiology*, *45*(1), 45–54.

Stratford, M. P., & Griffiths, A. J. (1978). Variations in the properties and morphology of cysts of Acanthamoeba castellanii. *Journal of General Microbiology*, *108*(1), 33–37.

Sun, X. (2018). Acanthamoeba keratitis: Diagnosis and treatment. *Acanthamoeba Keratitis:Diagnosis and Treatment*.

Takashiba, S., Dyke, T. E. Van, Amar, S., Murayama, Y., Soskolne, A. W., & Shapira, L. (1999). Differentiation of monocytes to macrophages primes cells for lipopolysaccharide stimulation via accumulation of cytoplasmic nuclear factor κB. *Infection and Immunity*, *67*(11), 5573–5578.

Takeuchi, O., & Akira, S. (2010). Pattern Recognition Receptors and Inflammation. *Cell*, *140*(6), 805–820.

Tan, S. Z., Walkden, A., Au, L., Fullwood, C., Hamilton, A., Qamruddin, A., Armstrong, M., Brahma, A. K., & Carley, F. (2017). Twelve-year analysis of microbial keratitis trends at a UK tertiary hospital. *Eye (Basingstoke)*, *31*(8), 1229–1236.

Tandon, N. N., Kralisz, U., & Jamieson, G. A. (1989). Identification of glycoprotein IV (CD36) as a primary receptor for platelet-collagen adhesion. *The Journal of biological chemistry*, *264*(13), 7576–7583.

Taravaud, A., Loiseau, P. M., & Pomel, S. (2017). In vitro evaluation of antimicrobial agents on Acanthamoeba sp. and evidence of a natural resilience to amphotericin B. *International Journal for Parasitology: Drugs and Drug Resistance*, *7*(3), 328–336.

Tarique, A. A., Logan, J., Thomas, E., Holt, P. G., Sly, P. D., & Fantino, E. (2015). Phenotypic,functional,and plasticity features of classical and alternatively activated human macrophages. *American Journal of Respiratory Cell and Molecular Biology*, *53*(5), 676–688.

Thompson, P. P., Kowalski, R. P., Shanks, R. M. Q., & Gordon, Y. J. (2008). Validation of Real-Time PCR for Laboratory Diagnosis of Acanthamoeba Keratitis. *Journal of Clinical Microbiology*, *46*(10), 3232–3236.

Toguri, J. T., Caldwell, M., & Kelly, M. E. M. (2016). Turning Down the Thermostat: Modulating the Endocannabinoid System in Ocular Inflammation and Pain. *Frontiers in Pharmacology*, *7*(SEP).

Toropainen, E., Hornof, M., Kaarniranta, K., Johansson, P., & Urtti, A. (2007). Corneal epithelium as a platform for secretion of transgene products after transfection with liposomal gene eyedrops. *The Journal of Gene Medicine*, *9*(3), 208–216.

Tran, M. T., Lausch, R. N., & Oakes, J. E. (2000). Substance P differentially stimulates IL-8 synthesis in human corneal epithelial cells. *Investigative Ophthalmology and Visual Science*, *41*(12), 3871–3877.

Tripathi, T., Smith, A. D., Abdi, M., & Alizadeh, H. (2012). Acanthamoeba-cytopathic protein induces apoptosis and proinflammatory cytokines in human corneal epithelial cells by cPLA2α activation. *Investigative Ophthalmology and Visual Science*, *53*(13), 7973–7982.

Trocme, S. D., & Aldave, A. J. (1994). The eye and the eosinophil. *Survey of Ophthalmology*, *39*(3), 241–252.

Tsuchiya, S., Yamabe, M., Yamaguchi, Y., Kobayashi, Y., Konno, T., & Tada, K. (1980). Establishment and characterization of a human acute monocytic leukemia cell line (THP-1). *International Journal of Cancer*, *26*(2), 171–176.

Tu, E. Y., & Joslin, C. E. (2010). Recent outbreaks of atypical contact lens-related keratitis: What have we learned? *American Journal of Ophthalmology*, *150*(5), 602.

Tu, E. Y., Joslin, C. E., Sugar, J., Booton, G. C., Shoff, M. E., & Fuerst, P. A. (2008). The relative value of confocal microscopy and superficial corneal scrapings in the diagnosis of acanthamoeba keratitis. *Cornea*, *27*(7), 764–772.

Underhill, D. M., & Ozinsky, A. (2002). Phagocytosis of microbes: Complexity in action. *Annual Review of Immunology* (Vol. 20, pp. 825–852).

Valenzuela, A. G., López-Corella, E., & De Jonckheere, J. F. (1984). Primary amoebic meningoencephalitis in a young male from northwestern Mexico. *Transactions of the Royal Society of Tropical Medicine and Hygiene*, *78*(4), 558–559.

Van Klink, F., Leher, H., Jager, M. J., Alizadeh, H., Taylor, W., & Niederkorn, J. Y. (1997). Systemic immune response to Acanthamoeba keratitis in the Chinese hamster. *Ocular Immunology and Inflammation*, *5*(4), 235–244.

Vasseneix, C., Gargala, G., François, A., Hellot, M. F., Duclos, C., Muraine, M., Benichou, J., Ballet, J. J., Brasseur, G., & Favennec, L. (2006). A keratitis rat model for evaluation of anti-Acanthamoeba polyphaga agents. *Cornea*, *25*(5), 597–602.

Vaure, C., & Liu, Y. (2014). A comparative review of toll-like receptor 4 expression and functionality in different animal species. *Frontiers in Immunology*, *5*(JUL).

Verma, A. K., Raizada, M. K., & Murti, C. R. K. (1974). Effect of bioamines on the cellular differentiation of Hartmannella culbertsoni. *Biochemical Pharmacology*, *23*(1), 57–63.

Visvesvara, G. S., & Stehr-Green, J. K. (1990). Epidemiology of Free-Living Ameba Infections. *The Journal of Protozoology*, *37*(4), 25s-33s.

Visvesvara, G. S., Martinez, A. J., Schuster, F. L., Leitch, G. J., Wallace, S. V., Sawyer, T. K., & Anderson, M. (1990). Leptomyxid ameba, a new agent of amebic meningoencephalitis in humans and animals. *Journal of Clinical Microbiology*, *28*(12), 2750–2756.

Vontobel, S. F. (2015). Corneal Penetration of Polyhexamethylene Biguanide and Chlorhexidine Digluconate. *Journal of Clinical & Experimental Ophthalmology*, *06*(03).

Walochnik, J., Duchene, M., Eibl, H., & Aspock, H. (2003). [Treatment of Acanthamoeba keratitis: possibilities, problems, and new approaches]. *Wien Klin Wochenschr*, *115 Suppl*, 10–17.

Walochnik, J., Obwaller, A., & Aspock, H. (2000). Correlations between morphological, molecular biological, and physiological characteristics in clinical and nonclinical isolates of Acanthamoeba spp. *Applied and Environmental Microbiology*, *66*(10), 4408–4413.

Walochnik, J., Scheikl, U., & Haller-Schober, E. M. (2015). Twenty years of Acanthamoeba diagnostics in Austria. *Journal of Eukaryotic Microbiology*, *62*(1), 3–11.

Walochnik, J., Sommer, K., Obwaller, A., Haller-Schober, E. M., & Aspöck, H. (2004). Characterisation and differentiation of pathogenic and non-pathogenic Acanthamoeba strains by their protein and antigen profiles. *Parasitology Research*, *92*(4), 289–298.

Wang, Y. E., Tepelus, T. C., Gui, W., Irvine, J. A., Lee, O. L., & Hsu, H. Y. (2019). Reduction of acanthamoeba cyst density associated with treatment detected by in vivo confocal microscopy in acanthamoeba keratitis. *Cornea*, *38*(4), 463–468.

Weisman, R. A. (1976). Differentiation in Acanthamoeba castellanii. *Annual review of microbiology* (Vol. 30, pp. 189–219).

Werfel, T., Sonntag, G., Weber, M. H., & Gotze, O. (1991). Rapid increases in the membrane expression of neutral endopeptidase (CD10), aminopeptidase N (CD13), tyrosine phosphatase (CD45), and Fcγ-RIII (CD16) upon stimulation of human peripheral leukocytes with human C5a. *The Journal of Immunology*, *147*(11), 3909–3914.

Whittaker, R. H. (1969). New concepts of kingdoms of organisms. *Science*, *163*(3863), 150–160.

Wilhelmus, K. R. (2001). The Draize eye test. *Survey of ophthalmology* (Vol. 45, Issue 6, pp. 493–515).

Willaert, E., Stevens, A. R., & Healy, G. R. (1978). Retrospective identification of Acanthamoeba culbertsoni in a case of amoebic meningoencephalitis. *Journal of Clinical Pathology*, *31*(8), 717–720.

Willoughby, C. E., Ponzin, D., Ferrari, S., Lobo, A., Landau, K., & Omidi, Y. (2010). Anatomy and physiology of the human eye: effects of mucopolysaccharidoses disease on structure and function - a review. *Clinical & Experimental Ophthalmology*, *38*, 2–11.

Wilson, S. E., & Hong, J. W. (2000). Bowman's layer structure and function: Critical or dispensable to corneal function? A Hypothesis. *Cornea* (Vol. 19, Issue 4, pp. 417–420). Cornea.

Wilson, S. L., Ahearne, M., & Hopkinson, A. (2015). An overview of current techniques for ocular toxicity testing. *Toxicology* (Vol. 327, pp. 32–46).

Wilson, S. L., Ahearne, M., & Hopkinson, A. (2015). An overview of current techniques for ocular toxicity testing. *Toxicology*.

Wolff, E., Bron, A. J., Tripathi, R. C., & Tripathi, B. J. (1997). *Wolff's anatomy of the eye and orbit*. London: Chapman & Hall medical.

Wynn, T. A. (2004). Fibrotic disease and the TH1/TH2 paradigm. *Nature Reviews Immunology* (Vol. 4, Issue 8, pp. 583–594).

Yamazaki, N., Kobayashi, A., Yokogawa, H., Ishibashi, Y., Oikawa, Y., Tokoro, M., & Sugiyama, K. (2012). Ex vivo laser confocal microscopy findings of cultured Acanthamoeba trophozoites. *Clinical Ophthalmology*, *6*(1), 1365–1368.

Yang, S., & Villemez, C. (1994). Cell surface control of differentiation in Acanthamoeba. *Journal of cellular biochemistry*, *56*(4), 592–596.

Yang, Z., Cao, Z., & Panjwani, N. (1997). Pathogenesis of Acanthamoeba keratitis: carbohydrate-mediated host-parasite interactions. *Infect. Immun.*, *65*, 439–445.

Yang, Z., Goldman, N., & Friday, A. (1994). Comparison of models for nucleotide substitution used in maximum- likelihood phylogenetic estimation. *Molecular Biology and Evolution*, *11*(2), 316–324.

Yona, S., Kim, K. W., Wolf, Y., Mildner, A., Varol, D., Breker, M., Strauss-Ayali, D., Viukov, S., Guilliams, M., Misharin, A., Hume, D. A., Perlman, H., Malissen, B., Zelzer, E., & Jung, S. (2013). Fate Mapping Reveals Origins and Dynamics of Monocytes and Tissue Macrophages under Homeostasis. *Immunity*, *38*(1), 79–91.

Youngson RM (2006). *Collins Dictionary of Human Biology*. Glasgow: HarperCollins. ISBN 978-0-00-722134-9.

Zamfir, O., Yera, H., Bourcier, T., Batellier, L., Dupouy-Camet, J., Tourte-Schaeffer, C., & Chaumeil, C. (2006). Diagnostic par PCR des kératites à Acanthamoeba spp. *Journal Francais d'Ophtalmologie*, *29*(9), 1034–1040.

Zetterberg, A., & Engström, W. (1981). Mitogenic effect of alkaline pH on quiescent, serum-starved cells. *Proceedings of the National Academy of Sciences of the United States of America*, *78*(7), 4334–4338.

Zhong, J., Li, X., Deng, Y., Chen, L., Zhou, S., Huang, W., Lin, S., & Yuan, J. (2017). Associated factors, diagnosis and management of Acanthamoeba keratitis in a referral Center in Southern China. *BMC Ophthalmology*, *17*(1), 1–8.

Zhou, J., Begley, C. G., Wright, A., Wilson, G., & Tokarski, T. (2000). Characterization of cells collected from the normal human ocular surface by contact lens cytology. *Cornea*, *19*(6), 824–832.

Ziegler-Heitbroc, H. W. L., Thiel, E., Futterer, A., Herzog, V., Wirtz, A., & Riethmüller, G. (1988). Establishment of a human cell line (mono mac 6) with characteristics of mature monocytes. *International Journal of Cancer*, *41*(3), 456–461.

Ziegler-Heitbrock, H. W., Schraut, W., Wendelgass, P., Ströbel, M., Sternsdorf, T., Weber, C., Aepfelbacher, M., Ehlers, M., Schütt, C., & Haas, J. G. (1994). Distinct patterns of differentiation induced in the monocytic cell line Mono Mac 6. *Journal of leukocyte biology* (Vol. 55, Issue 1, pp. 73–80).

Ziegler-Heitbrock, L. (2007). The CD14+ CD16+ blood monocytes: their role in infection and inflammation. *Journal of Leukocyte Biology*, *81*(3), 584–592.

Zuang, V., Desprez, B., Barroso, J., Belz, S., Berggren, E., Bernasconi, C., Bessems, J., Bopp, S., Casati, S., Coecke, S., Corvi, R., Dumont, C., Gouliarmou, V., Griesinger, C., Halder, M., Janusch-Roi, A., Kienzler, A., Landesmann, B., Madia, F., … Whelan, M. (2015). *EURL ECVAM Status Report on the Development, Validation and Regulatory Acceptance of Alternative Methods and Approaches (2015)*.